

UNITED KINGDOM • CHINA • MALAYSIA

Faculty of Medicine and Health Sciences

School of Medicine

An investigation of Chromosome 20q13 Amplification in Colorectal Cancer

Hussain Ali Al-masmoum

Bsc, Msc

Thesis submitted to the University of Nottingham for the Degree of Doctor of Philosophy

Declaration

This thesis entitled as „ An investigation of Chromosome 20q13 Amplification in Colorectal Cancer ‟ is the result of my own investigations and observations unless stated otherwise.

Acknowledgment

First and foremost I owe my successful completion to my almighty **Allah** for granting me the wisdom and health to undertake this research.

I would like to express my special heartfelt thanks and sincere appreciation to my supervisor **Professor Mohammed Ilyas**. Your kind guidance, encouragement, making yourself available to clarify my doubts and providing me with an opportunity to grow as a research scientist was really helpful.

I also would like to acknowledge a great source of collaboration and friendship; **members of the Pathology group** (University of Nottingham).

Special mention goes to **Dr Wakkas Fadhil**, whom I owe respect and gratitude, for his valuable suggestion, concise comments on my laboratory work and he has contributed immensely to my research at various stages of the programme.

During my work, obstacles were less because of the presence of **Mr. Mohammed Albanghali**. I will forever be thankful to him for his contributions and efforts in the statistical data analysis.

Many people, I cannot mention one by one, deserve my appreciation for their help and assistance. However, I should especially thank **Dr. Saleh Al-ghamdi** for the guidance and great advice during my early stage in the PhD wonderful journey.

Words cannot express how grateful I am for **my family**, without their unconditional support; this doctoral thesis was not possible to complete.

Dedication

I dedicate my thesis to my beloved wife and my family how supported me throughout the process. This work is also dedicated to my parents for their endless love and being a constant source of encouragement during the challenges in my PHD journey.

Hussain Almasmoum

Abstract

Background: Colorectal cancer (CRC) is the third most prevalent and second most fatal type of cancer in the Western world. 20q amplification has been identified in approximately 50% of CRC cases. 20q amplification and may be associated with liver metastasis. In our lab, a previous array comparative genomic hybridization (aCGH) study of a series of primary CRCs and corresponding liver metastases, found that the 20q13 was frequently amplified in both groups. Several known oncogenes are located at Chromosome 20q (for example *SRC*, *TPX2* and *CSE1L)* suggesting that 20q amplification may be an important event in the development and metastasis of CRC.

Hypothesis and Aim: Although there are many genes located in 20q identified to have role in developing CRC, other genes with potential role in tumour progression have not been studied in CRC. We hypothesized that 20q harboring genes have a potential role in CRC progression. Therefore, we aimed to (i) study the frequency of 20q amplification in CRC by validating our aCGH data by alternative method and screen larger sample set for 20q amplification. (ii) Protein expression of candidate genes was investigated. Then, candidate genes were evaluated in several cancer related processes including proliferation and cell motility.

Materials and Methods: The evaluation of 20q amplification was performed in DNA from FFPE of micro-dissected 20 CRCs and their matched liver metastasis, using comparative quantitative PCR (qPCR) based on 6 genes (*PTPN1*, *CSE1L*, *ADNP*, *PREX1*, *ELMO2* and *PTGIS*), which are located in the same region. It was found that quantification of two genes was sufficient to evaluate amplification and thus separate series of 103 cases were screened for 20q amplification based on qPCR of two genes (*ELMO2* and *PTPN1*). For studying the functional activity, *PTPN1*, *CD40*, *PREX1*, *ELMO2* and *PTGIS* were studied in CRC cell lines. To evaluate gene function, small interference RNAs (siRNAs) were used to knockdown genes of interest in CRC cell lines. Knockdown was validated by western blot and qPCR and the effect of knockdown was evaluated on cellular functions such as proliferation, cell migration, cell invasion and wound healing. Immunohistochemistry was used to investigate protein expression in primary CRCs.

Results: The amplification of 20q in CRC sample was studied by qPCR and aCGH. High concordance was found between the two methods aCGH, and high correlation coefficient between the qPCR results of the genes demonstrated the utility of this method for measuring amplification. In the combined data set, 20q amplification was seen in both primary tumours (51%) and metastases (60%). *TP53* mutation was associated with 20q amplification (p =0.010).

Then, we investigated the functional activity of 5 genes located on 20q, which might be has a role in CRC progression. (1) PTPN1 has been reported as tumour suppresser and oncogene. Therefore, we studied protein expression and its functional role in CRC cell lines. PTPN1 was overexpressed in 59% of primary tumours. Knockdown of PTPN1 reduced cell motility but did not affect cell proliferation. (2) CD40, previously, has been identified as a tumour suppresser in CRC. However, high CD40 expression was detected 25% of tumours. Functional assays showed CD40 promotes proliferation by altering subG1 phase of the cell cycle. Therefore, CD40 might promote tumour growth by inhibiting apoptosis. (3) PREX1 was expressed in 61% of primary tumours. Functional analysis showed that it promotes both cell proliferation and motility. (4) ELMO2 was expressed in 38% of primary tumours and functional analysis showed it promotes proliferation and cell migrations. (5) Finally, PTGIS is highly expressed in CRC and its expression associated with liver metastasis. However, PTGIS effect on tumour progression has not been studied. PTGIS knockdown had no effect on CRC cell lines growth and motility.

Conclusion: Using alternative methods to evaluate the 20q13 amplification, we have confirmed our previous aCGH and found a frequency similar to that reported in the literature. Amplification of 20q appears frequently in primary tumours but it not positively associated with metastasis. Many genes located in 20q have oncogenic effects which would support the hallmarks of cancer. Understanding their role in CRC development could reveal new avenue in understanding cancer biology and treatment.

.Thesis Related Publications

Presentations and Conference Communications

1- Protein tyrosine phosphatase, non-receptor type 1 gene functions as an oncogene and promotes cell motility in colorectal cancer.

Almasmoum, H; Fadhil, W; Jackson, D; Ilyas, M

Poster Presentation, the 26th European Congress of Pathology (ECP 2014) in London, UK, 30th of August to 3 September 2014.

2- Phosphatidylinositol 3,4,5-trisphosphate-dependent Rac exchanger 1 functions as an oncogene that promotes Proliferation migration and invasion in colorectal cancer.

Almasmoum, H; Fadhil, W; Jackson, D; Ilyas, M

Poster Presentation, the 26th European Congress of Pathology (ECP 2014) in London, UK, 30th of August to 3 September 2014.

3- Tumour Necrosis Factor Receptor, CD40, Gene Functions as an Oncogene and Promotes Cell Proliferation in Colorectal Cancer Cell Lines.

Almasmoum, H; Thorpe, H; Ilyas, M

Poster Presentation, 8th Joint Meeting of the British Division of the International Academy of Pathology and the Pathological Society of Great Britain & Ireland, 23 – 25 June 2015, 30th of August to 3 September 2014

In-process Publications:

1- PTP1B gene functions as an oncogene and promotes cell motility in colorectal cancer

2- Prex1 functions as an oncogene that promotes Proliferation migration and invasion in colorectal cancer

3- CD40, gene functions as an oncogene and reduces cell proliferation in colorectal cancer cell lines

List of Content

DECLARATION ..... **I**

ACKNOWLEDGMENT ..... **II**

DEDICATION ..... **III**

ABSTRACT ..... **IV**

.THESIS RELATED PUBLICATIONS ..... **VI**

PRESENTATIONS AND CONFERENCE COMMUNICATIONS VI

IN-PROCESS PUBLICATIONS: VI

LIST OF CONTENT ..... **VII**

LIST OF FIGURES ..... **X**

LIST OF ABBREVIATIONS ..... **XVII**

1 CHAPTER ONE: INTRODUCTION **1**

1.1 EPIDEMIOLOGY **2**

1.2 HEREDITARY CRC **4**

1.2.1 FAMILIAL ADENOMATOUS POLYPOSIS (FAP) 5

1.2.2 MUTYH-ASSOCIATED POLYPOSIS 5

1.2.3 POLYMERASE PROOFREADING-ASSOCIATED POLYPOSIS (PPAP) 6

1.2.4 HAMARTOMATOUS POLYPOSIS SYNDROMES 6

1.2.5 LYNCH SYNDROME 7

1.3 GENETICS OF SPORADIC CRC **7**

1.3.1 CHROMOSOMAL INSTABILITY PATHWAY (CIN) 11

1.3.2 MICROSATELLITE INSTABILITY (MSI) 18

1.3.3 CPG ISLAND METHYLATOR PHENOTYPE (CIMP) 21

1.4 GENETICS OF LIVER METASTASIS **22**

1.5 GENETICS IMPLICATION IN CRC TREATMENT **26**

1.6 20Q AMPLIFICATION **27**

1.6.1 TYROSINE-PROTEIN PHOSPHATASE NON-RECEPTOR TYPE (*PTPN1*) 35

1.6.2 CLUSTER OF DIFFERENTIATION 40 (CD40) 39

1.6.3 PHOSPHATIDYLINOSITOL (3,4,5)-TRISPHOSPHATE (PIP3)-DEPENDENT RAC EXCHANGER 1 (*PREX1*) 41

1.6.4 ENGULFMENT AND CELL MOTILITY (*ELMO2*) 43

1.6.5 PROSTAGLANDIN I2 (PROSTACYCLIN) SYNTHASE (*PTGIS*) 46

1.7 HYPOTHESIS AND AIMS OF THE STUDY **47**

1.7.1 Background: 47
1.7.2 Hypothesis 47
1.7.3 Aims 47

2 CHAPTER TWO: MATERIALS AND METHODS4 50

2.1 Tissue sample and DNA extraction 51
2.2 DNA copy number evaluation of 20q13 genes in colorectal cancer and liver metastasis 53
2.2.1 Sample quality control 53
2.2.2 Molecular analysis of tumour samples 53
2.2.3 Primer Design 53
2.2.4 Polymerase Chain Reaction (PCR) 56
2.3 Tissue Culture Studies: 58
2.3.1 Culturing of cell line 58
2.3.2 Sub-culturing of the cells (Passaging) 59
2.3.3 Cell transfection with Small Interfering RNAs (siRNAs) 59
2.3.4 RNA Extraction 62
2.3.5 Complementary DNA (c.DNA) generation 62
2.3.6 qPCR 62
2.3.7 Protein samples preparation and quantitation 63
2.3.8 Western blotting 63
2.3.9 Functional studies 65
2.4 Immunohistochemistry (IHC) 72
2.4.1 Tissue microarray construction and IHC 72
2.4.2 Immunohistochemistry staining 73
2.4.3 Optimisation of the antibody concentration 74
2.4.4 Evaluation of the immunohistochemical staining 75
2.5 Statistical Analysis 75

3 CHAPTER THREE: DNA COPY NUMBER EVALUATION OF 20Q GENES IN COLORECTAL CANCER AND LIVER METASTASIS 77

3.1 Introduction 78
3.2 RESULTS 82
3.2.1 Evaluation of the FFPE sample quality 82

3.2.2 PRIMER OPTIMISATION 84
3.2.3 AMPLIFICATION THRESHOLD IN QPCR 97
3.2.4 ROLE OF 20Q IN CRC LIVER METASTASIS 98
3.2.5 ROLE OF 20Q AMPLIFICATION IN DRIVING CRC 104
3.3 DISCUSSION 111

4 CHAPTER FOUR: EVALUATING CANCER-RELATED FUNCTION AND EXPRESSION OF GENES LOCATED ON 20Q 114

4.1.1 PTPN1 (PROTEIN TYROSINE PHOSPHATASE, NON-RECEPTOR TYPE 1) 116
4.1.2 CLUSTER OF DIFFERENTIATION 40 (CD40) 140
4.1.3 PHOSPHATIDYLINOSITOL (3,4,5)-TRISPHOSPHATE (PIP_3)-DEPENDENT RAC EXCHANGER 1 (*PREX1*) 166
4.1.4 ENGULFMENT AND CELL MOTILITY (ELMO2) 185
4.1.5 PROSTAGLANDIN I2 (PROSTACYCLIN) SYNTHASE (PTGIS) 199

5 CHAPTER FIVE: GENERAL DISCUSSION 207

5.1 DNA COPY NUMBER EVALUATION OF 20Q GENES IN COLORECTAL CANCER AND LIVER METASTASIS 208
5.2 EVALUATING CANCER RELATED PROGRESS OF GENES LOCATED AT 20Q 210
5.2.1 PTPN1 ENHANCES CELL MOTILITY IN CRC CELL LINES 210
5.2.2 CD40 ENHANCES CELL NUMBER IN CRC CELL LINES 211
5.2.3 PREX1 ENHANCES PROLIFERATION AND MOTILITY IN CRC CELL LINES 212
5.2.4 ELMO2 ENHANECS PROLIFERATION AND MOTILITY IN CRC CELL LINES 214
5.2.5 PTGIS ROLE IN COLORECTAL CANCER CELL LINES 214
5.3 LIMITATION OF THE THESIS: 216
5.4 POTENTIAL FUTURE STUDIES: 216
5.5 FINAL CONCLUSION 217

6 CHAPTER SIX: REFERENCES 218

7 CHAPTER SEVEN: APPENDIX 250

7.1 APPENDIX 2: DNA EXTRACTION 251
7.2 APPENDIX2: BCA PROTEIN ASSAY KIT INSTRUCTION 252

List of Figures

Figure 1-1 Estimated age-standardised colorectal cancer incidence for men in 2008 3

Figure 1-2 CRC classification in molecular subgroups 10

Figure 1-3 Genetic pathways of colorectal cancer (CRC) 12

Figure 1-4 Model of the 20q time of occurrence in colorectal cancer 25

Figure 1-5 Structural domains of PTPN1. 37

Figure 1-6 Oncogenic signaling of PTPN1. 38

Figure 1-7 PREX1 structure 42

Figure 1-8 Schematic representation of ELMO protein. 44

Figure 1-9 Recruitment of RHOG, ELMO2, and ILK to leading edges of migrating cells in response to EGF 45

Figure 1-10 The strategy used to investigate chromosome 20q13 amplification in Colorectal cancer. 49

Figure 2-2-1 Graphical representation of real time PCR data. 57

Figure 2-2 Methylene blue assay sensitivity assessment 67

Figure 2-3 Presto Blue assay sensitivity assessment 68

Figure 2-4 An example of marking the 6-well plate. 72

Figure 3-1 Ideogram and high resolution map of Chromosome 20q13 81

Figure 3-2. Quality of DNA from (FFPE) tissues. 83

Figure 3-3 agarose gel electrophoresis gradient temperature for ELMO2 primers optimisation. 85

Figure 3-4. Primer optimisation, thus, these primer were suitable for qPCR analysis. 86

Figure 3-5 Amplification plot of GAPDH primers and Melt Curve analysis 88

Figure 3-6 Amplification plot of PTGIS primers and Melt Curve analysis 89

Figure 3-7 Amplification plot of PTPN1 primers and Melt Curve analysis 90

Figure 3-8 Amplification plot of CSE1L primers and Melt Curve analysis..... 91

Figure 3-9 Amplification plot of ADNP primers and Melt Curve analysis 92

Figure 3-10 Amplification plot of ELMO2 primers and Melt Curve analysis 93

Figure 3-11 Amplification plot of PREX1 primers and Melt Curve analysis 94

Figure 3-12. A representative example of Linear regression slope of serial dilution of the reference sample. 95

Figure 3-13. Quantitative (q) PCR results from the normal colon DNA samples. . 97

Figure 3-14. A representative example of Relative quantitative (RQ) results and melting curve analysis post the real-time PCR. 103

Figure 3-15. Relative quantitative (RQ) comparative threshold results of 12 patients with CRC. 106

Figure 4-1. Low and high expression of PTPN1. 118

Figure 4-2. Pie chart showing the frequencies of high and low expression of PTPN1. 119

Figure 4-3. Western blot screening of PTPN1 expression in 7 CRC cell lines.... 122

Figure 4-4. PTPN1 knockdown in SW620, RKO, HCT116, DLD1, and HT29 cells. 123

Figure 4-5. HCT116, SW620, DLD1 and HT29 cells were transfected with a siRNA targeting the PTPN1 gene. 124

Figure 4-6. Effect of PTPN1 on cell proliferation and cell cycle in DLD1 and HT29 cells. 126

Figure 4-7. Effect of PTPN1 on cell cycle in HT29 cells. 127

Figure 4-8. Effect of PTPN1 on cell proliferation and cell cycle in HCT116 cells.128

Figure 4-9. Effect of PTPN1 on cell proliferation and cell cycle in RKO cells. 129

Figure 4-10. Effect of PTPN1 on cell proliferation and cell cycle in SW620 cells. 130

Figure 4-11. PTPN1 enhanced CRC cell motility in transwell migration assay... 132

Figure 4-12. Wound healing assay. 134

Figure 4-13. PTPN1 increases cell invasion ability. 136

Figure 4-14. Low and high expression of CD40 and CD40L. 143

Figure 4-15. Pie chart showing the frequencies of high and low cytoplasmic expression of CD40 and CD40L. 144

Figure 4-16. Pie chart showing the frequencies of high and low expression of CD40 and CD40L 145

Figure 4-17. Western blot screening of CD40 expression in 7 CRC cell lines. ... 153

Figure 4-18. CD40 knockdown in RKO, HCT116, DLD1, and HT29 cells. 154

Figure 4-19. Effect of CD40 on cell proliferation and cell cycle in HCT116 cells. 156

Figure 4-20. Effect of CD40 on cell proliferation in DLD1 cells. 157

Figure 4-21. Effect of CD40 on cell proliferation and cell cycle in HT29 cells. 158

Figure 4-22. Effect of CD40 on cell proliferation and cell cycle in RKO cells. 159

Figure 4-23. CD40 did not affect cell motility in transwell migration assay. 161

Figure 4-24. Wound healing assay. 162

Figure 4-25. Pie chart showing the frequencies of absence and presence of PREX1 expression. 168

Figure 4-26. PREX1 IHC in normal colon and malignant colonic tissues. 169

Figure 4-271. Western blot screening of PREX1 expression in 6 CRC cell lines. 174

Figure 4-28. PREX1 knockdown in SW620 and HCT116 cells. 175

Figure 4-29 PREX1 knockdown in SW620 and HCT116 cells qPCR 176

Figure 4-30. Effect of PREX1 on cell proliferation in SW620 and HCT116 cells. 178

Figure 4-31. PREX1 enhanced motility in transwell migration assay. 180

Figure 4-32. Wound healing assays. 181

Figure 4-33. PREX1 increase cell invasion ability. 182

Figure 4-34 No expression of ELMO2 and Expression of ELMO2 staining. 186

Figure 4-35 Pie chart showed the frequencies of high and low expression of ELMO2 186

Figure 4-36 ELMO2 knockdown in four different colorectal cancer cell lines 191

Figure 4-37 Effect of ELMO2 on cell proliferation and cell cycle in HT29. 193

Figure 4-38 Effect of ELMO2 on cell proliferation in SW620 and DLD1. 194

Figure 4-39 ELMO2 enhanced motility in wound healing Transwell migration assays. 196

Figure 4-40 Western blot screening of PTGIS expression in 4CRC cell lines. ... 200

Figure 4-41. PTGIS knockdown in SW620, SW480, and HCT116 cells. 201

Figure 4-42. Effect of PTGIS on cell proliferation in SW620, SW480, and HCT116 cells. 202

Figure 4-43. PTGIS did not affect cell motility in the transwell migration assay. 204

List of Tables

Table 1-1 The consensus molecular subtypes (CMSs)of colorectal cancer 9

Table 1-2 Genes containing coding repeats that are targets for mutation in colorectal cancer with microsatellite instability. (Iacopetta et al., 2010)..... 20

Table 1-3 List of studies previously carried out examining amplification of chromosome 20 in the context of colorectal cancer and liver metastasis. 28

Table 1-4 Frequency of the alterations in primary carcinomas and liver metastases at the chromosome band level. 32

Table 1-5 List of candidate genes located at chromosome 20. 34

Table 2-1: List of sample sets selected to study amplification of chromosome.20 and protein expression. 52

Table 2-2: Sequences of the primers produced by Eurofins MWG Operon. 55

Table2-2-3 The sequences of the siRNAs and its Identification code. 61

Table 2-4 list of antibodies used in western blot. 64

Table 2-5: List of antibodies used in immunohistochemsitry 74

Table 3-1. CRC cell lines that present with 20q amplification 79

Table 3-2. Primer pair efficiencies. 96

Table 3-3 the Relative quantitative data generated from qPCR analysis of 15 CRCs and secondary tumours. 100

Table 3-4. Chromosome 20q13 amplification status assessed by aCGH and qPCR. 101

Table 3-5. Ploidy status and mutation profile of 20Amp-CRCs and 20qSt-CRCs. 107

Table 3-6 molecular profile of 110 cases. 108

Table 4-1. PTPN1 staining overview. 120

Table 4-2. Overall frequency of PTPN1 expression in CRC tissues in different matched tumour sites. 120

Table 4-3. CD40 overall staining. 142

Table 4-4. CD40L overall staining. 142

Table 4-5. Overall frequency of CD40 expression in CRC tissues in different matched tumour sites. 146

Table 4-6. Overall frequency of CD40L expression in CRC tissue in different matched tumour sites. 148

Table 4-7. Cross tabulation of CD40 *vs.* CD40L membrane staining of luminal tumours. 150

Table 4-8. Cross tabulation of CD40 *vs*. CD40L membrane staining in middle tumours. 150

Table 4-9. Cross tabulation of CD40 *vs.* CD40L membrane staining of the edge of the tumours. 151

Table 4-10. PREX1 overall staining. 168

Table 4-11. Overall frequency of PREX1 expression in different matched CRC tumour sites. 170

Table 4-12. Cross tabulation of PREX1 edge tumour *vs.* PREX1 middle tumour staining. 171

Table 4-13. Cross tabulation of PREX1 luminal tumour *vs*. PREX1 middle tumour staining. 171

Table 4-14 Cross tabulation of PREX1 luminal tumour *vs.* PREX1 edge tumour staining. 172

Table 4-15 ELMO2 staining overview 187

Table 4-16 Overall frequency of ELMO2 in CRC tissue in different matched tumour sites. 187

Table 4-17 Crosstabulation of ELMO2 Middle Tumour Vs ELMO2 Edge Tumour 188

Table 4-18 Crosstabulation of ELMO2 Middle Tumour Vs ELMO2 Luminal Tumour 188

Table 4-19 Crosstabulation of ELMO2 Luminal Tumour Vs ELMO2 Edge Tumour 189

List of Abbreviations

AURKA: Aurora A kinase
CGH: Comparative genomic hybridization
CIMP: CpG Island Methylator Phenotype
CIMPL: CIMP low
CIN: Chromosomal instability pathway
CRC: Colorectal cancer
CSE1L: Chromosome segregation 1-like
DIDO1: Death-inducer obliterator 1
DC: Dendritic cell
DCC: Deleted in Colorectal Cancer
DMEM: Dulbecco's Modified Eagle's Medium
EGF: Epidermal growth factor
EGFR: Epidermal growth factor receptor
ELMO2: Engulfment and cell motility gene
EMT: Epithelial-mesenchymal transition
EpCAM: Epithelial cell adhesion marker
ERK: Extracellular regulated MAP-kinase
FAP: Familial adenomatous polyposis
FISH: Fluorescence *in situ* hybridization
FGF: Fibroblast growth factor
GEF: Guanine nucleotide exchange factors
GPCR: G protein-coupled receptor
IGFR: Insulin-like growth factor receptor
IHC: Immunohistochemistry
ILK: Integrin-linked kinase
KRAS: Kirsten RAS
HNPCC: Hereditary non-polyposis colorectal cancer
HRAS: Harvey RAS
JPS: Juvenile polyposis syndrome
LOH: Loss of heterozygosity
MAP: *MUTYH*-associated polyposis
MEK: MAP kinase/ERK kinase
MMR: mismatch repair

MSI: Microsatellite instability

MSS: Microsatellite stability

NRAS: neuroblastoma RAS

PARD6B: par-6 partitioning defective 6 homolog beta

PDK1: 3-phosphoinositide-dependent kinase 1

PIP2: Phosphatidylinositol 4,5 bisphosphate

PIP3: phosphatidylinositol 3,4,5-trisphosphate

PJS: Peutz-Jeghers syndrome

PPAR: peroxisomal-proliferator-activated receptor

PREX1: Phosphatidylinositol (3,4,5)-trisphosphate (PIP_3)-dependent Rac exchanger 1

PTEN: Phosphatase and tensin homolog

PTGIS: Prostaglandin I2 (prostacyclin) synthase

qPCR: Quantitative polymerase chain reaction

RAF: Root abundant factor

RTK: Receptor tyrosine kinase

siRNA: Small Interfering RNA

SNP: Single nucleotide polymorphism

TCF/LEF: T cell factor/lymphoid enhancer family

TMA: Tissue microarray

VEGF: Vascular endothelial growth factor

Wnt: Wingless signal transduction

1 Chapter One: Introduction

1.1 Epidemiology

Colorectal cancer (CRC) is the third most common cancer globally and the fourth most common cause of cancer-related death. There are 1,200,000 new cases and 600,000 deaths per year. (Brenner et al., 2014). In the population which is younger than 50 years, the incidence of CRC is low. However, the incidence of CRC strongly increases with age, and the median age of CRC diagnosis is 70 years (Siegel et al., 2012). The lowest incidence is reported in countries of central and south Asia and Africa, whereas the highest incidence is reported in countries of Europe and North America (Center et al., 2009). The estimated age-standardised incidence by region ranges from 4.3 cases out of 100,000 in central Africa to 45.7 cases out of 100,000 in Australia (Figure 1-1). In some developed countries, CRC incidence has stabilised or is starting to decrease. This may be linked with the use of sigmoidoscopy and colonoscopy with polypectomy (Stock et al., 2012).

The estimated mortality of CRC ranged from 3.5 per 100 000 in Central Africa to 20.1 in Eastern and Central Europe for men, and from 2.7 to 12.2 in the same regions for women (Brenner et al., 2014). However, the mortality rate in some East Asia and Eastern Europe countries has decreased. This may be associated with improved early detection and treatment. However, in countries with poor healthcare resources, the mortality rate is still increasing (Center et al., 2009).

The prognosis of patients with CRC has slowly improved in many countries in recent years. The percentage of patients with 5-year-relative survival is approximately 65% in developed countries such as Australia, USA, Canada, and several European countries. However, the 5-year-relative survival of patients with CRC in low income countries remains less than 50% (Siegel et al., 2012, Brenner et al., 2012, Sankaranarayanan et al., 2010). The relative survival decreases with age. However, for women at younger age than men, the relative survival is slightly higher (Siegel et al., 2012).

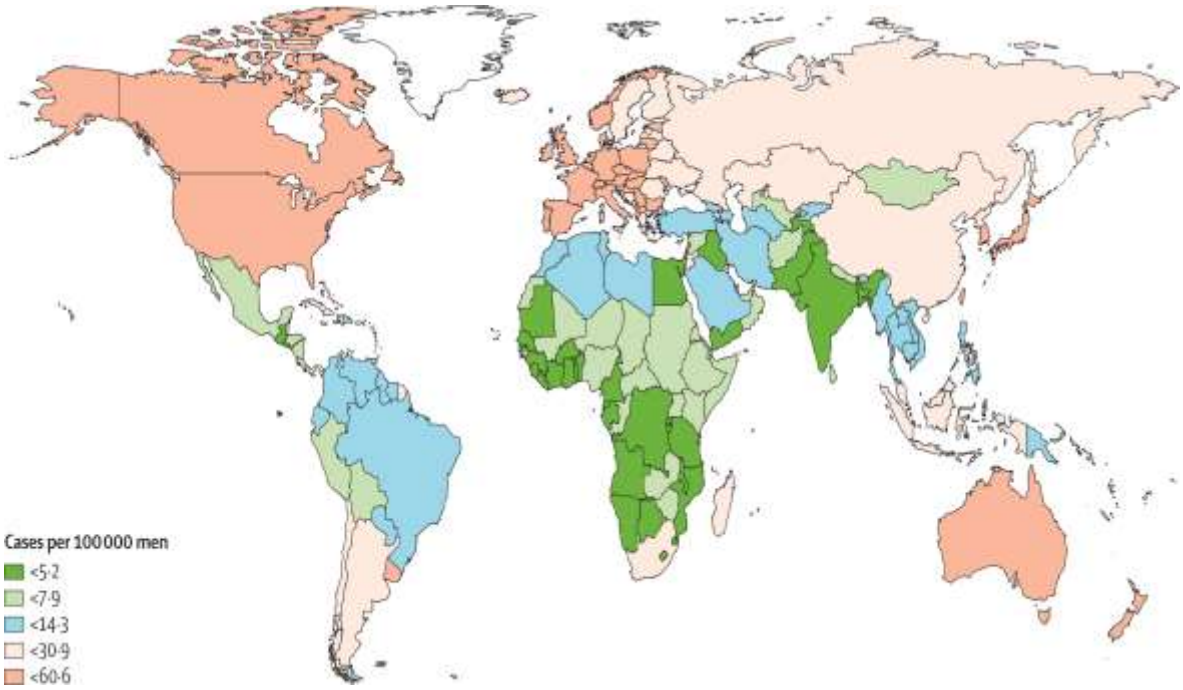


Figure 1-1 Estimated age-standardised colorectal cancer incidence for men in 2008

Colorectal cancer is the third most common cancer and the fourth most common cancer cause of death globally, accounting for roughly 1·2 million new cases and 600 000 deaths per year.Incidence is low at ages younger than 50 years, but strongly increases with age. Median age at diagnosis is about 70 years in developed countries. The highest incidence is reported in countries of Europe, North America, and Oceania, whereas incidence is lowest in some countries of south and central Asia and Africa. In 2008, estimated age-standardised incidence by region ranged from 4·3 cases per 100 000 people in central Africa to 45·7 per 100 000 in Australia and New Zealand in men (Brenner et al., 2014).

Risk factors for CRC have been identified in epidemiological studies and include inflammatory bowel disease (Jess et al., 2012), family history of CRC (Taylor et al., 2010), smoking (Liang et al., 2009), excessive alcohol consumption (Fedirko et al., 2011), high consumption of red meat (Chan et al., 2011), and obesity (Ma et al., 2013). The highest risk factors of developing CRC are the family history factor and history of inflammatory bowel disease. Another risk factor associated with increased risk of developing CRC is infection such as *Helicobacter pylori* and *Fusobacterium* (Sonnenberg and Genta, 2013, Kostic et al., 2012). The use of aspirin (Bosetti et al., 2012, Rothwell et al., 2011) and physical activity (Boyle et al., 2012) have been reported to reduce the risk of developing CRC up to 20–30%. The most effective method to prevent CRC is endoscopy with removal of pre-cancerous lesions (Brenner et al., 2011, Elmunzer et al., 2012) and this has been the basis of NHS bowel cancer screening program in the UK.

1.2 Hereditary CRC

Less than 5% of CRC occurs in the context of dominantly inherited mutations and a lower percentage accounts for recessive syndromes. There are two types of hereditary CRC, which are distinguished by the presence of adenomatous polyps or not. Familial adenomatous polyposis (FAP) is characterised by patient presenting with multiple polyps. One or more of these polyps may become malignant, in absence of preventive surgery. The other type, which is not associated with polyposis, is hereditary non-polyposis colorectal cancer (HNPCC) (Arvelo et al., 2015).

To date, rare mutations that underline these syndromes have been identified in only 14 genes (Peters et al., 2015). The identification of these genes started with the discovery of mutations in the *APC* gene (adenomatous polyposis coli), which is a predisposing factor for FAP syndrome (Bodmer et al., 1987). Then, mutations in the human DNA mismatch repair (MMR) genes were associated with HNPCC, which is also known as Lynch syndrome (Vasen et al., 2015, Vasen, 2000). Other mutations were then revealed in *MutY homologue* (*MUTYH*) (Al-Tassan et al., 2002), *PTEN (Mallory, 1995),* and *SMAD4,* which are the genetic bases of other polyposis syndromes. These genes are implicated in very important pathways that

play a large role in CRC development such as the wingless signal transduction (Wnt) signalling pathway.

1.2.1 Familial adenomatous polyposis (FAP)

FAP is an autosomal dominant inherited syndrome, which is characterised by early onset of multiple polyps. FAP accounts for 1% of all CRC cases (Lynch et al., 1990, Galiatsatos and Foulkes, 2006). Two phenotypes have been described: (1) the classic FAP, which is characterised by hundreds to thousands of adenomas and has a high risk of (up to 100%) developing into CRC. (2) Attenuated FAP, which presents with a lower number of adenomas and a much lower risk of CRC when compared to the classic FAP (Arvelo et al., 2015, Groen et al., 2008).

FAP is mainly caused by germline mutations in the *APC* gene, which is located on chromosome 5q. *APC* is a tumour suppressor gene, which plays a role in the Wnt signalling pathway. Somatic mutation in this gene is the first step of the adenoma-carcinoma sequence. The *APC* gene was discovered by the genetic study of families with FAP that were found to have germline mutation of the *APC* gene (Groden et al., 1991)

Germline mutations in the *APC* gene have been identified in 80% of patients with more than 1000 adenomas, 56% of patients with 100–1000 adenomas, 10% of patients with 20–100 adenomas, and 5% of patients with 10–20 adenomas (Nielsen et al., 2007). Normally, *APC* mutations are positioned in or near the functional domain, which binds to β-catenin. Recently, mutation in the *APC* gene promoter were shown to decrease *APC* transcription, which could result in FAP predisposition (Snow et al., 2014).

1.2.2 MUTYH-associated polyposis

MUTYH-associated polyposis (MAP) is an autosomal recessive syndrome, caused by germline mutation of two alleles in the *MUTYH* gene. Thirty percent of families with multiple polyps do not show autosomal dominant inheritance associated with FAP (Nielsen et al., 2005). The MAP's phenotype can overlap with that of FAP, in which patients show less than 100 adenomas (Cleary et al., 2009, Lubbe et al.,

2009). *MUTYH* gene is a base excision repair gene, which is located on chromosome 1p. It is involved in repairing DNA damaged by oxidative stress. MUTYH protein prevents G-C to T-A transversions. The most common germline mutations affecting *MUTYH* gene are the Y179C and G396D mutations. Patients carrying these mutations have a 28-fold increased risk of developing CRC compared to the general population (Theodoratou et al., 2010). Recently, no or minimal increased CRC risk was observed in individuals who are carriers of single allele mutation in the *MUTYH* gene (Balaguer et al., 2007).

1.2.3 Polymerase proofreading-associated polyposis (PPAP)

During DNA replication, polymerase errors may occur and cause mutation. Accurate replication occurs through Watson-Crick pairing and through a proof-reading exonuclease domain of the polymerase enzyme which detects and removes un-complementary bases in the daughter strand (Reha-Krantz, 2010). Recently, germline mutations in the proofreading domains of two DNA polymerases (POLE and POLD) were discovered by using whole genome sequencing of patients with multiple adenomas. POLE (p.Leu424Val) and POLD1 (p.Ser478Asn) mutations showed dominant inheritance and high penetrance which predispose to CRC (Palles et al., 2013). These mutations lead to the acquisition of a large number of somatic mutations, which are known as hyper-mutated tumours (Palles et al., 2013, Seshagiri, 2013).

1.2.4 Hamartomatous polyposis syndromes

Hamartomas are tumours characterised by an abnormal organisation of normal looking tissue. They may occur sporadically or as part of a hamartomatous polyposis syndrome arising from a germline mutation. The syndromes are associated with an increased risk of CRC.

Peutz-Jeghers syndrome (PJS) is an autosomal-dominant syndrome. It is caused by germline mutations in the *STK11* gene (Hemminki et al., 1997). *SKT11* gene encodes a tumour suppressor related to cellular energy homeostasis that targets mTOR, which is linked to the PI3K-AKT pathway (Vivanco and Sawyers, 2002a). Mutations of the *STK11* gene cause the hamartoma and other somatic mutations lead to adenomas, which subsequently lead to carcinoma (Miyaki et al., 2000).

Juvenile polyposis syndrome (JPS) is a very rare genetic disorder. JPS is an autosomal dominant inherited syndrome caused by germline mutations in *SMAD4* or *BMOR1A* genes. Germinal mutations have been described in the SMAD4 (MADH4) (chromosome 18q21.1) and in the BMPR1A (chromosome 10q 21-22) gene [21,22]. Genetic mutations have not been identified in all patients with JPS. SMAD4 mutations are more common and predispose to polyposis in the upper-digestive tract [23]. BMPR1A mutations are found in 40–100% of families without SMAD4 mutation.

1.2.5 Lynch syndrome

The Lynch syndrome or hereditary nonpolyposis colon cancer (HNPCC) is autosomal dominant and is the most common hereditary CRC (Hampel et al., 2006). It is caused by germline mutations in the DNA mismatch repair (MMR) genes (*MSH2, MLH1, MSH6, PMS2,* and *EPCAM).* The two most common mutations on the *MSH2* and *MLH1* genes account for approximately 90% of cases. The Lynch syndrome is characterised by an early onset at the age of 45 (Stoffel et al., 2009). Loss of MMR activity leads to defects in repairing the mismatch of single base, insertion, and deletion during the DNA replication. These errors in replication are especially common in nucleotide repeat sequences called microsatellites. The development of multiple mutations at these sites (called Microsatellite instability, MSI) is a marker for the Lynch syndrome diagnosis (Perucho, 1999).

1.3 Genetics of sporadic CRC

One million people develop CRC each year worldwide. Among these patients, 50% are expected to die within 5 years after diagnosis (Weitz et al., 2005). CRC is the third most common cancer after breast and lung cancers in the UK. CRC is a result of the accumulation of genetic and epigenetic alterations, which transform the normal epithelium into adenocarcinomas. Fearon and Vogelstein proposed a genetic pathway for the adenoma-carcinoma sequence (Fearon and Vogelstein, 1990), which advanced our understanding of CRC molecular pathogenesis.

Deregulation of homeostatic functions in cancer progression is caused by accumulation of mutations in key oncogenes and tumour suppressor genes. Recently, sequencing analysis of CRC DNA has identified 67 functionally

important genes mutations, which are located in a coding sequence (Sjöblom et al., 2006). However, the statistical analysis method of this study has been criticised (Getz et al., 2007). Cancer genome sequencing projects indicate that most cancer genomes present hundreds of mutations. This raises a challenge to evaluate which of these mutations play a role in cancer progression (driver mutations) and which mutation has no effect on this progression (passenger mutations). The interaction of mutation rates and clonal expansion is considered crucial in the dynamic of somatic evolution. The model of clonal evolution suggests a series of clonal expansions that result in the growth of a neoplasm (Beerenwinkel et al., 2007). This model highlights the central role of adenomatous precursor lesions and suggests that most CRCs present an early increased activation of the APC/β-catenin pathway followed by RAS/RAF mutations and losses of p53 functions in the later stages of tumour development (Fearon and Vogelstein, 1990). However, only 7% of patients with CRC present mutations in all three genes, indicating that there are other pathways involved in CRC progression (Smith et al., 2002). Recent studies suggest that genetic alteration is more complex and that epigenetic variations in genes related to cancer and expression of non-coding RNAs are also involved in cancer progression (Esteller, 2008). One example of epigenetic alteration is increased DNA methylation of CpG islands in the promoter regions of genes, also known as the CpG Island Methylator Phenotype (CIMP) (Samowitz et al., 2005). Thus, it is now well known that there are multiple molecular pathways that lead to the formation of adenomas and progression to CRC. These have been classified into five pathways (Jass, 2007) (Figure 1-2). Recently, four consensus molecular subtypes (CMSs) has been identified with distinguishing features: CMS1 (microsatellite instability immune, 14%), hyper-mutated, microsatellite unstable and strong immune activation; CMS2 (canonical, 37%), epithelial, marked WNT and MYC signalling activation; CMS3 (metabolic, 13%), epithelial and evident metabolic dysregulation; and CMS4 (mesenchymal, 23%), prominent transforming growth factor-β activation, stromal invasion and angiogenesis. Samples with mixed features (13%) possibly represent a transition phenotype or intratumoral heterogeneity (Guinney et al., 2015). The role of these genetic alterations in cancer formation, adenoma-carcinoma sequence, and in metastasis will be discussed, especially the role of the long arm of chromosome 20 amplification in CRC progression.

Table 1-1 The consensus molecular subtypes (CMSs)of colorectal cancer

Proposed taxonomy of colorectal cancer, reflecting significant biological differences in the gene expression-based molecular subtypes. The collaborative bioinformatics work on the largest collection of CRC cohorts with molecular annotation to date. A consensus molecular classification system allows the categorization of most tumors into one of four robust subtypes. Marked differences in the intrinsic biological underpinnings of each subtype support the new taxonomy of this disease (Guinney et al., 2015). CIMP, CpG island methylator phenotype; MSI, microsatellite instability; SCNA, somatic copy number alterations.

.

CMS1 MSI immune	CMS2 Cononical	CMS3 Metabolic	CMS4 Mesenchymal
14%	37%	13%	23%
MSI, CIMP high, hypermutation	SCNA High	Mixed MSI status, SCNA low, CIMP low	SCNA high
BRAF mutations		*KRAS* mutations	
Immune infiltration and activation	WNT and myc activation	Metabolic deregulation	Stromal infiltration, TGF-β activation, angiogenesis
Worse survival after relapse			Worse relapse-free overall survival

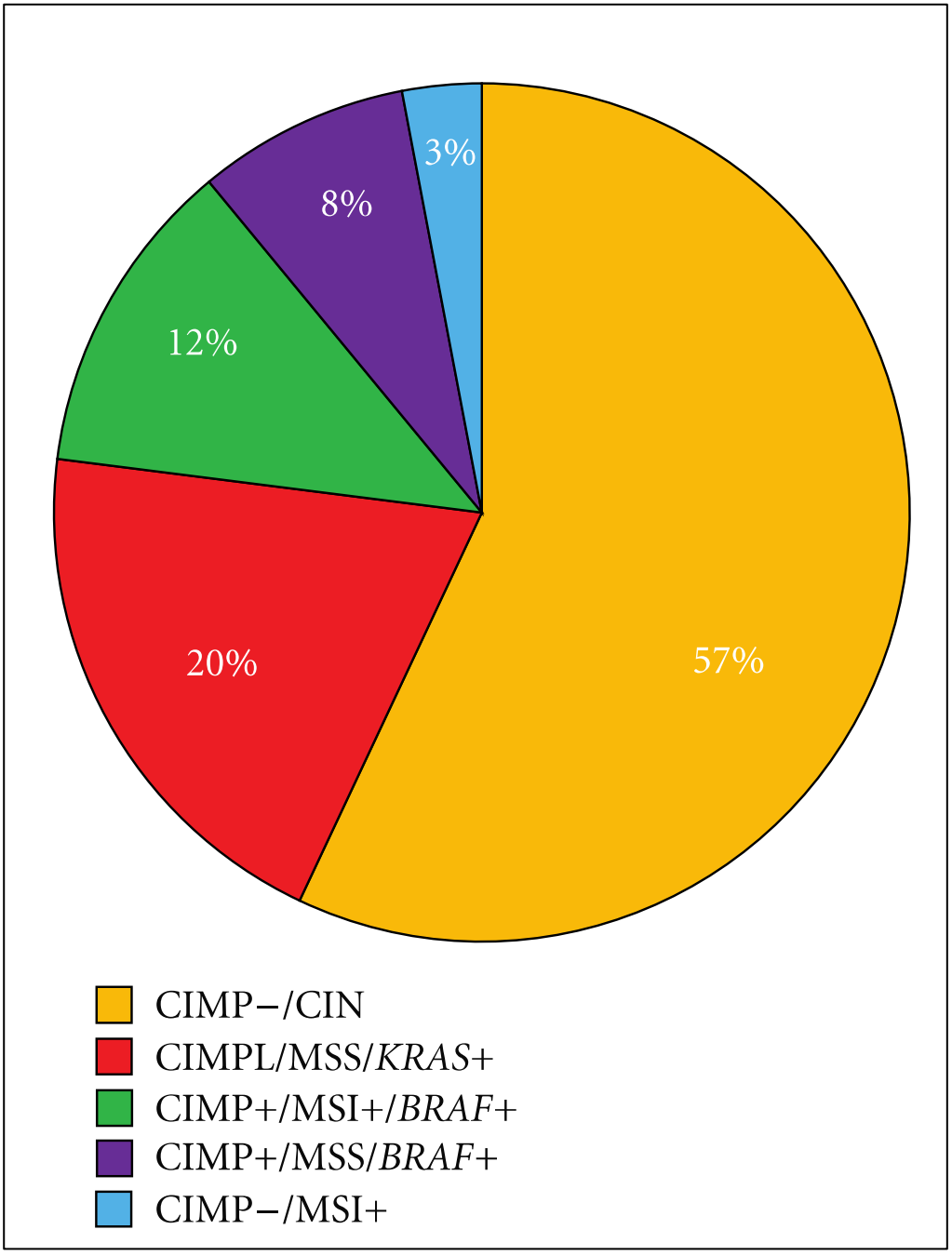


Figure 1-2 CRC classification in molecular subgroups
CRC is stratified based on genomic instability and presence or absence of the CpG Island methylator phenotype (CIMP). The approximate frequencies of each CRC subtype in the Western population are illustrated (Jass, 2007). Microsatellite instability (MSI); chromosomal instability (CIN); CIMP Low (CIMPL). microsatellite stable (MSS).

1.3.1 Chromosomal instability pathway (CIN)

CIN is the most common genetic defect. It has been reported in approximately 50 to 85% of all cases (Grady and Carethers, 2008b, Goel et al., 2007). CIN is recognised by aneuploidy and even structural alterations to chromosomes. It is usually assessed by DNA flow-cytometry (Walther et al., 2008). Mutation in the *APC* gene occurs early during the development of polyps. Kras mutations arise during the intermediate - late adenomas stage. p53 and deletion of 18q occur with the transition to malignancy. *SMAD2* and *SMAD4* are located on 18q, which contains the Deleted in Colorectal Cancer (*DCC*) gene. SMAD2 and SMAD4 are involved in the TGF-β signalling pathway (Figure-2) (Bellam and Pasche, 2010). It is well-established that CRC cases with CIN are associated with a much poorer prognosis (Pritchard and Grady, 2011). Deletion in chromosome 5, 18q, or 17p and gain in 8q, 13q, and 20q are frequently reported in CRC (Meijer et al., 1998b, Nakao et al., 2004). Amplification of chromosome 20 long arm has been reviewed in details later in section 1.6.

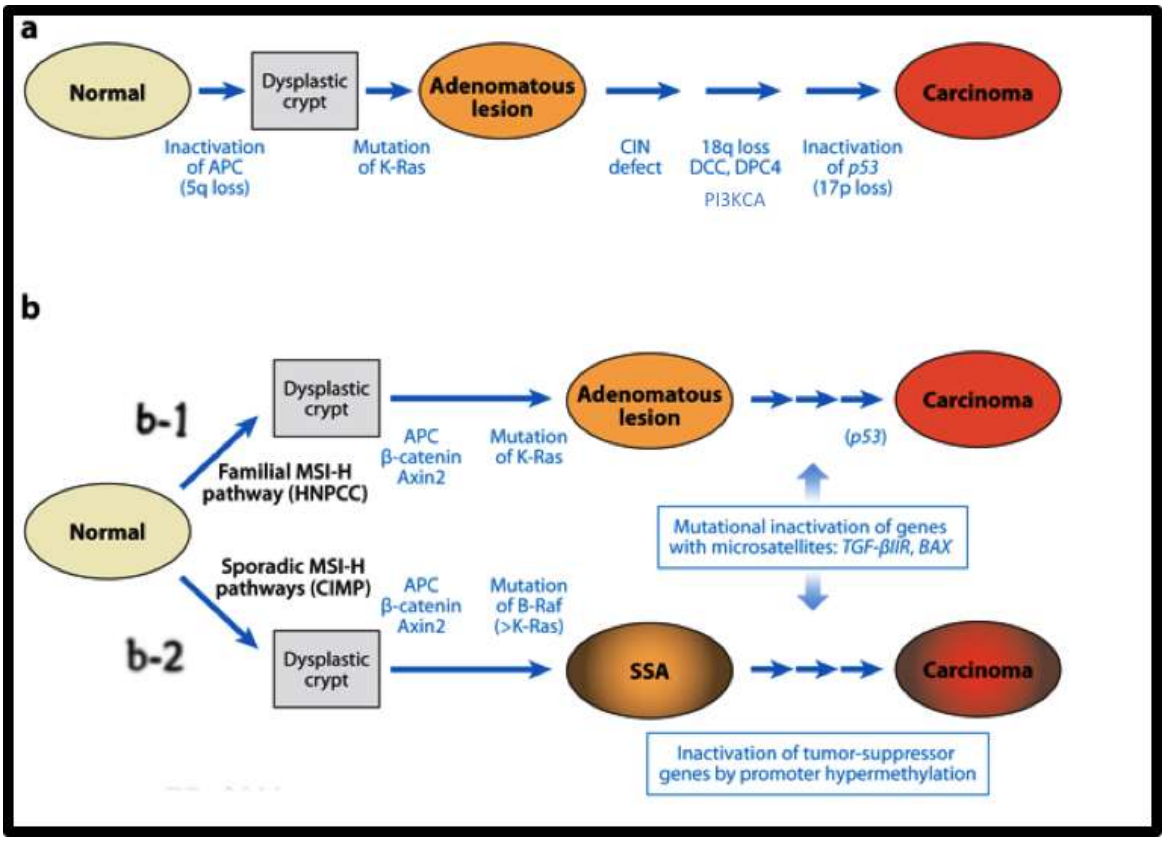


Figure 1-3 Genetic pathways of colorectal cancer (CRC)
(*a*) Most CRCs (50–85%) display CIN. (*b*) The minority of CRCs (15%) present high-frequency of microsatellite instability (MSI-H). (b-1) In familial (hereditary nonpolyposis colorectal cancer (HNPCC) syndrome) MSI-H tumours, patients carry germ-line mutations in one allele of one of the four main MMR genes and then somatic mutations (second hit) inactivate the remaining allele (b-2) in sporadic MSI-H tumours. Epigenetic changes generally lead to hypermethylation of the *MLH1* promoter. Presentation of sessile serrated adenomas (SSAs) through this pathway is common, together with other features such as the presence of hypermethylation in different genes and mutation of *BRAF* (Fearon, 2011b).

1.3.1.2 Wnt signalling pathway

APC is a tumour suppressor gene, which is located in chromosome 5 and plays a critical role in CRC development. Germline mutations in the *APC* gene cause FAP, which accounts for nearly 1% of all CRC cases (Lynch and de la Chapelle, 2003, Rustgi, 2007) and is characterized by the development of numerous adenomatous polyps in the gastrointestinal tract and early onset of CRC (Phelps et al., 2009). In addition, somatic mutations in *APC* were reported in 70–80% of sporadic CRC. Most of these mutations lead to the expression of a truncated APC protein (Kinzler and Vogelstein, 1996, Polakis, 2007, Segditsas and Tomlinson, 2006). Somatic *APC* mutations are reported with the same frequency in advanced adenoma, small adenoma, and carcinoma, suggesting that these mutations arise during the early stage of CRC (Polakis, 2007, Fearon and Vogelstein, 1990). Another point supporting this is that somatic mutations are reported even in microscopic adenomas with few dysplastic glands (Kinzler and Vogelstein, 1996). However, recent studies argued that the APC/β-catenin pathway is not necessarily the first genetic hit in CRC. A study reported that the frequency of *APC* mutation is 7% in flat tubular adenomas and 36% in polypoid tubular adenomas (Umetani et al., 2000). Other studies reported no *APC* mutation in dysplastic and non-dysplastic aberrant crypt foci (ACF) and no β-catenin accumulation in these lesions (Takayama et al., 2001).

The *APC* gene plays important roles in CRC by regulating the Wnt signalling pathway as well as by decreasing cell migration (Kroboth et al., 2007), cell adhesion (Faux et al., 2004), and apoptosis (Dikovskaya et al., 2007). The APC protein is regulating the β-catenin-dependent Wnt signaling pathway. Truncated APC protein results in a failure of the phosphorylation and destruction of β-catenin. Consequently, increase in the intracellular β-catenin levels results in the continuous activation of the Wnt pathway in CRC cells. β-catenin, subsequently, forms complexes with the T cell factor/lymphoid enhancer family (TCF/LEF) of DNA binding proteins. Next, this complex is translocated to the nucleus (Polakis, 2007, Aoki and Taketo, 2007). β-catenin activates the expression of many different genes which contain TCF DNA binding sites in key regulatory regions (Mosimann et al., 2009). Some of those genes are proto-oncogenes (CMYC (He et al., 1998)), gene encoding metalloprotease (MMP) 7 (Crawford et al., 1999),

and CD44 (Wielenga et al., 1999)), growth factors (fibroblast growth factor (FGF) 9 (Hendrix et al., 2006) and FGF20 (Chamorro et al., 2005)), and Wnt signalling pathway feedback regulators (AXIN2 (Lustig et al., 2002)).

1.3.1.3 Ras pathway

The Ras family (Rat Sarcoma) of G proteins (small GTP-binding proteins) plays a role at the molecular level, downstream of growth factor receptors (Malumbres and Barbacid, 2003). There are three members in the RAS family, Kirsten RAS (KRAS), Harvey RAS (HRAS), and neuroblastoma RAS (NRAS). Somatic mutations of these genes are reported in many human cancers (Malumbres and Barbacid, 2003). Most somatic mutations are observed in KRAS and are detected in nearly 40% of patients with CRC (Boughdady et al., 1992, Finkelstein et al., 1993). Most of the KRAS mutations are reported in codon 12/13 (located in exon 3) and other rare mutations are observed in codon 61 and codon 146. In patients with small adenomas (less than 1 cm), approximately 10% of the tumours contain KRAS mutations, while 40% of patients with larger adenomas (more than 1 cm) contain KRAS mutations (Vogelstein et al., 1988). This mutation occurs as intermediate - late in adenomas and results in an important growth advantage and clonal expansion (Klein and Stoecklein, 2009). In addition, the prevalence of KRAS mutation is higher in the late stage of cancer than during the early stage of cancer. This information supports the evolutionary concept in CRC progression. Although studies have shown that KRAS mutations are strongly associated with worst survival rates (González-Aguilera et al., 2004), the prognostic roles of KRAS mutations remain unclear. This may be associated with tumour heterogeneity. Therefore, studies designed to investigate the correlation between KRAS mutations and prognosis should avoid sampling error and should use only one cancer stage to avoid the heterogeneity effect in the statistical analysis.

An example of KRAS function in activating signalling from growth factor receptors is the epidermal growth factor receptor (EGFR) signalling pathway. The EGFR is stimulated by ligands such as epidermal growth factor (EGF). Ligand binding leads to dimerization and phosphorylation of the receptor, resulting in KRAS activation through adaptor molecules such as Grb2 and SOS, which stimulate the conversion of RAS from the GDP-bound form to the GTP-bound form. In turn, RAS activates root abundant factor (RAF), MAP kinase/ERK kinase (MEK), and

extracellular regulated MAP-kinase (ERK). Finally, translocation of ERKs to the nucleus leads to the transcription of genes involved in cell proliferation, differentiation, and apoptosis (Kolch, 2000).

1.3.1.4 PI3KCA

The *PI3KCA* gene encodes a protein (P110α) subunit that has a catalytic protein kinase domain. This subunit forms heterodimers with another protein (p85) subunit, which maintains the level of activity of P110α. It is activated by the upstream RTK (receptors tyrosine kinase) or RAS. In turn, it phosphorylates PIP2 (phosphatidylinositol 4,5 bisphosphate) at the third position of the inositol ring, which converts it into PIP3 (phosphatidylinositol 3,4,5-trisphosphate). PIP3 recruits 3-phosphoinositide-dependent kinase 1(PDK1) to the cellular membrane where PDK1 activates Akt, which phosphorylates different downstream proteins that affect cell cycle entry, cell growth, and survival (Zhao and Vogt, 2008). Somatic mutations in *PIK3CA* have been reported in 15–25% of patients with CRC, which reveals PIK3CA oncogenic role in CRC progression. Several studies indicated an increase in PIK3 activity in CRC (Phillips et al., 1998). Somatic mutations of this gene increase kinase activity, resulting in an increase in PIP3 production in tumours cells (Carson et al., 2008). However, amplification of *PIK3CA*, which is detected in a considerable percentage of CRCs, may also increase PIK3 activity (Vivanco and Sawyers, 2002b).

There is an interaction between the Ras and PI3K pathways in which activated RAS increases the activities of PI3K and vice versa (Rodriguez-Viciana et al., 1994, Rodriguez-Viciana et al., 1996). However, the mutant Kras protein is not very efficient in activating the PI3K signalling pathway (Li et al., 2004).

The phosphatase and tensin homolog (*PTEN*) gene, located on chromosome 10, encodes a protein that mediates the dephosphorylation of PIP3 to PIP2 (Chalhoub and Baker, 2009), thereby, reversing PIK3CA activity. Somatic mutations that inactivate PTEN are reported in only 10% of CRCs (Chalhoub and Baker, 2009, Danielsen et al., 2008), but other studies suggest that PTEN protein expression may be lost in 15–20% of CRCs (Laurent-Puig et al., 2009). Similar to *PIK3CA*

oncogenic mutations, *PTEN* tumour suppressor gene inactivation probably acts to enhance effects downstream of K-Ras protein via PIP3-mediated activation of AKT (Chalhoub and Baker, 2009).

1.3.1.5 18q LOH

LOH is located on chromosome 18q and observed in 60% of CRCs, specifically in 50% of late stage adenomas and 10% of early adenomas (Vogelstein et al., 1988, Fearon and Vogelstein, 1990). The18q deletion is associated with more aggressive clinical behaviour of CRCs. A region in the chromosome 18q contains several tumour suppressor genes such as Deleted in Colorectal Cancer (*DCC*), SMAD2 and SMAD4. The latter two are involved in the TGF pathway as downstream targets of the TGF β receptor in which phosphorylation of SMAD2 and SMAD3 allows proteins to traffic to the nucleus and form complexes with SMAD4 and this complex can then regulates gene transcription.

Somatic mutations that inactivate SMAD4 are reported in 10–15% of CRCs, and *SMAD2* mutations are reported in 5% of CRCs (Wood et al., 2007, Leary et al., 2008). Recently, mutations that inactivate SMAD3, located on chromosome 15, were reported in 5% of CRCs (Leary et al., 2008). Mutations in SMAD4 have also been shown to result in juvenile polyposis syndrome, which is also associated with CRC (Chow and Macrae, 2005).

1.3.1.6 P53

The *p53* gene is located on chromosome 17*,* which undergoes loss of heterozygosity in 70% of CRC cases (Fearon and Vogelstein, 1990, Vogelstein et al., 1988). Normally, p53 protein is involved in cell cycle checkpoints, promoting apoptosis and inhibiting angiogenesis by regulating the transcription of genes involved in these cellular processes (Vousden and Prives, 2009). It plays a crucial role in the transition from adenoma to carcinoma, in which the frequency of losing p53 functionality is gradually elevated during the adenoma-carcinoma sequence, which is 5–26% in early adenomas, 50% in late adenoma, and 70% in CRC (Pino and Chung, 2010). During the development of carcinomas, cancer cells undergo a variety of stresses such as hypoxia, DNA strand breakage, and cell cycle arrest.

The inactivation of p53 prevents proper responses to these stimuli and, consequently, enables the growth and invasion of tumour cells (Fearon, 2011b).

The *TP53* gene is thought to be the main target of 17p LOH because, in most CRCs with 17p LOH, the remaining *p53* allele carries a somatic mutation. Approximately 85% of the *p53* mutations in CRC are missense mutations, which mostly accumulate at codons 175, 245, 248, 273, and 282 (Baker et al., 1990). Few mutations are nonsense and frame-shift, which encode a considerable part of the *p53* open reading frame. In addition, it was reported that *p53* mutations or 17p LOH occur rarely in adenomas. In CRC, a small minority of patients present *p53* mutations without 17p LOH (Baker et al., 1990). Therefore, mutations of p53 and 17p LOH are associated with the adenoma to carcinoma transition.

1.3.2 Microsatellite instability (MSI)

Microsatellite instability is a common feature in several cancers such as gastric and ovarian cancer as well as CRC (Chiaravalli et al., 2001). Microsatellites are short repeat nucleotide sequences that are present throughout the whole genome. The mismatch repair (MMR) system contains at least seven different proteins (MLH1, MLH3, MSH2, MSH3, MSH6, PMS1, and PMS2) that form heterodimeric proteins. These heterodimers recognize and repair mismatch errors during DNA replication. Any mutations that reduce the efficacy of the MMR system would predispose to the development of MSI (Vilar and Gruber, 2010). Germline mutations in the MMR genes can also lead to MSI and can cause Hereditary Non Polyposis CRC (or Lynch syndrome) (Bellizzi and Frankel, 2009).

Promoter hypermethylation is another pathway that has been identified, which can also inhibit the MMR system by silencing the MMR genes. This seems to be the mechanism that underlies loss of MMR in sporadic MSI tumours. Specifically, a high degree of MLH1 promoter hypermethylation and consequent silencing of this gene has been noted in sporadic tumours with MSI (Auclair et al., 2011). Target genes for MSI are involved in various critical cell functions, including cell signaling, apoptosis, and DNA repair (Table 1).

The MSI pathway differs from the CIN pathway in that MSI cases display a normal karyotype with exceptional molecular genetic characteristics (Walther et al., 2009). Most research groups identify MSI as the presence of at least 30% unstable loci, present among a panel of five mononucleotide markers, BAT-25, BAT-26, NR-21, NR-24, and MONO-27, which are known to have a high sensitivity and specificity (Bacher et al., 2004). MSI positive tumours have also been subdivided into MSI-high (MSI-H) and MSI-low (MSI-L) depending on the quantitative differences in the degree of instability. Tumours with 10–29% unstable loci are designated as MSI-low. Patients with MSI positive tumours tend to have a better prognosis than those with CIN tumours (Guastadisegni et al., 2010, Sheffer et al., 2009b).

Although MSI CRC tumours have a distinct feature compared to the Microsatellite stability (MSS), there is an overlap between the two groups especially in the MSI-L group. This overlap may be due to the categorisation of MSI-L (Halford et al.,

2002), which is still questionable. Contradictory results have been published regarding the clinical and histological outcome between MSI-L and MSS cases (Kim et al., 2009, Wright et al., 2005). Therefore, these results may be explained by the use of a non-conclusive cut-off to distinguish between MSS and MSI–L cases. It could be argued that there is no convincing evidence showing molecular and physiological differences between CRC MSS and MSI-L. Thus, if the differences between features are minor; we may be able to only refer to MSI-H as MSI.

Table 1-2 Genes containing coding repeats that are targets for mutation in colorectal cancer with microsatellite instability. (Iacopetta et al., 2010)

Target genes for MSI are involved in various critical cell functions including cell signaling, apoptosis, and DNA repair Their mutation is believed to drive the oncogenic process through positive selection.

Function, *gene*	**Mononucleotide coding repeat**	**Frequency of mutation (%)**	**Function, *gene***	**Mononucleotide coding repeat**	**Frequency of mutation (%)**
DNA repair			Signal transduction		
MSH3	(A)	38	*TGFβRII*	(A)	81
MSH6	(C)	22	*ACTRII*	(A)	58
Apoptosis			Cell cycle		
BAX	(G)	45	*PTEN*	(A)	18
Caspase-5	(A)	48	*RIZ*	(A)	27

1.3.3 CpG Island Methylator Phenotype (CIMP)

The CIMP pathway accounts for about 15% of all sporadic CRCs, making it the second most common pathway, resulting in the malignant transformation of colonic tissue (Boland et al., 2009). It is characterized by epigenetic silencing of tumour suppressor genes by hypermethylation of the promoters and a co-existent global DNA hypomethylation (Kim et al., 2010). These promoters, which contain CpG islands (cytosine–guanosine), are exposed to hypermethylation at different levels, which are mainly determined by specific DNA sequences (Feltus et al., 2006). The exact molecular mechanisms underlying the promoter hypermethylation-induced silencing of genes and the global DNA hypomethylation is yet to be fully understood.

The role of CIMP in sporadic CRCs was identified when a group detected abnormal methylation pattern in several Tumour suppressor genes such as *TSP-1* and *IGF2*. There was a significant association of MSI tumour with CIMP (Ahuja et al., 1997).

It has been shown that 38% of non-MSI tumours are CIN negative (Goel et al., 2003, Fadhil et al., 2014, Silver et al., 2012). This subset of tumours underwent further investigation, revealing that the vast majority are associated with CIMP and BRAF V600E mutation (Weisenberger et al., 2006). In addition, CIMP is correlated with MSI, but not with LOH (Goel et al., 2007). Consequently, MSI is associated with CIMP in sporadic cases or Lynch syndrome in familial cases.

DNA methylation occurs early in the adenoma-carcinoma sequence. Thus, it can be used as a marker for CRC screening. Promoter methylation of p16 is aberrant in premalignant colonic adenomas (Rashid et al., 2001). Another study reported that the degree of aberrant methylation of MGMT, a DNA repair gene, increases throughout the normal to adenoma-carcinoma sequence (Nagasaka et al., 2008).

With regard to pharmacogenetic targeting, the reversibility of DNA methylation has attracted the interest to produce drugs that inhibit methylation in affected genes in tumours, thereby, restoring the activity of these genes. For example, azacitidine and decitabine are recognized as methylation inhibitors (Stresemann and Lyko, 2008)

1.4 Genetics of liver metastasis

CRCs are molecularly and clinically heterogeneous. The different oncogenic mechanisms confer differential clinical phenotypes and possible variability in survival (Sanchez et al., 2009). As the primary CRC lesions, the metastatic CRCs show molecular and genetic diversity and the type of genetic alterations may indicate the site and route of metastasis (Messick et al., 2009). Among patients with CRC who die of advanced carcinoma, 60 to 70% show liver metastasis. In non-resectable CRC liver metastases, the overall survival is only 2 years even with the use of targeted drugs. Moreover, only 30% of patients with resectable liver metastasis have an overall survival of 5 years and approximately 20% survive for 10 years. Decisions regarding hepatic surgery for patients with CRC who have developed liver metastasis relies whether adequate liver preservation can be ensured. Thus, early detection of liver metastases may help in more conclusive surgery and this will lead to long term survival (Abdel-Misih et al., 2009b).

As described earlier, different molecular mechanisms are involved in CRC tumorigenesis. However, further adaptions are required for the acquisition of metastatic capability. Colorectal liver metastasis is a complex process, which includes different steps such as the detachment of tumour cells, invasion, and migration through the stroma. Cells intravasate into lymphatic or venous vessels, and, in the latter case, they travel through the portal vein system. They extravaste into the liver, form micro-metastasis, and expand to macro-metastasis (Kawada et al., 2011). Thus, different cellular adaptions are essential for the metastatic capability and it would be expected that the expression of some tumour suppressor genes and oncogenes is significantly altered to drive the metastatic spread. Thus, understanding the molecular and cellular mechanism that causes CRC liver metastasis is important for early detection and therapeutic strategies.

Many genes located in 20q may be associated with CRC metastasis because they are functionally relevant to the molecular mechanism of metastasis. For example, *PTGIS*, encoded by a gene located on 20q, is an enzyme that catalyses prostaglandin H2 to PGI2 conversion. PGI_2 prevents apoptosis, thereby supporting the growth of CRC (Cutler et al., 2003). It has been reported that intracellular PGI2 activates nuclear receptor PPARdelta, which is a downstream target of the APC/β-

catenin pathway. This may contribute to CRC progression and angiogenesis (Park et al., 2001b). In patients with CRC who developed liver metastasis, *PTGIS* is highly expressed when compared to patients with CRC without metastasis. This overexpression is associated with liver metastasis and poor prognosis (Lichao et al., 2012b). These genes have not been studied in CRC cell lines. Studying the functional relevance of this gene may provide a better understanding of the mechanism underlying CRC metastasis. There are other proteins, which have also been reported in CRC liver metastasis. The E cadherin/α-catenin complexes , maintain the adhesion of tumour cells to each other. Downregulation of E-cadherin in favour of N-cadherin (known as the “cadherin switch”) is associated with epithelial - mesenchymal transition (EMT), which is involved in migration and stromal invasion (Kang and Massagué, 2004). In CRC, it has been reported that the expression of E-cadherin/α-catenin is low and it has been linked to high expression of β-catenin (Delektorskaia et al., 2005, Hayashida et al., 2005). This phenomenon is associated with metastatic potential and poorer prognosis (Raftopoulos et al., 1998). The epithelial cell adhesion marker (EpCAM) is highly expressed in CRC (Xie et al., 2005) and is involved in modulating cadherin mediated cell-cell interactions (Litvinov et al., 1997), in which it is associated with downregulation of cadherin levels (Winter et al., 2003). Thus, EpCAM may be involved in EMT.

During the invasion step, proteinases, which are produced by cancer cells or fibroblasts, degrade the basal membrane and ECM components and enable cells to detach from the primary site. Several enzymes are involved in degradation such as MMPs, plasminogen, and cathepsins. MMP7 (Matrylysin) belongs to the MMPs family. It is a proteolytic enzyme, which, in its activated form, binds to the tumour cell surface (Leeman et al., 2003). It has been reported that *MMP7* is overexpressed in CRC and its expression is associated with invasion and liver metastasis (Ishikawa et al., 1996). MMP7 degrades the membrane, allowing the cells to invade. It, also, promotes invasion by activating other MMPs. Another point is that MMP2 and MMP9 may be involved in CRC liver metastasis, as both have been observed in the stroma of both primary CRC and liver metastases (Mc Donnell et al., 1999).

In metastasis, angiogenesis is involved in regulating metastatic tumour cells outgrowth. Vascular endothelial growth factor (VEGF) is an important angiogenic stimulator. High expression level of VEGF-A is associated with poor prognosis in patients with CRC (Takahashi et al., 1995). Angiogenesis inhibitors can regulate liver metastasis growth. These inhibitors, including angiostatin, endostatin, and thrombospondin-1 (TSP-1), are secreted in CRC primary and metastatic cells (Maeda et al., 2001).

Once micro-metastasis is established in the liver, it needs growth factors in order to grow. It is likely that growth factor receptors are involved in the growth of CRC metastatic tumour cells. EGFR overexpression has been reported in a significantly high proportion of metastatic CRC. This is linked to more aggressive tumour and liver metastasis (Italiano et al., 2005). However, using immunohistochemistry to study EGFR expression did not allow the detection of an association between liver metastases and EGFR expression level (Kountourakis et al., 2006).

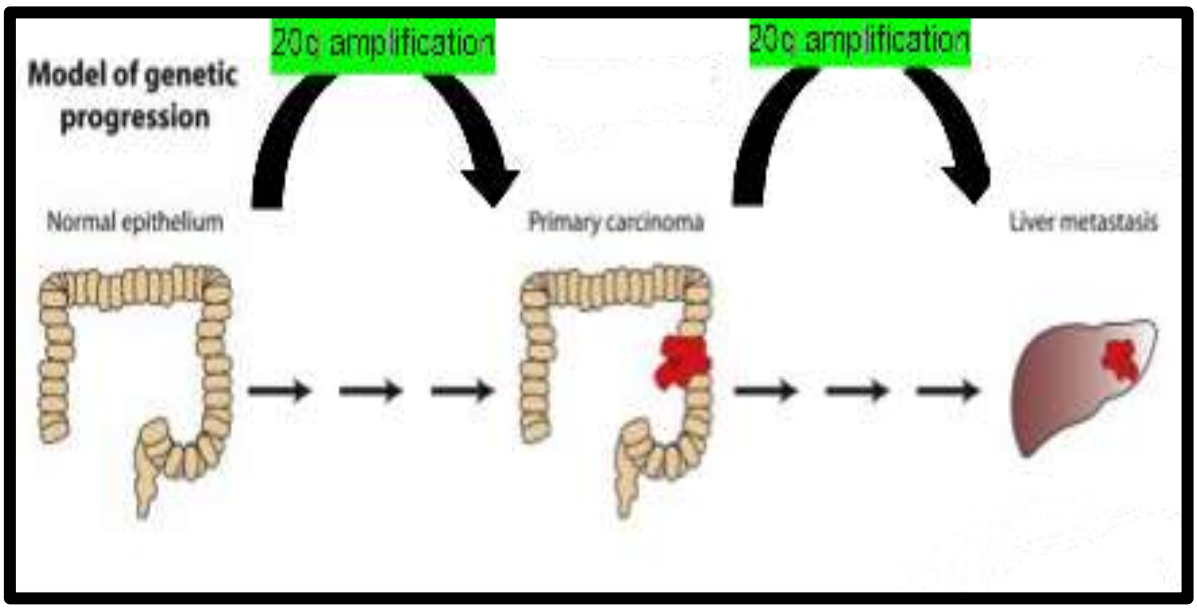


Figure 1-4 Model of the 20q time of occurrence in colorectal cancer

(Diep et al., 2006b).

1.5 Genetics implication in CRC treatment

CRC treatments have been improved in the last decade, particularly with the development of targeted therapies. Cetuximab is a monoclonal antibody that binds to the EGFR, consequently inhibiting tumour growth, invasion, angiogenesis, and metastasis. Some patients respond to the drug, while others do not. Genetic analysis revealed that 20–40% of patients with wild-type *KRAS* respond to the drug, whereas patients with mutant *KRAS* are resistant (Lièvre et al., 2008). However, some patients with wild-type KRAS do not respond to the drug, and further analysis reported that those patients carry a mutation in *BRAF* and possibly other genes (Laurent-Puig et al., 2009). Therefore, comparing the genetic alteration at the DNA and RNA levels could provide an explanation of the mechanism behind therapy resistance. Approaches could be used in order to compare genetic variations, comparing the expression profile of patients responding with patients not-responding by microarray analysis, and comparing the DNA copy number between these patients using CGH technology and SNP microarray. These approaches may allow us to identify genes that play a role in treatment resistance and use them as biomarker like KRAS mutation status for the anti-EGFR therapy.

1.6 20q amplification

Many studies have shown that chromosome 20 is frequently amplified in primary and liver metastasis tumour cells. In 1999, Meijer *et al.* used comparative genomic hybridization (CGH) in colorectal adenomas and carcinomas in order to study the gains and losses of chromosomes (Table 1-3). Regarding chromosome 20, the incidence of 20q gain in carcinomas compared with adenomas was 42%, which indicates that 20q may be involved in CRC progression from adenoma to carcinoma (Meijer et al., 1998b). De Angelis et al. reported that 20q gain in CRC cases was present in 67% of sporadic CRCs cases (De Angelis et al., 1999b). Rooney *et al.* performed CGH on micro-dissected tissues from patients with CRC and determined that gain of 20q accounts for 27.6% of cases. Moreover, this gain of 20q is observed in CRC cell lines such as R10 and HT29 (Rooney et al., 2001b). Recently, the 20q amplification was confirmed using SNP-Microarray (Sayagués et al., 2010b, Jasmine et al., 2012b, Andersen et al., 2007b). Analysis of DNA copy number changes at the gene level by multiplex ligation-dependent probe amplification showed that, in patients with CRC, 20q13, and 20q11 are frequently amplified (Postma et al., 2005b).

Recent GWAS (Genome-wide association study) of colorectal cancer has described six new susceptibility loci reaching a genome-wide threshold (Schumacher et al., 2015). In other word, presence of one of these loci increased the risk of developing CRC. One of these loci is rs6066825 that is located at 20q13(Schumacher et al., 2015). This SNP (single-nucleotide polymorphism) lies within an intron of the PREX1 gene, which we investigated this gene in more detail in this thesis1.1.1.1 (section1.6.3). Meta-analysis of GWAS studies has also identified susceptibility loci (rs4925386) located at 20q13 (Houlston et al., 2010). In summary, 20q amplification has been confirmed by different techniques and different sample sets, especially in sporadic CRC specimens. 20q amplification, also, occurs during the early stage of the adenoma-carcinoma sequence (Tabach et al., 2011). It has been suggested that genes located in this region may drive the progression from adenoma to carcinoma (Sillars-Hardebol et al., 2011b, Carvalho et al., 2009).

Table 1-3 List of studies previously carried out examining amplification of chromosome 20 in the context of colorectal cancer and liver metastasis.

List of studies previously carried out examining amplification of chromosome 20 in the context of colorectal cancer and liver metastasis. This list reported the study of chromosomal instability of CRC primary and secondary. In this table, we reported the method used for studying chromosomal aberration and summary of finding in research finding. Abbreviation: array Comparison Genomic Hybridisation (aCGH), Fluorescence in situ hybridization (FISH), Multiplex Ligation-dependent Probe Amplification (MLPA), Single nucleotide polymorphism array (SNP array), Genomic-wide association study (GWAS).

	Method	Finding
Meijer et al., 1998b	CGH	Increased number of chromosomal gains of 20q, involves in the progression of adenomas to carcinomas
, Korn et al., 1999b	CGH	27 liver metastases and 6 synchronous primary tumors. Amplification of 20q is found in 85% of the cases. colorectal metastases show chromosomal changes similar to those that have been reported for primary tumors
(De Angelis et al., 1999b)	CGH	Forty-five sporadic colorectal carcinomas show 20q amplification in 67% of cases. This amplification is associated with High tumour S phase fractions.
Parada et al., 1999	CGH	This study shows that 20q is frequently amplified in CRC primary and liver metastasis
Hidaka et al., 2000b	FISH	Amplification of the 20q13.2 region is investigated in 17 nonmetastatic colorectal cancers 18 primary CRC tumours with liver metastasis, and 18 metastatic lesions. The frequency of 20q amplification is higher in primary and liver metastatic lesions of CRC than in CRC lesions without liver metastasis
Aragane et	CGH	DNA copy number of 30 primary colorectal cancers

al., 2001b		and 16 liver metastases are screened. The incidence of liver metastases is higher in patients with primary colorectal cancer with 20q amplification.
Aust et al., 2004	FISH	Amplification of 20q13.2 is found in 78 cases (53%). Cases with gains on 20q13.2 shows worse outcome than cases without: the gain of 20q13.2
Postma et al., 2005b	CGH and MLPA	In both adenomas and carcinomas, high frequencies of 20q gain is found (83% and 92%, respectively)
Diep et al., 2006b	Meta-analysis of 31 CGH studies	Meta-analysis of data obtained from 31 comparative genomic hybridization (CGH) studies comprising a total of 859 CRCs conclude that 50% of primery CRC with 20q amplification and 75% of liver metastesis with 20q amplification
Andersen et al., 2007b	SNP arrays	The analysis shows genes in regions with increased copy number in 20q and these genes are predominantly upregulated
Carvalho et al., 2009	aCGH	Chromosome 20 is the most frequently altered in the progressed adenomas and carcinomas (in >60% of cases).
Sayagués et al., 2010b	SNP-Microarray	23 primary tumours from sporadic CRC patients who had developed liver metastasis. Amplification of 20q is the most frequent event (87%)
(Houlston et al., 2010)	Meta-analysis of three GWAS studies	CRC risk loci association is identified in rs4925386, which is located at 20q13.

Bruin et al., 2010b	aCGH	CRC patients who subsequently developed liver metastasis show frequent 20q amplification.
Jasmine et al., 2012b	SNP array	Paired (tumour and surrounding healthy) fresh frozen tissue from 86 CRC patients shows frequent amplification of 20q
Munoz-Bellvis et al., 2012	SNP array	An increased frequency of genetic lesions of chromosome 20 have been associated with metastatic colorectal. However, acquisition of new chromosomal abnormalities but not chromosome 20
Schumacher et al., 2015	GWAS	Association study with 18,299 cases of colorectal cancer and 19,656 controls shows CRC risk loci rs6066825, located at 20q13

Regarding CRC liver metastasis, one of the genetic alteration on metastatic cells is the chromosomal amplification and deletion (Table 1-3). Various studies have compared the genetic differences between CRC primary tumours and metastases at the DNA copy number and expression level. These studies reported an association between chromosomal abnormalities and CRC liver metastasis (Diep et al., 2006b, Hidaka et al., 2000b, Aragane et al., 2001b, Aust et al., 2004, Korn et al., 1999b). Other studies reported gene expression profiles for patients with CRC, but these studies only identified a few common genes (Arango et al., 2005, Eschrich et al., 2005, Wang et al., 2004). Regarding the chromosomal abnormalities, patients with CRC who develop liver metastasis tumour are reported to have 20q gain (Table **1-4**). CGH investigation by Korn *et al.* reported the occurrence of 20q gains (85%) in liver metastatic CRC specifically at 20q13.1 and 20q13.2 sub-bands (Korn et al., 1999b). In addition, fluorescence *in situ* hybridization (FISH) analysis conducted by Nanashima *et al.* indicated 20q gains in patients with CRC which had liver metastases (Nanashima et al., 1997b). Parada *et al*. compared the cytogenetic patterns of primary and liver metastatic CRC and reported the same result (Parada et al., 1999). Hidaka *et al.* also identify the 20q.13.2 sub-band amplification more frequently in primary CRC and liver metastases when compared to CRC without liver metastasis using FISH (Hidaka et al., 2000b). Aragane *et al.* reported gain in 20q in primary CRC (63%) and in metastatic CRC (81%) (Aragane et al., 2001b). Other recent studies also showed the gain of 20q and its correlation with CRC liver metastases using either High-Resolution SNP Array or CGH techniques (Sayagués et al., 2010b, Bruin et al., 2010b). 20q amplification is confirmed since different studies have replicated the results using different techniques in different sample series. However, the functional role of genes located in the 20q region that is highly amplified in CRC has not been studied.

Table 1-4 Frequency of the alterations in primary carcinomas and liver metastases at the chromosome band level.

Meta-analysis study of 31 Comparison Genomic Hybridisation (CGH) of primary CRC and liver metastasis shows the amplification frequency of 20q amplification (Diep et al., 2003).

	Losses		Gains	
Chromosome band	Primary carcinomas (n = 720)	Liver metastases (n = 139)	Primary carcinomas (n = 720)	Liver metastases (n = 139)
20q11	3%	0%	49%	72%
20q12	3%	1%	50%	73%
20q13	3%	1%	50%	75%

There are different genes located on 20q, which are reported to drive CRC progression (Table 1-5). Aurora A kinase (AURKA) is located on 20q13 and plays a role in the regulation of mitotic spindle formation. In addition, it is involved in regulating several important signaling pathways such as p53 and c-Myc (Katayama et al., 2004, Yang et al., 2004). AURKA and TPX2 are co-expressed at the DNA, mRNA, and protein levels. Knocking down both genes in CRC cells was recently shown to affect several processes such as invasion, anchorage-independent growth, and cell viability. AURKA and TPX2 promote 20q gain-driven colorectal adenoma-to-carcinoma progression (Sillars-Hardebol et al., 2011b) The Chromosome segregation 1-like (*CSE1L*) gene is located on 20q and is amplified in CRC specimens. CSE1L is a nuclear transport factor involved in chromosome segregation and in protein transportation from the cytoplasm to the nucleus (Kau et al., 2004). CSE1L gene affects cell viability and anchorage- independent growth (Sillars-Hardebol et al., 2011b). Alnabulsi *et al*. studied the effect of CSE1L in CRC cell lines and concluded that it affects apoptosis, cellular adhesion, and invasion (Alnabulsi et al., 2012). Overexpression of CSE1L has been linked to CRC tumour progression (Sillars-Hardebol et al., 2012b). Death-inducer obliterator 1 (DIDO1) is a tumour suppressor gene and early apoptosis regulator in other cancers. DIDO1 disruption can result in chromosomal instability. An *in vitro* study showed that DIDO1 affects anchorage-independent growth (Sillars-Hardebol et al., 2011b). Further functional analysis of this gene may clarify its role in CRC development.

BCL2L1, located on 20q, belongs to the family of Bcl-2 proteins. This protein family plays a role in the regulation of the mitochondrial pathway of apoptosis. There are two splice variants of BCL2L1, an anti-apoptotic (Bcl-x_L) and a pro-apoptotic (Bcl-x_S) splice variant. BCL2L1 is overexpressed in CRC (Krajewska et al., 1996). This overexpression (Bcl-xL) may lead to apoptosis resistance, which was linked to the development of tumour metastasis. Recently, BCL2L1 was reported to increase cell viability and anchorage-independent growth of CRC cell lines, but not invasion (Sillars-Hardebol et al., 2012a).

Table 1-5 List of candidate genes located at chromosome 20.

The candidate genes were chosen from the aCGH data. These genes showed highest amplification value. Furthermore, these genes functional role is associated with cancer progression. Some of these genes studied in CRC has shown controversial results and needs reinvestigation. Other genes have not been studied in CRC cells.

Gene	Function	Role in CRC
ADNP	**transcription factor**	**unknown**
AURKA	**Regulation of chromosome segregation**	**Oncogene (Sillars-Hardebol et al., 2011b)**
BCL2L1	**Apoptosis**	**Oncogene (Sillars-Hardebol et al., 2012a)**
CD40	**Apoptosis**	**Controversial role (Georgopoulos et al., 2007).**
CSE1L	**Regulation of chromosome segregation**	**Oncogene (Alnabulsi et al., 2012).**
DIDO1	**chromosomal instability**	**Oncogene (Sillars-Hardebol et al., 2011b)**
ELMO2	**Cell motility and inavsion**	**Unknown**
MMP9	**Invasion**	**Unknown**
PREX1	**Cell motility and invasion**	**Unknown**
PTGIS	**Protein expression associated with liver metastasis**	**Unknown**
PTPN1	**Proliferation and cell motility**	**Controversial role(Chen et al., 2014)**
SNAI1	**Transcription factor**	**Oncogene (Kwon et al., 2015)**
SRC	**Control several pathways**	**Oncogene (Sillars-Hardebol et al., 2011b)**
TPX2	**Regulation of chromosome segregation**	**Oncogene (Sillars-Hardebol et al., 2011b)**

In this thesis, five genes were studied in CRC cell lines (functional role)and tissue (for protein expression). The next sections (1.51.-1.5.3) would give review on the genes and their protein. Genes role in CRC and/or to other tumours, and justification of chosen these genes in our study.

1.6.1 Tyrosine-protein phosphatase non-receptor type (*PTPN1*)

PTPN1 gene is located on chromosome 20q13.13. It encodes for a protein that consists of 435 amino acid residues and is 50 kDa. PTPN1 protein has an N-terminal catalytic domain, an intervening region containing two proline-rich motifs, and a hydrophobic C-terminal (Figure 1-5). The C-terminal helps membrane localisation, which tethers the enzyme to face the endoplasmic reticulum (ER) (Frangioni et al., 1992). PTPN1 location at the ER surface may restrict its access to substrates. There are several mechanisms to control PTPN1 activities (Yip et al., 2010). The proline-rich motifs act as binding sites for p130Cas, Grb2, and Crk proteins (Liu et al., 1996).

Tyrosine kinases play an important role in signalling pathways that affect several physiological processes. In tumour, tyrosine kinases are hyper-activated. This hyper-activation increases the activation of downstream signalling cascade, which leads to the promotion of malignancy in humans. Tyrosine kinases are classified in two groups, (1) non-receptor tyrosine kinases and (2) receptor tyrosine kinases. Protein tyrosine phosphatase, non-receptor type 1 (*PTPN1*) is a non-transmembrane protein tyrosine phosphatase 1 (Sastry and Elferink, 2011). It has been involved in several physiological processes such as cell survival, proliferation, and motility (Scott et al., 2010, Julien et al., 2011).

The role of PTPN1 in tumours remains unclear despite evidence suggesting that PTPN1 can show both tumour suppressing and tumour-promoting effects (Lessard et al., 2010). On one hand, a wide range of receptor tyrosine kinase (RTK) signalling pathways are suppressed by PTPN1, including Met, EGFR, and platelet derived growth factor (PDGF) receptor (Stuible and Tremblay, 2010, Stuible et al., 2010). Knockdown and overexpression of PTPN1 in *in vitro* studies suggest the direct dephosphorylation of activated Met and EGFR. In transformed mouse fibroblasts, PTPN1 overexpression diminishes the tumorigenic feature (Brown-Shimer et al., 1992, Stuible et al., 2010). Moreover, PTPN1 can promote apoptosis

by facilitating caspase activities (Lessard et al., 2010, Akasaki et al., 2006) or downregulation of pro-survival signalling (González-Rodriguez et al., 2007, Sangwan et al., 2006). Furthermore, p53 and PTPN1 double knockout mice exhibit an increase in B cell lymphoma and decreased survival compared to p53 only knockout mice (Dubé et al., 2005).

On the other hand, there is evidence suggesting that PTPN1 might play a role in tumorigenicity. PTPN1 overexpression is associated with tumour growth in CRC cell lines (Zhu et al., 2007). PTPN1 overexpression is associated with tumour progression in CRC tissues (Chen et al., 2014). Cellular adhesion to the extracellular matrix (ECM) is an important factor in the migration and invasion of cells. Binding of integrins (a family of cell-surface transmembrane proteins) to the ECM leads to activation of C-SRC and other protein tyrosine kinases (). In breast and colon cancer cell lines, PTPN1 dephosphorylates the C-SRC inhibitory site, which retains C-SRC in its active form (Zhu et al., 2007, Bjorge et al., 2000). Furthermore, in both carcinoma and lymphoma cell lines, PTPN1 is able to block anti-tumour signalling pathways (Lu et al., 2008). Moreover, PTPN1 overexpression was reported in ovarian carcinoma (Lu et al., 2008) and squamous cell carcinoma (Nanney et al., 1997). In addition, PTPN1 is important in CRC. *PTPN1* is located on chromosome 20q13.13, a region frequently amplified in CRC and other cancers. Therefore, we investigated PTPN1 functional activities in CRC cell lines to confirm PTPN1 role in CRC progression.

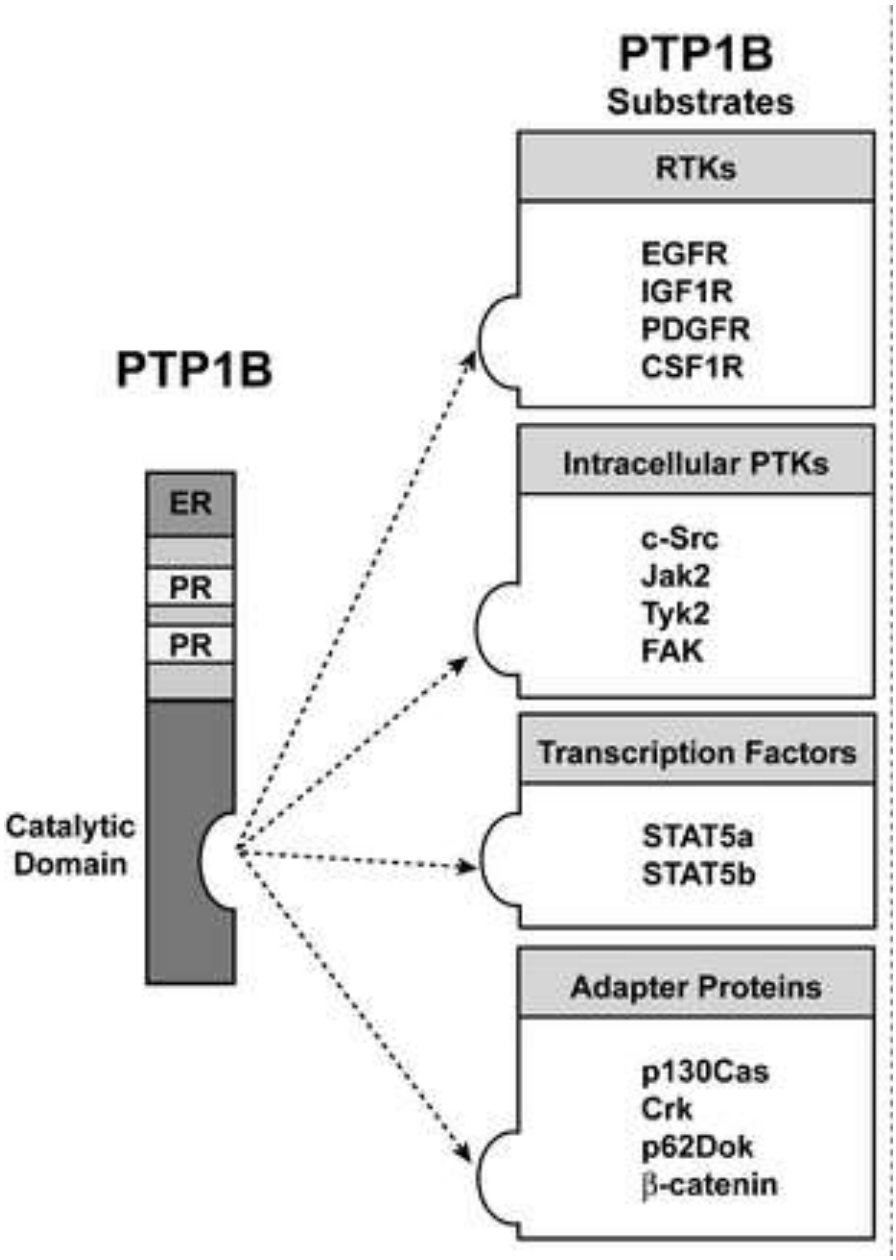


Figure 1-5 Structural domains of PTPN1.
Schematic representation of the structure of PTPN1 and its respective substrates linked to cancer. PTP1B contain similar N-terminal catalytic domains. PTP1B C-terminus localises on the endoplasmic reticulum (ER). It also contains two central proline-rich motifs (PR). RTKs Receptor tyrosine kinases (Stuible et al., 2008).

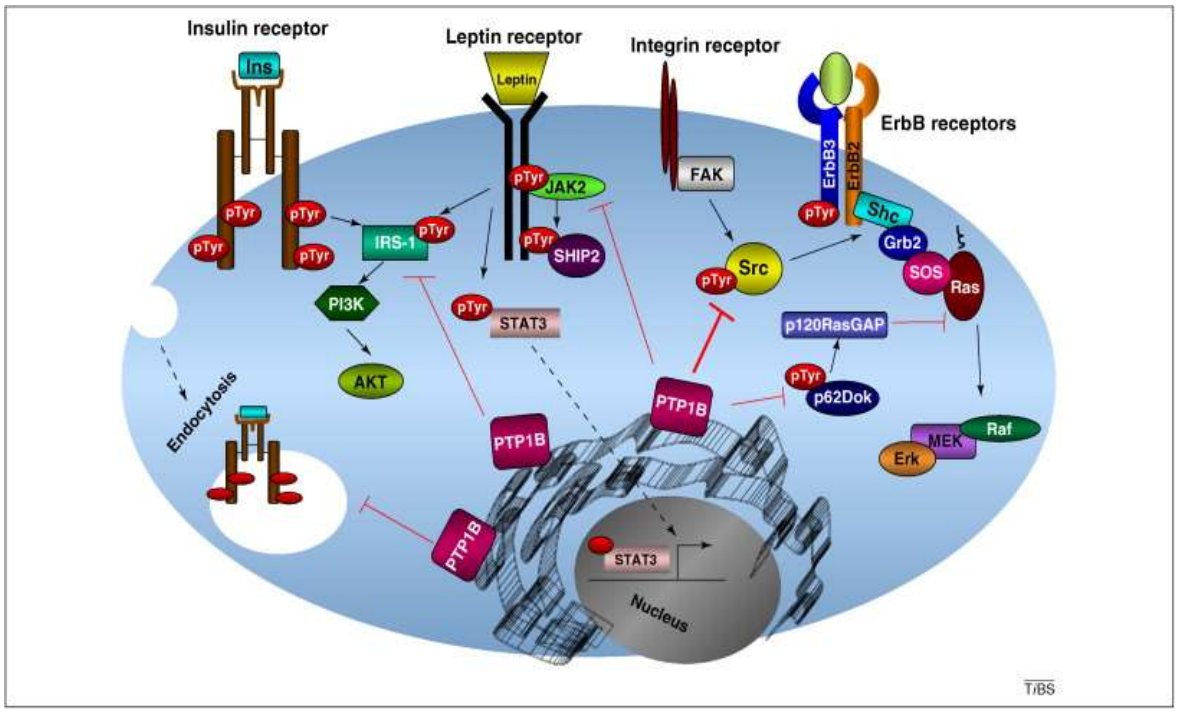


Figure 1-6 Oncogenic signaling of PTPN1.
PTP1B exerts a positive role in ErbB2 (Neu)-induced tumorigenesis. Insulin stimulation is followed by autophosphorylation and activation. Consequently, tyrosine phosphorylation of insulin receptor substrate-1 (IRS-1) leads to phosphatidyl-inositol 3 kinase (PI3K) and AKT activation. The leptin receptor promotes the recruitment and tyrosine phosphorylation of JAK2, which facilitates the activation of STAT3-mediated transcription. JAK2-STAT3 is also known as a target of PTPN1. PTPN1 dephosphorylates $p62^{Dok}$, which inhibits $p120^{RasGAP}$. Consequently, this process activates Ras-MAPK-mediated cell proliferation. Similarly, PTPN1 dephosphorylates Src at the inhibitory site (Y530), allowing the activation of small GTPases such as Ras and Rac (Yip et al., 2010).

1.6.2 Cluster of differentiation 40 (CD40)

CD40 is a member of the TNF receptor (TNFR) superfamily member. Its gene maps to chromosome 20q13.12 and encodes a 277 amino acid protein of 45–50 kDa. CD40 protein consists of a large extracellular domain containing 193 amino acids, a 22 amino-acid leader sequence, and a 66 amino-acid intracellular domain in humans. There are 22 cysteine residues in the CD40 extracellular domain that are conserved between the members of the TNFR superfamily (van Kooten and Banchereau, 2000). The intracellular domain of CD40 protein lacks intrinsic kinase activity. It largely signals through the recruitment of adaptor proteins of the TNF receptor associated factors (TRAF) family (Tsukamoto et al., 1999). CD40 expression was initially identified on the surface of B cells and on dendritic cells (DCs), platelets, monocytes, and macrophages. Interestingly, it is also expressed by non-hematopoietic cells such as fibroblasts, epithelial, and endothelial cells (Banchereau et al., 1995, van Kooten and Banchereau, 1997). The isolation of the ligand for CD40 (CD40L/CD154), was achieved in 1992. It is predominantly expressed in activated T cells (Armitage et al., 1992). CD40L is a type II transmembrane protein, which presents a variable molecular weight of 32–39 kDa due to post-translation modifications (van Kooten and Banchereau, 2000). Its extracellular domain consists of a β-sheet, α-helix loop, and a β-sheet(Karpusas et al., 1995).

The widespread expression of CD40 in haematological and solid tumours suggests that this receptor may play a role in carcinogenesis. CD40 plays a controversial role in cancer development as a tumour suppressor or oncogene. In follicular lymphoma, CD40, once activated by its ligand CD40L can stimulate proliferation by rendering the cells resistant to apoptosis (Johnson et al., 1993). In different haematological tumours, *in vitro* ligation of CD40 on the surface of the non-Hodgkin's lymphoma, Burkitt's lymphoma, and chronic lymphocytic B-cell leukaemia cells showed tumourigenic effects by inhibiting apoptosis (Kitada et al., 1999). CD40-CD40L interaction was disrupted by CD40L-neutralising antibodies and this activity resulted in the suppression of B cell malignant growth (Pham et al., 2002). A similar CD40 activity was detected in breast and kidney cancer (Bussolati et al., 2002, Tong et al., 2001). In human lung carcinoma, CD40 expression was studied in both cell lines and clinical samples. Its expression is

associated with the metastatic spread of lung cancer (Sabel et al., 2000). Furthermore, the expression of both CD40 and CD40L has been reported to increase proliferation and cell motility in primary renal carcinoma (Bussolati et al., 2002). An *in vivo* study showed that constitutive CD40 signaling exerts transforming activity. This transforming activity may occur due to selective activation of MAPKs, JNK, the non-canonical NF-κB pathway, and Erk (Homig-Holzel et al., 2008).

However, other studies have indicated that CD40 induces apoptosis or has anti-proliferative effects in haematological and non- haematological tumours (Dallman et al., 2003). The anti-cancer effect of CD40 ligation has been proposed as a potential therapeutic approach by using CD40 agonistic antibodies (Vonderheide and Glennie, 2013).

Interestingly, the physiological responses to CD40 activities are variable and may depend on the cellular context of the receptor and its ligand (CD40/CD40L) (Eliopoulos and Young, 2004). Constitutive activation of CD40 with low level of its ligand may play a role in tumorigenesis, whereas saturation of CD40 receptor with its ligand may be able to induce negative effects on tumour survival or growth (Eliopoulos and Young, 2004). In pancreatic ductal adenocarcinoma, co-expressing CD40 and CD40L is associated with more aggressive tumours, which may occur through autocrine signalling, although overexpression of CD40L is associated with better prognosis (Shoji et al., 2011). Furthermore, Bussolati *et al.* (Bussolati et al., 2002), showed that co-expression of CD40 and CD40L in renal cell carcinoma is highly associated with tumour metastatic spread. Similarly, CD40 overexpression in non-small cell lung carcinoma is associated with poor prognosis (Ishikawa et al., 2008).

Normal colon tissue does not express CD40 protein at detectable levels (Gelbmann et al., 2003). However, CD40 overexpression in CRC has been identified in approximately 50% of the cases (Wu et al., 2008). CD40 overexpression in CRC and not in normal colon tissue may suggest that CD40 is acting as an oncogene. However, *CD40* is located on chromosome 20q13, a frequently amplified region in CRC. This may explain CD40 overexpression as a passenger effect. However, an *in vitro* study suggests that ligation of CD40 with membrane bound CD40L induces apoptosis in CRC cells (Georgopoulos et al.,

2007). CD40 effects in CRC are thus controversial and, studying the functionality of CD40 and its expression in CRC cell lines and clinical tissues may help us determine whether CD40 acts as an oncogene or a tumour suppressor in CRC.

Therefore, studying the expression and function of CD40 in CRC cell lines and its expression in clinical tissues may indicate whether CD40 acts as an oncogene or a tumour suppressor in CRC and whether it could be used as a therapeutic target.

1.6.3 Phosphatidylinositol (3,4,5)-trisphosphate (PIP3)-dependent Rac exchanger 1 (*PREX1*)

Phosphatidylinositol (3,4,5)-trisphosphate (PIP_3)-dependent Rac exchanger 1 (*PREX1*) gene is located on chromosome 20q13.13. It encodes a 1,659 amino acid protein of 186 kDa. RHO GTPases are a large family of small G proteins that includes RHOA, Rac, Cdc42 amongst others. RHO GTPases regulate cell cycle progression, cytoskeletal organization, and gene expression and are involved in tumorigenesis and metastatic progression (Jaffe and Hall, 2005, Aspenstrom et al., 2007). The activation of RHO GTPases is regulated by guanine nucleotide exchange factors (GEFs), in which RHO GTPases convert from GDP bound to active GTP-bound (Schmidt and Hall, 2002). PREX1 is a large multi-domain GEF that can catalyse nucleotide exchange for the Rac subfamily of RHO GTPases to control cell motility and cell morphology (Herter et al., 2013, Waters et al., 2008).

PREX1 consists of an N-terminal DH-PH tandem domain (). This domain forms a catalytic subunit *in vitro* (Hill et al., 2005). The C-terminal contains two Dishevelled, EGL-10, Pleckstrin (DEP) domains, two postsynaptic density protein, discs large, zona occludens-1(PDZ) domains, and a large inositol polyphosphate 4-phosphatase (IP4P) homology domain (Lucato et al., 2015). PREX1functions as an integration point for signals downstream of RTKs and G protein-coupled receptors (GPCRs) (Welch et al., 2002). EGFR is one of the RTK receptor that activates PREX1 in breast cancer cells. When PREX1 is activated, it promotes cell proliferation and migration (Sosa et al., 2010). PREX1 protein functions as an integration point for signal downstream of RTKs (Welch et al., 2002). Stimulation of RTK activates the PI3K pathway to phosphorylate PIP2 to PIP3 (Barber et al., 2007).

In addition, PREX1 can be activated by GPCR, thereby, regulating endothelial cell angiogenesis *in vitro* (Carretero-Ortega et al., 2010). GPCR stimulation dissociates heterotrimeric G protein into Gα and Gβγ subunits. PIP3 and Gβγ subunits possibly synergistically activate PREX1at the plasma membrane (Barber et al., 2007).

The role of PREX1 in tumorigenesis has been studied in different tumours. Evidence indicated that PREX1 is overexpressed in breast and prostate cancer (Qin et al., 2009, Montero et al., 2011). *In vitro* studies showed that knockdown of PREX1 inhibits cell migration and invasion in ovarian, melanoma, and prostate cancer (Qin et al., 2009, Kim et al., 2011, Lindsay et al., 2011). Furthermore, *PREX1* mRNA expression has been studied in human melanoma cell lines and human melanomas. *PREX1* expression is elevated (Lindsay et al., 2011). Lindsay *et al.* (Lindsay et al., 2011) also showed that PREX1 promotes melanoblast migration through Rac activation. Additionally, a melanoma-model mouse with deleted PREX1 is more resistant to metastasis (Lindsay et al., 2011).

Although evidence indicates that PREX1 has an oncogenic role in tumorigenesis, PREX1 has not been studied in CRC cell lines. In this study, we investigated PREX1 expression in CRC tissues and cell lines. Moreover, functional studies were performed to clarify the role of PREX1 in the proliferation and motility of CRC cell line.



Figure 1-7 PREX1 structure
A schematic representation of the domain layout of PREX1. N-terminal DH-PH tandem domain forms the catalytic subunit of the protein DH: (yellow) PH (purple) domains, DEP :Disheveled, EGL-10, pleckstrin. two PDZ (postsynapticdensity protein, discs large, zona occludens-1) domains, and a large IP4P (inositol polyphosphate 4-phosphatase) Adapted from (Lucato et al., 2015)

1.6.4 Engulfment and cell motility (*ELMO2*)

ELMO2 gene is located on chromosome 20q13.13. It encodes a 720 amino acid protein of 182 kDa. ELMO2 belongs to the family ELMO that plays a role in cytoskeletal rearrangements required for cell motility and phagocytosis of apoptotic cells (Gumienny et al., 2001). ELMO2 interacts with DOCK180 to activate RAC1. GEFs for RHO GTPases are divided into two main families, (1) the classical DH-PH domains containing family (PREX1 is one of these), and (2) Dock180-related proteins that contain the Dock homology region (DHR)-2 domain (Schmidt and Hall, 2002). Dock-180 is classified as a binding protein for the SH3 domain of the proto-oncogene product c-Crk through its C-terminal PxxP region (Hasegawa et al., 1996). ELMO2 is a scaffold protein that shows no catalytic activity. It contains armadillo repeats at the N-terminus, a PH domain, and a complex proline rich region at the C-terminus. Evidence indicates that ELMO binds to DOCK180, thereby activating its catalytic activity toward RAC (Brugnera et al., 2002). Mutation of DOCK180 on the ELMO binding site inhibits RAC activation (Grimsley et al., 2004). Active RHOG GTPase binds to the N-terminal portion of ELMO (Katoh and Negishi, 2003). In addition, ELMO downregulation reduces cell migration through interrupting RHO GTPase activation (Katoh and Negishi, 2003). During migration, formation of stable lamellipodia is important to maintain the orientation of the leading edge. This is accomplished by activation and translocation of RHO GTPases to the plasma membrane (Petrie et al., 2009). Evidence indicates that integrin-linked kinase (ILK) binds to ELMO2 protein. Activation of RHOG recruits the ELMO2/ILK complex, where ELMO2 serves as a bridge, which links RHOG with ILK. This activation occurs in response to EGFR stimulation. The formation of ILK/ELMO2/RHO activates RAC1, which leads to actin polymerization () (Ho and Dagnino, 2012). Furthermore, the ELMO2/ILK/RHO complex is involved in microtubule regulation(Jackson et al., 2015), in which instability of these microtubules is critical for cellular function, including chromosome segregation (Rohena and Mooberry, 2014). Studies of ELMO2 in cancer are limited. *Li et al. (Li et al., 2013),* showed that ELMO2 is expressed in breast cancer cell lines and tissues. In addition, ELMO2 is overexpressed in breast cancer metastases when compared to non-metastasised cases. The role of ELMO2 in cancer development and metastasis remains

unclear. Exploring the role of ELMO2 in CRC could reveal its role in cancer development and/or metastasis.

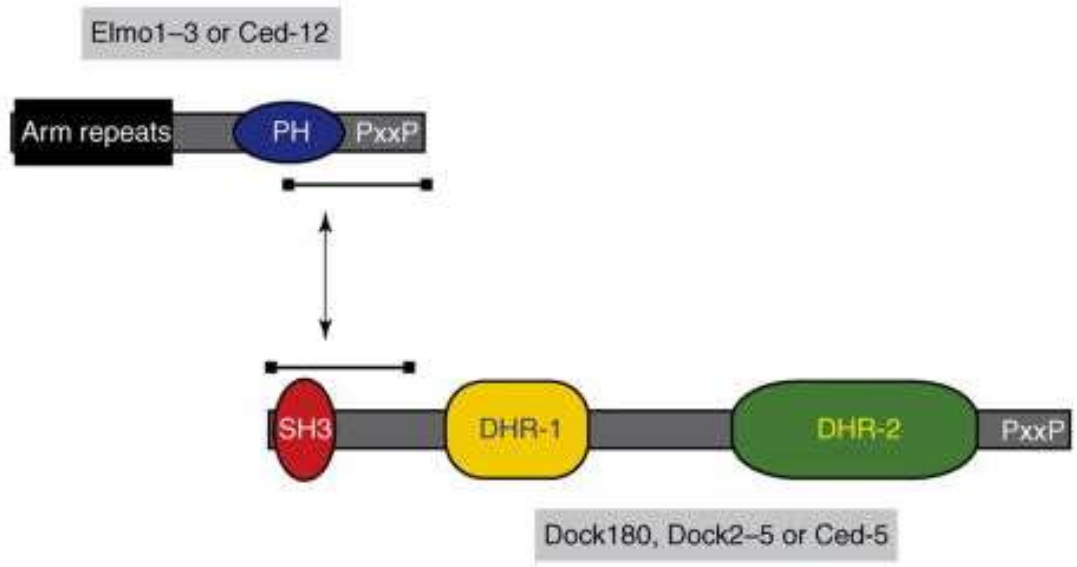


Figure 1-8 Schematic representation of ELMO protein.
A large portion of the C-terminal domain of Elmo, including part of the PH domain and the proline-rich region (black bar), is required for Elmo to interact with the Dock180-related proteinsc (double-headed arrow). The N-terminal portion of Dock180, in turn, is required for Dock180 to bind to the Elmo proteins. Although the SH3 domain of Dock180 can bind to Elmo in vitro, some studies suggest that this domain is dispensable for the Dock180–Elmo interaction in cells(Cote and Vuori, 2007).

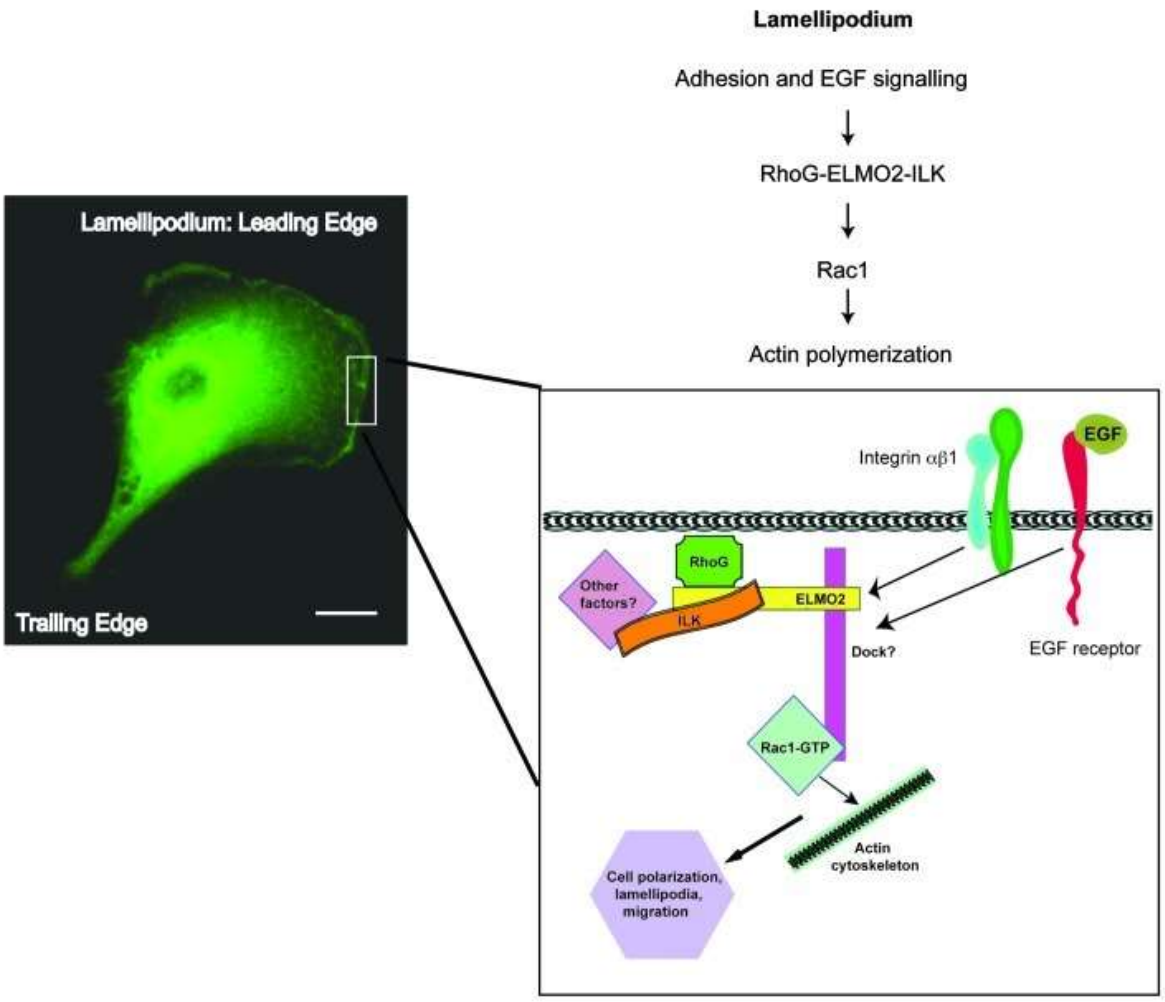


Figure 1-9 Recruitment of RHOG, ELMO2, and ILK to leading edges of migrating cells in response to EGF

Recruitment of RHOG, ELMO2 and ILK to leading edges of migrating cells in response to EGF. ELMO2, RHOG and ILK interact and localize to the cell front in response to EGF. This complex is necessary for normal RAC1 activation and forward movement. Whether RAC1 is directly activated by Dock proteins, or by other guanine exchange factors in association with the RhoG-ELMO2-ILK complex remains to be determined (Ho and Dagnino, 2012).

1.6.5 Prostaglandin I2 (prostacyclin) synthase (*PTGIS*)

PTGIS gene is located on chromosome 20q13.13. It encodes a 500 amino acid protein and has a molecular weight of 57 kDa. *PTGIS* plays an important role in the prostaglandin endoperoxide synthase pathway (cyclooxygenase pathway). Cyclooxygenase-2 plays a key role in the conversion of arachidonic acid to prostaglandin H2, while *PTGIS* catalyses the transformation of prostaglandin H2 to PGI2. The latter interacts with PPAR peroxisomal-proliferator-activated receptors, which may be involved in cancer progression (Lim et al., 1999). Furthermore, PPAR is considered as a downstream effector of the APC/β-catenin pathway (Munemitsu et al., 1995). It may be implicated in CRC progression by preventing apoptosis (He et al., 1999).

Lichao *et al.* (Lichao et al., 2012a) determined the expression of *PTGIS* protein in CRC tissue samples and showed that it was expressed in approximately 60% of the cases. *PTGIS* expression was higher in CRC cases with liver metastasis than in CRC cases without liver metastasis. *PTGIS* expression was higher in hepatic metastases when compared to the matched primary colon tumours.

However, a study of 100 CRC cases demonstrated the hypermethylation of the *PTGIS* promoter in 43 cases (Frigola et al., 2005). *PTGIS* mRNA expression was studied. It was overexpressed in benign tissue when compared to the tumour. The same group investigated the methylation status of the *PTGIS* gene promoter and confirmed that *PTGIS* was hypermethylated in 60% of CRC (Cebola et al., 2015).

On one hand, overexpression of *PTGIS* indicates the oncogenic role of this protein in CRC progression. On the other hand, hypermethylation of *PTGIS* promoter suggests a tumour suppressor effect in CRC. However, no investigation has been conducted to determine the functional activity of *PTGIS* and its possible effect on CRC progression. In summary, *PTGIS* is located in a frequently amplified region (20q13) and investigating its role in CRC is important to understand the role of the COX pathway in CRC. Therefore, *PTGIS* functional role in CRC was investigated in this study.

1.7 Hypothesis and Aims of the study

1.7.1 Background:

Many studies showed that the 20q is frequently amplified in primary and metastatic liver tumour cells. Different techniques have been used to study DNA copy number in CRC and liver metastasis and most of them agreed that 20q is frequently amplified. These studies conclude that 20q amplification occurs during the early stage of CRC. Furthermore, several genes have been identified in 20q, which drives the adenoma to carcinoma sequence in CRC. Other genes identified in 20q normally play a role in invasion, accurate chromosomal segregation, proliferation, apoptosis, and migration although their role in tumours in unknown. In addition, 20q may be involved in the development of CRC liver metastasis, when it is amplified in these cells. Genes on 20q may drive the progression from adenoma to carcinoma, but may also be important in driving tumour metastasis.

1.7.2 Hypothesis

Reviewing literature indicates several studies were found to link amplification of chromosome 20 with progression of CRC (Table 1-3). Furthermore, multiple genes on this chromosome found to directly play an oncogenic role in CRC (Table **1-4**). Giving that other genes on chromosome 20 have not been yet investigated in relation to CRC. Perhaps, one could hypothesis that further genes on this chromosome might play an oncogenic function in CRC. Noteworthy, success in defining further genes with potential oncogenic role in CRC could help better evidence-based apply of personalised medical approach.

1.7.3 Aims

This study was designed to investigate the amplification frequency of chromosome 20 and its association with other molecular alteration. In addition, to investigate the functional role of candidate genes (Table 1-5) located in chromosome 20 (Figure 1-10).

1) Investigation the frequency of 20q amplification in CRC and its association with genetic alteration.

a) To develop qPCR method, validate our aCGH data from a series of 20 micro-dissected CRC primary and their matched liver metastasis samples.
b) To screen another series of 103 CRC cases for 20q amplification applying the developed qPCR at (a).
c) To investigate the association of 20q amplification with *KRAS, PIK3CA, TP53*, and ploidy status.

2) Exploring the functional role of candidate genes located on chromosome 20 in CRC.
   a) To explore protein expression of candidate genes (located on chromosome 20q13) in CRC cell lines and tumour tissues.
   b) To study the functional activities of *PTPN1, CD40, PREX1, ELMO2* and *PTGIS* genes in CRC cell lines by gene knockdown, and investigate the effect on cell proliferation and motility.

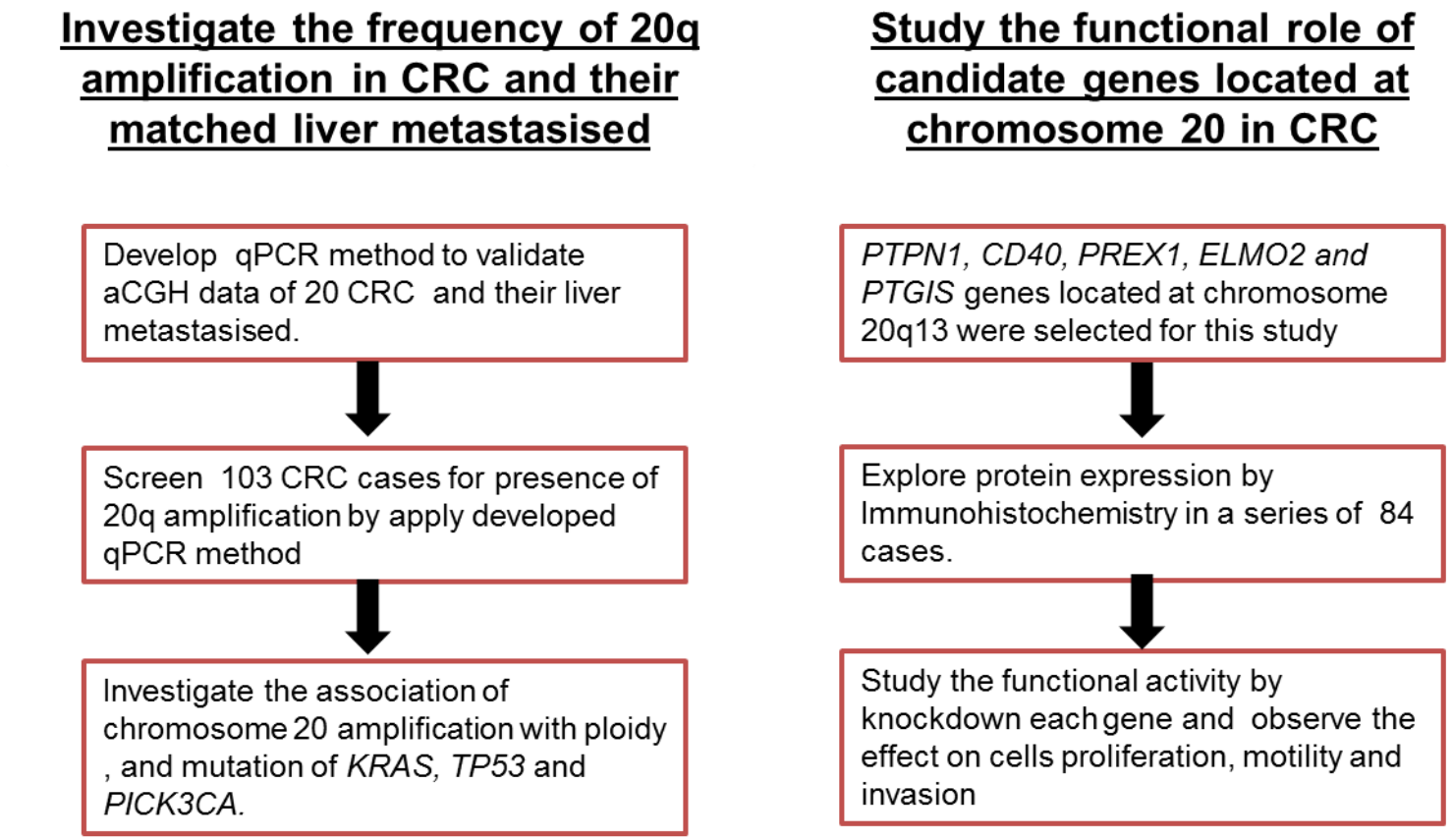


Figure 1-10 The strategy used to investigate chromosome 20q13 amplification in Colorectal cancer.

Abbreviation: CRC: colorectal cancer, qPCR: quantitative PCR, aCGH: array CGH

2 **Chapter Two: Materials and Methods4**

2.1 Tissue sample and DNA extraction

In this study, three different sample sets of CRCs were tested (Table 2-1). The first set was a series of 20 cases of paired primary CRCs and corresponding liver metastases selected from the archives for this study. Dr Wakkas Fadhil performed the DNA extraction and the assessment of the quality of DNA.. After histopathological review of these cases, DNA was isolated from microdissected FFPE tumour samples. This set was tested previously (by our group) for chromosomal instability by aCGH. The aCGH result was validated by qPCR.

The second set of tumours used was a series of 110 non-microdissected primary CRC cases randomly selected for this study. For this sample set, 20q amplification was screened. Dr Wakkas Fadhil performed histopathological review of these cases, DNA extraction and the determination of the DNA quality (Fadhil et al., 2014).

The method used for DNA extraction from these tissues is provided in Appendix 2: DNA extraction. The ethical approval for both sets of cases was obtained (Reference No C02.310).

The third sample set, was archival FFPE blocks of a random series of CRC 84 cases retrieved from Nottingham Health Science Biobank (ethical approval, APC 147). Dr Saira Sajid and Dr Maham Akhlaq reviewed Eighty-five primaries CRC FFPE samples. Tissues microarray was built from this set and tested by immunohistochemistry.

Table 2-1: List of sample sets selected to study amplification of chromosome.20 and protein expression.

Samples Set	Tests applied	Chapter
20 CRC primary and their matched liver metastasised	20 microdissected cases of paired primary CRCs and corresponding liver metastases selected. Samples tested by aCGH and qPCR.	Chapter 3
110 primary CRC	7 cases were microsatellite instable and were excluded from following analysis. 103 cases were screened for 20q amplification by qPCR	Chapter 3
84 CRC	After reviewing the cases, 84 cases were selected for studying protein expression using Immunohistochemistry	Chapter 4

2.2 DNA copy number evaluation of 20q13 genes in colorectal cancer and liver metastasis

2.2.1 Sample quality control

All DNA samples were tested for quality using four pairs of primers amplifying across the GAPDH gene (used as Reference gene) in a multiplex PCR (Fadhil et al., 2014), This would give products of 100, 200, 300 and 400bp (van Beers et al., 2006).

For 20 cases set, the quality assessment was performed to ascertain of the quality of the samples. PCR was performed in a total volume of 10 µl which contains 1×HotShot master mix (Cadama Medical Ltd), 250nM of primers, and 20 ng templates DNA.

The PCR conditions were as follows: initial denaturation at 95°C for 5 min followed by 35 cycles of denaturation at 95°C for 30 s, annealing temperature 62°C for 30 s, and an extension phase at 72°C for 1 s. A final elongation at 72°C for 10 min followed these cycles. PCR products were analysed using gel electrophoresis on a 2% agarose gel and 1xTBE buffer (0.089 M Tris, 0.089 M boric acid, 0.002 M EDTA, pH 8.2–8.3).

2.2.2 Molecular analysis of tumour samples

Testing for MSI and *KRAS, PICK3CA, and TP53* mutation screening were performed by Dr Wakkas Fadhil as previously described (Fadhil et al., 2012, Fadhil et al., 2010). In addition, Dr Wakkas Fadhil measured the DNA content of tumour cells by flow cytometry.

2.2.3 Primer Design

Primers were designed for the DNA copy number analysis of genomic DNA and c.DNA of Cell lines. The genomic DNA sequences of the genes of interest were obtained from the NCBI (http://www.ncbi.nlm.nih.gov/nuccore/). It was taken into account that the efficiency of PCR will depend on the quality of the DNA

When DNA is extracted from FFPE, it is usually compromised by the process of fixation and this, in turn, can influence the efficiency of the PCR. Quantitative analysis depends on highly efficient PCR. In order to maximise efficiency in degraded templates, it is best to design primers for small amplicons. Primers were designed to amplify amplicons of 110 to 180 base pairs (bps). In addition, since primers were to be used for both gDNA and cDNA, they were anchored in the exonic region of the genes of interest and were not intron-spanning. Primer3 software (http://frodo.wi.mit.edu/) was used to generate the primers sequence. Then, these primers underwent in-silico analysis using the UCSC (University of California Santa Cruz) In-Silico PCR software (http://genome.ucsc.edu/cgi-bin/hgPcr?command=start) to ensure that the primers would amplify the expected fragment of the genes of interest. The sequences of the primers are provided in Table 2-2.

Table 2-2: Sequences of the primers produced by Eurofins MWG Operon.

Genes	Forward primer 5'–> 3'	Reverse primer 5'–> 3'	NCBI Reference Sequence	Product size
PTPN1	AATGAGGAAGTTTCGGATGG	GAAGAGTCCCCCATGATGAA	NG_012119	102bp
PTGIS	GACAAGGACCACATGTGCAG	TGCATCTCCTCTGACACACC	NG_007940.1	143bp
CSE1L	GCTGCTTGTGATCTGGTACG	GCTGCATCTTTGTGTTTCCA	NM_001316.2	137bp
PREX1	ACAGCGTCTTCGTGGAGAAC	AATGCTCTCCAGCTTGGTGT	NM_020820.3	110bp
ELMO2	GGAGCTGAGGGAGAAGATCC	GGCGGTTCCCAATCTTTC	NM_133171.3	104bp
ADNP	CTTGGGTCAGAGCAGAGGTC	CTGGATGCCTGTGACTGAGA	NC_000020.11	119bp
GAPDH	GAGAAGTATGACAACAGC	CAAGTCAGGGGAGCGTGT	NC_000012.11	99bp

2.2.4 Polymerase Chain Reaction (PCR)

2.2.4.1 Primer optimisation

In order to ascertain the optimal annealing temperature, each primer pair was initially tested on a gradient PCR machine (Primus96 advanced® Gradient). A PCR reaction with a 12 temperature gradient at the annealing stage was performed (usually with a temperature range of 55°C – 65°C). The reaction was undertaken in a final volume of 12.5µL in which each reaction contained X1 SensiFast SYBR Lo-ROX PCR Master Mix (Bioline), forward and reverse primers pair at 250nM, 10ng template DNA and water to complete the total volume.

The PCR conditions were as follows: Initial denaturation at 95°C for 5 min followed by 35 cycles of denaturation at 95°C for 30 s, annealing (Temperatures vary) for 30 s, extension at 72°C for 45 s. A final elongation for 7 min at 72°C followed these cycles. Finally, PCR products were analysed using gel electrophoresis on a 2% agarose gel.

2.2.4.2 qPCR

For the quantification experiments, 5.71 ng of the DNA template was used. Target genes copy number was determined by the relative quantitative ($2^{-\Delta\Delta Ct}$) method using GAPDH as the reference gene (normalising control).

The relative quantitation $2^{-\Delta\Delta CT}$ method relies on assumption that PCR reaction efficiency of primers of target genes and reference are approximately equal. Reactions with 100% efficiency indicate that each PCR cycle produces a double time of product. Therefore, in our experiments, the primers optimised to reach efficiency of 100 ± 10%. The second assumption is that the reference gene is expressed at a constant level between the samples. GAPDH is the reference gene used for normalisation.

The threshold cycle (CT) is the intersection between the amplification curve and the threshold line (Figure 2-2-1). The ΔCT is the CT value of the target gene minus the CT value of the reference gene. Thus, the ΔΔCT is the ΔCT of the sample minus the ΔCT of the calibrator (Reference sample) and this value is used in the equation $2^{-\Delta\Delta Ct}$ which produce a value called relative quantitative (RQ) value.

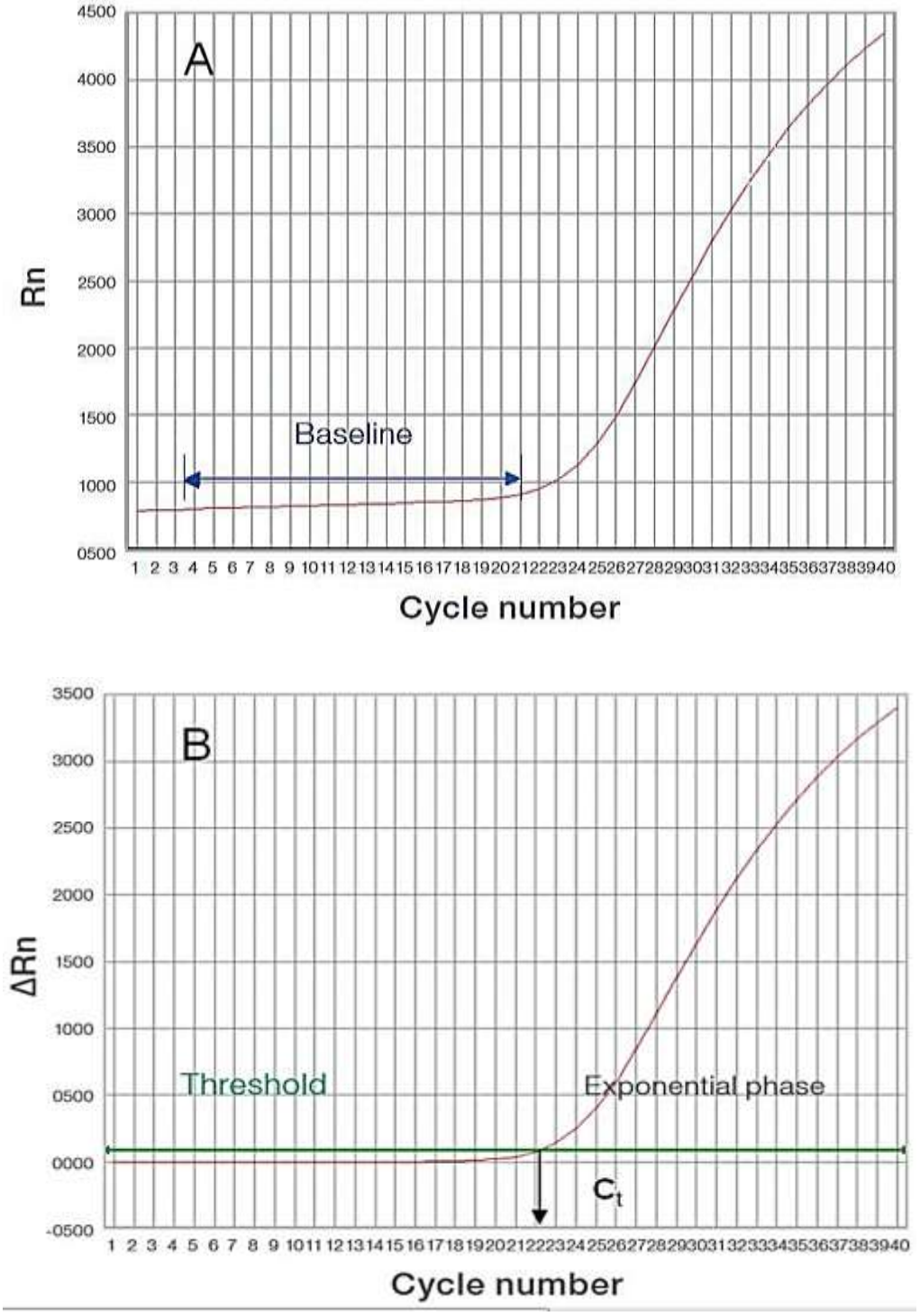


Figure 2-2-1 Graphical representation of real time PCR data.
(A) Amplification plot showing Rn plotted against cycle number showing the baseline. Baseline is the amount of fluorescence detected in the initial cycle of PCR reaction. (B) Amplification plots showing the ΔRn against the cycle number.
Rn: is the amount of fluorescence detected from the reporter dye (Syber green) normalised to the amount of fluorescence of the passive dye (ROX).
ΔRn: is Rn minus the baseline (Life-Technologies, 2011)

In this method, the relative copy-number difference of the target gene in tumour sample against a reference calibrator sample (consisting of 10 pooled DNA samples obtained from normal FFPE colonic tissue) is provided by the $2^{-\Delta\Delta Ct}$ equation. Data evaluation was performed using the ABI 7500 Fast System software and RQ software (Applied Biosystems).

PCR was performed in a total volume of 12.5 µl and consisted of X1 GoTaq® qPCR Master Mix (Promega), forward and reverse primers pair at 200nM, except one primer pair for PREX1 150nM (to avoid primer dimers), and water. The PCR reaction was performed in triplicate using the following PCR condition: 95°C for 5 min followed by 35 cycles at 95°C for 10 s, 60°C for 30 s and 77°C for 10 s.

An additional melting curve stage was included at the end of the PCR. Melting data can be used to check product specificity and the melting protocol consisted of one cycle of 95°C for 15 s, 65°C for 45 s at maximum ramping speed, then gradual heating (ramping speed rate at 1%) to 95°C.

In order to perfom qPCR, it was important to perform standard curve initially in order to evaluate the primers' efficiency. Pooled DNA obtained from 10 non-tumour FFPE colonic tissue samples were used as template for the initial standard curve experiments at a concentration of 40ng. Three serial dilution (1:7) points were used to set up the standards. Primer pairs with efficiencies ranging from 95%–105% were used in subsequent analysis. Standard curve was performed on ABI 7500 Fast System (Applied Biosystems).

2.3 Tissue Culture Studies:

2.3.1 Culturing of cell line

The Colorectal cancer cell lines (HCT116, RKO, SW480, SW620, HT29, and DLD1) were obtained from the Molecular and Population Genetics Laboratory, London Research Institute, Cancer Research, London, UK. The identity of the cell lines was validated by Dr Wakkas Fadhil through analysis of the known mutation profile for each cell line (Seth et al., 2009).

Cell lines were cultured in 75cm^2 flasks in Dulbecco's Modified Eagle's Medium (DMEM) containing 10% foetal calf serum (Invitrogen), 1% (100 units/ml) penicillin/streptomycin (Invitrogen). Cells were incubated for at 37°C in an atmosphere containing 5% CO_2 and split at 90% confluence. Cells were checked on a daily basis under the microscope for degree of confluence, presence of excessive number of floating cells and fungal /bacterial infection

2.3.2 Sub-culturing of the cells (Passaging)

Once the cells reached 90–95% confluence, the growth medium was removed and cells were washed twice with PBS. Then, cells were trypsinised using 2ml of Trypsin EDTA and incubated at 37°C for 5 min to detach the cells. Fresh DMEM was added to neutralise the trypsin (at a ratio of 1ml of Trypsin EDTA+ 9ml DMEM) and then cells were pelleted by centrifugation at 1000rpm for 5 minutes. The supernatant was removed and the cell pellet was resuspended with 10 ml DMEM. One mililiter of the suspension was added to 9 ml of DMEM and it was pipetted to 75 cm^2 flasks.

For cell counting, cells were detached from the flasks or 6 well plates, pelleted, and then suspended in growth medium in a 0.5 mL tube. Ten microlitres of the suspension was mixed with 10 µL of TC10 Trypan Blue dye 0.4% (BioRad) and cells were counted using the TC10™ automated cell counter (BioRad).

2.3.3 Cell transfection with Small Interfering RNAs (siRNAs)

siRNAs were used to knockdown candidate genes located on chromosome 20. The siRNA sequences are presented in Table2-2-3. Commercially validated siRNAs (Invitrogen) were used for knockdown of PTPN1, CD40, PREX1 and *ELMO2* genes . The siRNA used to knockdown *PTGIS* gene was validated and purchased from Ambion. The non-target siRNA (targeting Luciferase) was synthesised by Eurofins MWG/Operon (Germany) and used as a negative control.

The final concentration of siRNA in all experiments was 66nM which provided the highest knockdown efficiency. Increasing the concentration of the siRNAs might lead to off-target effects (Caffrey et al., 2011).

Approximately 150,000 cells were seeded into each well of 6 well plates. Cells were transfected with siRNA when they had reached 30-40% confluence. For transfection, 66nM (per well) of the siRNA and 5µl (per well) of lipofectamine 2000 were diluted in 250µl of Opti-MEM media in separate eppendorf tubes and incubated for 5 min at room temperature.

The siRNA and lipofectamine 2000 were then mixed and incubated for 20 minutes at room temperature. The mixture was added to each well containing 1.5 mL of Opti-MEM media, providing a total volume of 2 mL and incubated at 37oC for 6 h. The Opti-MEM media was replaced with DMEM plus 10% FBS. The cells were allowed to grow for 48 h before being harvested for further experiments.

Table2-2-3 The sequences of the siRNAs and its Identification code.

Gene	Sequences	siRNA ID
PTGIS	Sense GACUUUUACAAGGAUGGGAUU Antisense UCCCAUCCUUGUAAAAGUCUU	S11506 (Ambion, UK)
PTPN1	Sense UUGAUGUAGUUUAAUCCGACUAUGG Antisense CCAUAGUCGGAUUAAACUACAUCAA	PREX1HSS126496 (Invitrogen, UK)
CD40	Sense ACCUGUGAAGAAGGCUGGCACUGUA Antisense UACAGUGCCAGCCUUCUUCACAGGU	CD40HSS141508 (Invitrogen, UK)
PREX1	Sense GGACAACAUUCAGAGAUAUGUGGAA Antisense UUCCACAUAUCUCUGAAUGUUGUCC	PTPN1VHS41290 (Invitrogen, UK)
ELMO2	Sense CCCAGAGUAUUAUACCCUCCGUUAU Antisense AUAACGGAGGGUAUAAUACUCUGGG	ELMO2HSS127210 (Invitrogen, UK)
Luciferase	Sense CAGUGUAGUAGUCGUUUC Antisense GAAACGACUACUACACUG	(EurofinsMWG/Operon, Germany)

2.3.4 RNA Extraction

Once cells reached 90% confluent, they were harvested by washing the cultures with PBS followed by trypsinisation. The cell suspension was centrifuged for 5 minutes at 300g speed to pellet the cells. Total RNA was extracted using RNeasy Mini kit (QIAGEN) according to the manufacture's instruction. The RNA yield was then measured using the NanoDrop ND-1000 UV-Vis Spectrophotometer (LabTech International Ltd, Ringmer, UK). All samples showed optical density ratios from1.96 to 2.05, which indicates relative purity of the sample.

2.3.5 Complementary DNA (c.DNA) generation

Complementary DNA was generated from 1µg of total RNA, in a total volume of 50µl. The mixture contained 1 µM random Hexamers (Invitrogen). The mixture was incubated for 10 min at 70°C.

During incubation time, mixture of 200 U of M-MLV reverse transcriptase (Invitrogen), 10 mM dithiothreitol (DTT; Invitrogen), 0.5mM of Deoxyribonucleotides triphosphate (dNTP) and 1× M-MLV RT buffer were prepared and it was then added. The mixture was incubated for 60min at 37°C and then incubated for 10 min at 70°C. RT-negative samples (RT-cDNA) were prepared to ensure the purity of the RNA from contamination with genomic DNA. In these, 1.5µl of RNase-free water were included instead of reverse transcriptase enzyme and RNase block. RT- cDNA controls were important for detecting genomic DNA contamination.

2.3.6 qPCR

The cDNA samples were diluted five times with RNA free Water. The qPCR was in final volume of a final volume of 10µl. each reaction consisted of 1X GoTaq® qPCR Master Mix (Promega), forward and reverse primers each at final concentration of 0.200µM, and template consisting of 3 µl cDNA. Controls included PCR whereby template was replaced by RNA free water (Negative contro) or RT- cDNA.

The relative expression difference of the target gene in Knockdown cells against reference sample (RNA extracted from cells transfected with an

siRNA targeting luciferase gene) is given by $2^{-\Delta\Delta Ct}$ equation. The house keeping gene Hypoxanthine phosphoribosyl-transferase 1 (HPRT1) expression was used as endogenous control to normalise data from candidate genes. The ABI 7500 Fast System software and RQ software (Applied Biosystems) was used to analyse the data.

2.3.7 Protein samples preparation and quantitation

For protein extraction, tissue culture media was aspirated and cells were washed with ice-cold PBS (1X). Ice-cold RIPA buffer (Thermo scientific) and a 1% protease and phosphatase inhibitor cocktail (Thermo scientific) were added to cells and incubated for 20 minutes on ice. Then the mixture was centrifuged at 4^{o}C at 13,000 rpm for 30 minutes to pellet the cellular debris.

The supernatant fluid was transferred into an eppendorff tube and kept on ice. Proteins were quantified by performing Pierce® BCA Protein Assay kit (Thermo scientific, UK) following the manufacturer instructions. Absorbance was measured by the plate reader (Labsystems, UK) at 550nm wavelength (Appendix2: BCA protein Assay kit instruction).

2.3.8 Western blotting

Protein lysate (50µg) was mixed with NuPAGE® LDS Sample Buffer (4X) supplemented with 5% β-mercaptoethanol (βME). Lysate was heated at 95^{o}C for 5 minutes. Then, the mixture was run on a NuPAGE 4-12% bis-tris gel (Invitrogen) at170 volt for 60 minutess. Protein was transferred to PVDF membrane (Amersham Hybond-P, GE Healthcare), which had been activated with methanol, by using the Trans-Blot Semi-Dry Transfer Cell (BioRad) at 20 V for 30 minutes. After that, the PVDF membranes were blocked with either 5% milk (powdered milk dissolved in PBS, 2.5g/50ml) or 5% Bovine Serum Albumin (BSA) diluted in PBS with 0.1% Tween-20 (Sigma) for 1 hour at room temperature. Then, membranes were incubated with primary antibodies in 5% BSA/milk and 5% milk at 4C^{o} overnight.

Membranes were, then, washed three times with PBS-Tween (0.1 %) and then incubated for 1 hour at room temperature with HPR-conjugated secondary Anti-Rabbit or Anti- mouse antibodies (Sigma). The membranes

were then washed two times with PBS-Tween and once with PBS. Finally, membranes were incubated for 5 minutes with Enhanced Chemiluminescence (ECL) Prime detection kit (Abersham) and then exposed to X-ray film (Kodak) from 3 s to 1 minute. X-ray film was passed through developer, fixer (Sigma) and finally washed with water. The band intensity was analysed using ImageJ 1.47 software.

Table 2-4 list of antibodies used in western blot.

Antibody	Source	Dilution/Blocking
PTGIS	Sigma ab23668	1/500 5% BSA
PTPN1	Cell signalling ab75856	1/1000 5%BSA
CD40	Abcam ab13545	1/5000 5%milk
CD40L	Abcam ab65854	1/2000 5%milk
PREX1	Cell signalling (D8O8D)	1/1000 5%BSA
ELMO2	Abcam ab181234	1/500 5%BSA
β-Actin	Sigma A2228	1/50,000 5%milk

2.3.9 Functional studies

2.3.9.1 Cells number assessment (Proliferation assay)

There are two methods used in our lab to study cell proliferation of control and treated cells. The first is the Methylene Blue assay, which is based on methylene blue dye is absorbed into both live and dead cells. However, the methylene blue is not washed out with water in live cells, but non-viable cells cannot retain the dye after washing.

The other method is Presto Blue assay, which is resazurin-based compound. Presto blue is converted to the reduced form by mitochondrial enzymes of viable cells. Presto Blue exhibits a change in a colour and a shift in its fluorescence, as a consequence of the reduction. Thus, it can be quantified using fluorometric approach.

In addition, Presto Blue is a non-toxic dye, thus it can be used to monitor cell viability in time point. According to the manufacture (Invitrogen), it is the fastest live assay for assessing cell viability with short incubation (10 minutes). Furthermore, It is a very sensitive assay which may can detect 12 viability of cells per well.

Firstly, comparison of the sensitivity of Presto Blue and Methylene Blue assays was performed. SW620 cell lines were harvested by aspirating growth media from flask 75cm^2 and flask was washed twice by PBS. Then, the cells were detached and counted as described earlier. After that, 20000, 40000, 80000, 160000 and 360000 cells were seeded into 24 well-plates in triplicate, and incubated at 37Cº and 5% CO2 for 4 hours to make sure the cells were adhered.

For the methylene blue assay, the growth media was aspirated slowly, and then the cells were fixed by adding 200µl 100% methanol to each well and incubate at room temperature for 30 min. After that, the excessive methanol was removed were left at air to dry for 5min. Then, 200µl Methylene blue (1gm methylene blue hydrate (Sigma, UK) dissolved in 100ml of water) was added to wells and incubate for 30 min at room temperature, and then the

remain methylene blue was removed. 100µl of ethanol/HCl (1:1) was added to each well to release the dye from the DNA. Ethanol/HCl was incubated for 2 min and then 100 µl of the stained ethanol/HCl was transferred into wells of a 96-well plate. Finally, the absorbance at 650nm wavelength nanometre (nm) was measured on a plate-reader Figure 2-2 (Labsystems, UK).

For the Presto Blue, the growth media was aspirated also for this assay, but the cells did not have to be fixed. Then, the mixture of PrestoBlue (10X)/ growth media (1X) (1:10 ratio) was prepared with not exposing the mixture for lights for a long time. Then, the 400µl PrestoBlue was added to each well, and then incubated at 37Cº and 5% CO2 for 1 hour.

Finally, 100µl of solution from each well was then sampled in triplicate into a 96 well plate, and then the fluorescence intensity (relative fluorescence units-RFUs) was measured using for excitation at 495nm and a filter for emission at 580nm. For background control, the mixture was added to one well with no cell seeded in, and fluorescence intensity was measured to subscribe the background effect. The fluorescence intensity was measured and background subscribed by FLUOstar optima (BMG Labtech) Figure 2-3.

The Methylene blue assay had poorer performance when compared to Presto Blue. At the lower end, it was not able to discriminate between the 20,000 cells and 40,000 cells. At the higher end, it was not able to discriminate between 160,000 and 320,000 cells Figure 2-2. Thus, the methylene blue assay might not detect small differences between the cells number in studying the effect of gene knockdown and control.

However, Presto blue was able to discriminate wells with 20,000 cells from wells with 40,000 cells, and it was able to discriminate between 160,000 and 320,000 cells. The sensitivity of Presto Blue assay was accurate in comparing with methylene blue. Thus, the PB assay was used to study the proliferation pattern of the cells after manipulation.

For gene knockdown experiments, cells were harvested 48h after siRNA transfection. Then, cells ($2X10^4$) were seeded into 24 well-plates in triplicate. Then, cells were left for 4h to adhere to wells. After that, growth media was

aspirated very slowly and carefully. A Mixture of Presto Blue and growth media was added and fluorescence measured as described above.

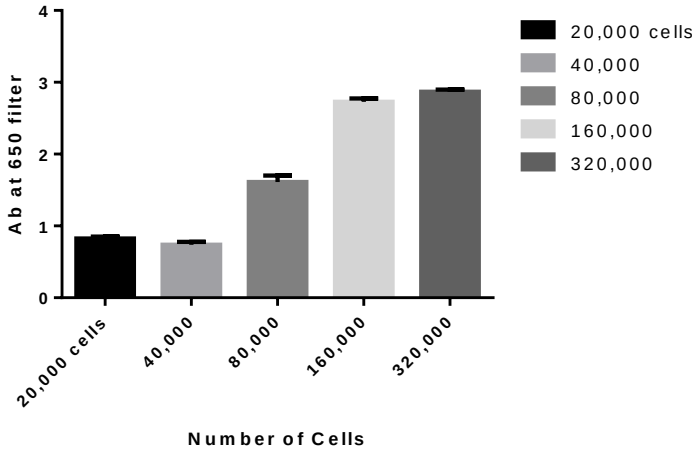


Figure 2-2 Methylene blue assay sensitivity assessment
Comparison of the sensitivity of Presto Blue and Methylene Blue assays was performed. SW620 cell lines were seeded in 20000, 40000, 80000, 160000 and 360000 cells into 24 well-plates in triplicate, and incubated at 37C^{o} and 5% CO2 for 4 hours. The cells were fixed by 100% methanol and stained with, Methylene blue. Then, ethanol/HCl (1:1) was added to release the dye from the DNA. The absorbance at 650nm wavelength nanometre (nm) was measured on a plate-reader. , Methylene Blue was not able to distinguish between the 20,000 cells and 40,000 cells, and between 160,000 and 320,000 cells

.

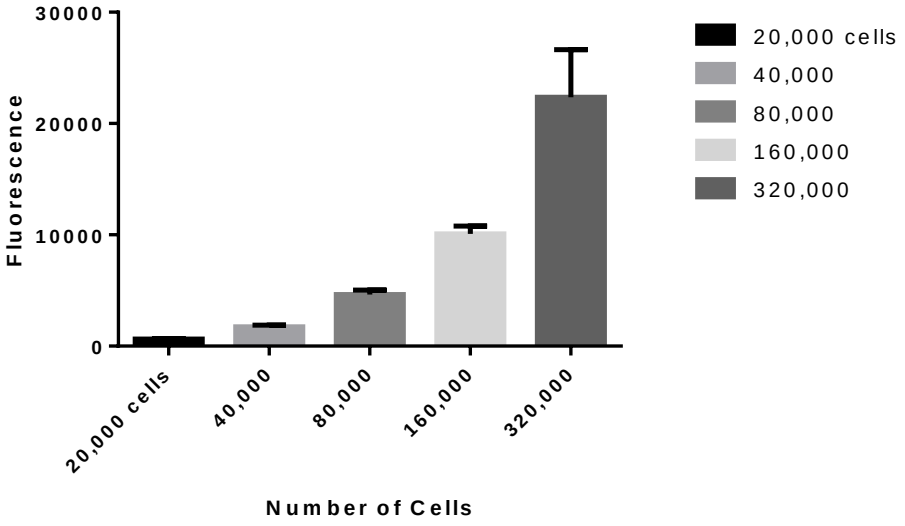


Figure 2-3 Presto Blue assay sensitivity assessment

Comparison of the sensitivity of Presto Blue and Methylene Blue assays was performed. SW620 cell lines were seeded in 20000, 40000, 80000, 160000 and 360000 cells into 24 well-plates in triplicate, and incubated at 37Cº and 5% Presto Blue was added to each well, and then the fluorescence intensity (relative fluorescence units-RFUs) was measured using for excitation at 495nm and a filter for emission at 580nm. Presto Blue could categorize between 20,000 cells from wells with 40,000 cells, and it was able to classify between 160,000 and 320,000 cells.

2.3.9.2 Cell cycle analysis by flow cytometry

Cell cycle analysis was conducted to study the effects of candidate genes located at chromosome 20q13. Knockdown was performed as described earlier, and after 48 hours cells were harvested by aspirating the growth media and then washed twice by PBS. After that, 200µl of trypsin EDTA was added to each well and incubated at 37Cº and 5% CO2 for 5 minutes to detach the cells.

Then, 1.5ml of growth media was added to neutralise the trypsin EDTA and cells were transferred to eppendorff tube and centrifuged at 1000 rpm for 5 minutes. The supernatant was aspirated and pellet remained at the bottom of the tube. The pellet was resuspended in PBS and then again centrifuged at 1000 rpm for 5 minutes. This step was repeated and then, the cells were fixed with 70% ice cold ethanol overnight at - 20°C. After the fixation, cells were washed twice with PBS and centrifuged for 10 minutes at 1500rpm. After removing the PBS by careful pipetting, cells was re-suspended in 500µl PBS contained 25µl Propidium iodide (PI) solution (Sigma, R4864, 1mg/ml), 0.1% fetal serum albumin (FSA) (Promega, UK), and 10 µl DNase free Rnase solution (Sigma, R6513, 5mg/ml).

Then, the mixture was incubated for 20 minutes at 37°C in dark. The samples were transferred to ice until the analysis. Using the FC-500 Beckman Coulter flow cytometry Machine (Beckman Coulter, USA) $30x10^3$ events were analysed and the generated data were analysed by Weasel software Version 2.7 (Walter and Elisa Hall Institute, Australia). The results were considered after exclusions of duplets. Cell cycle analysis was performed in triplicate.

2.3.9.3 Cell migration and invasion assays

After 48 hours of knockdown, cells were harvested by trypsin/EDTA as described earlier. Then, trypsin/EDTA was neutralised by add growth media and then mixture was centrifuged at 1000rmp for 5 minutes then the supernatant was aspirated. The pellet, then, was resuspended in 1000µl

growth media and cells were counted as described using TC10™ automated cell counter (Biorad).

The cell migration assay was performed to study cell motility after knockdown of candidate genes. Transwell migration assays were performed by using 24 transwell chambers (8µm pore size, Corning). This consists of a well-shaped insert which fits in the wells of a 24 well plate. The insert's base has a membrane with 8µm pore size which allows cells to migrate to the bottom of the 24 well plates. Cells which migrate through the pores fall of the well and sink to the bottom of the well where they can be counted by using an inverted microscope.

In order to activate the membrane of the transwell, the lower chamber of 24-well plate was filled 600µl growth media and the insert was applied to the well, and then incubated for 2 hours at 37Cº and 5% CO2 before performing migration assay.

Then, the inserts were transferred to another 24-well plate, in which the lower chamber had been filled with 600µl of growth media containing a total of 20%FBS. 150,000 cells from the suspension was mixed together with growth media (containing 10% FBS) to give a total of 200µl and that was added to the upper chamber of the well. Then, the 24 well-plate was incubated for 48 hours at 37Cº and 5% CO2 to allow the cells to migrate. After 48 hour of incubation, cells attached to bottom of the well were counted by using 10X objective microscope. The assay was perfumed always in triplicate.

Cell invasion was performed to study the ability of the cells to digest and invade basement membrane matrix. This assay was performed as described in cell migration assay. In the invasion assay, however, the filter membrane of the upper chamber was coated with 100µl of Matrigel (Basement Membrane Matrix, Growth Factor Reduced), (BD Biosciences, UK). The stock concentration of the matrigel was 6.9mg/ml and it was diluted 1:3 with non-serum growth media. The matrigel was left to thaw overnight at 4ºC. Pipette tips and tubes were pre cooled to prevent solidification.

In order to coat the membrane with matrigel, 100µl of thawed and diluted matrigel was added to the upper chamber and incubated at 37Cº for 8 hours to allow gelling of the matrigel. Then, 200,000 cells were suspended in growth media in a total volume of 100µl and added to the upper chamber. As in the migration assay, the lower chamber was filled with 600µl growth media with 20%FBS. The plates were incubated at 37Cº and 5% CO2 for 48h to 72h. Cells invading through the coated membrane and attached to the bottom of the well were counted by 10X objective microscope. The assay was performed always in triplicate.The wound healing assay

2.3.9.4 Wound healing assay

The wound healing assay or the scratch assay was used as a validation of the migration assay that can measure the effect of genes knockdown in cell motility. It was performed in 6 well plate, in which 3 wells were transfected with siRNA targeting Luciferase as a control and 3 well were transfected with siRNA targeting one of the candidate genes.

After 48 hours of the knockdown, cells were reached about 90% confluency and serum deprived for 24h in non-serum growth media. A sterile 200µl pipette tip was used to scratch the cells in three separate parallel scratches for each well.

After the scratches were performed, cells migration across the wound line was assessed after 24 and 48 h. The initial reading (0 h) was acquired immediately after the scratches were performed. The outer surface of the 6-well plates was marked as shown in Figure 2-4, to ensure that the photographs were taken acquired for the same site each time.

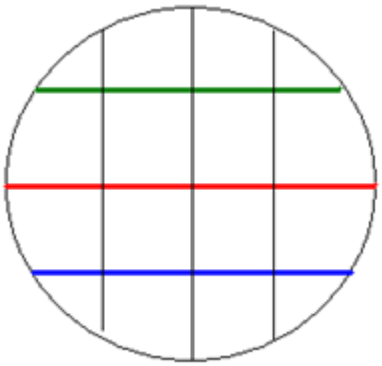


Figure 2-4 An example of marking the 6-well plate.

The photographs were taken at 0, 24, and 48 h by using a charge-coupled device (CCD) camera (Canon, Japan), which was attached to an inverted phase-contrast microscope (Zeiss, Germany). The percentage of wound area was measured and compared by ImageJ 1.47 Software. The proportion of wound area (percentage) at 24 and 48 h was calculated by normalising the reading to the 0 h reading. The data were analysed and presented using Graph Pad Prism 6 software.

2.4 Immunohistochemistry (IHC)

2.4.1 Tissue microarray construction and IHC

The luminal, middle and edge tumours, and non-tumour colon tissues were marked for each case and correspond areas in the blocks were marked. Then, array recipient blocks were prepared by applying molten paraffin into mould. Then, the paraffin was mounted in histopathological tissue cassette and incubated on ice to harden. The wax trimmed until it became flat surface ready to receive the cores.

Specimens from the cases were arrayed onto a Tissue microarray (TMA) slides (Clipped Corner X-tra® Adhesive Slides, Leica Microsystems) by Dr Saira Sajid, Dr Maham Akhlaq, and myself. For each case, three cores, with a core size of 0.6 µm and 0.8 mm apart from each other, were arrayed.

Blocks were then placed into a fully automated TMA arrayer, TMA Grand Master® (3D HISTECH®, Budapest, Hungary). Ten blocks were loaded each time and the machine captured a picture. Marked areas were recognised

easily and cores were taken into receipt blocks. Three cores were taken from each site for each case. The sections were cut by biobank staff, City hospital, Nottingham.

2.4.2 Immunohistochemistry staining.

IHC for TMA slides were stained by using NovolinkTM polymer detection system (Novocastra,UK) according to the manufacture's recommendation. First of all, slides were deparaffinised by using Leica Autostainer. Slides were placed on the hotplate for 10min at 60Cº. The TMA, then, was dewaxed by incubating slides in xylene for 5 minutes twice. After that, each slide was rehydrated through three changes of alcohol, in which it was incubated for 2 minutes in 100% ethanol, 90% ethanol and 70% ethanol, respectively. Then, the TMA slides were placed in water for 5 minutes. Antigen retrieval was performed by microwave for 20 minutes and the slides were incubated in sodium citrate buffer (pH 6.0), and slides, then, were washed by water.

The slides, then, were placed to Sequanza trays, and washed with Tri Buffered saline pH 7.6 (TBS) twice. During the washing step, it was necessary to watch the TBS flow through to ensure there were no air bubbles in the Sequanza trays, which might affect the staining. After that, peroxidase activity were neutralised by applying peroxidase block for 5 minutes and then washed twice by TBS for 5 minutes each. Then, the NovocastraTM Protein Block was applied for 5 minutes to reduce non-specific binding of the antibodies and polymer.

After two washing steps with TBS, the antibodies were diluted in Leica antibody diluent, and then incubated for various time listed in the Table 2-5. Then, the slides were washed twice with TBS for 5 minutes to remove unbound antibodies. Post primary antibody, Novolink was applied for 30 minutes and then washed twice with TBS. Then, NovoLink Polymer, Anti-mouse/rabbit IgG-Poly-HRP antibody (secondary antibodies) was applied and incubated for 30 min and then washed twice with TBS. Slides were then incubated with chromogen, 3,3' - diaminobenzidine (DAB), prepared from DAB Chromogen and NovolinkTM DAB Substrate Buffer (Polymer) for 5 minutes. .

Finally, the slides were incubated with Novolink Haematoxylin for 6 minutes and then slides removed from the Sequanza trays, and washed with water. Slides were then dehydrated by autostainer, in which slides were incubated in 70%, 90% and 100% ethanol for 2 minutes each, respectively. Then, the slides incubated in xylene for 5 min twice and the TMAs were mounted with DPX.

Table 2-5: List of antibodies used in immunohistochemsitry

Antibody	Source	Dilution	Incubation Period	Antigen Retrieval
PTPN1	Cell Signalling	1/20	Overnight	sodium citrate buffer (pH 6.0),
CD40	Abcam	1/300	30 minutes	sodium citrate buffer (pH 6.0),
CD40L	Abcam	1/350	30 minutes	sodium citrate buffer (pH 6.0),
PREX1	Cell Signalling	1/50	Overnight	sodium citrate buffer (pH 6.0),
ELMO2	Abcam	1/50	Overnight	sodium citrate buffer (pH 6.0),

2.4.3 Optimisation of the antibody concentration

The staining was performed for CD40 and CD40L using several different concentrations ranging from 1/100 to 1/1000. The concentrations used for final staining were 1/300 and 1/350 for CD40 and CD40L, respectively.

With regard to PTPN1, PREX1 and ELMO2, the initial concentrations used were 1/20, 1/50, 1/100 and 1/200, and were incubated for 30 minutes. However, none of these concentrations had worked. Then, the highest concentration was used for overnight incubation. PREX1 and ELMO2

antibodies were over stained. The concentration of PTPN1 antibody for final staining was 1/20 and incubated overnight. The concentrations used for final staining of PREX1 and ELMO2 antibodies were 1/50 and incubated for overnight.

2.4.4 Evaluation of the immunohistochemical staining

All slides were initially reviewed by light microscope to assess the staining of the tissues, and the negative control which was tissue stained without the primary antibodies. Then, slides were cleaned and scanned at X20 by NanoZoomer slide scanner (Hamamatsu Photonics, Welwyn Garden City, UK) at histopathological department, QMC hospital. Nanozoomer software was used to view the scanned slides. The H scoring system was used to evaluate the presence and intensity of the immunoreactivity. It was perfumed by multiplying the percentage of the stained cells (from 0-100%) by intensity of the staining (absence=0, weak=1, medium=2 and strong=3).

2.5 Statistical Analysis

- The paired T-test was used to compare the relative quantitative PCR results of primary and secondary CRC tumours. $p < 0.05$ was considered statistically significant.
- Spearman correlation, r, test was performed in order to determine the correlation between the qPCR data for the target genes.
- Tumours were considered to show amplification if the relative quantitative value (RQ) was ≥1.5 and any tumour with a RQ of less than 1.5 were considered as no amplification. The amplification cut off was obtained as explained in Chapter 3.2.3.
- Categorical data were tested for association using a two sided Fisher's exact test (p value of two-side with Bonferroni

correction for multiple testing if appropriate). All statistical analysis were carried out by using SPSS v.21 and in all cases a probability value of $p < 0.05$ was considered statistically significant.

- All graphs and statistical analysis of the functional analysis were produced and analysed by GraphPad-Prism software.
- Two way-Anova was used to assess statistical significant of proliferation assay. Unpaired two tailed T-test was performed.
- The frequencies of the staining and all graphs were produced using SPSS software. Statistical test used in order to measure the level of the agreement between the staining of different tumour sites.
- Kappa test was performed by using SPSS software the significance was considered when p value is less than 0.05.

3 Chapter Three: DNA Copy Number Evaluation of 20q Genes in Colorectal Cancer and Liver Metastasis

3.1 Introduction

Traditionally, genomic instability in CRC has been classified in two types, chromosomal instability (CIN) and microsatellite instability (MSI). The former is the most common genetic defect observed in patients with CRC. It has been identified in approximately 85% of all cases (Grady and Carethers, 2008a, Ilyas et al., 1999, Jass, 2007, Fearon, 2011a).

CIN is generally detected by the presence of aneuploidy (Lengauer et al., 1997). CRCs with MSI are distinct. MSI results in the loss of mismatch repair genes' function. Generally, it appears from genetic aberrations (mutations or epigenetic inactivation) in one of four genes (MLH1, MSH2, PMS2, and MSH6) (Abdel-Rahman et al., 2006, Borresen et al., 1995, Thibodeau et al., 1993). The loss of mismatch repair function leads to a failure to repair base-pair mismatches and insertion / deletion (indel) mutations resulting in increased mutation rate.

A variety of older studies, before the identification of the MSI genotype, have shown that 11–68% of all cases of CRC are diploid or near diploid (Armitage et al., 1991, Flyger et al., 1999, Heimann et al., 1990, Tang et al., 1995). Given that MSI will account for 10-15% of diploid CRCs, this would suggest that some of the microsatellite stable (MSS) tumours are likely to be diploid and therefore not CIN. Our group has shown that 43% of MSS tumours are neither MSI nor CIN (Fadhil et al., 2014). These have been termed as Microsatellite and Chromosome Stable (MACS) CRCs and there is a strong possibility that MACS-CRCs might be a third genetic type of CRCs (Silver et al., 2012).

In CIN-CRCs, several deletions in chromosome 5, 18q, or 17p and gains of chromosome regions 8q, 13q, and 20q have been reported (Rowan et al., 2005). Furthermore, the 20q amplification was confirmed by using another technique, high-resolution SNP array (Sayagués et al., 2010a, Jasmine et al., 2012a, Andersen et al., 2007a). Analysis of DNA copy number changes at the gene level by multiplex ligation-dependent probe amplification (MLPA) and fluorescence in situ hybridization (FISH) have also shown that in CRC, 20q13 and 20q11 are frequently amplified (Postma et al., 2005a, Nanashima

et al., 1997a). In addition, 20q amplification has been identified in several CRC cell lines Table 3-1.

About 60 to 70% of patients with CRC who die from CRC have liver metastasis. For patients with non-resectable CRC liver metastases, the overall survival is only 2 years with the use of targeted drugs. However, of CRC cases with resectable liver metastasis approximately 30% survive for 5 years and 20% survive for 10 years (Abdel-Misih et al., 2009a).

Table 3-1. CRC cell lines that present with 20q amplification
CGH: Comparative Genomic Hybridization, aCGH: array Comparative Genomic Hybridization.

CRC cell lines	Method	Reference
R1	CGH	(Rooney et al., 2001a)
H630	CGH	(Rooney et al., 2001a)
HT29	CGH and aCGH	(Rooney et al., 2001a, Sillars-Hardebol et al., 2011a)
CACO2	CGH and aCGH	(Andersen et al., 2007a, Sillars-Hardebol et al., 2011a)
BE	CGH	(Andersen et al., 2007a)
LOVO	CGH	(Andersen et al., 2007a)
SW480	aCGH	(Sillars-Hardebol et al., 2011a)

As far as CRC liver metastasis is concerned, 20q amplification is also frequent in patients with CRC who developed liver metastasis. CGH investigations reported the occurrence of 20q gains in liver metastatic CRC (Aragane et al., 2001a, Korn et al., 1999a), specifically at the 20q13.1 and 20q13.2 sub-bands (Korn et al., 1999a). The meta-analysis study demonstrated that approximately 73% of CRC liver metastasis showed 20q amplification which was more frequent than primary tumour(Diep et al., 2006a). Other recent studies using either High-Resolution SNP Array or aCGH techniques also showed the gain of 20q and its correlation with CRC liver metastases. The 20q amplification is more frequently reported in primary tumours cases with liver metastasis than non-metastasised cases (Sayagués et al., 2010a). Nevertheless, the 20q amplification was not different in liver metastasises compared to the primaries (Bruin et al., 2010a, Munoz-Bellvis et al., 2012), which agreed with our aCGH data.

Our aCGH data in a series of 20 CRC specimens and their matched liver metastasis specimens indicated the amplification of 20q, particularly the 20q13 cyto-band. However, there was no difference found between 20q amplification in primaries and their liver metastasis. This is not consistent with other studies which show more frequent 20q amplification in liver metastasis compared to primary tumour.(Jasmine et al., 2012a, Postma et al., 2005a, Hidaka et al., 2000a). Therefore, the aim of this study is to develop a qPCR based methodology to test for 20q amplification and then use that methodology to validate our results in the 20 microdissected CRC specimens and their matched liver metastasis specimens and to test another series of 103 CRC cases to ascertain the frequency of 20q amplification. In addition, the association of 20q amplification was studied in CRC specimens with *KRAS, PIK3CA, TP53*, and ploidy status.

The principle of our qPCR assay was that, if a region was amplified, then all the genes in that region should be amplified and to a similar level. Since 20q13 is a very “gene-rich” region, we were able to identify 6 closely located genes - *CSE1L*, *PTPN1*, *PREX1*, *ADNP, ELMO2,* and *PTGIS* which spanned a region of 5 Mb Figure 3-1 to use for our assay

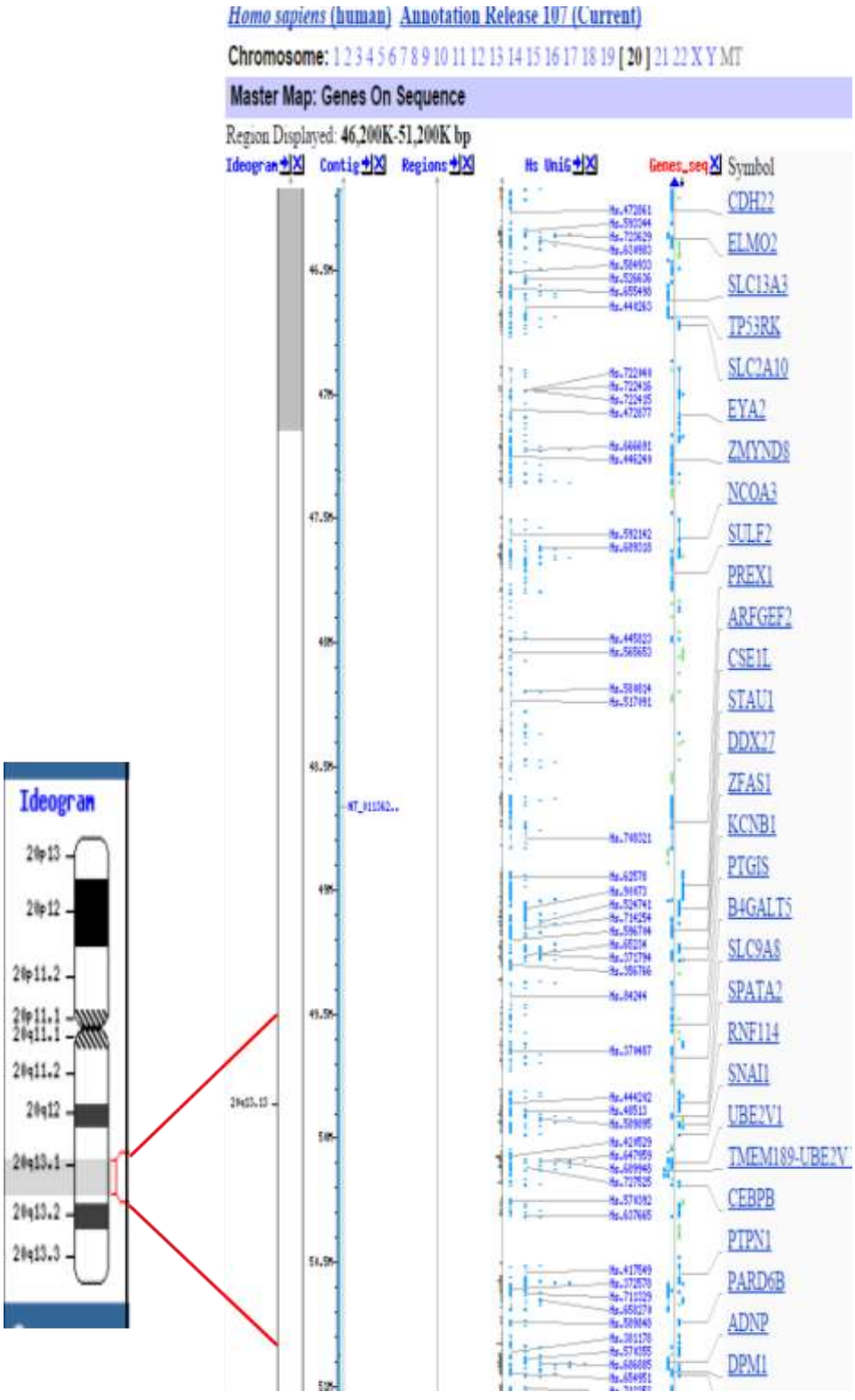


Figure 3-1 Ideogram and high resolution map of Chromosome 20q13

3.2 RESULTS

3.2.1 Evaluation of the FFPE sample quality

DNA quality assurance of both sets had been previously performed by member of our group, Dr Wakkas Fadhil. For validation purpose, the quality of the DNA materials of the 20 microdisscted CRC specimens and their matched liver metastasis specimens was tested by multiplex PCR using four pairs of primers amplifying 100, 200, 300, 400 bp genomic regions of the *GAPDH* gene. DNA quality of 15 out of 20 (75%) primary tumours and 15 out of 20 (75%) secondary tumours showed minimum three bands at the expected sizes. The DNA quality of 103 CRC series had been tested previously (Fadhil et al., 2014). On the other hand, samples showing no amplification or only one band on gel electrophoresis were considered of insufficient quality for qPCR analysis and were omitted from the subsequent analysis Figure 3-2.

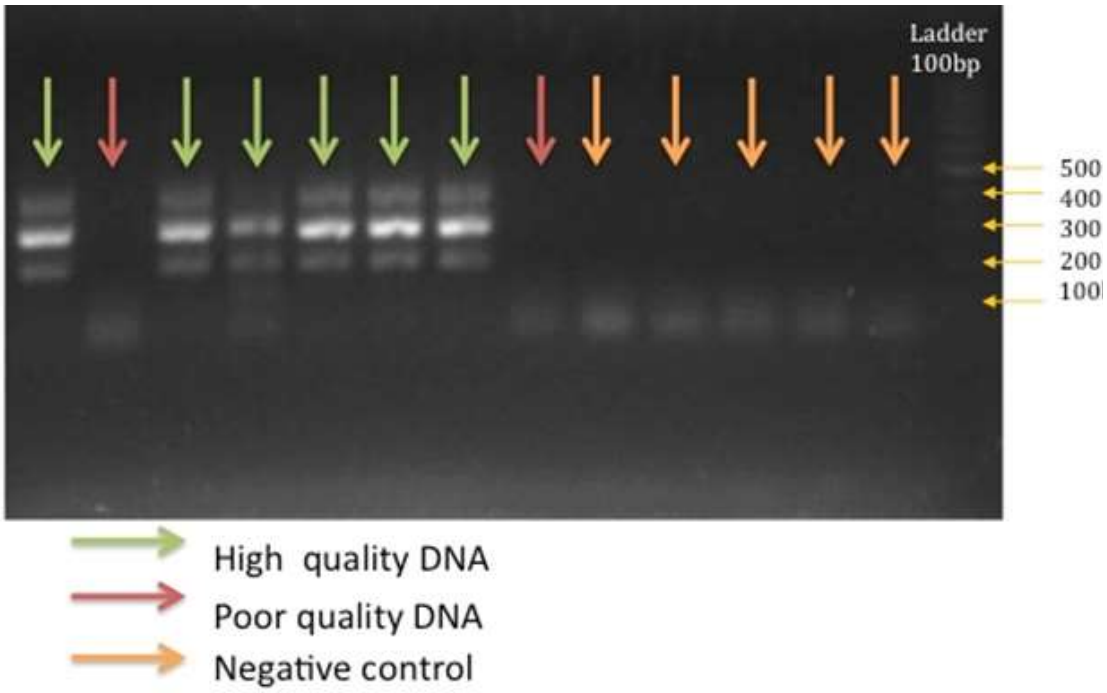


Figure 3-2. Quality of DNA from (FFPE) tissues.
A multiplex PCR was performed and the PCR products were analysed using 2% gel electrophoresis. DNA from the FFPE samples produced bands of 200, 300, and/or 400 bp. (Arrowed in green) Samples of low quality produced only a single band or no PCR amplification and they were considered of poor quality for qPCR analysis (Arrowed in red). The negative control (arrowed in orang) showed no amplification: from left to right primers for GAPDH 100, 200, 300 and 400bps and the fifth lane showed the multiplex primers did not show amplification. DNA quality of 15 out of 20 (75%) primary tumours and 15 out of 20 (75%) secondary tumours showed minimum three bands at the expected sizes.
.

3.2.2 Primer optimisation

Gradient-PCR was conducted to determine the ideal annealing temperature for all oligonucleotides. A representative example of Gradient PCR for ELMO2 primers optimisation showed in Figure 3-3. Optimum amplification was achieved when using 60°C for all primer pairs and a single band was seen on gel electrophoresis. Since qPCR is dependent on measuring fluorescence, melting curve analysis was also performed to ensure that the primers were truly amplifying. Thus; these primers were suitable for qPCR (Figure 3-4).

It was also important to determine the primers efficiency prior to performing qPCR, since variation in primer efficiency between the target gene and the housekeeping/reference gene is an important confounder that may raise a false positive/negative result. Therefore, standard curves were obtained in order to evaluate the primers efficiency. The efficiency for all primers was calculated using serial dilutions of a calibrator (a DNA sample pooled from 10 non-tumour colonic tissues). Amplification plots of all primers were illustrated in Figure 3-5 to Figure 3-11and Figure 3-12. All primer pairs showed efficiencies ranging from 97–110%. The R2 values were close to 1.0 (ideal R2) and the slope values were close to -3.32 (Table 3-2). The amplification efficiency of the primers of interest was nearly the same as the reference gene's primers. Therefore, we could rule out confounders that could affect our experiment.

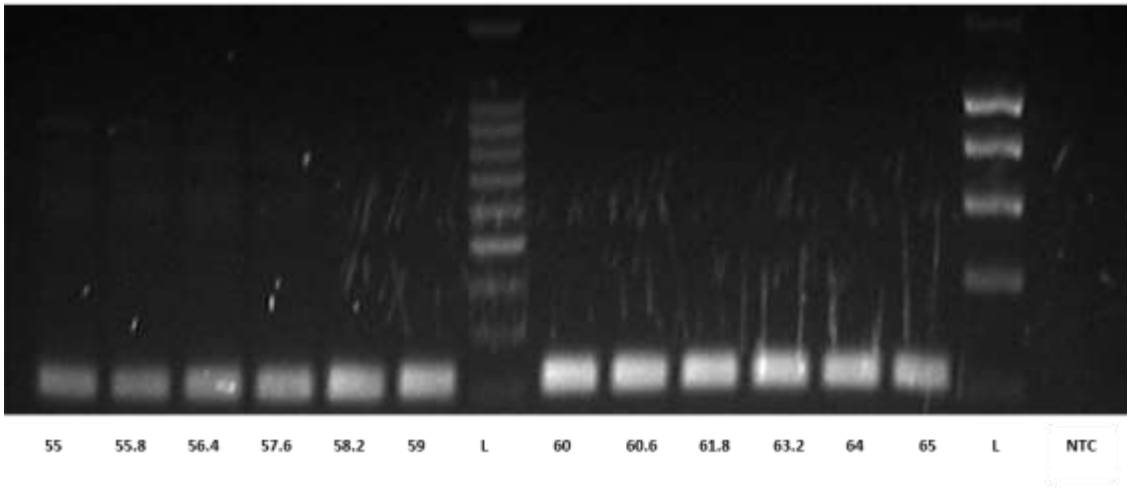


Figure 3-3 agarose gel electrophoresis gradient temperature for ELMO2 primers optimisation.

In order to ascertain the optimal annealing temperature, each primer pair was initially tested on a gradient PCR machine (Primus96 advanced® Gradient). A PCR reaction with a 12 temperature gradient at the annealing stage was performed (usually with a temperature range of 55°C – 65°C). The reaction was undertaken in a final volume of 12.5µL in which each reaction contained X1 SensiFast SYBR Lo-ROX PCR Master Mix (Bioline), forward and reverse primers pair at 250nM, 10ng template DNA and water to complete the total volume. A PCR reaction with a 12 temperature gradient at the annealing stage was performed (usually with a temperature range of 55°C – 65°C). The reaction was undertaken in a final volume of 12.5µL in which each reaction contained X1 SensiFast SYBR Lo-ROX PCR Master Mix (Bioline), forward and reverse primers pair at 250nM, 10ng template DNA and water to complete the total volume. Templet used non-tumour colonic FFPE genomic DNA sample (20ng), 60°C gave the most intense band.

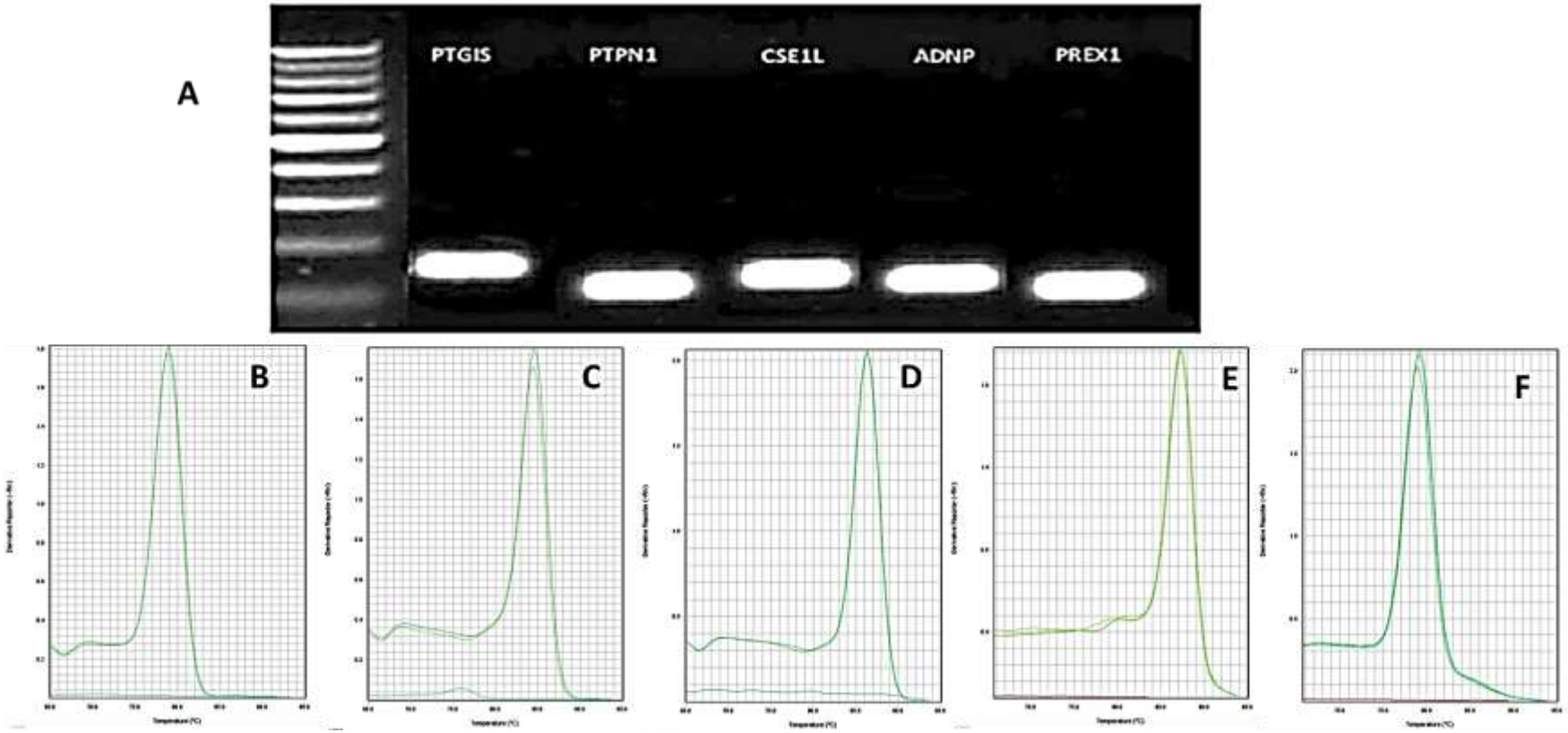


Figure 3-4. Primer optimisation, thus, these primer were suitable for qPCR analysis.

(A) 2% Gel electrophoresis A PCR reaction with a 60°C annealing temperature. The reaction was undertaken in a final volume of 12.5µL in which each reaction contained X1 SensiFast SYBR Lo-ROX PCR Master Mix (Bioline), forward and reverse primers pair at 250nM, 10ng template DNA and water to complete the total volume. Bands were showing that all primers amplified the expected size. (B-F) The melting curve was obtained to show that all primer pairs were forming a single peak. Melting data can be used to check product specificity and the melting protocol consisted of one cycle of 95°C for 15 s, 65°C for 45 s at maximum ramping speed, then gradual heating (ramping speed rate at 1%) to 95°C. The melt curve was obtenied by X-axis: showed the temperature. Y-axis : showed Derivative Reporter (-Rn).

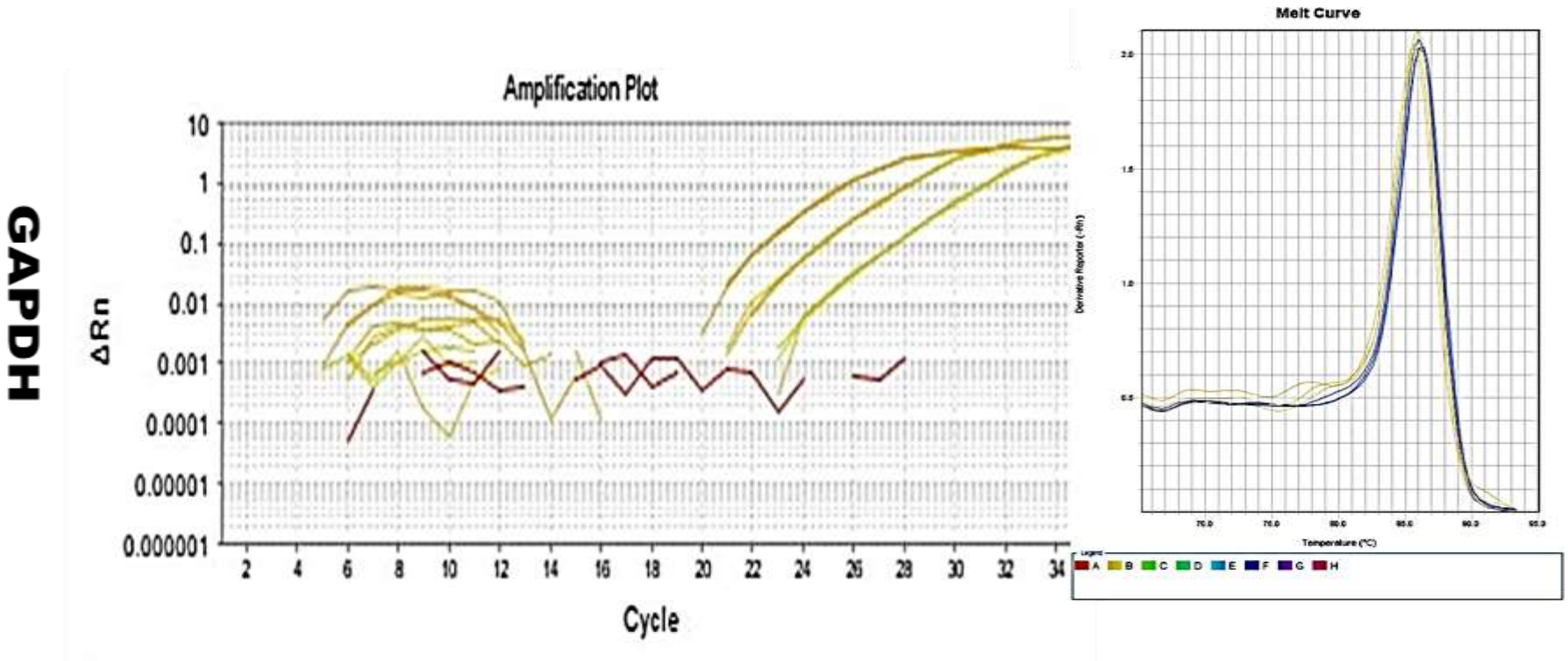


Figure 3-5 Amplification plot of GAPDH primers and Melt Curve analysis

Amplification plots for GAPDH showed the ΔRn against the cycle number. The amplification plot showed the quality of the primer pair to produce a steady amplification in different sample concentration. PCR was performed in a total volume of 12.5 µl and consisted of X1 GoTaq® qPCR Master Mix (Promega), forward and reverse primers pair at 200nM, and water. The PCR reaction was performed in triplicate using the following PCR condition: 95°C for 5 min followed by 35 cycles at 95°C for 10 s, 60°C for 30 s and 77°C for 10 s. Melting curve used to check product specificity. This ligand explain this figure and figures 3-6 to 3-11

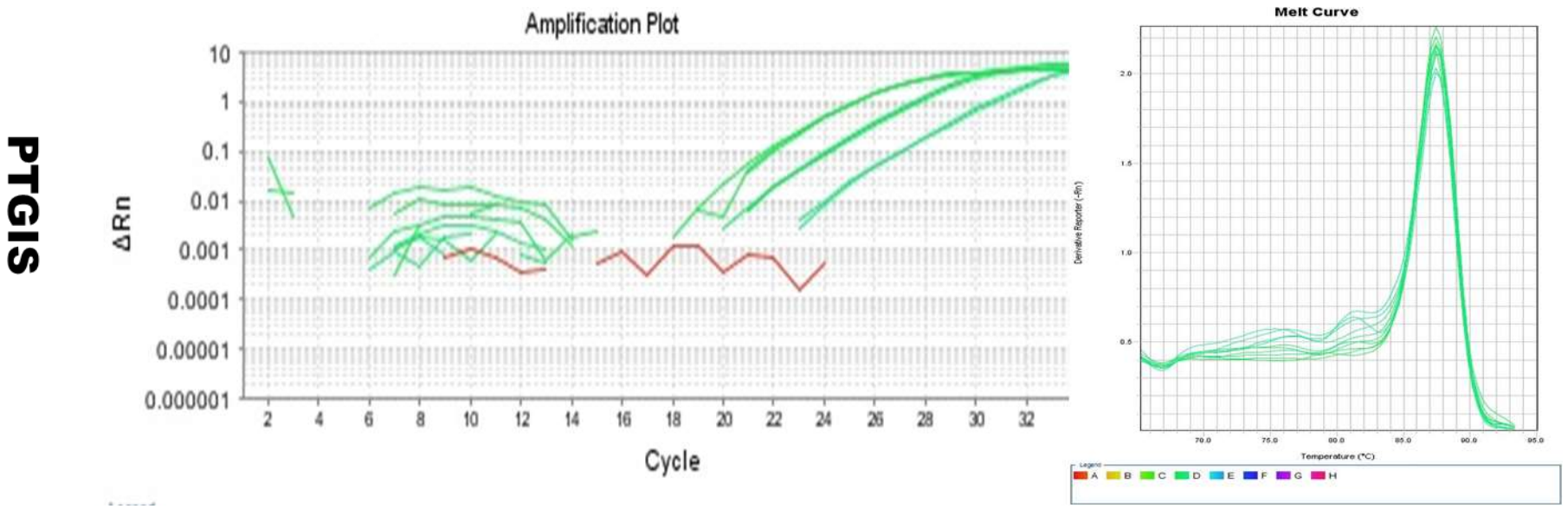


Figure 3-6 Amplification plot of PTGIS primers and Melt Curve analysis
PCR reaction for PTGIS showed Amplification plots and Melt curve. The details explained in ligand of figure 3-5.

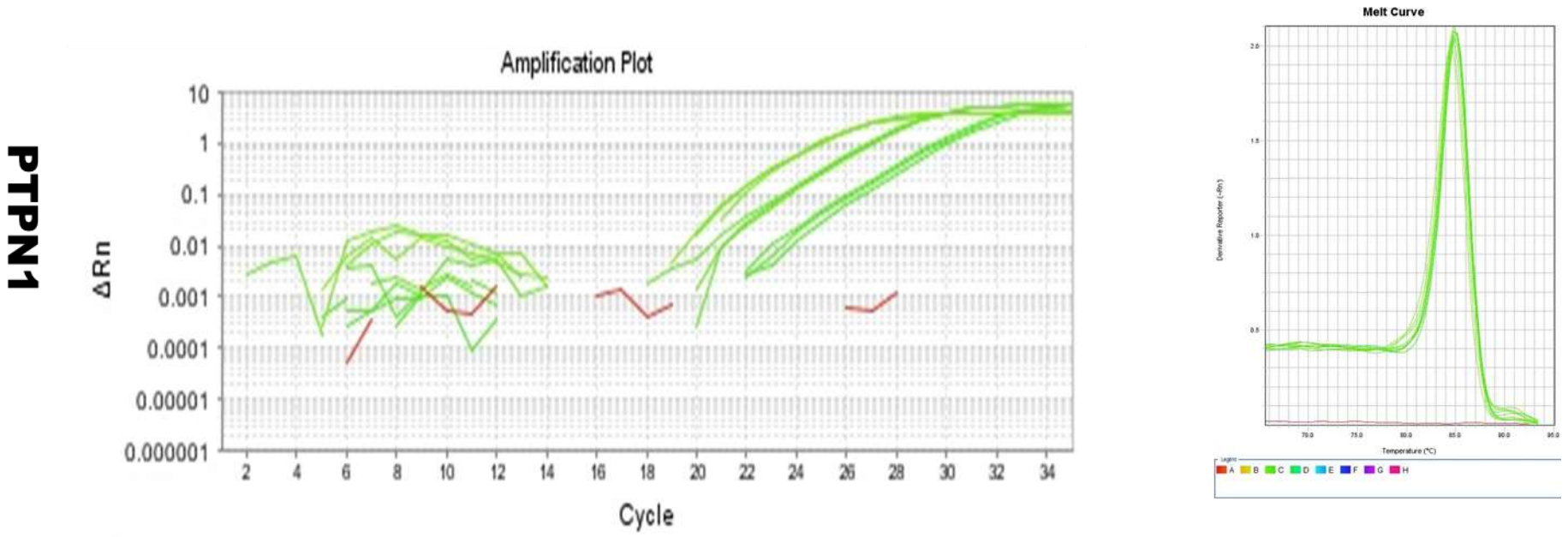


Figure 3-7 Amplification plot of PTPN1 primers and Melt Curve analysis
PCR reaction for PTPN1 showed Amplification plots and Melt curve. The details explained in ligand of figure 3-5.

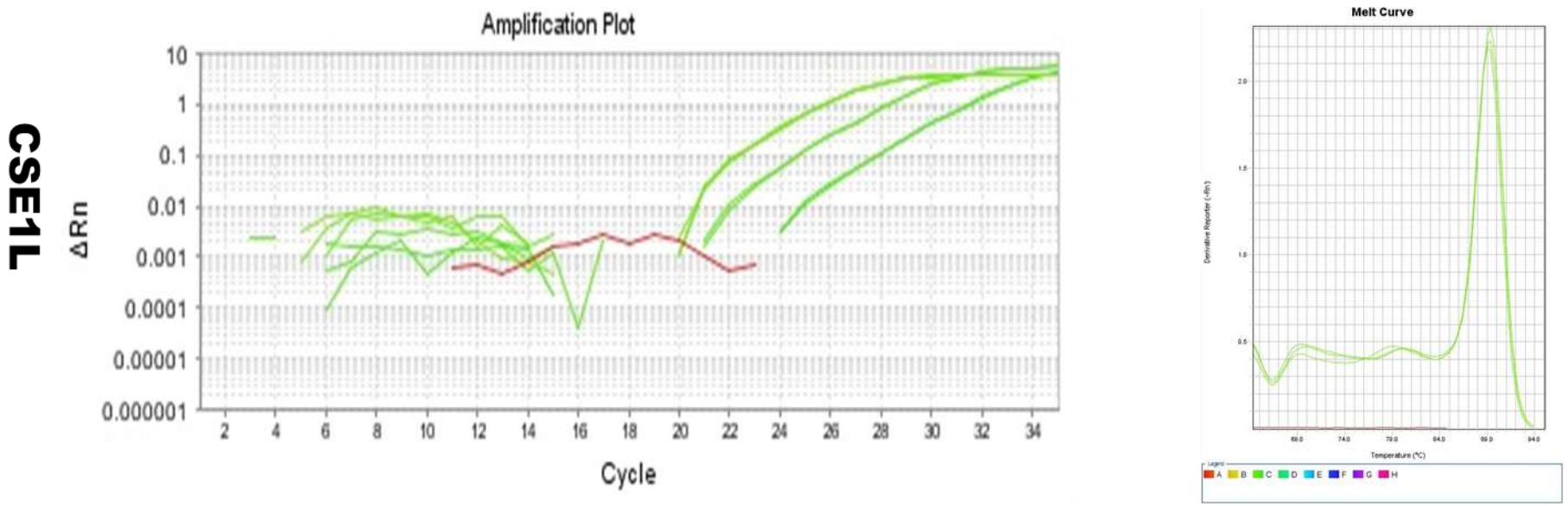


Figure 3-8 Amplification plot of CSE1L primers and Melt Curve analysis
PCR reaction for CSE1L showed Amplification plots and Melt curve. The details explained in ligand of figure 3-5.

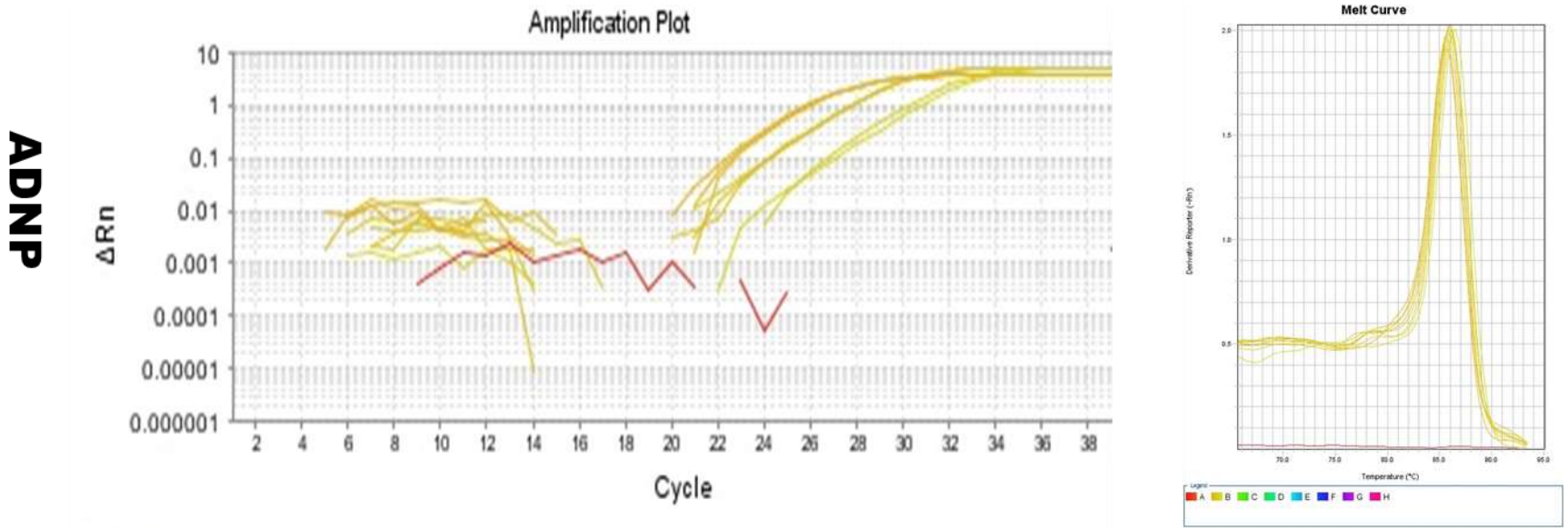


Figure 3-9 Amplification plot of ADNP primers and Melt Curve analysis
PCR reaction for ADNP showed Amplification plots and Melt curve. The details explained in ligand of figure 3-5.

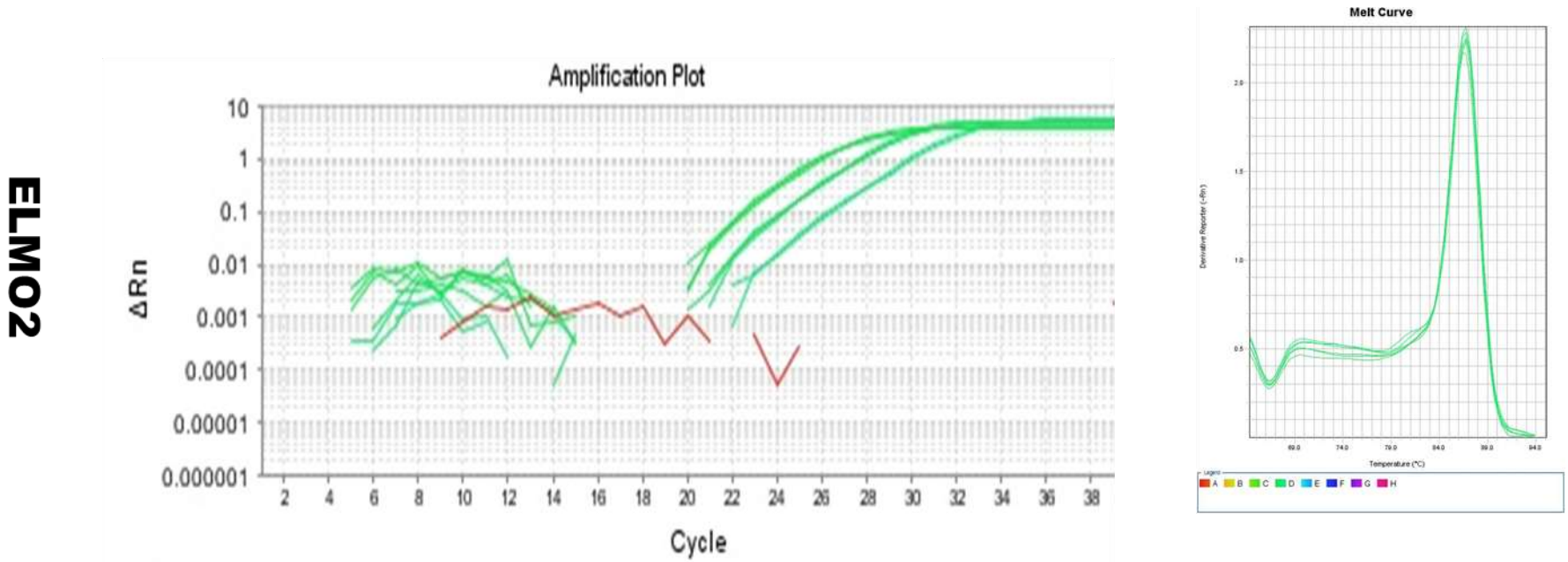


Figure 3-10 Amplification plot of ELMO2 primers and Melt Curve analysis
PCR reaction for *ELMO2* showed Amplification plots and Melt curve. The details explained in ligand of figure 3-5.

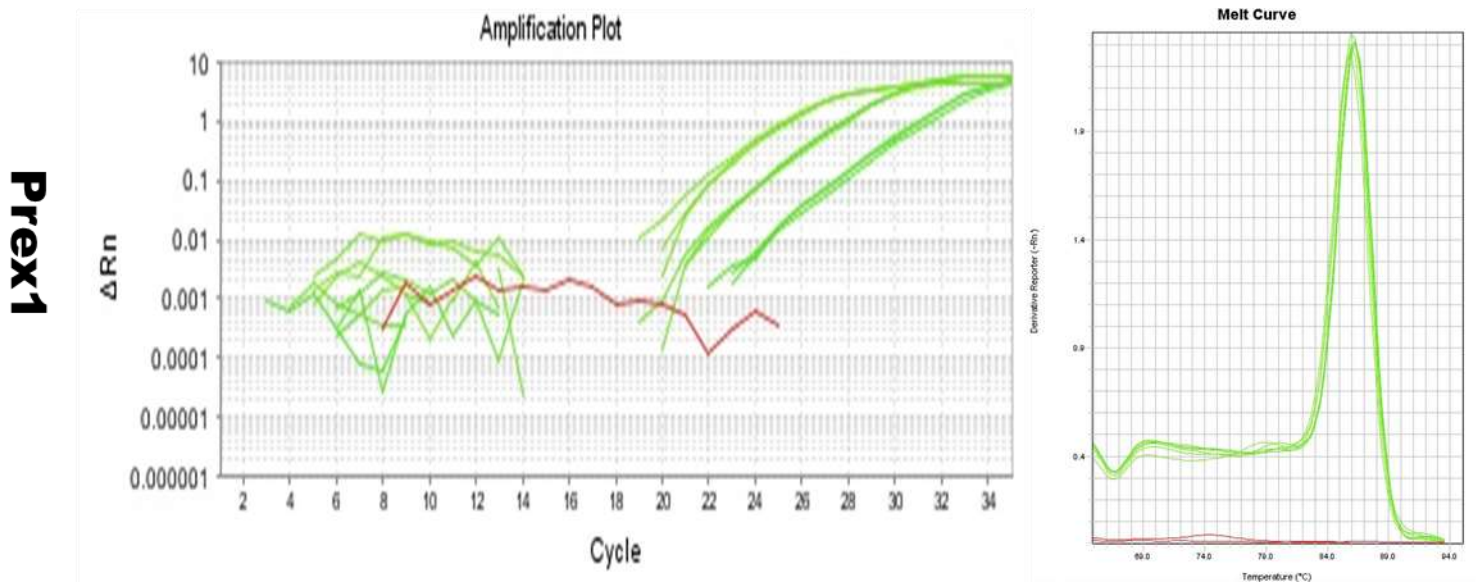


Figure 3-11 Amplification plot of PREX1 primers and Melt Curve analysis
PCR reaction for PREX1 showed Amplification plots and Melt curve. The details explained in ligand of figure 3-5.

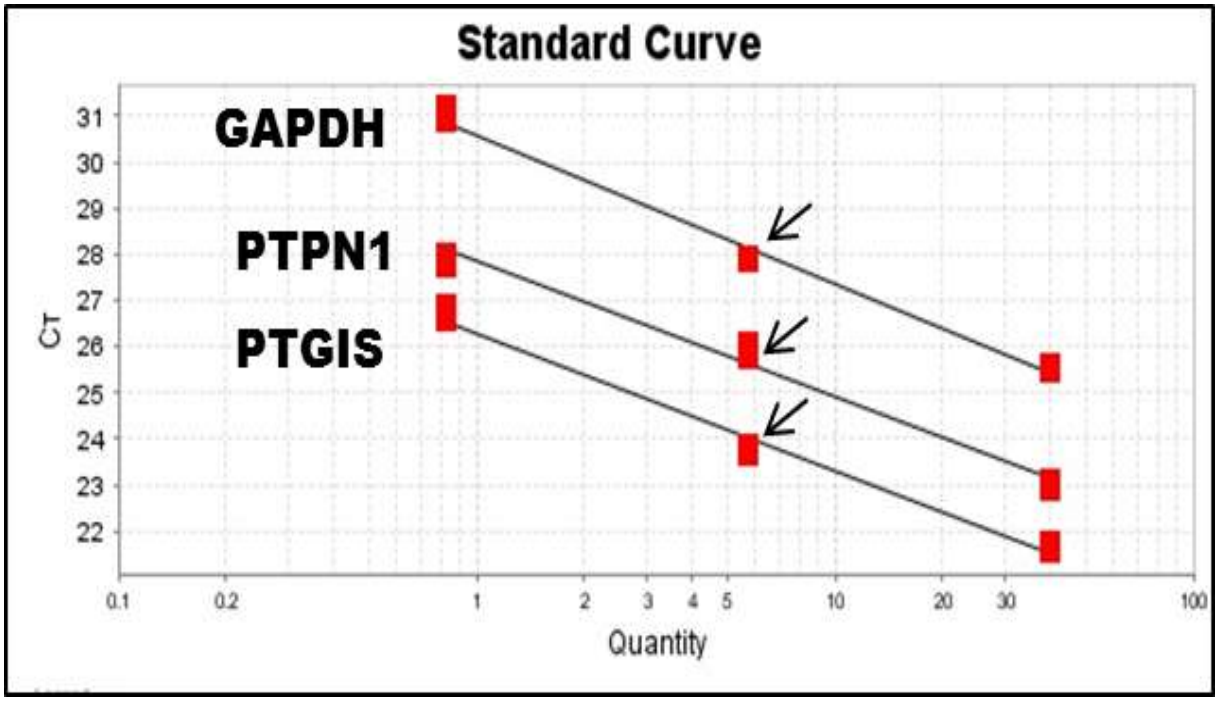


Figure 3-12. A representative example of Linear regression slope of serial dilution of the reference sample.

Serial dilutions of a10 pooled DNA non-tumour FFPE colonic tissue sample were used to calculate *GAPDH*, *PTPN1,* and *PTGIS* primer pairs' efficiency. The primers efficiently amplified the template at 5.71 ng (Arrowed). Thus, in the comparative experiment, the amount of DNA samples used was 5.71 ng. In order to perfom qPCR, it was important to perform standard curve initially in order to evaluate the primers' efficiency. Three serial dilution (1:7) points were used to set up the standards. Primer pairs with efficiencies ranging from 95%–105% were used in subsequent analysis. Standard curve was performed on ABI 7500 Fast System (Applied Biosystems).

Table 3-2. Primer pair efficiencies.

Primers pair efficiencies was acquired by performing standard curve. Standard curve was obteind a real time PCR for a serial dilutions of a10 pooled DNA non-tumour FFPE colonic tissue sample. Primer pairs with efficiencies ranging from 95%–105% were used in subsequent analysis. Standard curve was performed on ABI 7500 Fast System (Applied Biosystems)

Genes	EFF	R2	Slope
GAPDH	97.537	0.99	-3.382
PTPN1	108.3	0.991	-3.137
PTGIS	109.261	0.986	-3.118
CSE1L	105.108	.994	-3.205
ADNP	101.23	.971	-3.293
PREX1	101.209	0.998	-3.293
ELMO2	103.23	0.995	-3.312

3.2.3 Amplification threshold in qPCR

Thirteen normal colon DNA samples were used as templates to set the amplification threshold (Figure 3-13). Relative quantitative PCR was performed using non-tumour colonic DNA samples derived from FFPE tissues. *GAPDH* was used as the endogenous control, while the calibrator DNA sample was prepared by pooling DNA from additional 10 non-tumour colonic FFPE samples. The relative quantitative data from 6 targeted genes located on 20q (*CSE1L, PTPN1, PREX1, ADNP, ELMO2, and PTGIS*) showed that RQ values ranging from 0.89 to 1.13 RQ, which demonstrated that RQ ≥1.5 can be considered as an amplification threshold.

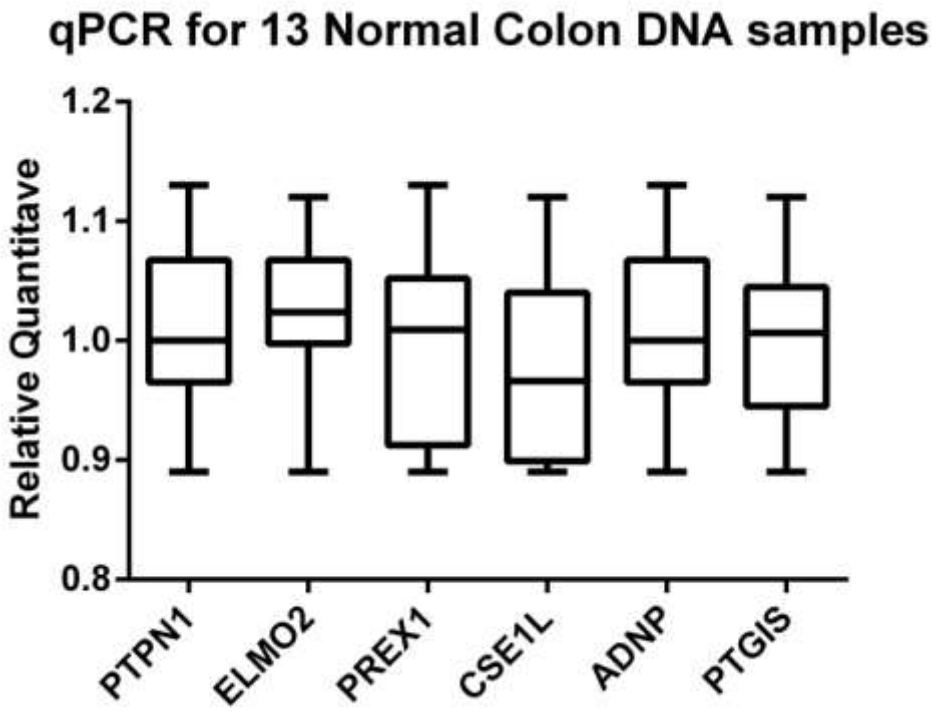


Figure 3-13. Quantitative (q) PCR results from the normal colon DNA samples.

qPCR analysis was performed using *PTPN1, PTGIS, PREX1, CSE1L, ADNP* and *ELMO2* genes to screen the 20q status in 13 normal colon specimens in triplicate. Relative quantitative data showed that all cases did not exceed the 1.13 RQ. Calibrator (Cal) is a pooled DNA sample obtained from 10 non-tumour FFPE colonic tissue samples. This results allowed to set an 20q amplification at RQ of 1.5. qPCR was performed on ABI 7500 Fast System (Applied Biosystems). . All data are expressed mean ± SD.

3.2.4 Role of 20q in CRC liver metastasis

Array CGH data of 15 CRC and their matched liver metastasis specimens demonstrated abnormal DNA copy number profiles. The most frequent amplification was noted in the 20q aCGH data. However, 20q13 amplification was not different in both primary and metastasised tumours. Therefore, this study was to validate those data. Quantitative PCR was performed to test the 20q amplification in a series (*n = 15*) of CRC specimens and their matched liver metastases (Table 3-3).

GAPDH gene was used as the endogenous control/ reference gene and the reference DNA sample (calibrator) was pooled from 10 non-tumour colonic tissue samples. At the end of the qPCR reaction the dissociation curve was determined to test the specificity of the PCR products (Figure 3-14). Then, co-amplification of the 6 genes was tested by performing Spearman correlation test (r). This analysis was performed by testing correlation of the relative quantitative data from each gene to *ADNP*. There was significant moderate to strong positive correlation between them in which the r values ranged from 0.543 to 0.874 Table 3-3. This positive correlation of fold changes in the target genes indicated that these genes were co-amplified.

The frequency of 20q amplification in the primary tumours (66.7%) was not different from the frequency of 20q amplification which was detected in the secondary tumours (60%), as listed in Table 3-3. However, in two cases the relative quantitative value of the primary tumour was higher than that of the secondary tumour (Figure 3-14). Furthermore, there was one case showed amplification in liver metastasis but not in the primary tumour. This indicates that 20q amplification was not driving CRC liver metastasises in this set of matched primary and liver metastasised tumour.

The aCGH data, then, were compared to the qPCR results (Table 3-4). The aCGH data showed 20q as frequently amplified region amplified in primaries CRC and their corresponding metastases (17 out of 30 subjects). A high degree of concordance was found between aCGH and qPCR, of data (28/30 cases, 93%). In addition, Kappa test high degree of agreement (0.862) between the two sets of

data. Thus, qPCR results validated the aCGH data regarding the 20q amplification status in both primaries and their liver metastases

Table 3-3 the Relative quantitative data generated from qPCR analysis of 15 CRCs and secondary tumours.

Cases with more than 4 genes' RQ exceeded 1.5 considered 20q amplified. P: Primary. S: Secondary RQ: relative quantitative value. ** The Spearman correlation test was significant at the 0.01 level (2-tailed).

Sample	PTGIS	CSE1L	ADNP	PTPN1	PRXE1	ELMO2	Number of Amplified genes
P1	2.38	2.45	1.55	1.72	1.8	2.36	6/6
S1	0.54	1.12	0.92	1.07	1	1.14	0/6
P2	2.42	1.7	1.73	1.89	2.2	2.46	6/6
S2	0.98	0.72	0.76	0.91	1.11	1.32	0/6
P3	1.21	0.99	1.22	1.27	1.19	1.43	0/6
S3	1.87	1.09	1.81	1.55	1.8	2.54	5/6
P4	3.04	2.42	2.4	2.4	2.56	2.29	6/6
S4	2.53	2.12	1.88	2.09	2	2.1	6/6
P5	4.02	3.15	2.66	1.95	3.34	2.59	6/6
S5	4.12	2.27	2.99	2.48	3.62	3	6/6
P6	0.9	1.49	1.08	1.33	1.33	1.51	1/6
S6	1.34	1.26	1.46	1.6	1.12	1.36	1/6
P7	1.93	3.07	2.79	2.89	3.97	2.2	6/6
S7	1.63	1.51	1.17	1.58	2.11	3.23	5/6
P8	1.94	3.07	2.79	2.89	3.97	3.96	6/6
S8	1.63	1.65	1.46	1.58	2.11	2.71	5/6
P9	1.48	1.43	1.31	1.31	2.36	0.83	1/6
S9	1.12	0.91	0.98	1.01	2.16	1.2	1/6
P10	4.09	1.01	1.76	2.12	2.97	4.71	5/6
S10	2.56	1.09	1.54	1.77	1.76	3.97	5/6
P11	1.49	1.17	0.64	0.8	0.69	1.93	1/6
S11	0.99	1.81	0.98	0.99	1	1.78	2/6
P12	2.3	2.44	1.25	1.58	3.57	2.2	5/6
S12	2.87	1.58	1.4	1.59	2.02	3.29	5/6
P13	1.61	2.41	1.23	1.92	2.88	3.86	5/6
S13	2.45	1.92	1.48	1.72	1.67	2.91	5/6
P14	0.64	1.81	1.28	1.69	0.99	1.46	2/6
S14	1.47	1.98	1.27	1.22	1.15	1.11	1/6
P15	3.54	2.79	1.46	2.06	2	3.13	5/6
S15	4.02	1.55	1.82	2.8	2.1	1.23	5/6
Correlation co-efficient of RQ data	**0.7617 P< 0.0001**	**0.6286 p=0.0027**	**1**	**0.8753** P< 0.0001**	**0.0.6227 P0.0002**	**0.5378 P= 0.0132**	
Total:	20q amplified in Primary CRC: 10/15 (66.7%) 20q amplified in liver metastasised CRC: 9/15 (60%)						

Table 3-4. Chromosome 20q13 amplification status assessed by aCGH and qPCR.

The aCGH previously performed and only 20q13 status was analysed. The qPCR was performed on 15 CRC and their liver metastasised on six genes located on 20q13. Then the data was analysed by delta-delta CT method. The level of agreement of 20q amplification between aCGH and qPCR methods was high. The Kappa test value was 0.862, which indicated a strong agreement between the two methods.

Cases	aCGH 20q13 amplification	qPCR 20q13 amplification
1P	YES	YES
1S	No	No
2P	YES	YES
2S	No	No
3P	No	No
3S	YES	YES
4P	YES	YES
4S	YES	YES
5P	YES	YES
5S	YES	YES
6P	No	No
6S	No	No
7P	YES	No
7S	YES	No
8P	YES	YES
8S	YES	YES
9P	No	No

9S	No	No
10P	YES	YES
10S	YES	YES
11P	No	No
11S	No	No
12P	YES	YES
12S	YES	YES
13P	YES	YES
13S	YES	YES
14P	No	No
14S	No	No
15P	YES	YES
15S	YES	YES

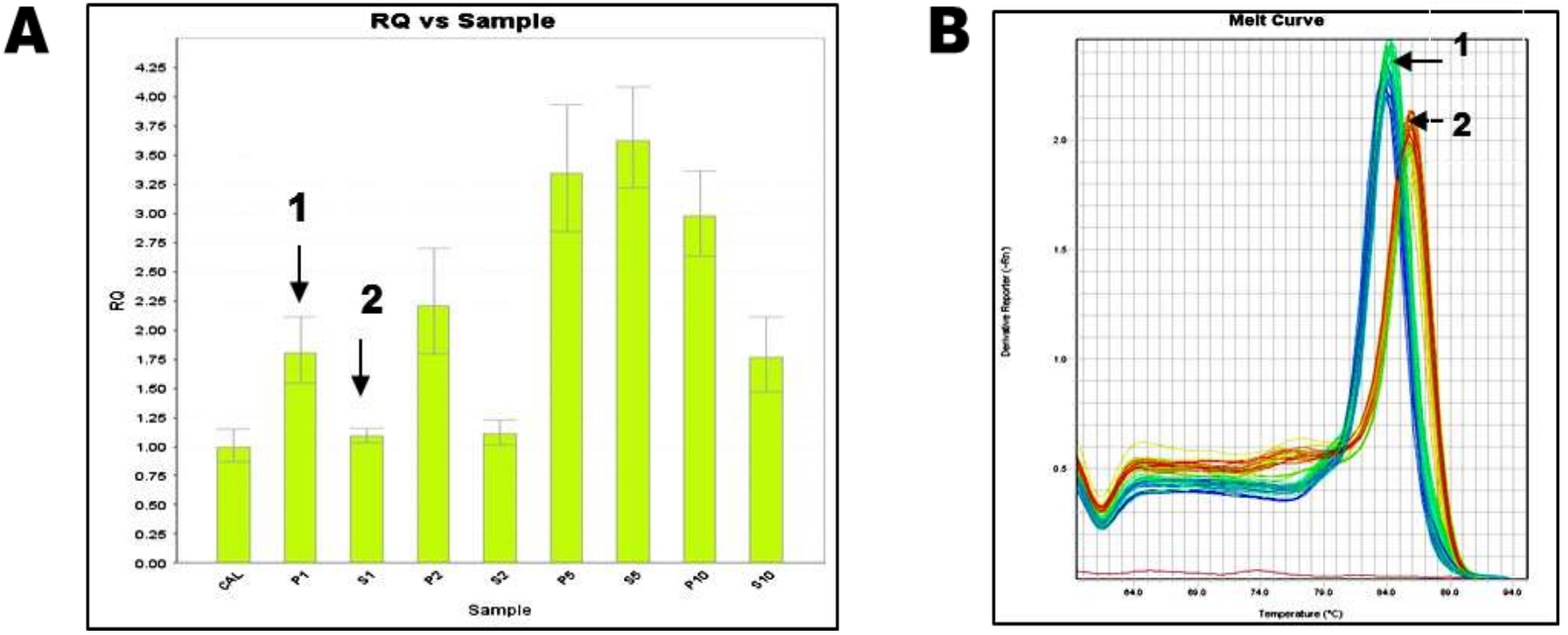


Figure 3-14. A representative example of Relative quantitative (RQ) results and melting curve analysis post the real-time PCR.

(a) The qPCR analysis showed the relative quantitative data of primary and secondary tumours in triplicate. In some cases, the primary tumour RQ (Arrowed in 1) was higher than that of the secondary tumours (Arrowed in 2). (b) The melting curve, post-real-time PCR, was obtained to assess the quality of the qPCR reaction. As expected, the quality was good for both *GAPDH* (the reference gene arrowed in 1) and *PTGIS* (Arrowed in 2).

3.2.5 Role of 20q amplification in driving CRC

Flow cytometry data and mutation profiles were not available for 4 patients and 7 patients presented with MSI-CRC. These patients were excluded from the analysis. PTPN1 and ELMO2 were nominated to study the 20q status in a series of 103 cases. A strong positive correlation between PTPN1 and ELMO2 qPCR data was observed for relative quantitative values, Spearman of R = 0.911, p<0.0001(Figure 3-15). Of the 103 CRCs tested, a total of 53 (51.4%) were 20q amplified whilst 50(50.6%) were not 20q amplified. In order to investigate further the role of 20q amplification in CRC, tumour genetic profile and ploidy status of those 103 CRC specimens were studied in relation to their 20q status. DNA content of 103 primary CRC was analysed using flow cytometry, as previously described (Fadhil et al., 2014). The ploidy status was characterised and 62 (60%) specimens presented aneuploidy (i.e., CIN-CRCs), whilst 41 (40%) were diploid or near-diploid (i.e., MACS-CRCs). Therefore, a high proportion of the tumours tested were of the CIN-CRCs genotype. In studying molecular differences between CRC cases, two subgroups were observed, one was considered as 20q amplified (20qAmp-CRC) and the other was 20q stable (20qSt-CRC). The statistical analysis showed that the frequency of 20q amplification was higher in CIN-CRCs than in the chromosomal stable tumours, but this association did not reach the level of statistical significance were not associated with 20qAmplified tumours (P = 0.046), in which 70% of 20qAmplified-CRCs were aneuploid. Thus, more than half of the 20q amplified CRCs might develop through the CIN-CRC pathway.

The genetic profile of 103 CRC tumour specimens for the presence of mutations in *KRAS*, *PIK3CA*, and *TP53* genes was previously determined (Table 3-5). With regard to the association of 20q with the mutation profile, it was found that the mutation distribution for those genes was not associated with the status of 20q amplification (Table 3-5). Nevertheless, it was noted that 38/53 (72%) of 20qAmp-CRC presented *TP53* mutations (P = 0.01, Fisher exact test), while only 27/50 (54%) of the 20qSt-CRCs presented *TP53* mutation. Another point of interest was that 19/53 (36%) patients with 20qAmp-CRC presented with *KRAS* mutation, while

52% of patients with 20qSt-CRC presented with *KRAS* mutation, which could indicate that CRC tumours with 20q amplification might prefer to develop through the KRAS-independent pathway.

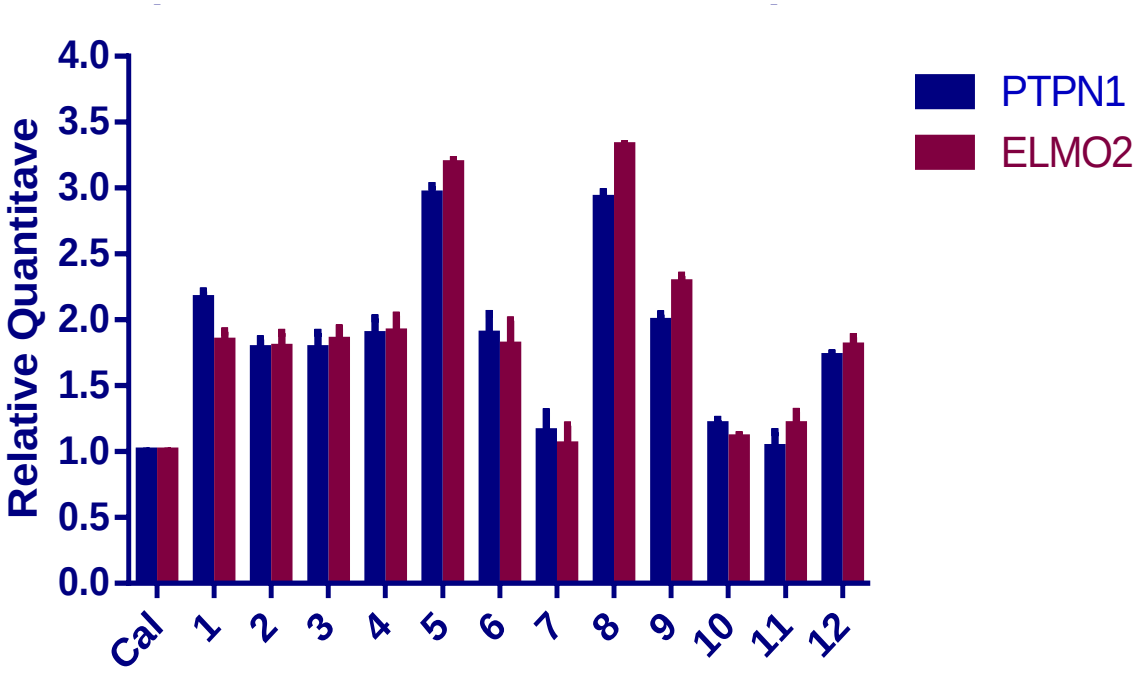


Figure 3-15. Relative quantitative (RQ) comparative threshold results of 12 patients with CRC.

The relative copy-number difference of the target gene in tumour sample against a reference calibrator sample (consisting of 10 pooled DNA samples obtained from normal FFPE colonic tissue) is provided by the 2–ΔΔCt equation. Data evaluation was performed using the ABI 7500 Fast System software and RQ software (Applied Biosystems). PCR was in triplicate using the following PCR condition: 95°C for 5 min followed by 35 cycles at 95°C for 10 s, 60°C for 30 s and 77°C for 10 s.The qPCR analysis showed the relative quantitative data of CRC primary tumours in triplicate. Samples number 1 to 6, 8, 9, and 12 exceeded the 1.5 RQ value and were considered as amplified. Samples 7, 10, and 11 were close to the calibrator (Cal) and these samples were considered as 20q stable. The error bars ±SD.

Table 3-5. Ploidy status and mutation profile of 20Amp-CRCs and 20qSt-CRCs.

The mutation for KRAS and PIK3CA was not associated with the status of 20q amplification. Ploidy status was not associated with 20q amplification in CRC cases. KRAS, PICK3CA, TP53 mutations were screened using high resolution melt curve analysis and confirmed by sanger sequencing. Cell cycle analysis was achieved by flow cytometry. Chi Square test was used and p values (after Bonferroni correction) <0.0125 were considered as statistically significant (*).

		20qAmp CRC	20qSt-CRCs		Total sample
Ploidy status	Aneuploid	37(70%)	25 (50%)	P VALUE 0.046	62 (60%)
	Diploid	16 (30%)	25 (50%)		41 (40%)
KRAS	*Mutant*	19 (36%)	26 (52%)	P VALUE 0.115	45 (44%)
	Wild type	34 (64%)	24 (48%)		58 (56%)
PIK3CA	*Mutant*	9 (16%)	6 (12%)	P VALUE 0.580	15 (15%)
	Wild type	44 (84%)	44 (88%)		88 (85%)
TP53	*Mutant*	38 (72%)	23 (46%)	P VALUE 0.010*	61 (59%)
	Wild type	15 (28%)	27 (54%)		42 (41%)

Table 3-6 molecular profile of 110 cases.

Testing for MSI and KRAS, PICK3CA, and TP53 mutation screening were performed by using high-resolution melt curve analysis. The DNA content of tumour cells by flow cytometry. 20q amplification was measured by qPCR analysis using delta-delta CT method.

MMS: Microsatellite stable, MSI: Microsatellite instability, MUT: mutant, WT: wild type. A: aneuploidy, D: diploid. 20q Amp: 20q amplified, non-Amp: 20q not amplified.

ID	PIK3CA	KRAS	P53	PLOIDY STATUS	20q STATUS
1	WT	MUT	MUT	A	non-Amp
2	MUT	WT	WT	A	20q Amp
3	WT	WT	MUT	A	20q Amp
4	MUT	WT	WT	A	non-Amp
5	MUT	MUT	WT	D	non-Amp
6	WT	WT	MUT	A	20q Amp
7	WT	WT	MUT	D	non-Amp
8	WT	MUT	WT	D	non-Amp
9	WT	WT	MUT	A	20q Amp
10	WT	MUT	MUT	D	20q Amp
11	WT	WT	MUT	D	non-Amp
12	WT	WT	MUT	A	non-Amp
13	WT	MUT	MUT	D	20q Amp
14	WT	WT	WT	A	20q Amp
15	WT	MUT	WT	A	non-Amp
16	WT	MUT	MUT	A	non-Amp
17	WT	MUT	MUT	A	20q Amp
18	WT	MUT	MUT	D	non-Amp
19	WT	MUT	WT	D	non-Amp
20	WT	WT	WT	A	non-Amp
21	WT	WT	MUT	A	20q Amp
22	WT	MUT	WT	A	non-Amp
23	WT	MUT	MUT	D	non-Amp
24	WT	MUT	WT	A	non-Amp
25	MUT	WT	MUT	D	20q Amp
26	MUT	MUT	MUT	A	20q Amp
27	WT	WT	MUT	A	non-Amp
28	WT	MUT	WT	D	non-Amp
29	WT	MUT	MUT	A	non-Amp
30	WT	MUT	WT	D	non-Amp
31	WT	WT	WT	D	non-Amp
32	MUT	WT	MUT	A	non-Amp
33	WT	WT	MUT	A	20q Amp
34	WT	WT	MUT	A	20q Amp

35	WT	MUT	MUT	D	20q Amp
36	MUT	MUT	MUT	A	20q Amp
37	WT	MUT	MUT	D	non-Amp
38	WT	WT	WT	D	20q Amp
39	WT	WT	MUT	A	20q Amp
40	MUT	MUT	MUT	D	20q Amp
41	WT	WT	MUT	D	non-Amp
42	WT	MUT	MUT	A	20q Amp
43	WT	WT	MUT	D	20q Amp
44	WT	MUT	MUT	D	20q Amp
45	WT	WT	MUT	A	20q Amp
46	WT	WT	MUT	A	non-Amp
47	WT	WT	MUT	D	20q Amp
48	WT	WT	MUT	A	20q Amp
49	WT	MUT	WT	D	20q Amp
50	WT	WT	WT	D	non-Amp
51	WT	WT	WT	A	20q Amp
52	WT	WT	MUT	D	non-Amp
53	WT	MUT	MUT	A	20q Amp
54	WT	WT	MUT	A	non-Amp
55	WT	WT	MUT	A	non-Amp
56	WT	WT	WT	D	20q Amp
57	WT	MUT	WT	A	20q Amp
58	WT	WT	WT	D	non-Amp
59	WT	MUT	MUT	D	20q Amp
60	WT	MUT	MUT	A	20q Amp
61	WT	WT	MUT	A	20q Amp
62	MUT	WT	WT	A	20q Amp
63	MUT	MUT	WT	A	20q Amp
64	MUT	MUT	MUT	A	20q Amp
65	WT	MUT	WT	D	non-Amp
66	WT	WT	MUT	D	20q Amp
67	WT	WT	MUT	A	20q Amp
68	WT	WT	WT	D	20q Amp
69	WT	WT	WT	A	non-Amp
70	WT	MUT	WT	A	non-Amp
71	WT	WT	MUT	A	20q Amp
72	WT	MUT	MUT	A	non-Amp
73	MUT	WT	WT	A	non-Amp
74	WT	MUT	WT	A	non-Amp
75	WT	MUT	WT	D	non-Amp
76	WT	MUT	MUT	D	non-Amp
77	WT	MUT	MUT	A	20q Amp
78	WT	MUT	WT	D	non-Amp

79	WT	WT	MUT	A	20q Amp
80	WT	MUT	WT	D	non-Amp
81	WT	WT	MUT	A	non-Amp
82	WT	WT	WT	A	non-Amp
83	WT	WT	MUT	A	20q Amp
84	WT	MUT	MUT	D	20q Amp
85	WT	WT	WT	D	non-Amp
86	MUT	MUT	MUT	A	non-Amp
87	WT	WT	WT	D	non-Amp
88	WT	WT	MUT	A	20q Amp
89	WT	WT	WT	D	non-Amp
90	WT	WT	MUT	A	non-Amp
91	WT	MUT	WT	D	non-Amp
92	WT	WT	MUT	D	20q Amp
93	WT	WT	WT	A	20q Amp
94	WT	MUT	WT	A	20q Amp
95	WT	WT	WT	A	20q Amp
96	MUT	WT	MUT	A	20q Amp
97	WT	WT	MUT	A	20q Amp
98	WT	WT	WT	A	20q Amp
99	MUT	MUT	WT	A	non-Amp
100	WT	WT	MUT	A	20q Amp
101	WT	MUT	MUT	D	non-Amp
102	WT	WT	WT	A	20q Amp
103	WT	WT	MUT	A	non-Amp

3.3 Discussion

Many studies have demonstrated that chromosome 20 is frequently amplified in CRC, particularly 20q. The 20q amplification has also been reported in CRC liver metastasis (Aragane et al., 2001a, Korn et al., 1999a). Furthermore, several genes located on 20q affect CRC progression such as AURKA and BCL2L1. Thus, We aimed to validate previous results from an aCGH study on CRC samples, which also showed that 20q was amplified in primary tumours and liver metastases but there was no significant difference. This was tested by qPCR to determine the amplification of candidate genes located on 20q13 in CRC FFPE DNA samples. A series of 103 patients with CRC was screened using comparative quantitative PCR. In addition, the association of 20q amplification in CRCs with KRAS, PIK3CA, TP53 and ploidy status was studied.

In our aCGH data, the 20q amplification was noticed in primary and secondary CRC tumours, particularly in the 20q13 cyto-band. Consistent with the aCGH findings, the analysis of the same sample set by qPCR based on genes located in 20q13 showed frequent amplification (concordance= 93%). The similarity of our results using an alternative method (qPCR) validated the results generated by the aCGH analysis. The relative quantitative results from the candidate genes were strongly correlated. This suggests that those genes were co-amplified. The co-amplification of genes located at 20q agreed with the findings of a previously reported study that the whole 20q is amplified in CRC tumours (Sillars-Hardebol et al., 2011b).

Having validating the aCGH data, we detected the amplification of 20q13 in the 15 primaries and their liver metastasised cases in 66.7% of primary tumours. The liver metastatic tumours showed 20q amplification in 60% of the cases. The insignificant difference between the 20q amplification status of both primaries and liver metastasised tumours agreed with the studies of (Bruin et al., 2010a, Munoz-Bellvis et al., 2012). Therefore, 20q amplification did not drive liver metastasis in this sample set. However, previous studies have showed that 20q is amplified more frequently in patients with liver metastases compared with primary CRCs (Aragane et al., 2001a, Korn et al., 1999a). Those previous studies have

compared copy number variation between primary CRC without liver metastases and primary CRC with liver metastases. This might explained the difference between our observation and their observation.

In two cases, the primaries were 20q amplified and their liver metastases were not. This phenomenon could be explained in two ways. Firstly, this may be due to the presence of small subclones in the primary tumour without 20q amplification undergoing metastasis (Jones et al., 2008). Secondly, it could be due to technical issues linked to stromal contaminations in the metastatic samples, although it was microdissected.

Having qPCR method validated, we determined the amplification of 20q in 103 primary CRC tumours. In screening for 20q status in a series of CRC cases, 46.5% of primary CRC tumours were 20q amplified, which is in agreement with the literature (De Angelis et al., 1999a, Postma et al., 2005a, Hidaka et al., 2000a). This agreement suggests that 20q amplification is an important driver of CRC progression. Furthermore, Chromosomal abnormalities occurred more frequently than *KRAS* and *TP53* mutations (Leslie et al., 2003). However, our results showed that the frequency of *TP53* mutations is higher than that of the frequency of 20q amplification.

Having confirmed 20q amplification in our CRC series, we evaluated 20q amplification associations with other molecular features. There is a paucity of data in the literature regarding the coexistence of chromosomal aberrations and mutations of *p53* and *KRAS*, and none for *PIK3CA* in the same CRC tumours. In MSS, the association of ploidy status and 20q amplification was unknown. Comparison of the two genetic pathways (MACS-CRCs and CIN-CRCs) with 20qAmp-CRCs showed no significant differences. A higher portion of 20qAmp-CRCs (70%) was CIN-CRCs, which indicates that 20q amplification is more frequent in CIN-CRCs.

Genes commonly mutated in CRCs were screened, which showed no significant differences except from a greater frequency of *TP53* mutation in the 20qAmp-CRC tumours. Our results imply that *TP53* mutation, but not *KRAS* or *PIK3CA* mutation, is associated with a more unstable 20q. A higher frequency of *P53* mutation has been observed in advanced-stage tumours (Russo et al., 2005, Iacopetta et al.,

2006). However, 20q amplification occurs in the early stage of the adenoma-carcinoma sequence (Diep et al., 2006a, Sillars-Hardebol et al., 2011a). Furthermore, the co-existence of 20qAmp-CRC and *TP53* mutation in CRCs in our study is consistent with the Leslie *et al.* study (Leslie et al., 2003). Amplification of the 20q and the *TP53* mutation are common events, they could simply co-segregate as a result of their high frequency. With regard to *KRAS* and *PIK3CA* mutations, our CRC series presented an insufficient number of cases to allow the detection of small or moderate frequency differences between the two groups.

In conclusion, qPCR was performed for 6 genes (*PTPN1*, *CES1L*, *ADNP*, *PTGIS*, *ELMO2* and *PREX1*) located in 20q to evaluate the DNA copy number and compare it with our aCGH results. The high concordance of qPCR and aCGH data validated the results of the aCGH study. In agreement with other studies, we confirmed that 20q is frequently amplified in CRCs using qPCR in a series of CRCs. The frequency of 20q amplification was higher in CRC with chromosomal instability than in CRC with microsatellite stable and chromosomal stable. 20q amplification was associated with the *TP53* mutation, but not with the *KRAS* or *PIK3CA* mutation. A study using higher numbers of CRC cases may allow us to detect small differences between those mutations and 20q amplified cases.

4 Chapter Four: Evaluating Cancer-Related Function And Expression Of Genes Located On 20q

The amplification of 20q is a common event in CRCs. Thus, the hypothesis was that 20q contains genes which are tumour drivers. Some of these driver genes have not been studied in CRC. In previous chapter (chapter3), we showed that 20q amplification is a common event, in which 51.4% of CRC cases were 20q amplified. Candidate genes located at this region were amplified, and this amplification might upregulate their protein expression. *PTPN1* and *CD40* genes has been investigated previously in CRC. However, studies have showed contradictory results regarding both gene. Therefore, we reinvestigate the functional role of both genes in CRC. Regarding *PTGIS*, overexpression of PTGIS protein has been reported in CRC. However, PTGIS functional role has not been investigated in CRC. Therefore, we investigated functional activities of several genes that map to 20q in CRC cell lines. *ELMO2* and *PREX1* genes have not been studied before in CRC. Interestingly, both genes have showed an oncogenic effect on other tumours. Thus, we aim to investigate *ELMO2* and *PREX1* role in CRC. In this chapter, protein expression of these genes were investigated by IHC for a series of 84 CRC cases, which is independent from the sample sets studied in previous chapter. Then, we studied the effect of gene knockdown on proliferation, migration and invasion. In summary, protein expression and functional role of candidate genes located at 20q13 were studied.

4.1.1 PTPN1 (Protein Tyrosine Phosphatase, Non-receptor Type 1)

4.1.1.1 Introduction

PTPN1 is a protein tyrosine phosphatase which is involved in the dephosphorylation of a number of Receptor Tyrosine Kinases such as IGFR (Sastry and Elferink, 2011). It is involved in cell proliferation and motility (Scott et al., 2010, Julien et al., 2011), although its role in cancer development is uncertain. Evidence suggests that PTPN1 can exhibit both tumour suppressing and tumour-promoting effects (Lessard et al., 2010). PTPN1 was reviewed in detail in section (1.6.1).We reinvestigated PTPN1 functional activities in CRC cell lines to confirm PTPN1 role in CRC progression.

4.1.1.2 Result

4.1.1.2.1 PTPN1 Immunohistochemistry

PTPN1 protein expression has been studied in CRC tissue. PTPN1 has been associated with poor prognosis (Chen et al., 2014). Specimens from a series of 84 patients with CRC were available for evaluation. This CRC series is independent from tested set in previous chapter (chapter 3).The cores were harvested from three different sites in the tumour. They were obtained from the luminal side of the tumour, the central part of the tumour and the advancing edge of the tumour. In addition, matched non-tumour colonic tissues were obtained from each case and included in the TMA in triplicate.

PTPN1 staining was detected in all tumour sites and matched non-tumour tissues (Figure 4-1) and was quantified using the H-score. The data were divided into two different categories, “low expression” and “high expression” of PTPN1. The low expression was calculated from the highest H scoring of the non-tumour colonic tissue staining. It was set as 100 H scoring (Table 4-1). Consequently, PTPN1 staining with H score above 100 was considered as high PTPN1 protein expression.

High PTPN1 expression in luminal tumour was observed in specimens from 20 (25.6%) cases (

Table 4-2). The frequency of high PTPN1 expression did not change in the middle of the tumour and was approximately the same (26%). However, at the advancing edge of the tumour, the frequency of high PTPN1 expression significantly increased. More than half (59.4%) of the cases showed high expression of PTPN1.

The Kappa test was performed to measure the level of agreement between expression patterns within different tumour sites. The highest level of agreement in term of PTPN1 expression was observed between the luminal and middle tumour (Kappa value was 0.332, P = 0.005).

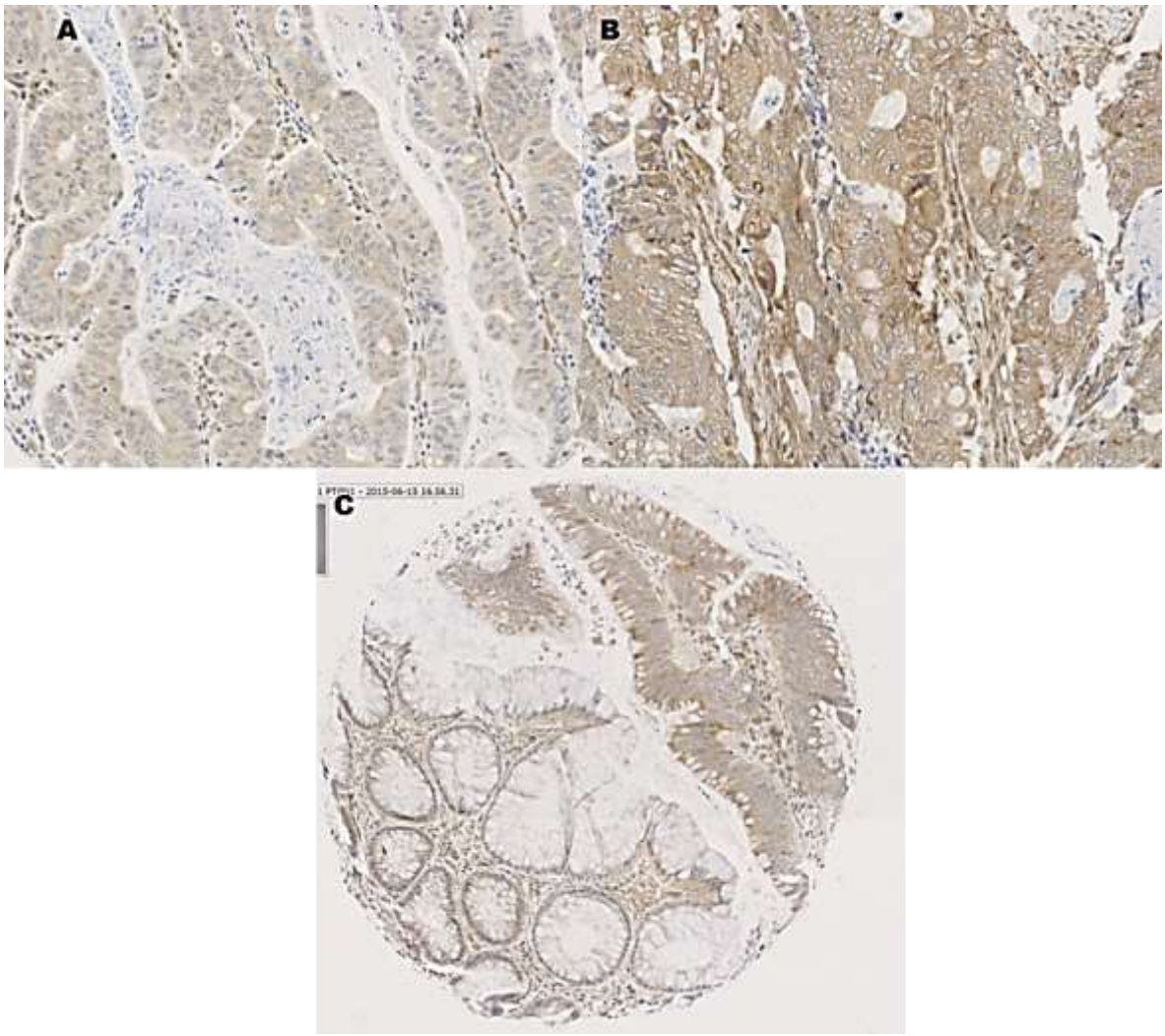


Figure 4-1. Low and high expression of PTPN1.
Figure (A) is a representative image of a low (Weak) expression of PTPN1 in CRC tumour tissue. (B) Tumour tissue highly expressing PTPN1. (C) PTPN1 expression in the tumour and matched non-t tissues, which presented a low PTPN1 expression. PTPN1 was expressed in the cytoplasm in all normal and tumour tissues. In Figure A and B, the pictures were acquired at 20× and, in Figure C, the picture was acquired at 5×.

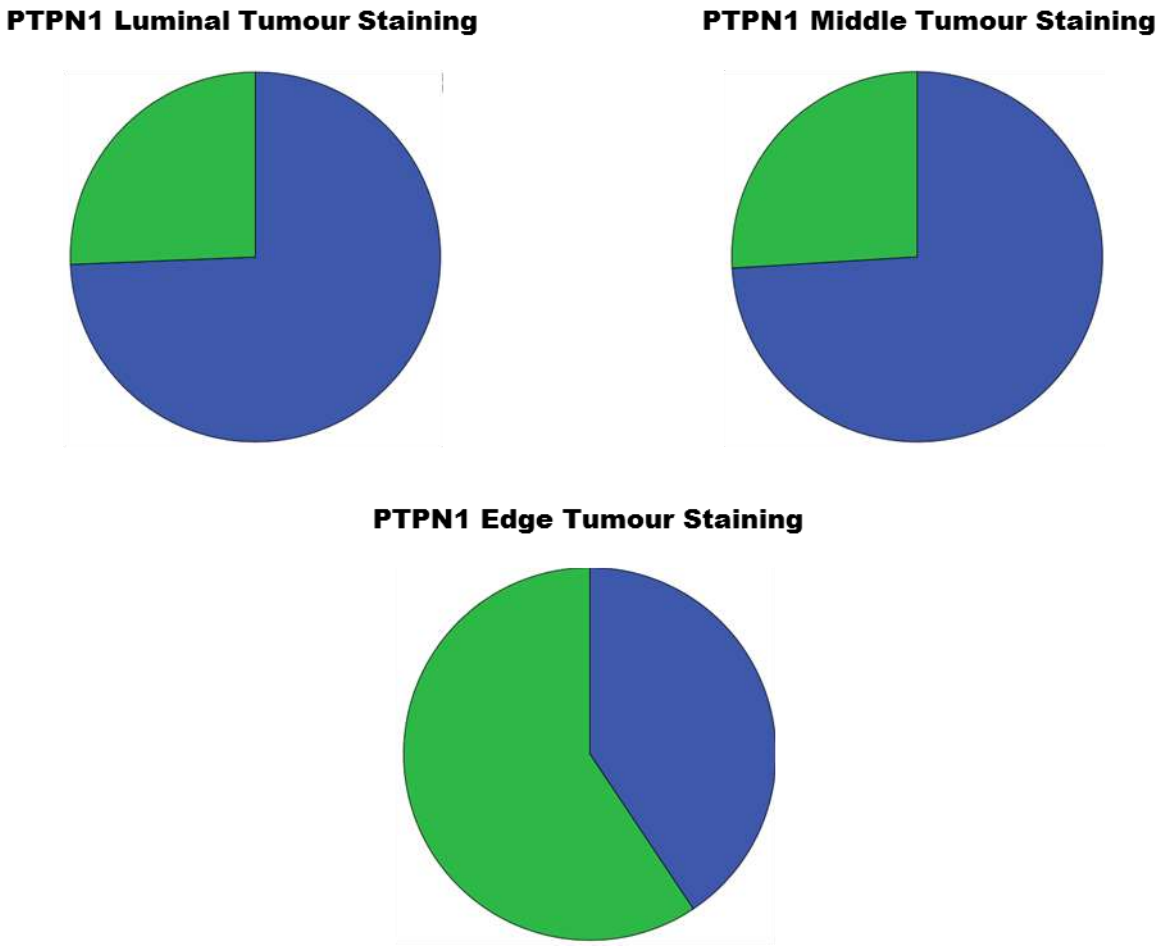


Figure 4-2. Pie chart showing the frequencies of high and low expression of PTPN1.

Immunohistochemistry of 84 CRC series was performed to study protein expression. This pie chart describe the frequency of protein expression in our series. The blue sections indicate low PTPN1expression and green sections represent high PTPN1 expression in different tumour sites

Table 4-1. PTPN1 staining overview.
Immunohistochemistry of 84 CRC series was performed to study protein expression

	PTPN1 luminal tumour staining	PTPN1 middle tumour staining	PTPN1 edge tumour staining	PTPN1 non-tumour colonic tissue staining
Minimum H scoring	20.00	100.00	100.00	20.00
Maximum H scoring	220.00	200.00	200.00	100.00

Table 4-2. Overall frequency of PTPN1 expression in CRC tissues in different matched tumour sites.
The overall frequency of low and high PTPN1 expression is listed. Low in the Table indicates the frequency of low PTPN1 expression and high means the frequency of high PTPN1 expression.

		Frequency	Percent (%)
PTPN1 Luminal Tumour Staining	Low	58	74.4
	High	20	25.6
PTPN1 Middle Tumour Staining	Low	57	74.0
	High	20	26.0
PTPN1 Edge Tumour Staining	Low	26	40.6
	High	38	59.4
PTPN1 non-tumour tissue Staining	Low	63	100
	High	0	0

4.1.1.2.2 PTPN1 knockdown

In order to find cell lines suitable for Gene knockdown, PTPN1 protein expression in CRC cell lines was studied by western blotting. Thirty micrograms of proteins from 7 CRC cell line lysates were separated on 4–12% Bis-Tris Plus Gel. A PTPN1 antibody was used to detect PTPN1 protein expression.

All tested cell lines expressed PTPN1 protein, although there were variations in protein expression levels (Figure 4-3). After measuring the band intensity and densitometry and after normalisation to β-actin expression, the highest PTPN1 protein expression was observed in HCT116 and HT29 cells. However, RKO, DLD1, and G2DP cells were moderately positive. Interesting patterns were seen in the cell lines SW620 and SW480.These are derived from the same patient but SW620 was derived from a metastatic tumour whilst SW480 was derived from the primary tumour. PTPN1 was expressed at a higher level in the primary-derived SW480 cells than in the metastasis-derived SW620 cells.

PTPN1 knockdown was performed by transfection of a siRNA targeting PTPN1 into cell lines (cell line siRNA PTPN1) and control cells were transfected with a siRNA targeting luciferase (cell line siRNA Luciferase). A total of 5 cell lines were tested HT29, RKO, DLD1, SW620 and HCT116. Of these, HT29, SW620 had 20q amplification and, DLD1 and HCT116 did not have this amplification. In PTPN1 knocked down cell lines, PTPN1 was significantly downregulated when compared to control cells. PTPN1 knockdown was validated by western blots and qPCR analysis in each transfection experiment (Figure 4-4) and (Figure 4-5). The knockdown efficiency in CRC cell lines was approximately 48-77%. qPCR was used to validate the knockdown efficiency in different cell lines at the mRNA level.

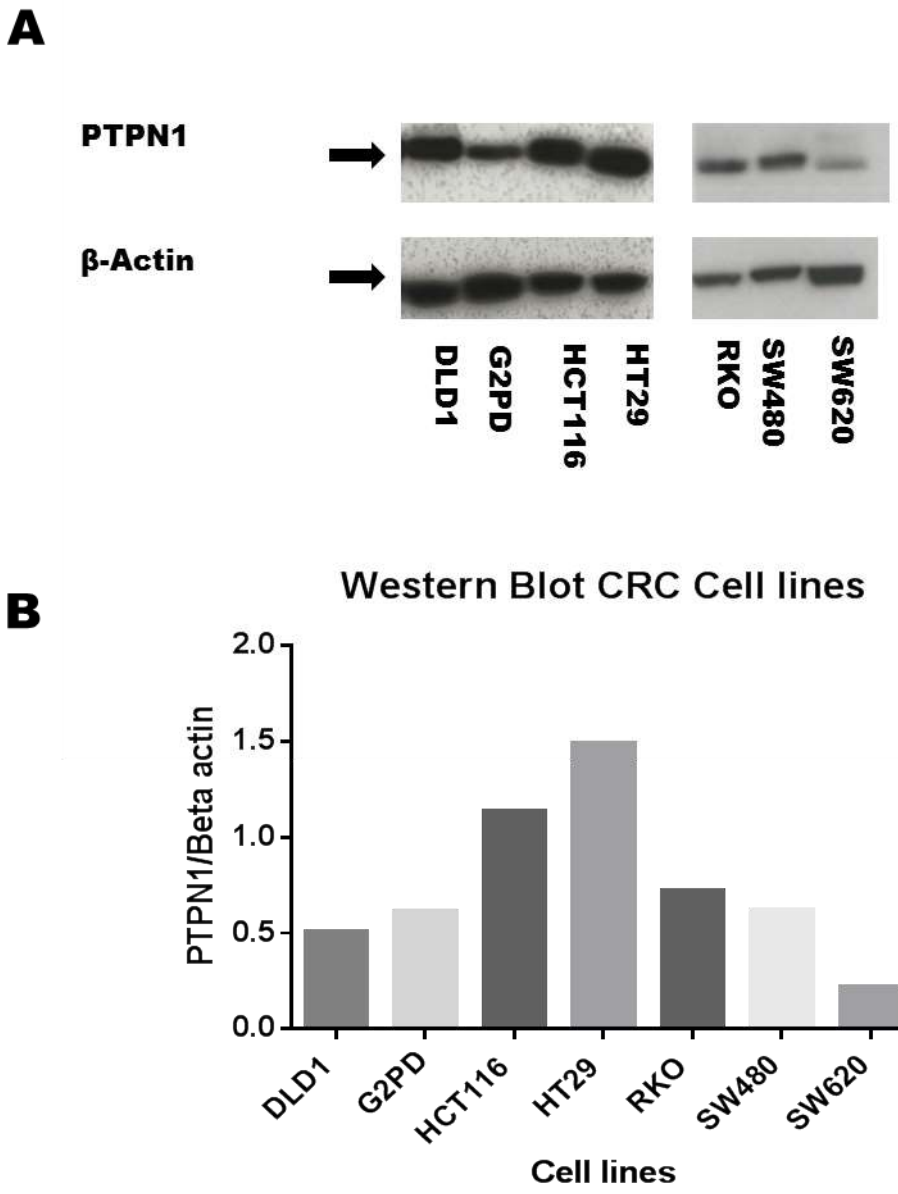


Figure 4-3. Western blot screening of PTPN1 expression in 7 CRC cell lines.
(A) Cell lysates (30µg) were analysed using 4–12% Bis-Tris Plus Gel. A PTPN1 antibody was used to detect PTPN1 protein expression levels. The loading control was the housekeeping protein ß-actin (1:50,000). (B) Histogram represented western blot intensities analysed by ImageJ software. Band intensity detected by PTPN1 antibody was normalised by its relevant ß-actin band. The highest PTPN1 protein expression was observed in HCT116 and HT29 cells. PTPN1 was expressed at a higher level in the primary-derived SW480 cells than in the metastasis-derived SW620 cells

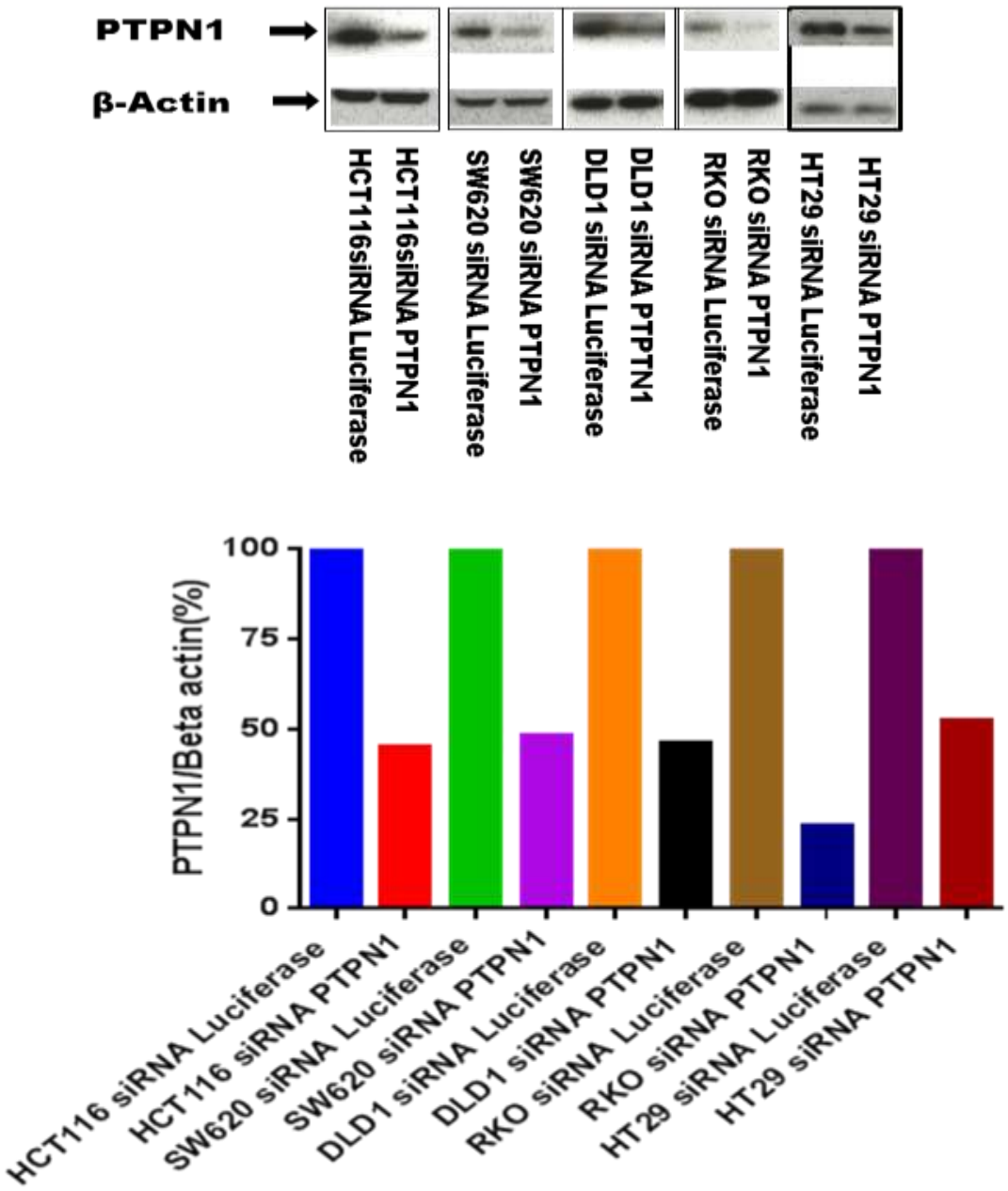


Figure 4-4. PTPN1 knockdown in SW620, RKO, HCT116, DLD1, and HT29 cells.

All cell lines were transfected with a siRNA targeting PTPN1 (cell line $^{siRNA\ PTPN1}$) or a siRNA targeting luciferase (cell line $^{siRNA\ Luciferase}$). Knockdown was validated by western blot in all tested CRC cell lines.β–actin was used as a loading control. Lower panel: Histogram represented western blot intensities analysed by ImageJ software. Band intensity detected by PTPN1 antibody was normalised by its relevant ß-actin band. In RKO cell line, the efficiency of the knockdown was 77%. In SW620 cell line, the knockdown efficiency was 52%. Similarly for both HCT116 and DLD1, the knockdown efficiencies were 55% and 54%, respectively. In HT29 cell line, the knockdown efficiency was 48%.

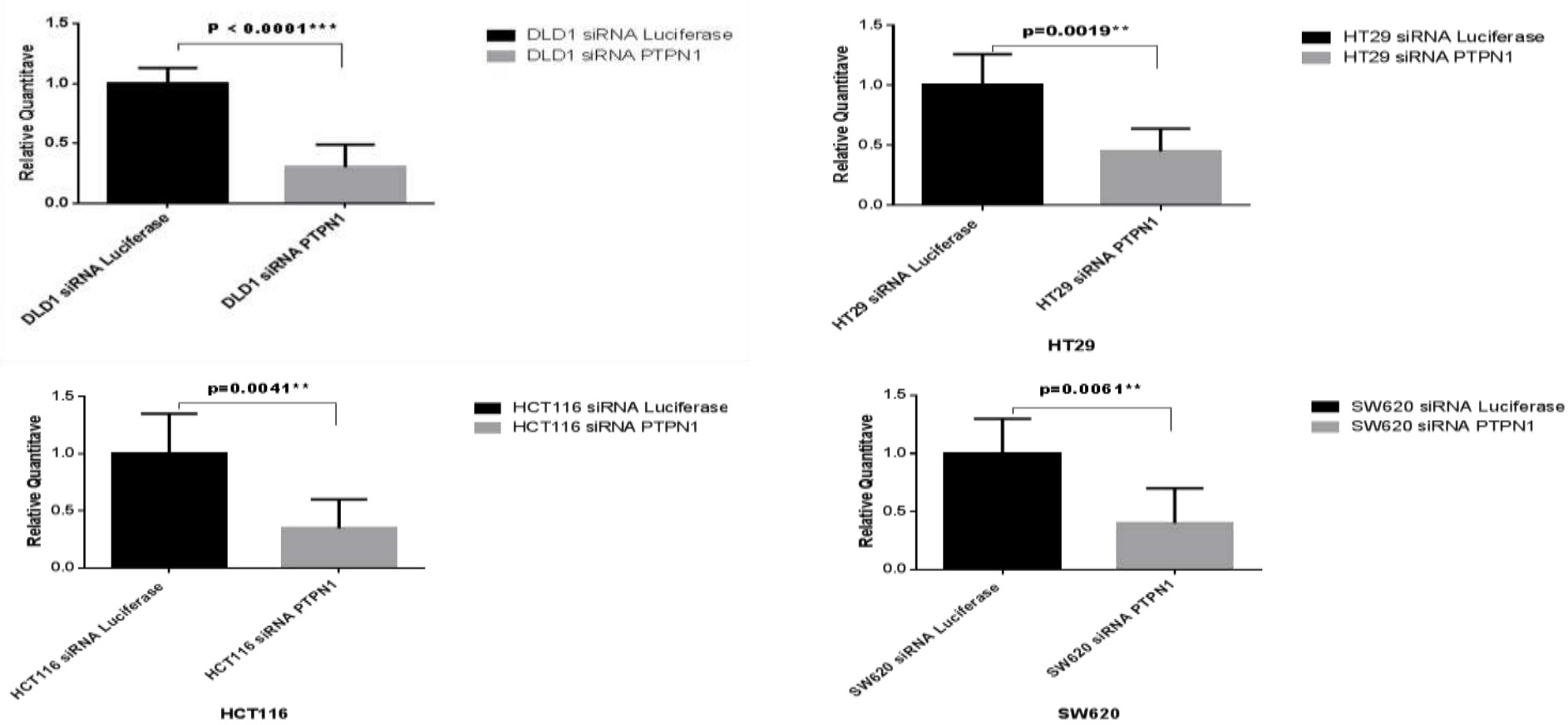


Figure 4-5. HCT116, SW620, DLD1 and HT29 cells were transfected with a siRNA targeting the PTPN1 gene.

HCT116, SW620, DLD1 and HT29 cells were transfected with a siRNA targeting the PTPN1 gene. Knockdown was validated by RT-qPCR The relative expression difference of the target gene in Knockdown cells against reference sample (RNA extracted from cells transfected with an siRNA targeting luciferase gene) is given by 2–ΔΔCt equation. The house keeping gene Hypoxanthine phosphoribosyl-transferase 1 (HPRT1) expression was used as endogenous control to normalise data from candidate genes. The ABI 7500 Fast System software and RQ software (Applied Biosystems) was used to analyse the data. Unpaired t-test was used for statistical analysis.

4.1.1.2.3 PTPN1 did not affect cell proliferation in CRC cell lines.

PTPN1 enhances cell proliferation in CRC cell lines (Zhu et al., 2007). On the other hand, in other cancers (Lessard et al., 2010, Akasaki et al., 2006), PTPN1 decreases cell proliferation. The effect of PTPN1 knockdown on the proliferation of several CRC cell lines was assessed in a time course assay (4 time points) using the Presto Blue assay. The proliferation pattern of DLD1 $^{siRNA\ PTPN1}$ cells did not significantly change when compared to that of DLD1 $^{siRNA\ Luciferase}$ cells (P = 0.0965, Two way-Anova test) (Figure 4-6A). Moreover, the proliferation of HT29 $^{siRNA\ PTPN1}$ cells was not altered when compared to that of HT29 $^{siRNA\ Luciferase}$ cells (P = 0.1096, Two way-Anova test) (Figure 4-6B). In addition, cell cycle analysis of PTPN1 knocked down cells showed no effect of PTPN1 knockdown on the cell cycle (Figure 4-6C). Similar experiments were performed using HCT116, RKO, and SW620 cell lines and showed no difference in term of proliferation rates and cell cycle patterns (P = 0.976, P = 0.132, and P = 0.2034, respectively, Two way-Anova test) (Figure 4-8, Figure 4-9, and Figure 4-10). In conclusion, PTPN1 did not alter the proliferation rate of the tested CRC cell lines.

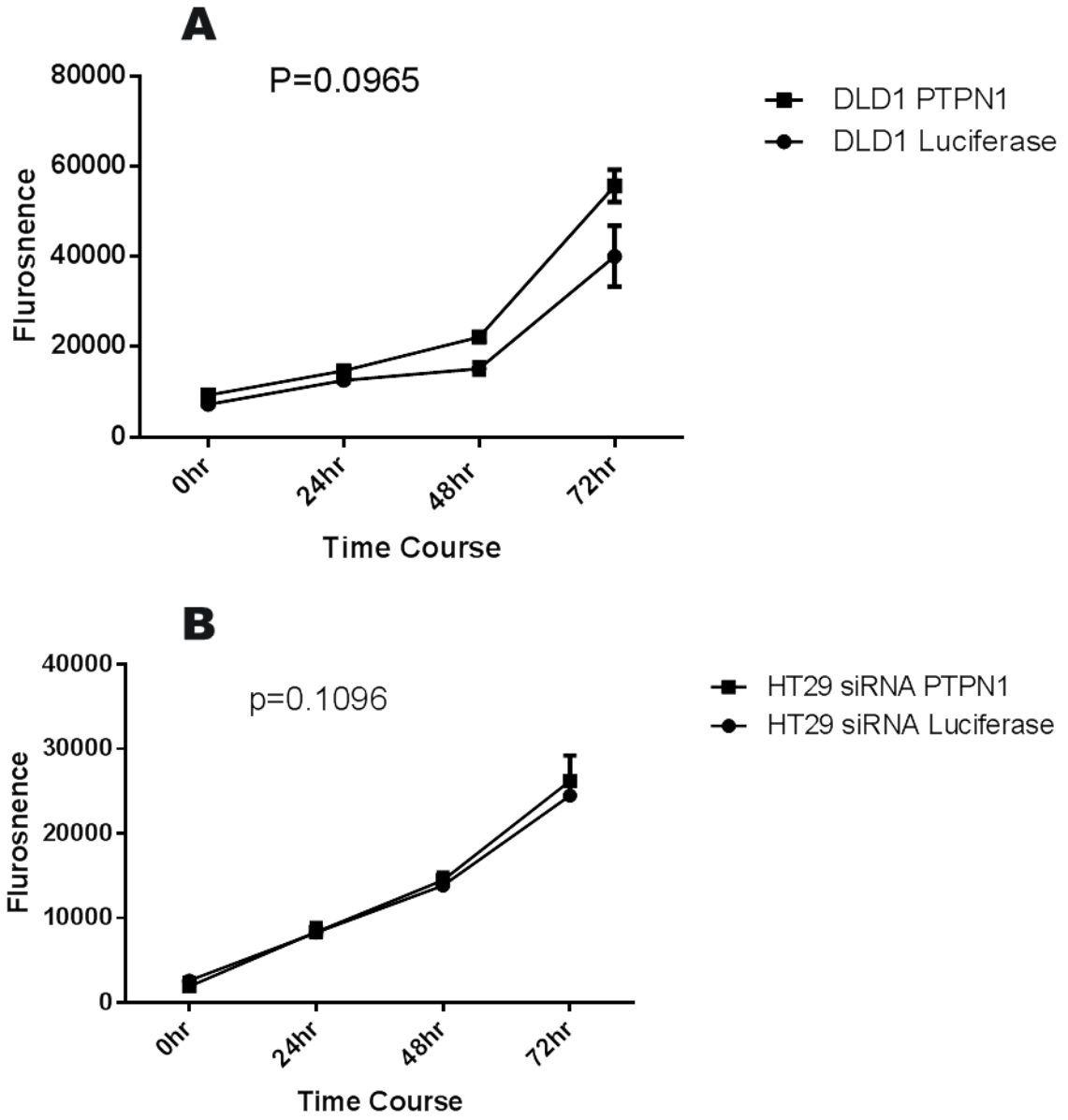


Figure 4-6. Effect of PTPN1 on cell proliferation and cell cycle in DLD1 and HT29 cells.

(A) and (B) Proliferation time course assay: Cells were harvested 48h after siRNA transfection. Then, cells ($2X10^4$) were seeded into 24 well-plates in triplicate. Presto Blue was added to each well, and then the fluorescence intensity (relative fluorescence units-RFUs) was measured using for excitation at 495nm and a filter for emission at 580nm. Proliferation was measured at 4 time points after PTPN1 knockdown in DLD1 and HT29 cells. PTPN1 did not affect cell proliferation. All data are expressed mean ± SD of three independent experiments.

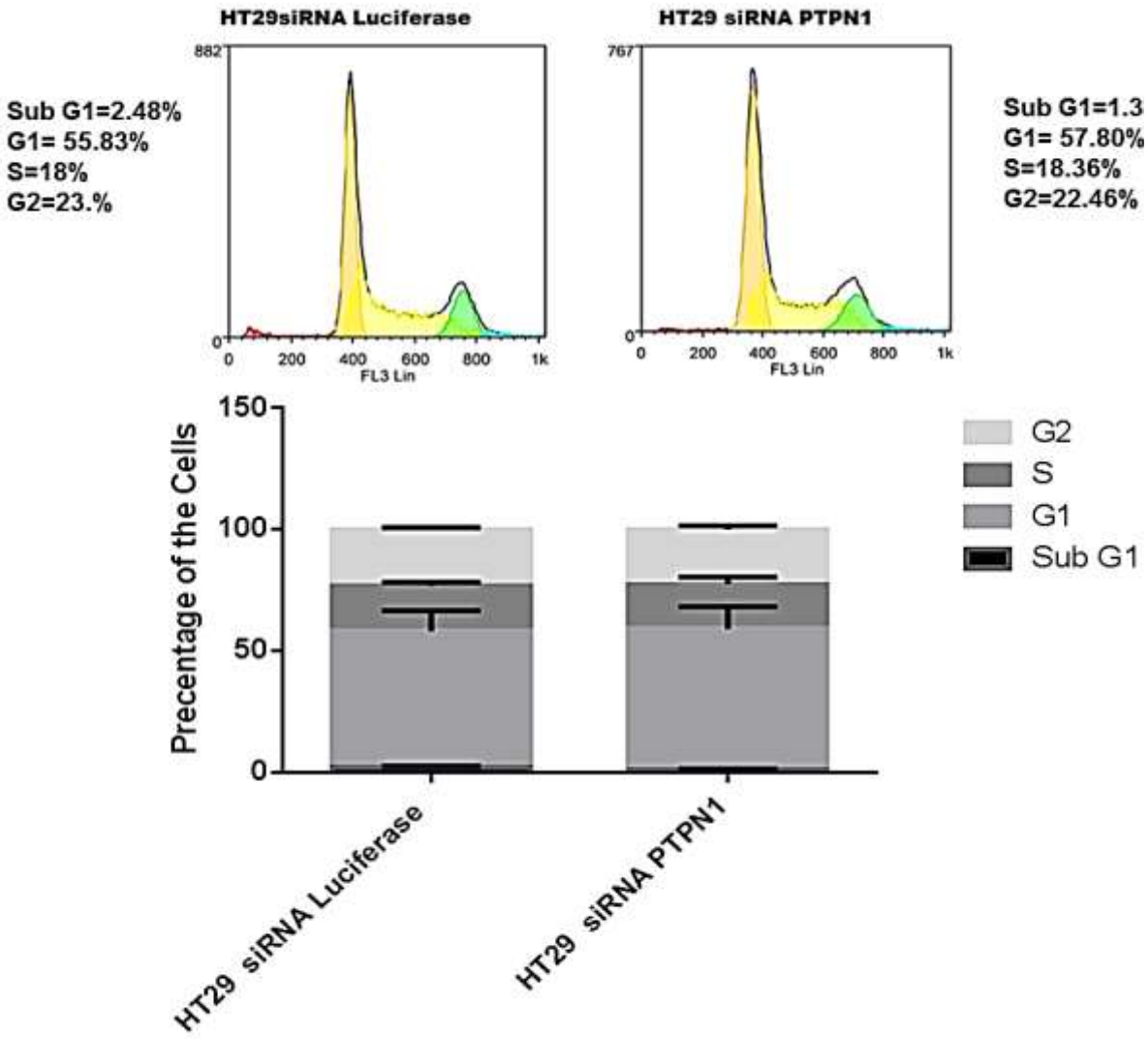


Figure 4-7. Effect of PTPN1 on cell cycle in HT29 cells.

Cell cycle patterns were analysed by Weasel software. The upper panel showed the cell cycle histogram in which the X-axis represents the fluorescence intensity and the Y-axis represents the number of cells. The percentages of cells in each cell cycle phases for both PTPN1 knocked down and control cells were not significantly different. The lower panel in graph represent the results of the cell cycle analysis of the PTPN1 knocked down and control HT29 cells. All data are expressed mean ± SD of three independent experiments

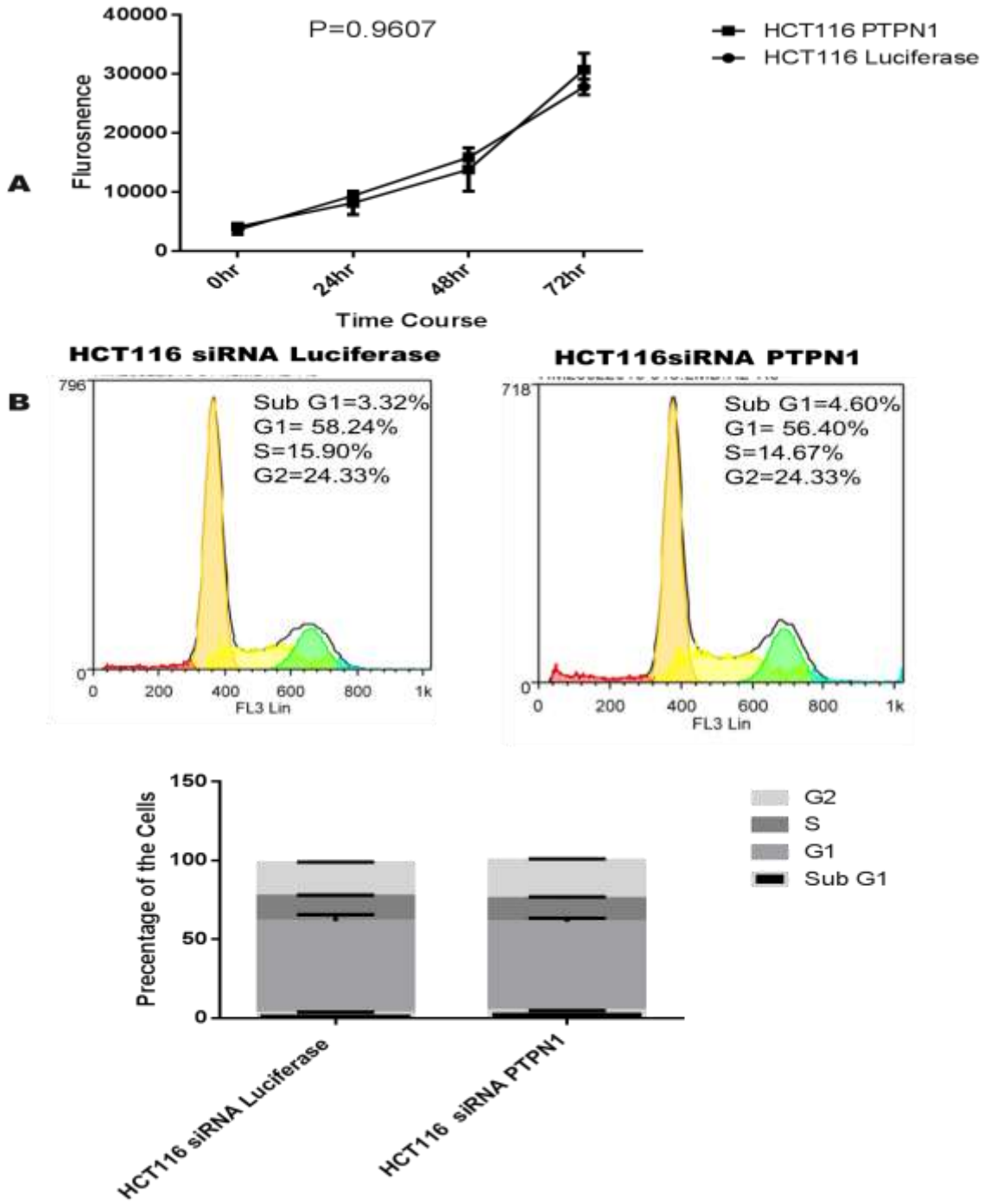


Figure 4-8. Effect of PTPN1 on cell proliferation and cell cycle in HCT116 cells.

(A) Proliferation time course assay: Proliferation was measured at 4 time points after PTPN1 knockdown in HCT116 cells. Cell viability was measured by fluorescence. (B) The percentages of cells in each cell cycle phases for both PTPN1 knocked down and control HCT116 cells were not significantly different. The lower panel in graph (B) represents the results of the cell cycle analysis of the PTPN1 knocked down and control HCT116 cells. All data are expressed as mean ± SD of three independent experiments.

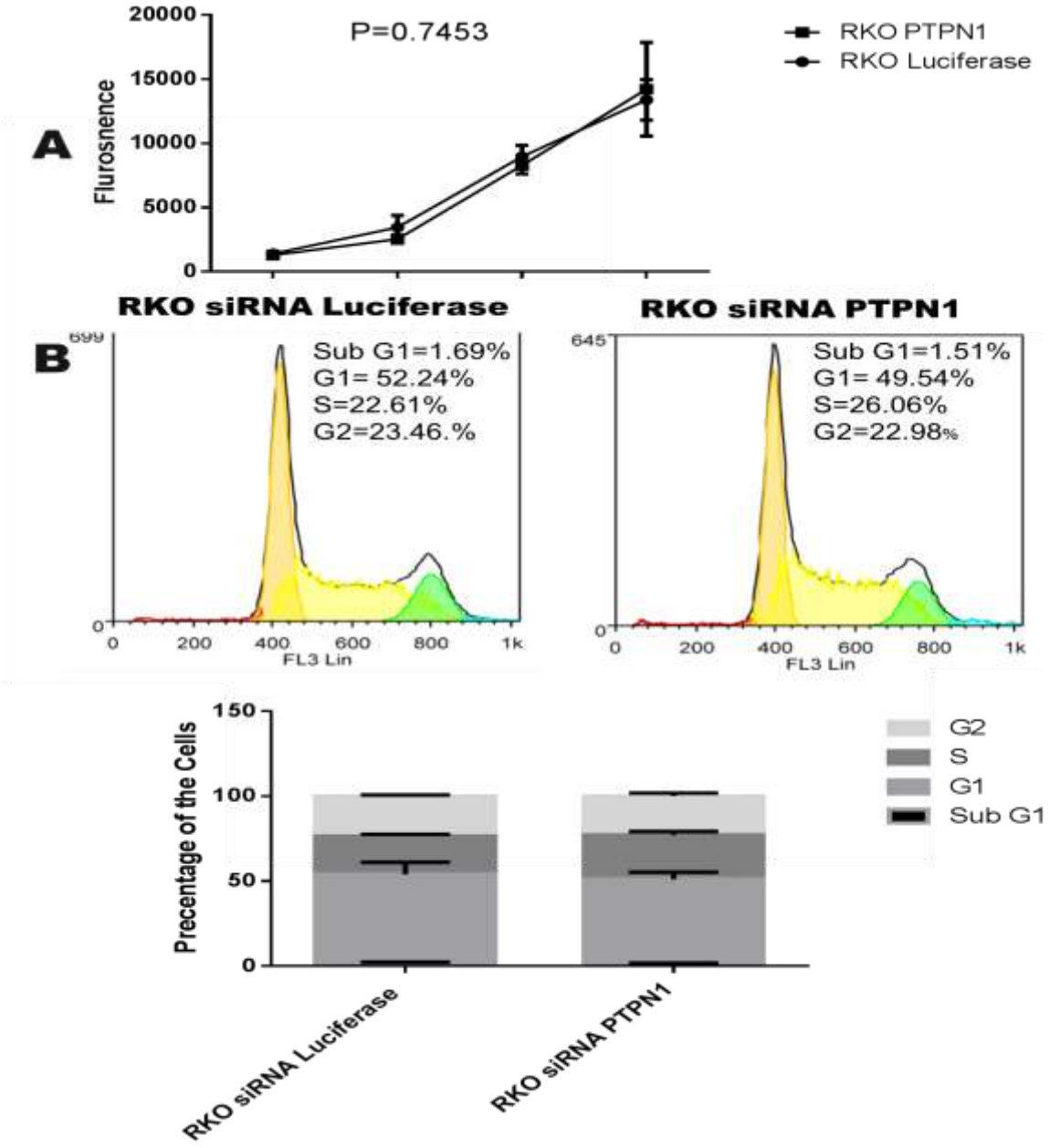


Figure 4-9. Effect of PTPN1 on cell proliferation and cell cycle in RKO cells.
(A) Proliferation time course assay: Proliferation was measured at 4 time points after PTPN1 knockdown in RKO cells. Cell viability was measured by fluorescence. (B) The percentages of cells in each cell cycle phases for both PTPN1 knocked down and control RKO cells were not significantly different. The lower panel in graph (B) represent the results of the cell cycle analysis of the PTPN1 knocked down and control RKO cells. All data are expressed as mean ± SD of three independent experiments.

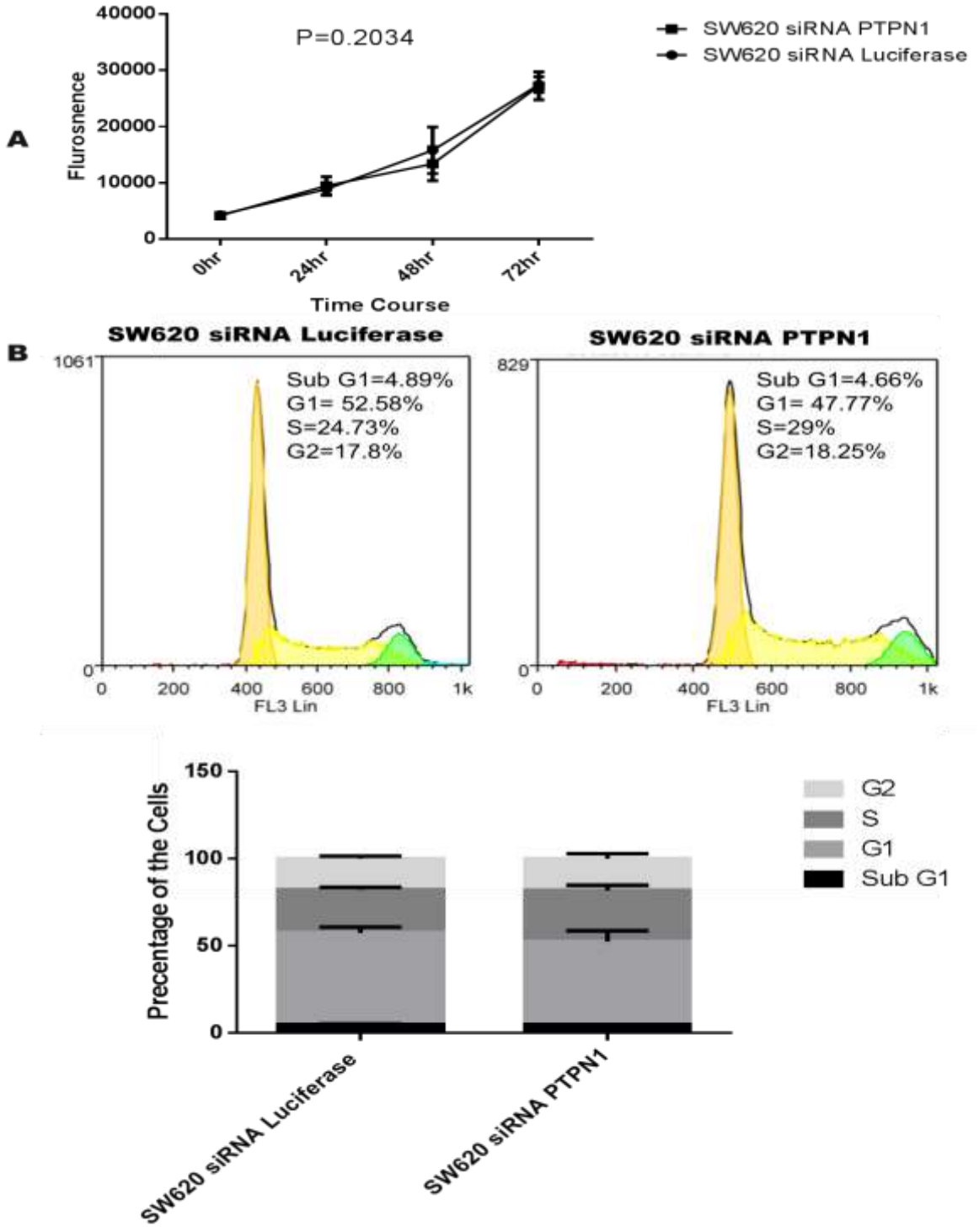


Figure 4-10. Effect of PTPN1 on cell proliferation and cell cycle in SW620 cells.

(A) Proliferation time course assay: Proliferation was measured at 4 time points after knockdown of PTPN1 in SW620 cells. Cell viability was measured by fluorescence. (B) The percentages of cells in each cell cycle phases for both PTPN1 knocked down and control SW620 cells were not significantly different. The lower panel in graph (B) represents the results of the cell cycle analysis of the PTPN1 knocked down and control SW620 cells. All data are expressed as mean ± SD of three independent experiments.

4.1.1.2.4 PTPN1 enhanced cell motility in CRC cell lines

PTPN1 has been reported to enhance cell motility in CRC cell lines (Zhu et al., 2007). In order to study the effect of PTPN1 on cell motility, transwell migration assays were performed using CRC cells knocked down for PTPN1.

4.1.1.2.4.1 Transwell migration

The cell lines, SW620 and HCT116, were transfected with the siRNA targeting PTPN1 or the siRNA targeting luciferase (Control). Following PTPN1 knockdown in HCT116 and SW620 cell lines, cells exhibited a significant decrease in motility. (HCT116 $^{siRNA\ PTPN1}$ versus HCT116$^{siRNA\ Luciferase}$, P = 0.0098; and SW620 $^{siRNA\ PTPN1}$ versus SW620$^{siRNA\ Luciferase}$, P = 0.0132, T-Test analysis).

To validate these results, other CRC cell lines were studied by transwell migration assay. HT29 $^{siRNA\ PTPN1}$ cells migrated more slowly than HT29 $^{siRNA\ Luciferase}$ (P = 0.0116, T-Test analysis). Furthermore, RKO $^{siRNA\ Luciferase}$ and DLD1 $^{siRNA\ Luciferase}$ cells migrated faster than cells knocked down for PTPN1 (P = 0.0069 and P = 0.0202, T-Test analysis) (Figure 4-11).

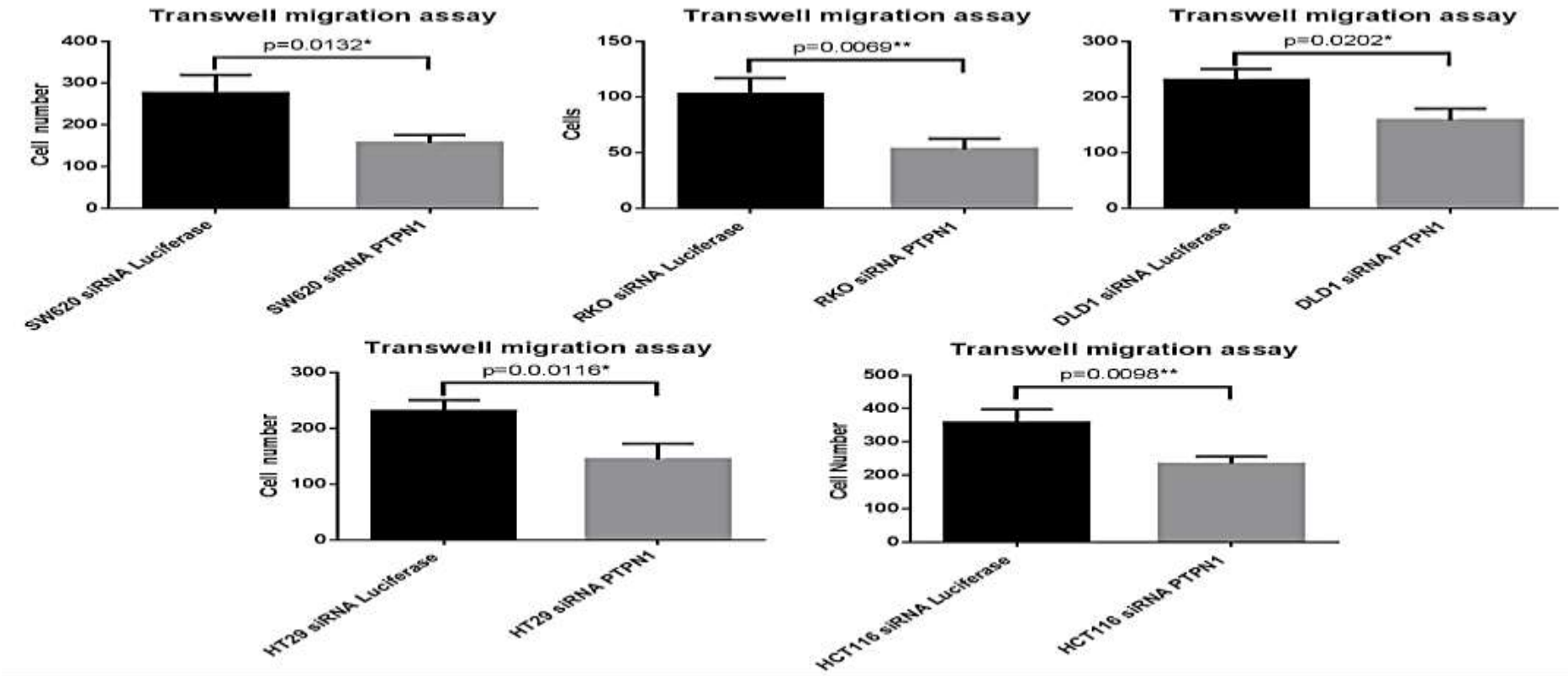


Figure 4-11. PTPN1 enhanced CRC cell motility in transwell migration assay.
Transwell migration assay was performed to study the migration of CRC cell lines. Migration of SW620 $^{siRNA\ PTPN1}$, RKO $^{siRNA\ PTPN1}$, DLD1 $^{siRNA\ PTPN1}$, HT29 $^{siRNA\ PTPN1}$, and HCT116 $^{siRNA\ PTPN1}$ cells was compared with that of the relevant $^{siRNA\ Luciferase}$ cell lines. For all tested cell lines, PTPN1 downregulation slowed the migration when compared to that of the control cells. PTPN1 enchanced cell migration in vitro. All results are expressed as means ± SD. All experiments were performed in triplicate.

4.1.1.2.4.2 Wound healing

The transwell assays suggested that PTPN1 plays a role in supporting cell motility. In order to validate this, we sought to assess motility using a different assay. The wound healing assay (also known as the “scratch assay”) measures migration of cells across a wound created in a confluent layer of cells.

.HCT116 $^{siRNA\ PTPN1}$ cells migrated more slowly across the wound than HCT116 $^{siRNA\ Luciferase}$ cells (P = 0.0135, T-Test analysis) (Figure 4-11A). For further validation, wound healing assay was performed by using the SW620 cell line. Similarly, SW620 $^{siRNA\ luciferase}$ migrated more quickly across the wound than SW620 $^{siRNA\ PTPN1}$ cells (P = 0.0189, T-Test analysis) (Figure 4-11B). Thus, all results showed that PTPN1 increased cell motility in CRC cell lines.

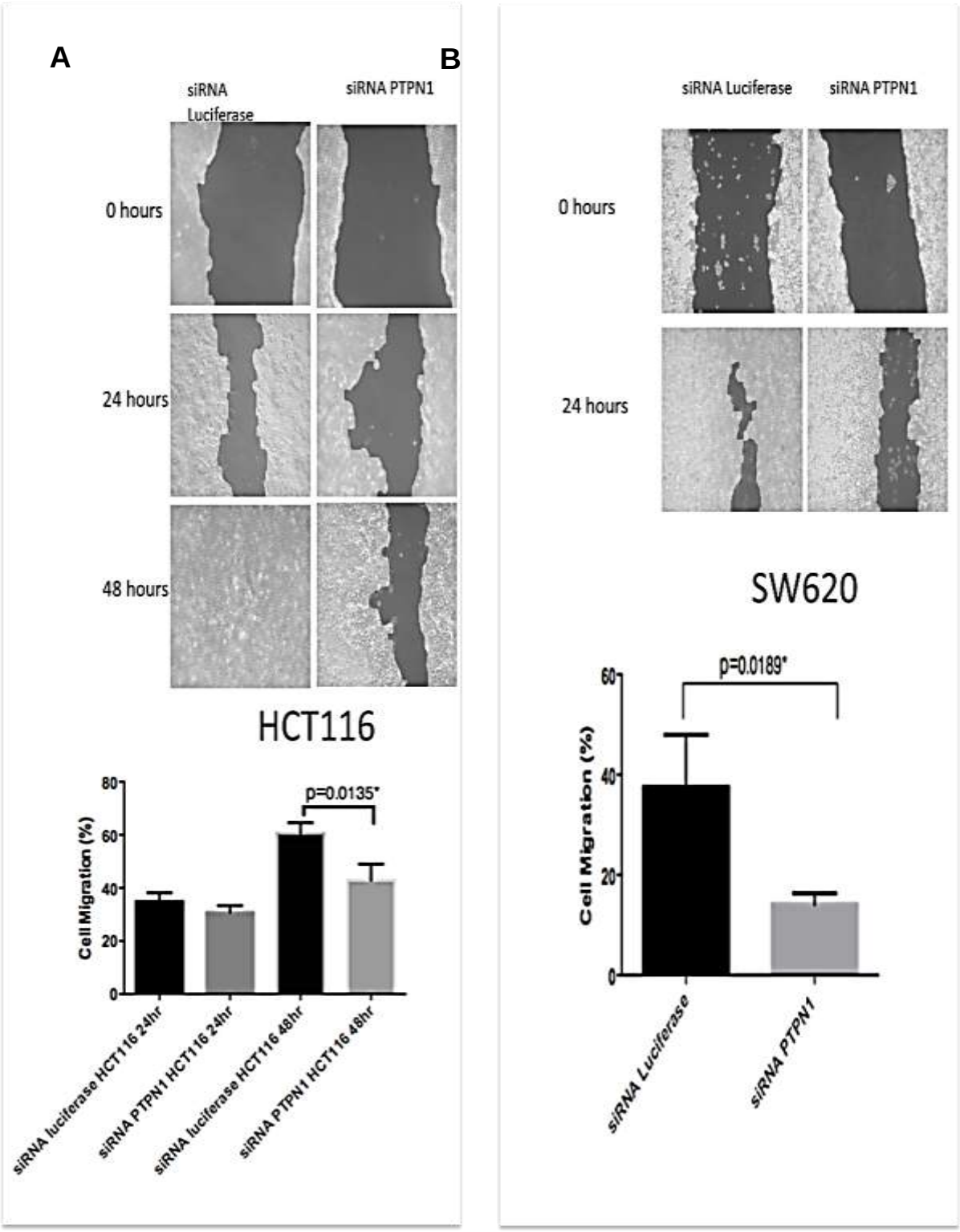


Figure 4-12. Wound healing assay.
After 48 h of PTPN1 knockdown, wound healing assay was performed for two cell lines. PTPN1 downregulation reduced the ability of cells to pass through the scratch as observed in Figure (A) and (B). The wound healing assays were performed twice. Knockdown PTPN1 migrated slower than the control. PTPN1 enhanced cell motility in CRC.

4.1.1.2.5 PTPN1 enhances cell invasion in CRC HCT116 cell line

The transwell migration and wound healing assays measure the speed of cell motility. In cancers, cells usually have to migrate through extracellular matrix. The nearest *in-vitro* approximation to this is the transwell invasion study in which migration of tumour cells across a layer of matrigel. Thus, a cell invasion assay was performed in the same way as the transwell migration assay, except that a matrigel layer was added to the upper chamber of the transwell.

The ability of HCT116 siRNA PTPN1 cells to invade the transwell covered with matrigel was compared with that of HCT116siRNA Luciferase cells. The number of HCT116siRNA Luciferase cells invading the membrane was significantly greater than that of HCT116 siRNA PTPN1 cells (HCT116 siRNA PTPN1 versus HCT116siRNA Luciferase, $P < 0.001$, T-Test analysis) (Figure 4-10). However, while we tried to validate these findings in other cell lines, not enough cells invaded the membrane to compare the cell invasion ability of SW620 $^{\text{siRNA PTPN1}}$ and SW620$^{\text{siRNA Luciferase}}$ cells. The same assay was performed using other cell lines, HT29, DLD1, and RKO. However, again not enough cells invaded the membrane to compare the invasion ability of PTPN1 knocked down and control cells.

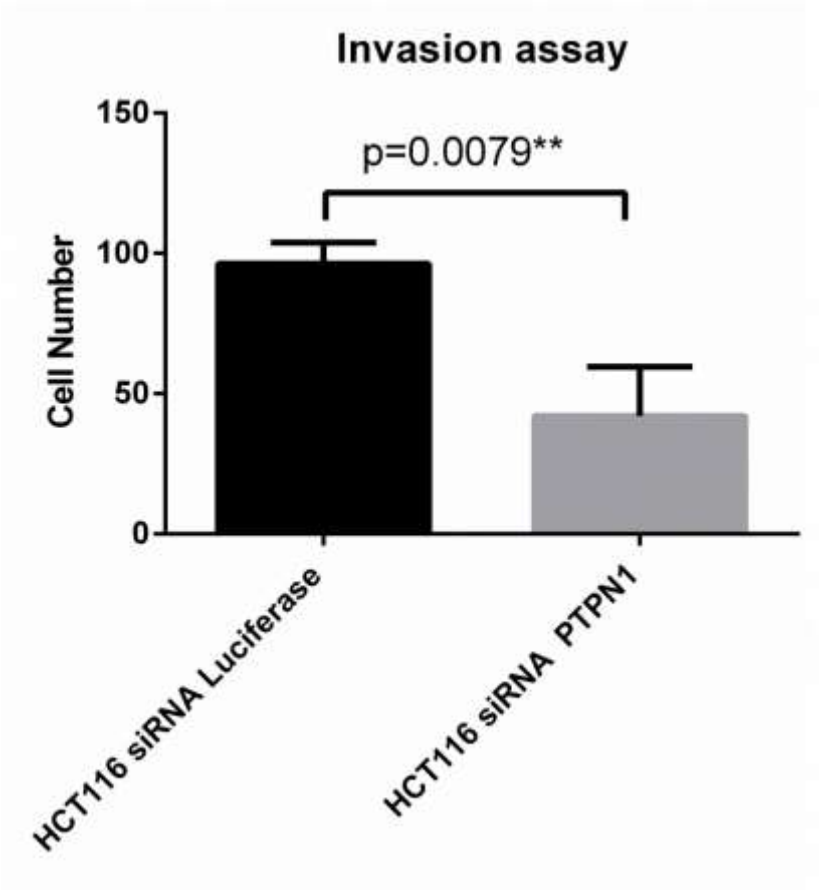


Figure 4-13. PTPN1 increases cell invasion ability.
There was a significant decreased in the number of HCT116 $^{siRNA\ PTPN1}$ cells which invaded the membrane when compared to HCT116 $^{siRNA\ Luciferase}$ cells. 24 transwell chambers (8µm pore size, Corning) was used after added a layer of matrigel. The invaded cells were counted under the microscope. Values are expressed as means ± SD. The experiment was performed in duplicate.

4.1.1.3 Discussion

PTPN1 is located on chromosome 20q13.13, a region frequently amplified in CRC and other cancers, and it is therefore relevant to this study. PTPN1 is a non-transmembrane protein tyrosine phosphatase 1(Sastry and Elferink, 2011) reported to be involved in regulating cell proliferation and motility (Scott et al., 2010, Julien et al., 2011). Contradictory results have been reported regarding the role of PTPN1 in tumour development. PTPN1 has been shown to exert both tumour suppressor and oncogenic activities (Lessard et al., 2010, Zhu et al., 2007).

We examined PTPN1 expression using IHC in a series of 84 primary CRC tissues in a TMA. There were 3 cores from each tumour but they were taken from different sites in the tumour: luminal side, central area and advancing edge. In addition, there were cores from normal tissue.

The presence of cores of normal colon allowed us compare tumour with normal and to set a threshold for scoring a case as positive for overexpression if it had a higher score than that of normal tissue. PTPN1 overexpression was observed in 25% of luminal and middle tumour tissues. Overexpression increased significantly in the advancing edge of the tumour tissues, in which PTPN1 overexpression was observed in over half of the cases (59%). Our results are not in agreement with those of Chen *et al*. (Chen et al., 2014). They reported that approximately 70% of the non-tumour colonic tissues do not express PTPN1 and only exhibited a faint expression when it was present. However, this study reported PTPN1 overexpression in 60% of CRC tissues which is similar to our score at the advancing edge. It is possible that technical differences account for the discrepancies between the two studies. Chen et al, also reported that PTPN1 overexpression is correlated with lymph node metastasis and depth of invasion as well as shorter overall survival (Chen et al., 2014). Therefore, PTPN1 overexpression in the edge of the tumour could be an indication of a role in regulating cell motility and invasion in CRC.

PTPN1 overexpression is not always associated with developing cancer. PTPN1 overexpression inhibits the transformation of fibroblasts into chronic myeloid leukaemia cells (Woodford-Thomas et al., 1992). Furthermore, PTPN1 expression in oesophageal cancer cells was lower than that in normal tissues. This low

expression was associated with differentiated oesophageal carcinoma without lymph node metastasis (Warabi et al., 2000). Together with other studies, our results suggest that PTPN1 expression and activity may be tissue specific.

PTPN1 was evaluated by gene knockdown using RNA interference. In order to identify suitable cell lines (i.e. those expressing high levels of PTPN1), a series of CRC cell lines were screened for PTPN1 expression. The expression was detected in all tested cell lines (Figure 4-3) as previously described (Zhu et al., 2007). PTPN1 protein expression was high in HCT116 and HT29 cell lines. HT29 and SW480 cells are 20q amplified (Rooney et al., 2001a, Sillars-Hardebol et al., 2011a), and, therefore, the high PTPN1 expression might be a consequence of this amplification. However, HCT116 is not 20q amplified and, yet, it highly expresses PTPN1. This high expression of PTPN1 might indicate the oncogenic role of PTPN1 in CRC carcinogenesis. Interestingly, two cell lines in our panel were derived from the same patient. SW480 was derived from the primary tumour whilst SW620 was derived from a metastasis. However levels of PTPN1 were higher in SW480 than SW620. The variation in PTPN1 expression in these two cell lines might indicate that PTPN1 regulation is complex.

To study PTPN1 effect on CRC, a PTPN1 siRNA was transfected into 5 CRC cell lines and growth and motility assays were performed. The proliferation rate of PTPN1 knocked down CRC cells was the same as that of the control cells in all 4 tested cell lines. This result is not consistent with previously published studies which have reported that PTPN1 promotes proliferation in CRC and breast cancer (Zhu et al., 2007, Arias-Romero et al., 2009). We cannot explain the differences between these studies and our study. Since we have tested 4 different cell lines, we feel our data are robust and the differences may be due to experimental methodology.

PTP1B has been shown to promote cell motility in CRC and breast cancer cell lines (Zhu et al., 2007) and this consistent with our data. We used two methods were used to study the effect of PTPN1 on cell migration - transwell migration and wound healing assays. The number of cells migrating across the transwell and the rate of wound closure were significantly decreased after PTPN1 knockdown in several CRC cell lines (Figure 4-11). Thus our data suggest PTPN1 promotes cell motility in CRC cell lines.

The effect of PTPN1 on invasiveness of CRC cells was studied. The number of cells that migrated across the matrigel was lower when the cells were transfected with PTPN1 siRNA and this is consistent with previous studies (Zhu et al., 2007, Lessard et al., 2012). Invasion requires degradation of the extracellular matrix as well as migration and, at this stage, we cannot be certain whether the results are due to PTPN1 enhancing both of these features or is mostly due to enhanced speed of migration. Together with the IHC data, the cell motility study suggests that PTPN1 overexpression at the advancing edge of the tumour may be to promote cell motility and invasiveness.

In conclusion, this study has confirmed that PTPN1 can promote CRC migration and invasion and that the enhanced expression at the advancing edge (compared to luminal and central areas) may be a reflection of this. . Studying PTPN1 signalling pathway in CRC cell lines is necessary to ascertain the mechanism of activity and possibly identifying targets for PTPN1 pathway inhibitors in the treatment of CRC. The expression data were not accompanied with clinical data and further study is necessary to determine whether PTPN1 could be a novel molecular marker to indicate CRC progression and prognosis in patients.

4.1.2 Cluster of differentiation 40 (CD40)

4.1.2.1 Introduction

CD40, TNF receptor superfamily member 5, is located on chromosome 20q13.12. CD40 expression is observed in hematopoietic and non-hematopoietic cells such as fibroblasts, epithelial, and endothelial cells (Banchereau et al., 1995, van Kooten and Banchereau, 1997). In addition, CD40 expression in haematological and solid tumours has been reported. Therefore, evidence suggests that this receptor may play a role in carcinogenesis although published data regarding this role are contradictory. This gene was reviwed previously in section (1.6.2). Therefore, studying the expression and function of CD40 in CRC cell lines and its expression in clinical tissues may indicate whether CD40 acts as an oncogene or a tumour suppressor in CRC and whether it could be used as a therapeutic target.

4.1.2.2 Results

4.1.2.2.1 CD40 Immunohistochemistry

CD40 protein expression has been studied in CRC tissues. CD40 was expressed in CRC tissues in approximately 50% of the cases and it was associated with lymph node metastasis (Wu et al., 2008). The number of specimens available for CD40 evaluation was 84 as previously described. This CRC series is independent from tested set in previous chapter (chapter 3). It has been reported that CD40L activates CD40 (Shoji et al., 2011). Thus, CD40 and its ligand expressions were studied. The expression of CD40 and CD40L was detected in the cytoplasm and membrane. Therefore, the H score for each case was obtained for the membrane and cytoplasmic staining.

Data were divided into three categories: (1) no expression of CD40/CD40L. (2) low expression, and (3) high expression (Figure 4-14). The low expression was calculated from the highest H scoring of the non-tumour colonic tissue staining. The expression of both CD40 and CD40L in the non-tumour colonic tissue was only detected in the cytoplasm. The expression of CD40 was not detected in 52% of non-tumour tissues and the highest H score reported was 100. Consequently, CD40 staining with H score above 70 was considered as high CD40 protein

expression. CD40 staining scored between 1 and 70, considered as low CD40 protein expression. The same method was used to categorise CD40L expression data. The highest H scoring was 110 and higher H scoring was considered as high CD40L protein expression.

High CD40 expression in the cytoplasm of luminal tumour was only observed in two cases (2.5%) (Table 4-5 and Figure 4-15). The frequency of high CD40 expression did not change in the middle and edge of the tumour (3.8–4%) (Table 4-5). Regarding the expression of CD40L in the cytoplasm, CD40L overexpression was not detected in our series in all different tumour sites. (Table 4-6 and Figure 4-15).

The overexpression of CD40 was detected in the membrane of luminal tumour site (16%). (Table 4-5) The frequency of CD40 expression in the membrane increased slightly in the middle and edge of the tumour tissues, 25% and 20%, respectively. As with CD40, CD40L membrane expression was not detected in non-tumour colonic tissues (Table 4-6). CD40L expression in the membrane was detected in 26% of luminal tumour sites. The expression was also observed in the middle and edge of the tumour tissues. The percentage of cases that expressed CD40L increased in the middle (30.7%) and edge (25.5%) of the tumour when compared to the number of cases showing CD40L luminal expression.

The association of membranous CD40 and CD40L expression in all tumour sites was studied (Table 4-7, Table 4-8 and

Table 4-9). There was no significance between CD40 and CD40L expression patterns in different sites of the tumour. Only two cases showed high CD40 and CD40L expression in the luminal and edge of the tumours in the membrane. In the middle of the tumour, both CD40 and CD40L were found highly expressed only in 7 cases.

Table 4-3. CD40 overall staining.

Immunohistochemistry of 84 CRC series was performed to study protein expression

	Minimum H score	Maximum H score
CD40 cytoplasmic Luminal Tumour Staining	0	170
CD40 cytoplasmic middle Tumour Staining	0	200
CD40 cytoplasmic edge Tumour Staining	0	230
CD40 cytoplasmic non-Tumour Staining	0	70
CD40 membrane Luminal Tumour Staining	0	180
CD40 membrane middle Tumour Staining	0	240
CD40 membrane edge Tumour Staining	0	215
CD40 membrane non-Tumour Staining	0	0

Table 4-4. CD40L overall staining.

Immunohistochemistry of 84 CRC series was performed to study protein expression

	Minimum H score	Maximum H score
CD40L cytoplasmic Luminal Tumour Staining	0	89
CD40L cytoplasmic middle Tumour Staining	0	87
CD40L cytoplasmic edge Tumour Staining	0	85
CD40L cytoplasmic non-Tumour Staining	0	90
CD40L membrane Luminal Tumour Staining	0	150
CD40L membrane middle Tumour Staining	0	130
CD40L membrane edge Tumour Staining	0	215
CD40L membrane non-Tumour Staining	0	0

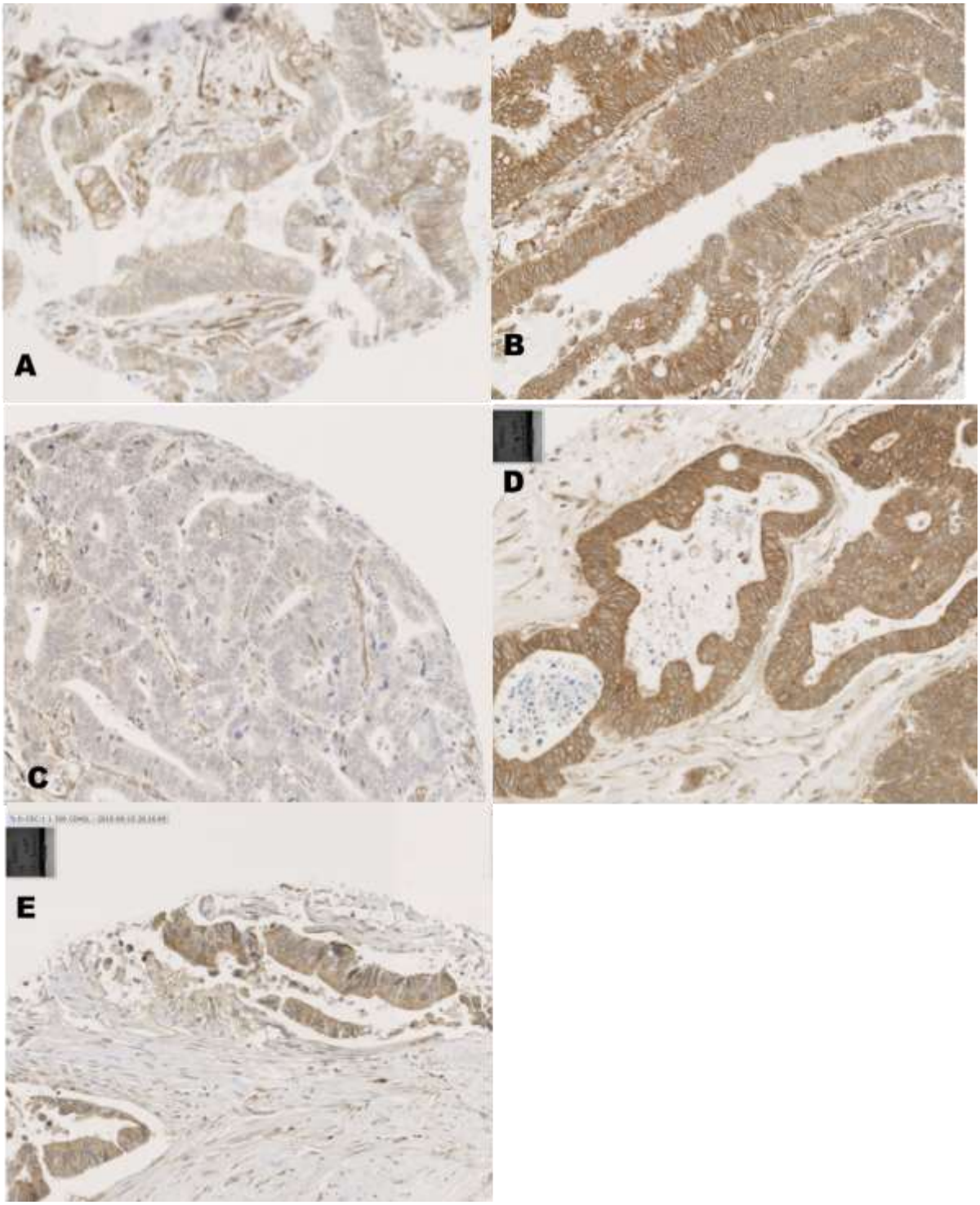


Figure 4-14. Low and high expression of CD40 and CD40L.
Figure (A) is a picture of a low (Weak) CD40 expression in CRC tumour tissue. (B) CD40 was highly expressed in tumour tissue. (C) CD40 was not expressed in the tumour. (D) CD40 expression was low (Weak) in CRC tumour tissue (E) CD40L was highly expressed in tumour tissue. CD40 and CD40L showed cytoplasmic and membrane staining in tumour tissues. All pictures were acquired at 20×.

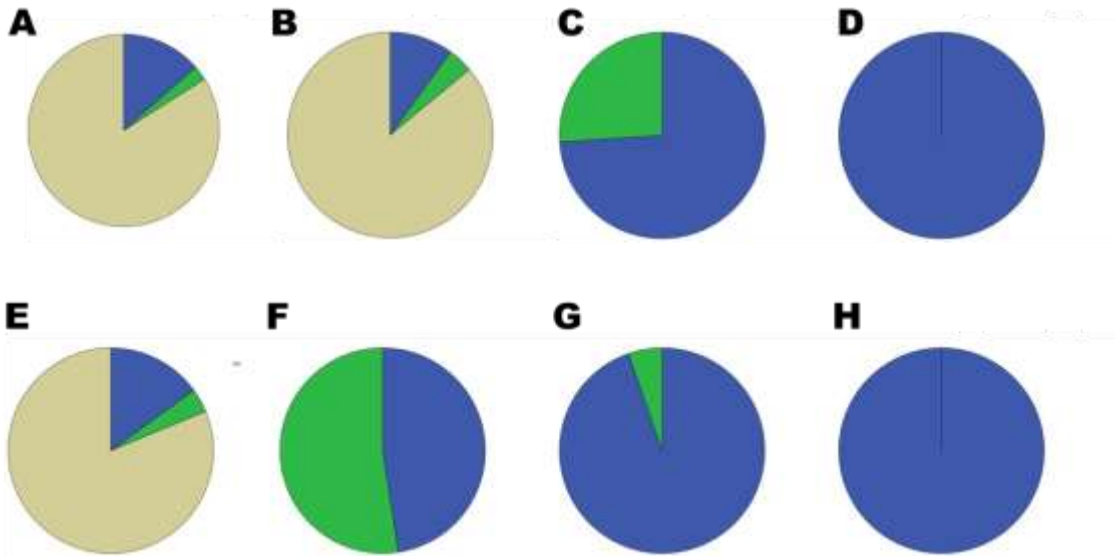


Figure 4-15. Pie chart showing the frequencies of high and low cytoplasmic expression of CD40 and CD40L.

Immunohistochemistry of 84 CRC series was performed to study protein expression. This pie chart describe the frequency of protein expression in our series. The blue sections indicate the cytoplasmic low CD40/CD40L expression and the green sections indicate the high CD40/CD40L expression, in different tumour sites. Grey section indicate absence of expression(A) CD40 cytoplasmic luminal tumour staining. (B) CD40 cytoplasmic edge tumour staining. (C) CD40L cytoplasmic luminal tumour staining (D) CD40L cytoplasmic non-tumour staining (E) CD40 cytoplasmic middle tumour staining. (F) CD40 cytoplasmic non-tumour staining (G) CD40L cytoplasmic middle tumour staining (H) CD40L cytoplasmic edge tumour staining.

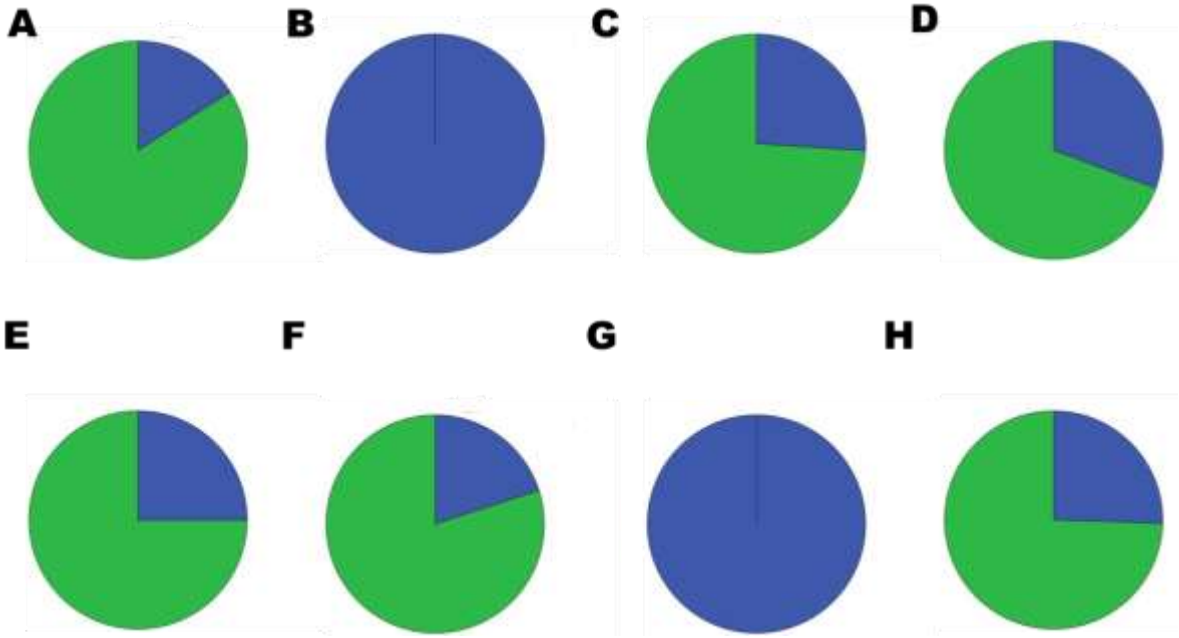


Figure 4-16. Pie chart showing the frequencies of high and low expression of CD40 and CD40L

Immunohistochemistry of 84 CRC series was performed to study protein expression. This pie chart describe the frequency of protein expression in our series. The blue sections indicate the membrane low CD40/CD40L expression and the green sections indicate the high CD40/CD40L expression, in different tumour sites. (A) CD40 luminal tumour staining. (B) CD40 non-tumour staining. (C) CD40L luminal tumour staining (D) CD40L middle tumour staining (E) CD40 middle tumour staining. (F) CD40 edge tumour staining (G) CD40L middle tumour staining (H) CD40L edge tumour staining.

Table 4-5. Overall frequency of CD40 expression in CRC tissues in different matched tumour sites.

Immunohistochemistry of 84 CRC series was performed to study protein expression

		Frequency	Percentage (%)
CD40 cytoplasmic Luminal Tumour Staining	Absence	68	84
	Low	11	13.6
	High	2	2.5
CD40 cytoplasmic Middle Tumour Staining	Absence	65	81.3
	Low	12	15
	High	3	3.8
CD40 cytoplasmic Edge Tumour Staining	Absence	43	86
	Low	5	10
	High	2	4
CD40 cytoplasmic non-tumour tissue Staining	Absence	32	52.5
	Low	29	47.5
	High		
CD40 membrane Luminal Tumour Staining	Absence	68	84
	Low	0	0
	High	13	16
CD40 membrane middle Tumour Staining	Absence	60	75
	Low	0	0
	High	20	25
CD40 membrane Middle Tumour	Absence	40	80
	Low	0	0

Staining	High	10	20
	Absence	60	100
CD40 membrane Edge Tumour Staining	Low	0	00
	High		

Table 4-6. Overall frequency of CD40L expression in CRC tissue in different matched tumour sites.

Immunohistochemistry of 84 CRC series was performed to study protein expression

		Frequency	Percent (%)
CD40L cytoplasmic Luminal Tumour Staining	Absence	19	26
	Low	54	74
	High	0	0
CD40L cytoplasmic Middle Tumour Staining	Absence	4	5.3
	Low	71	94.7
	High	0	0
CD40L cytoplasmic Edge Tumour Staining	Absence	0	0
	Low	51	100
	High	0	0
CD40L cytoplasmic non-tumour tissue Staining	Absence	0	0
	Low	51	100
	High		
CD40L membrane Luminal Tumour Staining	Absence	54	74
	Low	0	0
	High	19	26
CD40L membrane middle Tumour Staining	Absence	52	69.3
	Low	0	0
	High	23	30.7
CD40L membrane edge Tumour Staining	Absence	38	74.5
	Low	0	0

CD40L membrane Edge Tumour Staining	High	13	25.5
	Absence	51	100
	Low	0	00
	High		

Table 4-7. Cross tabulation of CD40 *vs.* CD40L membrane staining of luminal tumours.

Immunohistochemistry of 84 CRC series was performed to study protein expression. In this table, the correlation of CD40 membrane of luminal tumour staining compared to CD40L membrane of luminal tumour staining.

			CD40L membrane staining luminal tumour		Total
			Low expression	High expression	
CD40 membrane staining Luminal tumour	Low expression	Count	44	17	61
		% of Total	60.3%	23.3%	83.6%
	High expression	Count	10	2	12
		% of Total	13.7%	2.7%	16.4%
Total		Count	54	19	73
		% of Total	74.0%	26.0%	100.0 %

Table 4-8. Cross tabulation of CD40 *vs*. CD40L membrane staining in middle tumours.

Immunohistochemistry of 84 CRC series was performed to study protein expression. In this table, the correlation of CD40 membrane of central tumour staining compared to CD40L membrane of central tumour staining.

			CD40L membrane staining middle tumour		Total
			Low expression	High expression	
CD40 membrane staining Middle tumour	Low expression	Count	41	16	61
		% of Total	54.7%	21.3%	76%
	High expression	Count	11	7	18
		% of Total	14.7%	9.3%	24%
Total		Count	52	23	75
		% of Total	69.3%	30.7%	100.0 %

Table 4-9. Cross tabulation of CD40 *vs.* CD40L membrane staining of the edge of the tumours.

Immunohistochemistry of 84 CRC series was performed to study protein expression. In this table, the correlation of CD40 membrane of advancing tumour staining compared to CD40L membrane of advancing tumour staining.

			CD40L membrane staining edge tumour		Total
			Low expression	High expression	
CD40 membrane staining Edge tumour	Low expression	Count	26	8	34
		% of Total	60..5%	18.6%	79.1%
	High expression	Count	7	2	9
		% of Total	16.3%	4.7%	20.9%
Total		Count	33	10	43
		% of Total	76.7%	23.3%	100.0%

4.1.2.2.2 CD40 knockdown

In order to find cell lines suitable for Gene knockdown, CD40 protein expression in CRC cell lines was studied by western blotting. Thirty micrograms of proteins from 7 CRC cell line lysates were separated on 4–12% Bis-Tris Plus Gel. A CD40 antibody was used to detect CD40 protein expression.

CD40 protein is not detected in normal colon specimens (Gelbmann et al., 2003). In order to find cell lines suitable for Gene knockdown, CD40 protein expression in CRC cell lines was studied by western blotting. Five out of seven tested CRC cell lines expressed CD40 protein. However, SW480 and SW620 cell lines, cells derived from the same patient, did not express CD40 protein. Different levels of CD40 expression were detected by western blot (Figure 4-17). G2DP expressed a very low CD40 protein. Interestingly, three CRC cell lines are not 20q amplified (DLD1, HCT116, and RKO) showed highest CD40 protein expression. HT29 cell line showed moderate expression, although it is 20q amplified.

CD40 knockdown was performed by transfection of a siRNA targeting CD40 into cell lines (cell line $^{siRNA\ CD40}$) and control cells were transfected with a siRNA targeting luciferase (cell line $^{siRNA\ Luciferase}$). In the CD40 knocked down cell lines, CD40 was significantly downregulated when compared to the control cells. CD40 knockdown was assessed by western blot analysis. Knockdown efficiencies in CRC cell lines were 48% -83% (Figure 4-18).

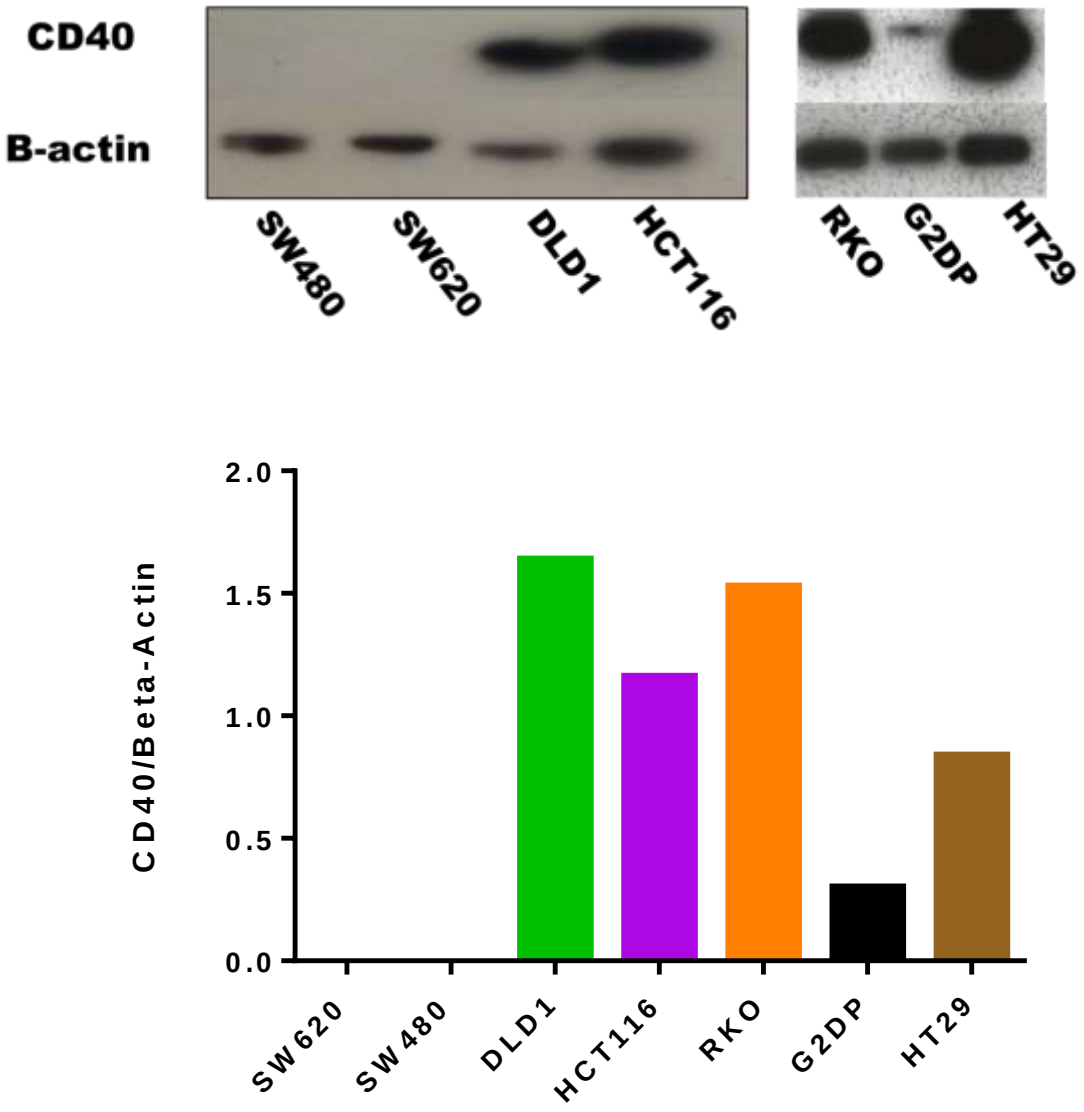


Figure 4-17. Western blot screening of CD40 expression in 7 CRC cell lines.
Cell lysates (30µg) were analysed using 4–12% Bis-Tris Plus Gel. A CD40 antibody was used to detect CD40 protein expression levels. The loading control was the housekeeping protein, ß-actin (1:50,000). Histogram represented western blot intensities analysed by ImageJ software. Band intensity detected by CD40 antibody was normalised by its relevant ß-actin band.

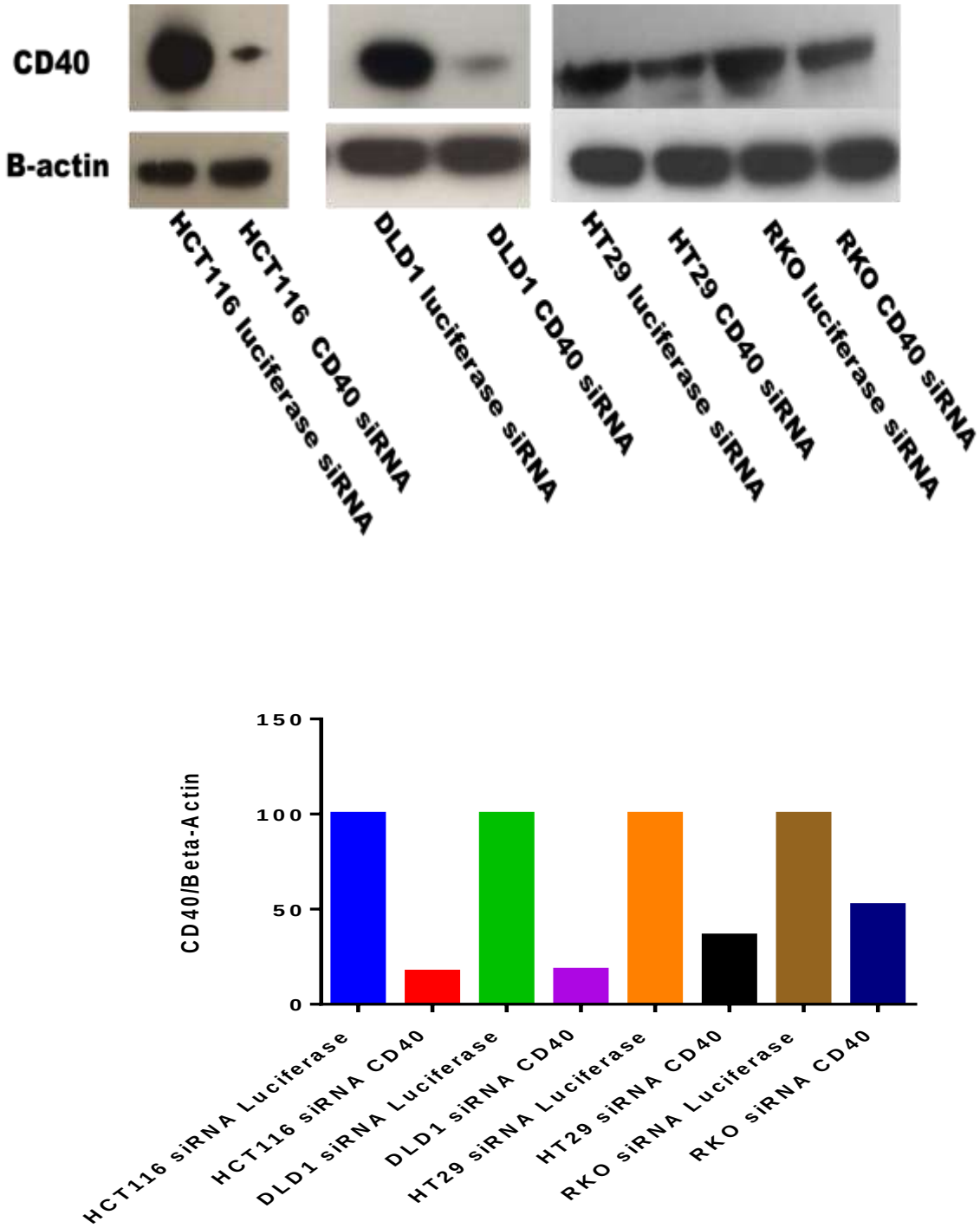


Figure 4-18. CD40 knockdown in RKO, HCT116, DLD1, and HT29 cells.
All cell lines were transfected with a siRNA targeting CD40 (cell line $^{siRNA\ CD40}$) or a siRNA targeting luciferase (cell line $^{siRNA\ Luciferase}$). Three days after knockdown, western blot were performed to assess CD40 expression in all tested CRC cell lines. β–actin was used as a loading control. Lower panel: Histogram represented western blot intensities analysed by ImageJ software. Band intensity detected by CD40 antibody was normalised by its relevant ß-actin band. In HCT116 and DLD1 cell lines, the efficiency of the knockdown was 83% and 82% respectivly. In HT29 cell line, the knockdown efficiency was 64%. For RKO cell line, the knockdown efficiencies were 48%.

4.1.2.2.3 CD40 enhances cell number in CRC cell lines

CD40 enhances cell growth in breast cancer and melanoma. Proliferation assay was performed at 4 time points to assess the effect of CD40 knockdown on cell proliferation using Presto Blue assay. The proliferation rate of HCT116 $^{siRNA\ CD40}$ cells significantly decreased when compared to that of HCT116 $^{siRNA\ Luciferase}$ cells ($P = 0.0144$, Two way Anova test) (Figure 4-19-A). In addition, cell cycle analysis of CD40 knocked down cells indicated the presence of more apoptotic (HCT116 $^{siRNA\ CD40}$ cells= 8.77% when compared to HCT116 ^{Luciferase} = 2.44%) ($P = 0.0004$, unpaired T-test). The number of CD40 knocked down cells in the G2 phase significantly decreased (22.39%) when compared to the control (29.61%) ($P = 0.0028$, unpaired T-test) (Figure 4-19-B). To validated previous result, CD40 effect on cell number was examined on other CRC cell lines. Downregulation of CD40 expression in HT29 cell line resulted in a significant decrease in cell number when compared to the control ($P < 0.0001$, Two way Anova test) (Figure 4-21-A). Further analysis of HT29 $^{siRNA\ CD40}$ cell cycle revealed that there was an increase in the number of apoptotic cells (2.49%) when compared to the cell cycle analysis of the control cells (6.34%) ($P =0.0003$, unpaired T-test) (Figure 4-21-B). In G2 phase, there was no significant difference in either condition.

The proliferation assay was also performed using the DLD1 cell line. The assay showed that downregulation of CD40 decreased the proliferation of DLD1 cells ($P = 0.002$, Two way Anova test) (Figure 4-20)

Although, CD40 is highly expressed in RKO cells, there was no significant difference in cell numbers between the proliferation rate of RKO $^{siRNA\ CD40}$ and that of the control RKO $^{siRNA\ Luciferase}$ cells ($P = 0.5289$, Two way test) (Figure 4-22-A). In order to validate the previous results, cell cycle analysis was performed on RKO $^{siRNA\ CD40}$ and RKO $^{siRNA\ Luciferase}$ cells. There was no significant change in the cell cycle pattern in either condition (Figure 4-22-B). SW620 cell line does not express CD40. There was no difference in the proliferation rate of both SW620 $^{siRNA\ Luciferase}$ and SW620 $^{siRNA\ CD40}$ cells, indicating that the CD40 siRNA did not have any non-target effects.

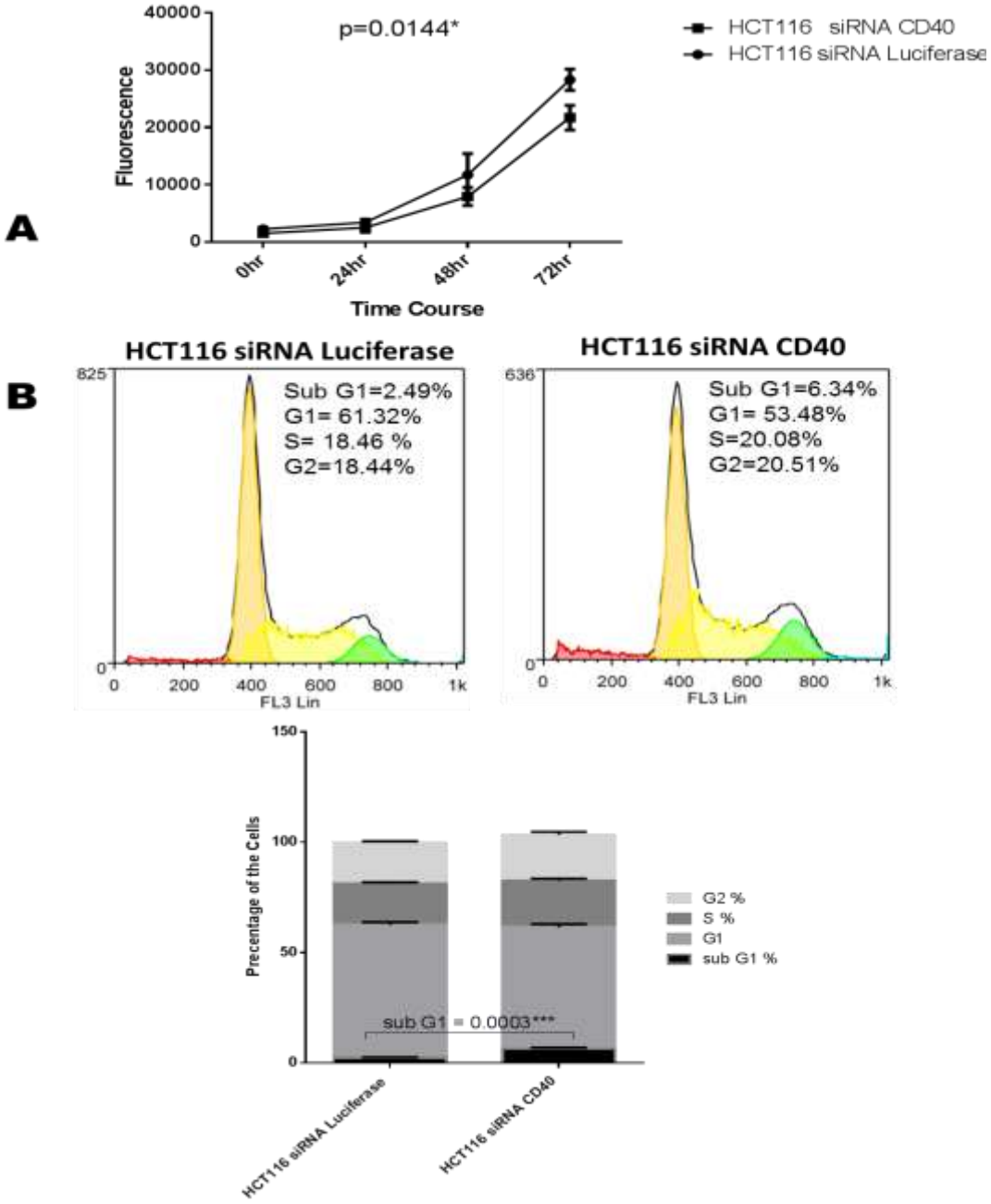


Figure 4-19. Effect of CD40 on cell proliferation and cell cycle in HCT116 cells.

(A) Proliferation time course assay:: Cells were harvested 48h after siRNA transfection. Then, cells ($2X10^4$) were seeded into 24 well-plates in triplicate. Presto Blue was added to each well, and then the fluorescence intensity (relative fluorescence units-RFUs) was measured using for excitation at 495nm and a filter for emission at 580nm Proliferation was assessed at 4 time points after CD40 knockdown in HCT116 cells and the cell viability was measured by fluorescence. (B) The cell cycle was analysed by Weasel software. The upper panel showed cell cycle histogram in which the X-axis was the fluorescence intensity and the Y-axis was the number of cells. The percentage of cells in each cell cycle phase for CD40 knockdown and control were significantly different. The lower panel in graph (B) represents the results of the cell cycle analysis of CD40 knocked down and control HCT116 cells. All data are presented as mean ± SD of three independent experiments.

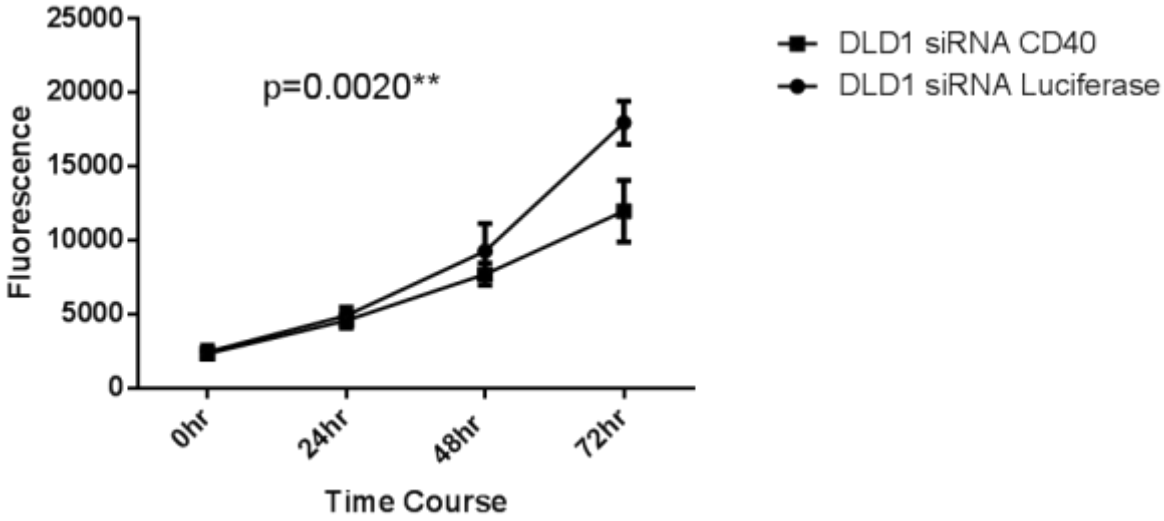


Figure 4-20. Effect of CD40 on cell proliferation in DLD1 cells.

Proliferation time course assay: : Cells were harvested 48h after siRNA transfection. Then, cells ($2X10^4$) were seeded into 24 well-plates in triplicate. Presto Blue was added to each well, and then the fluorescence intensity (relative fluorescence units-RFUs) was measured using for excitation at 495nm and a filter for emission at 580nm Proliferation was assessed at 4 time points after CD40 knockdown in DLD1 cells. Cell viability was measured by fluorescence. All data are presented as mean ± SD of three independent experiments.

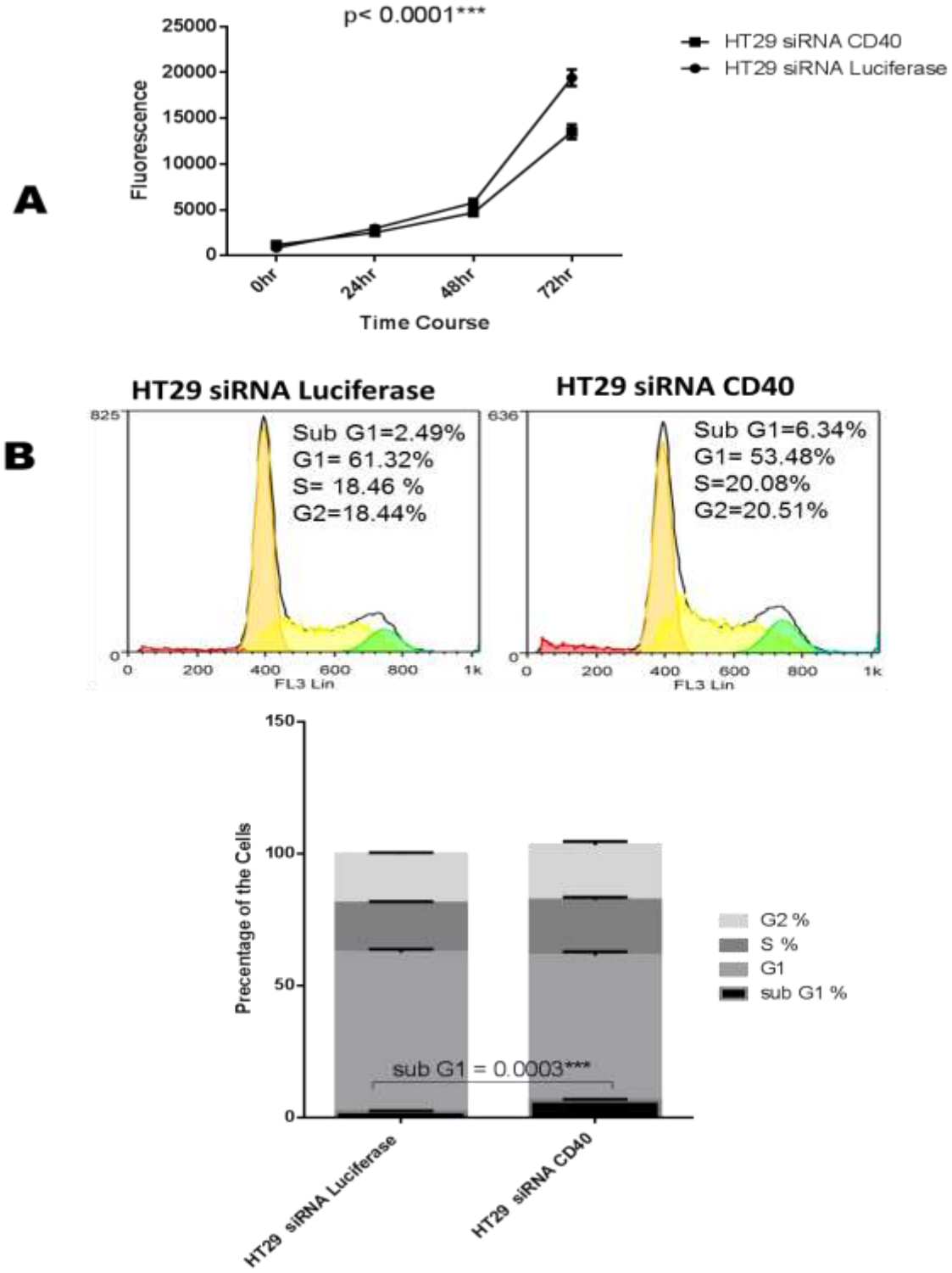


Figure 4-21. Effect of CD40 on cell proliferation and cell cycle in HT29 cells.
(A) Proliferation time course assay: Proliferation was assessed at 4 time points after CD40 knockdown in HT29 cells viabilities were measured by fluorescence. (B) The percentage of cells in each cell cycle phases in both CD40 knocked down and control HT29 cells were not significantly different. The lower panel in graph (B) represents the results of the cell cycle analysis of CD40 knocked down and control HT29 cells. All data are presented as mean ± SD of three independent experiments.

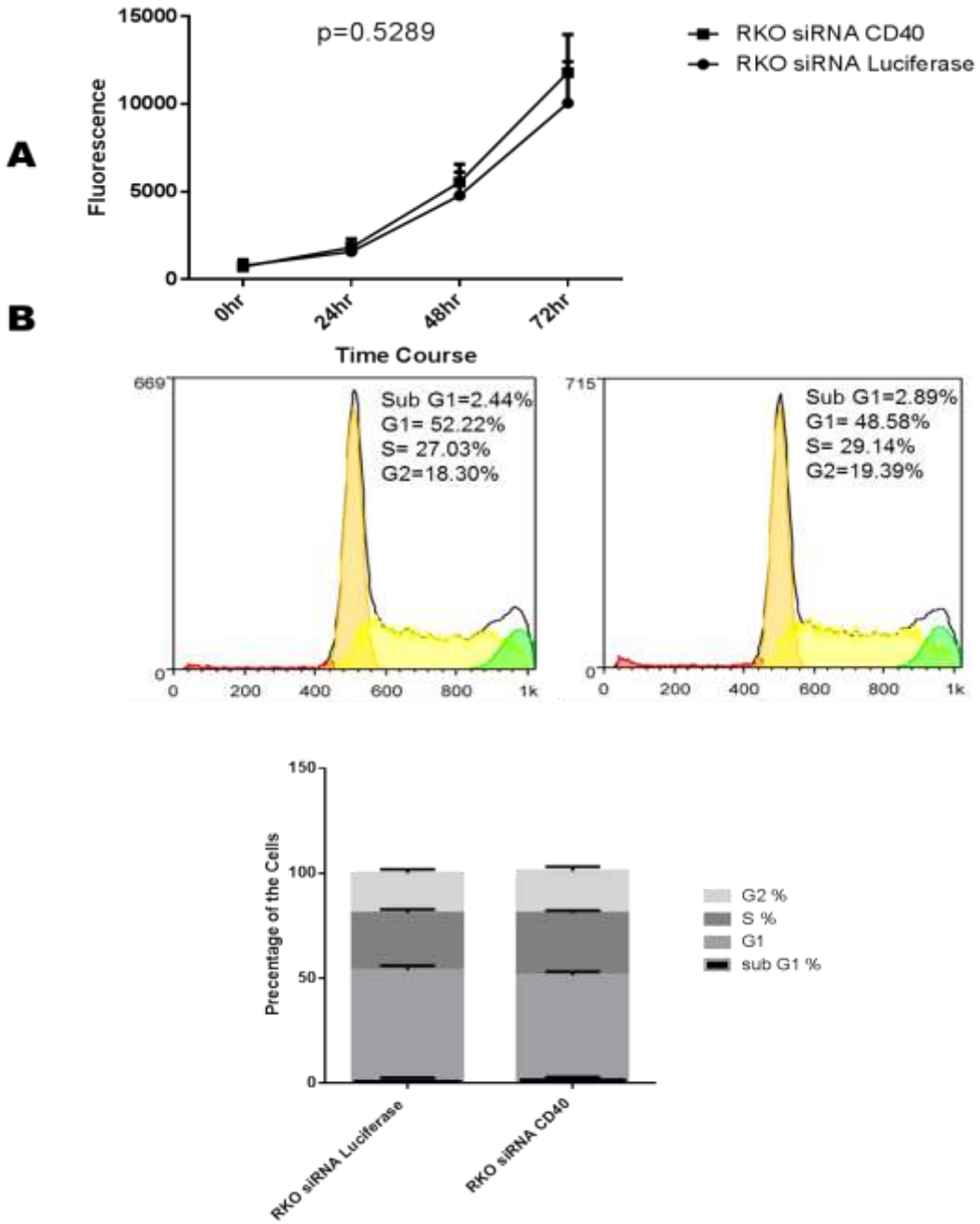


Figure 4-22. Effect of CD40 on cell proliferation and cell cycle in RKO cells.
(A) Proliferation time course assay: Cells were harvested 48h after siRNA transfection. Then, cells ($2X10^4$) were seeded into 24 well-plates in triplicate. Presto Blue was added to each well, and then the fluorescence intensity (relative fluorescence units-RFUs) was measured using for excitation at 495nm and a filter for emission at 580nm. Proliferation was assessed at 4 time points after CD40 knockdown in RKO cells. Cell viability was measured by fluorescence. (B) The percentages of cells in each cell cycle phases in both CD40 knocked down and control RKO cells were not significantly different. The lower panel in graph (B) represents the results of the cell cycle analysis of the CD40 knocked down and control RKO cells. All data are presented as mean ± SD of three independent experiments.

4.1.2.2.4 CD40 did not regulate cell motility in CRC cell lines

It has previously been reported that CD40 enhances cell motility in melanoma. Thus, we studied CD40 effect on cell motility using transwell migration assays. Following CD40 knockdown, HCT116 cells did not exhibit any decrease or increase in the number of cells that migrated through the transwell membrane. To validate this result, wound healing assay was performed. HCT116 $^{siRNA\ CD40}$ cells migrated at the same rate as HCT116 $^{siRNA\ Luciferase}$ cells across the wound. Similar results were obtained using SW620 cells.

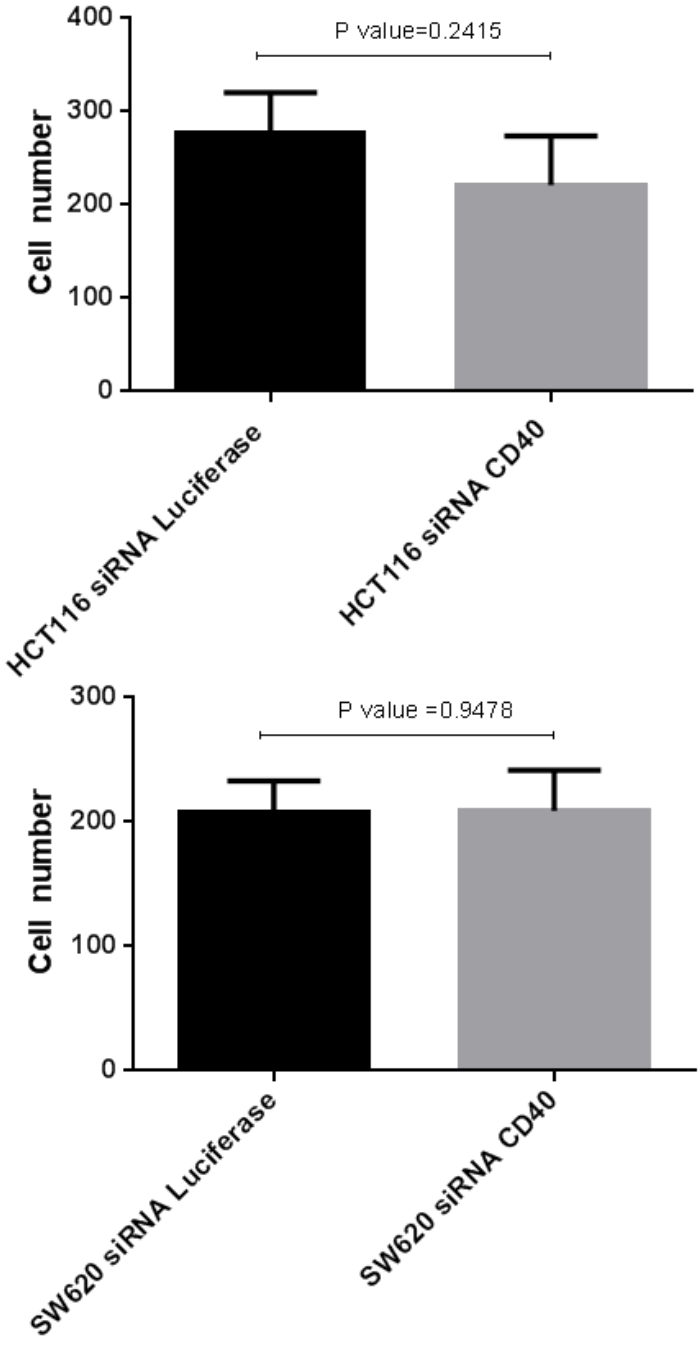


Figure 4-23. CD40 did not affect cell motility in transwell migration assay.
Transwell migration assay was performed to study cell migration in CRC cell lines. Migration of HCT116 $^{siRNA\ CD40}$ and SW620 $^{siRNA\ CD40}$ cells was compared with that of HCT116 $^{siRNA\ Luciferase}$ and SW620 $^{siRNA\ Luciferase}$, respectively. CD4 downregulation in both cell lines had no significant effect on cells when compared to the control. Results are expressed as means ± SD. All experiments were performed in triplicate.

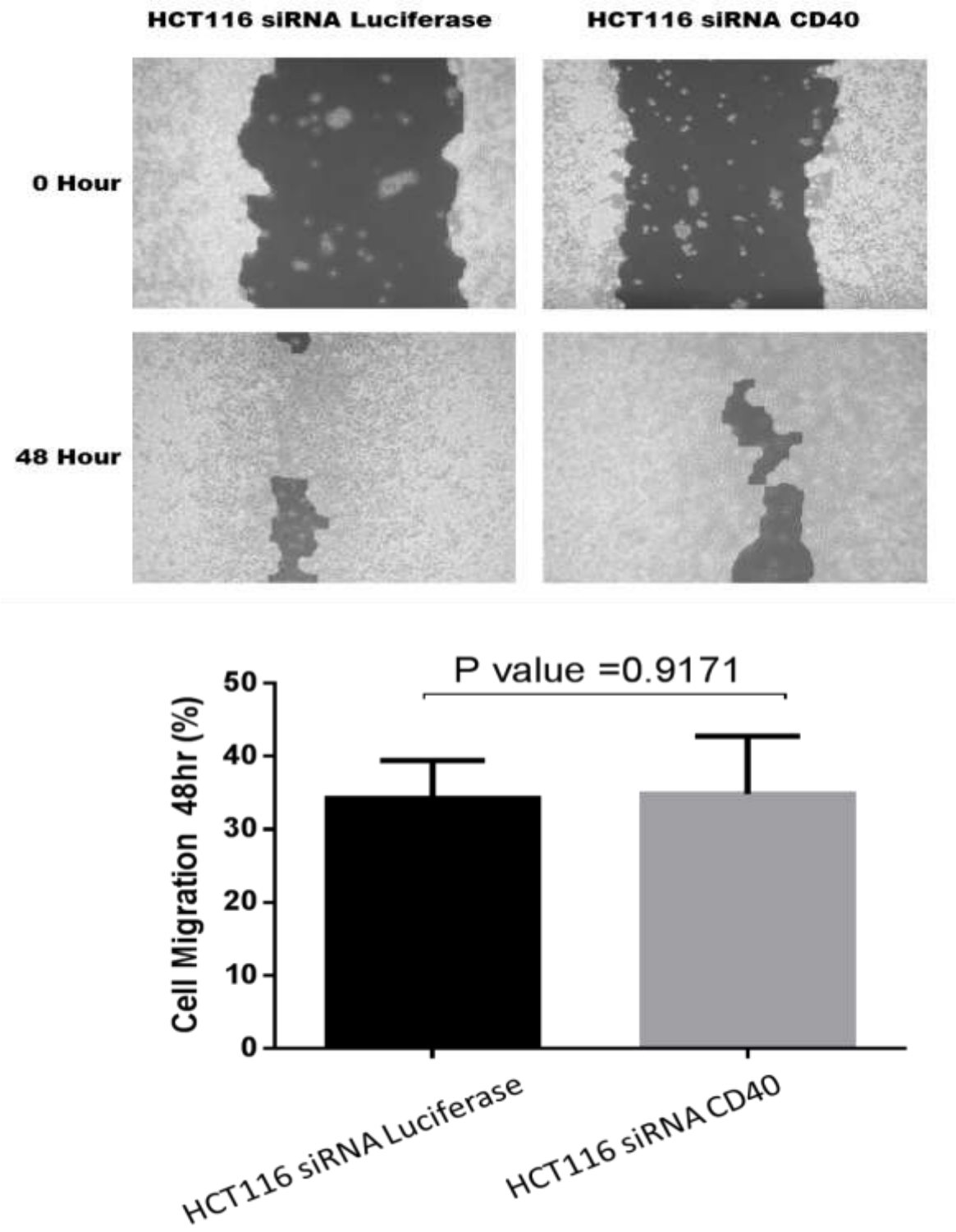


Figure 4-24. Wound healing assay.
After 48 h of CD40 knockdown, wound healing assay was performed using HCT116 cell lines. CD40 downregulation did not change the ability of the cells to migrate through the scratch. The wound healing assays were performed in two independent experiments.

4.1.2.3 Discussion

The expression of CD40, TNF receptor superfamily member 5, has been reported in haematological and solid tumours. On one hand, CD40 is reported as a tumour suppressor in several haematological tumours (Dallman et al., 2003, Vonderheide and Glennie, 2013). On the other hand, CD40 plays an oncogenic role in several solid tumours (Bussolati et al., 2002, Tong et al., 2001, Sabel et al., 2000, Homig-Holzel et al., 2008). CD40 is activated by its ligand (CD40L) (Johnson et al., 1993). CD40-CD40L interaction has been reported that it induces tumour growth (Bussolati et al., 2002, Tong et al., 2001). In CRC, however, this interaction has been reported that it induces apoptosis (Georgopoulos et al., 2007). CD40 is located on chromosome 20q13, a region frequently amplified in CRC. Thus, CD40 functional activity in CRC was investigated.

CD40 and CD40L expression in human CRC primary tumour tissues in TMA was examined by IHC. The expression of CD40 was detected in cytoplasm and membrane. The membrane and cytoplasm expressions were scored separately. Although both proteins were detected in the cytoplasm of non-tumour tissues, they were not expressed in the membrane. As CD40 expression was not detected in membrane of non-tumour tissues, there is a possibility that the expression detected in the cytoplasm might be an artefact. The very low frequency of CD40 and CD40L overexpression in the cytoplasm of CRCs indicates that cytoplasmic staining was an artefact. In addition, CD40 expression was detected in CRC cell lines but not detected in other CRC cell lines. This suggests that CD40 is not expressed in normal colon cells. Therefore, expression detected in the cytoplasm of colonic tissues might be an artefact. This finding supports that CD40 is not expressed in normal colonic epithelial cells, which agreed with previous studies. (Georgopoulos et al., 2007). The other possibility is that CD40 might function depending on its cellular localisation. In addition, the fact that CD40 is expressed in malignant cells, but not in normal colonic cells suggests that CD40 plays an oncogenic role in CRC.

In the cytoplasm, CD40 overexpression was found in only 2 out of 84 (2.5%) luminal tumour tissues and similar results were obtained for the middle and edge tumour. Regarding CD40L cytoplasmic expression, no overexpression was detected in the different tumour sites. CD40 and CD40L are mainly expressed in

the membrane, which is more relevant to the function of these proteins, as one is a receptor and the other is its ligand.

The membranous CD40 expression was detected in 16% of luminal tumour, 25% middle tumour, and 20% edge tumour tissues. CD40L expression was also found in 25% to 30% of the different sites of tumour tissues. CD40 overexpression has been reported in previous study (Georgopoulos et al., 2007). The overexpression of CD40 might be due to its oncogenic role in CRC.

CD40 overexpression is associated with poor prognosis in CRC and non-small lung cancer (Wu et al., 2008, Sabel et al., 2000). A study showed that both CD40 and CD40L are expressed at the same time in (85%) breast cancer tissues (Baxendale et al., 2005). Our results showed only 2 cases expressing CD40 and its ligand at the same time in each tumour sites. CD40-CD40L interaction induces apoptosis in CRC (Georgopoulos et al., 2007). As only 2 cases showed CD40-CD40L interaction, CD40 might induce apoptosis in small fraction of CRCs.

In order to study CD40 expression in CRC cell lines, western blot was used. Results showed that CD40 is expressed in HCT116, DLD1, RKO, and HT29. However, it was not expressed in SW480 cell line and its metastatic counterpart, SW620 cell line. Our results are in agreement with previous studies in which HCT116 cells highly expressed CD40, which was not detected in SW480 (Wu et al., 2008, Georgopoulos et al., 2007). However, another study indicated that CD40 was not expressed on HT29 cells, which is inconsistent with our finding that HT29 cells express CD40 as detected in western blot (Georgopoulos et al., 2007). Interestingly, cell lines that not 20q amplified (HCT116, RKO and DLD1) showed higher expression of CD40 compare to 20q amplified (HT29). Therefore, CD40 is not overexpressed due to 20q amplification; it might be due to its role as oncogene.

CD40 overexpression in CRC tumours suggests that CD40 promotes CRC progression. We used siRNA to knockdown CD40 and tested CD40 function in CRC cell lines. Proliferation assay results showed that CD40 knockdown reduced cell number in 3 out of 4 tested cell lines. The cell number of CD40 knocked down HCT116 cells decreased when compared to the control cells. cell cycle analysis

showed that increased of number of apoptotic cells when CD40 was knockdowned. This suggests that CD40 increased cell number by reducing apoptosis. The same effect was observed for CD40 knocked down HT29 and DLD1 cells. CD40 knockdown in RKO cells did not have the same effect, suggesting a cell line specific effect (Gillet et al., 2013).

Only two studies reported the function of CD40 in CRC. Both studies showed that CD40 promotes apoptosis in CRC cell lines (Wu et al., 2008, Georgopoulos et al., 2007). Both studies studied the apoptotic effect of CD40 when activated with recombinant soluble CD40L or membrane CD40L. However, they did not study the effect of CD40 knockdown or overexpression. It might be that CD40 reduces apoptosis and when interacts with CD40L it activates the apoptosis in CRC. Our results suggest that CD40 inhibits apoptosis in CRC. An in *vivo* study showed that constitutive CD40 signaling exerts transforming activity. This transforming activity may occur due to selective activation of MAPKs, JNK, the non-canonical NF-κB pathway, and Erk. Therefore, studying CD40 signalling pathway in CRC might reveal which pathway is affected by existence of CD40 in CRC cell.

These results are in agreement with a study indicating that CD40 increases the growth of breast cancer *in vivo* (Baxendale et al., 2005). Cell motility of CRC cells knocked down for CD40 was studied. Transwell migration assay showed no effect of CD40 knockdown on cell migration. These results were confirmed by the wound healing assay. In CRC, CD40 inhibit apoptosis in colorectal cancer cells and does not regulate cell moiltity.

In conclusion, this study has investigated CD40 expression and function. We have found CD40 is overexpressed in approximately 20% of tumours and the studies with cell lines show that it can occur even without 20q amplification. CD40 is generally expressed in all locations within the tumour and does not require CD40L co-expression. Our study confirmed that CD40 can promote CRC proliferation by inhibiting apoptosis .It does not however affect cell motility. Studying CD40 signalling pathway in CRC cell lines could provide more information, which could be used for future applications of CD40 antibody in the treatment of CRC. As for PTPN1, expression data were not linked with clinical data. Such data could be used to assess the potential of CD40 as a novel molecular marker to indicate the progression and prognosis for patients with CRC.

4.1.3 Phosphatidylinositol (3,4,5)-trisphosphate (PIP_3)-dependent Rac exchanger 1 (*PREX1*)

4.1.3.1 Introduction

PREX1 is a large multi-domain of guanine nucleotide exchange factors (GEF), which catalyses nucleotide exchange for the RAC subfamily of RHO GTPases. RHO Importantly, PREX1 oncogenic role has been reported in breast, melanoma and prostate cancer (Qin et al., 2009, Wong et al., 2011, Sosa et al., 2010). This gene was previously reviewed in detail in section 1.6.3. However, it role in CRC has not been investigated. Therefore, investigation, PREX1 role in CRC tumorigenesis would clarify its role in CRC.

4.1.3.2 Results

4.1.3.2.1 IHC

PREX1 protein expression has not been studied in CRC tissue. Nevertheless, PREX1 expression has been studied in melanoma tissues and its up regulation is associated with tumour growth. Thus, observing PREX1 expression in CRC tissues could show up regulation of PREX1. We evaluated PREX1 expression in 84 CRC cases arrayed in a TMA. The data were divided into two different categories; no expression of PREX1 and expression of PREX1 (Figure 4-26). Expression of PREX1 was not seen in any of the normal colonic epithelial tissues and it was considered as the 0 H scoring (Table 4-10). Consequently, any PREX1 staining was considered as PREX1 tissue expression.

However, PREX1 expression was detected in the cytoplasm of the different tumour sites. PREX1 expression was detected in the luminal tumour of 36 cases (46%). PREX1 expression was observed in the middle and the edge of the tumour in 61% of the cases (Table 4-11).

The association between PREX1 expression in the different tumour sites was studied (Table 4-12, Table 4-13, and Table 4-14). There was no significant association between PREX1 expression patterns in the different tumour sites. However, 34% concordance was observed between cases expressing PREX1 in both the middle and the edge of the tumour and 31% of concordance was

observed between the luminal and middle tumour sites. The level of concordance (27%) was not different between the luminal and edge tumour site.

Table 4-10. PREX1 overall staining.
Immunohistochemistry of 84 CRC series was performed to study protein expression.

	PREX1Luminal Tumour Staining	PREX1Middle Tumour Staining	PREX1Edge Tumour Staining	PREX1non-tumour colonic tissue Staining
Minimum H scoring	0	0	0	0
Maximum H scoring	130	170	137	100.00

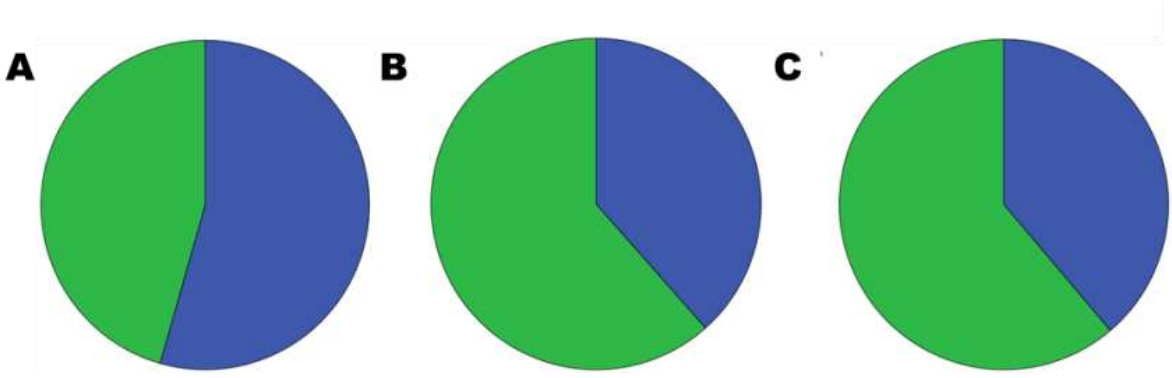


Figure 4-25. Pie chart showing the frequencies of absence and presence of PREX1 expression.
Immunohistochemistry of 84 CRC series was performed to study protein expression. This pie chart describe the frequency of protein expression in our series. The blue sections indicate absence of PREX1 protein expression and green sections indicate PREX1 expression in different tumours sites. (A) PREX1 luminal tumour staining. (B) PREX1 middle tumour staining (C) PREX1 edge tumour staining.

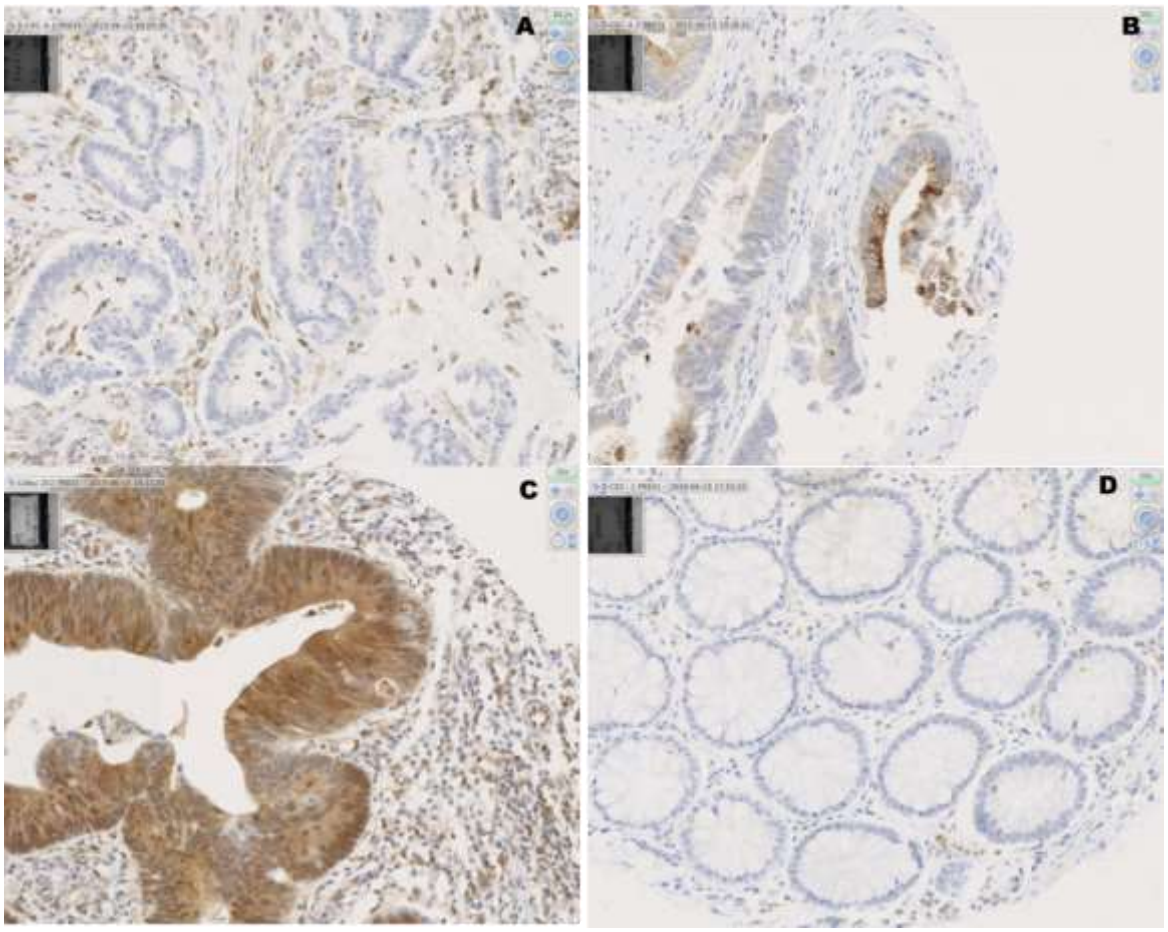


Figure 4-26. PREX1 IHC in normal colon and malignant colonic tissues.
Figure (A) shows the absence of PREX1 expression in CRC tumour tissues. (B) Weak PREX1 expression in tumour tissues. (C) Strong PREX1 expression in tumour tissues. (D) Absence of expression in normal colonic epithelial tissue. PREX1 is expressed in the cytoplasm tumour tissues. All pictures were acquired at 20×

Table 4-11. Overall frequency of PREX1 expression in different matched CRC tumour sites.

Immunohistochemistry of 84 CRC series was performed to study protein expression.

		Frequency	Percent (%)
PREX1Luminal Tumour Staining	No expression	43	54
	PREX1expression	36	46
PREX1 Middle Tumour Staining	No expression	30	39
	PREX1expression	48	61
PREX1Edge Tumour Staining	No expression	26	39
	PREX1expression	41	61
PREX1non-tumour tissue Staining	No expression	63	100
	PREX1expression	0	0

Table 4-12. Cross tabulation of PREX1 edge tumour *vs.* PREX1 middle tumour staining.

Immunohistochemistry of 84 CRC series was performed to study protein expression. In this table, the correlation of PREX1 expression of advancing tumour compared to PREX1 expression central tumour.

			PREX1Edge tumour		Total
			no PREX1expression	PREX1expression	
PREX1Middle tumour	no PREXession	Count	11 (17%)	15 (24%)	26
	PREX1expr	Count	15 (24%)	21 (34%)	36
Total		Count	26	36	62

Table 4-13. Cross tabulation of PREX1 luminal tumour *vs*. PREX1 middle tumour staining.

Immunohistochemistry of 84 CRC series was performed to study protein expression. In this table, the correlation of PREX1 expression of luminal tumour compared to PREX1 expression central tumour.

			PREX1Luminal tumour		Total
			no PREX1expression	PREX1expression	
PREX1Middle tumour	no PRression	Count	19 (26%)	11 (14%)	30
	PREX1exp	Count	21 (28%)	23 (31%)	44
Total		Count	40	34	74

Table 4-14 Cross tabulation of PREX1 luminal tumour *vs.* PREX1 edge tumour staining.

Immunohistochemistry of 84 CRC series was performed to study protein expression. In this table, the correlation of PREX1 expression of luminal tumour compared to PREX1 expression advancing tumour.

			PREX1Luminal tumour		Total
			no PREX1expression	PREX1expression	
PREX1Edge tumour	no PREX1expression	Count	12 (19%)	11 (17%)	23
	PREX1expression	Count	23 (37%)	17 (27%)	40
Total		Count	35	28	63

4.1.3.2.2 PREX1 knockdown

PREX1 protein expression has not been previously studied in CRC tissue or cell lines. PREX1 protein expression in CRC cell lines was studied by western blotting. Thirty micrograms of proteins from 6 CRC cell line lysates were separated on 4–12% Bis-Tris Plus Gel and a PREX1 antibody was used to detect PREX1 protein expression. After measuring the band intensity and densitometry and after normalisation to β-actin expression, the HT29 cells (20q amplified) showed weak PREX1 expression. Furthermore, SW480cells, which is 20q amplified, did not express PREX1, but SW620 (secondary tumour of SW480) did. DLD1 cells highly expressed PREX1. PREX1 expression detected by western blot varied from one cell line to the other from no expression to high expression (Figure 4-27).

PREX1 knockdown was performed by transfection of a siRNA targeting PREX1 into cell lines (cell line $^{siRNA\ PREX1}$) and control cells were transfected with a siRNA targeting luciferase (cell line $^{siRNA\ Luciferase}$). PREX1 expression was successfully knocked down in CRC cell lines when compared to control cells. PREX1 knockdown efficiencies in CRC cell lines were determined by western blot and were approximately 60-67.5% (Figure 4-28-A). PREX1 knockdown was confirmed by real time PCR. PREX1 was downregulated by approximately 60% compared to the control (Figure 4-28-B).

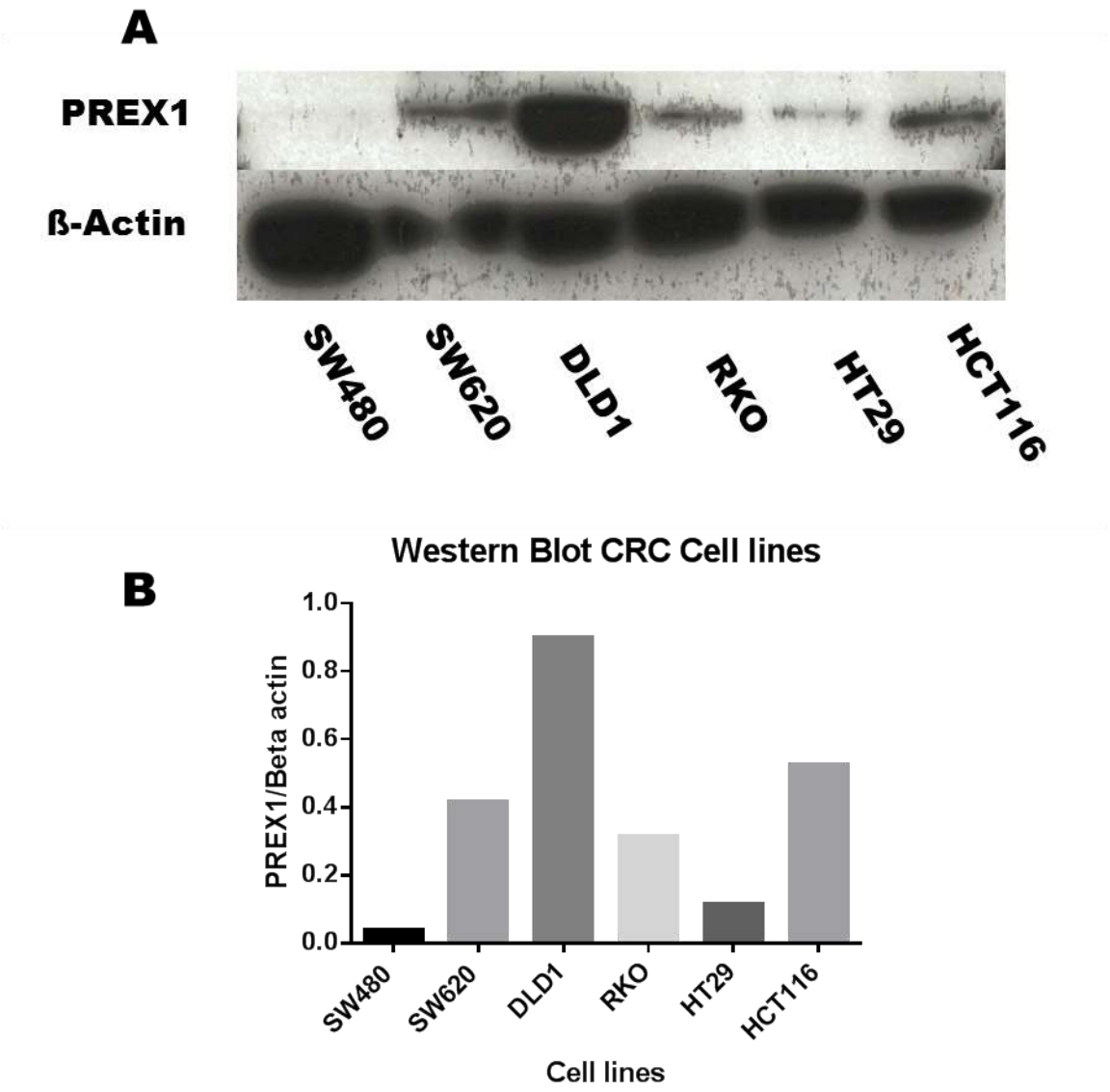


Figure 4-271. Western blot screening of PREX1 expression in 6 CRC cell lines.

(A) Cell lysates (30µg) were analysed using 4–12% Bis-Tris Plus Gel. A PREX1 antibody was used to detect PREX1 protein expression levels. The loading control was the housekeeping protein ß-actin (1:50,000). (B) Histogram represents the western blot intensities analysed by ImageJ software. The band intensity detected by the PREX1 antibody was normalised by its corresponding ß-actin band.

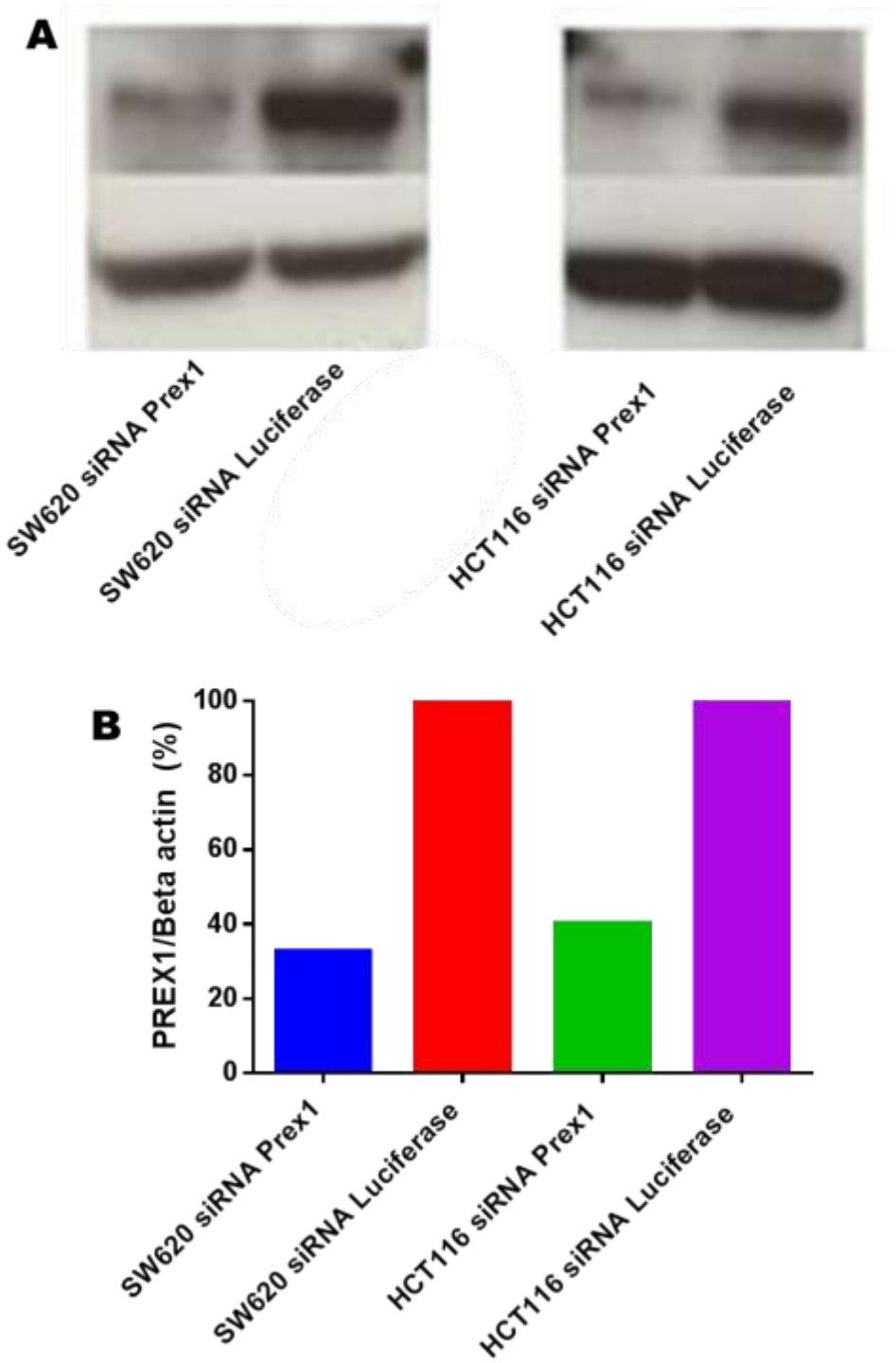


Figure 4-28. PREX1 knockdown in SW620 and HCT116 cells.
(A) All cell lines were transfected by a siRNA targeting PREX1 (cell line $^{siRNA\ PREX1}$) or a siRNA targeting luciferase (cell line $^{siRNA\ Luciferase}$). After three days of knockdown, western blot was performed to confirm PREX1 downregulation in all tested CRC cell lines. β-actin was used as a loading control. In HCT116 cell line, the knockdown effeminacy was 67.5% and 60% in HCT116 cell line

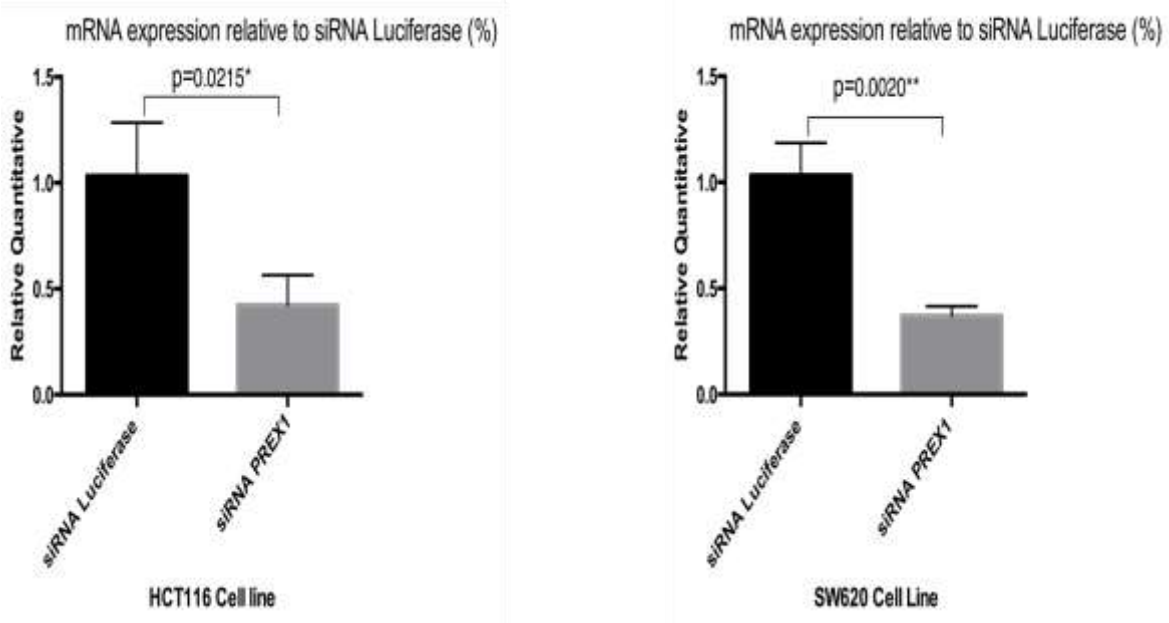


Figure 4-29 PREX1 knockdown in SW620 and HCT116 cells qPCR

Figures show PREX1 expression in HCT116 and SW620 cells transfected with a siRNA targeting *PREX1* gene. PREX1 knockdown was validated by RT-qPCR. The relative expression difference of the target gene in Knockdown cells against reference sample (RNA extracted from cells transfected with an siRNA targeting luciferase gene) is given by 2–ΔΔCt equation. The house keeping gene Hypoxanthine phosphoribosyl-transferase 1 (HPRT1) expression was used as endogenous control to normalise data from candidate genes. The ABI 7500 Fast System software and RQ software (Applied Biosystems) was used to analyse the data.

4.1.3.2.3 PREX1 enhances cell proliferation in CRC cell lines

PREX1 has been reported to enhance cell proliferation in breast cancer and melanoma cell lines. PREX1 functions have not been studied in CRC cell lines. Therefore, proliferation was assessed at 4 different time points in a number of CRC cell lines to determine the effect of PREX 1knockdown on cell proliferation using Presto Blue assay. Proliferation of SW620 $^{siRNA\ PREX1}$was significantly decreased when compare to that of SW620 $^{siRNA\ Luciferase}$ (P = 0.0097**, Two way anova test) (Figure 4-30). Moreover, the proliferation rate of HCT116 $^{siRNA\ PREX1}$ cells decreased when compared to that of HCT116 $^{siRNA\ Luciferase}$ (P > 0.0001*** Two way anova test) (Figure 4-30).

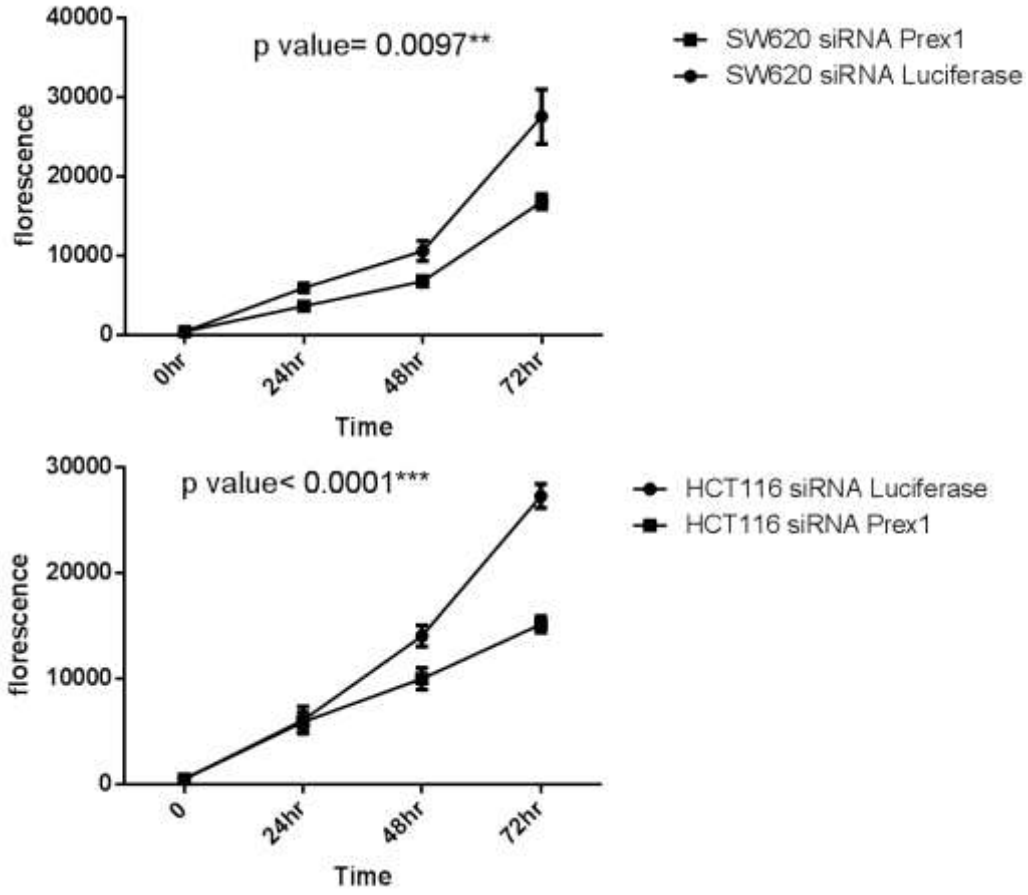


Figure 4-30. Effect of PREX1 on cell proliferation in SW620 and HCT116 cells.

Proliferation time course assay : Cells were harvested 48h after siRNA transfection. Then, cells ($2X10^4$) were seeded into 24 well-plates in triplicate. Presto Blue was added to each well, and then the fluorescence intensity (relative fluorescence units-RFUs) was measured using for excitation at 495nm and a filter for emission at 580nm. Proliferation was assessed at 4 time points after PREX1 knockdown in SW620 and HCT116 cells. Cell viability was measured by fluorescence. All data are expressed as mean ± SD of three independent experiments.

4.1.3.2.4 PREX1 enhances cell motility in CRC cell lines

Transwell migration assay was used to study the effect of PREX1 downregulation on the motility of CRC cell lines. SW620 cells were transfected with the siRNA targeting PREX1 and the siRNA targeting luciferase (control). SW620 $^{siRNA\ PREX1}$cells migrated slower than SW620 $^{siRNA\ Luciferase}$ cells (P = 0.0001, unpaired T-test). Furthermore, HCT116 $^{siRNA\ Luciferase}$ cells migrated significantly faster than HCT116 $^{siRNA\ PREX1}$ (P = 0.0202, unpaired T-test) (Figure 4-31). In order to validate these results, wound healing assay was performed using HCT116 cells. Cells transfected with PREX1 siRNA migrated across the wound more slowly than the control cells (P = 0.0218, unpaired T-test) (Figure 4-32). Invasion assay was performed to study the effect of PREX1on cell motility. HCT116 $^{siRNA\ PREX1}$ capability to invade the transwell covered with matrigel was lower than that of HCT116$^{siRNA\ Luciferase}$ cells (P = 0.0012, unpaired T-test).

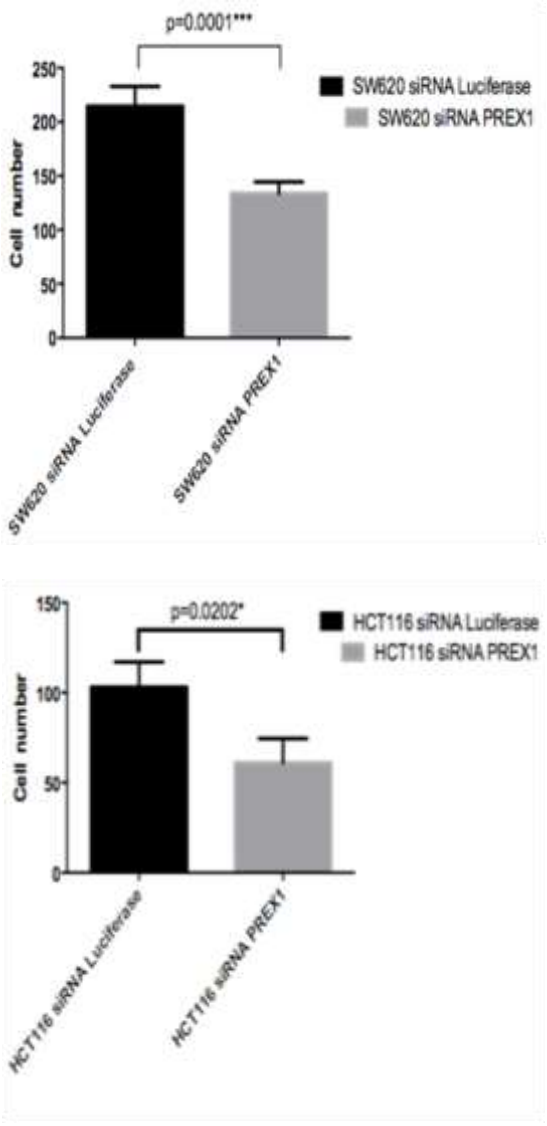


Figure 4-31. PREX1 enhanced motility in transwell migration assay.
Transwell migration assay was performed to study cell migration in CRC cell lines. Migration of SW620 $^{siRNA\ PREX1}$ and HCT116 $^{siRNA\ PREX1}$ cells were compared to that of the relevant control cell lines. For all tested cell lines, PREX1 downregulation resulted in a decrease in the migration when compared to that of the control cells. All results are expressed as means ± SD. All experiments were performed in triplicate.

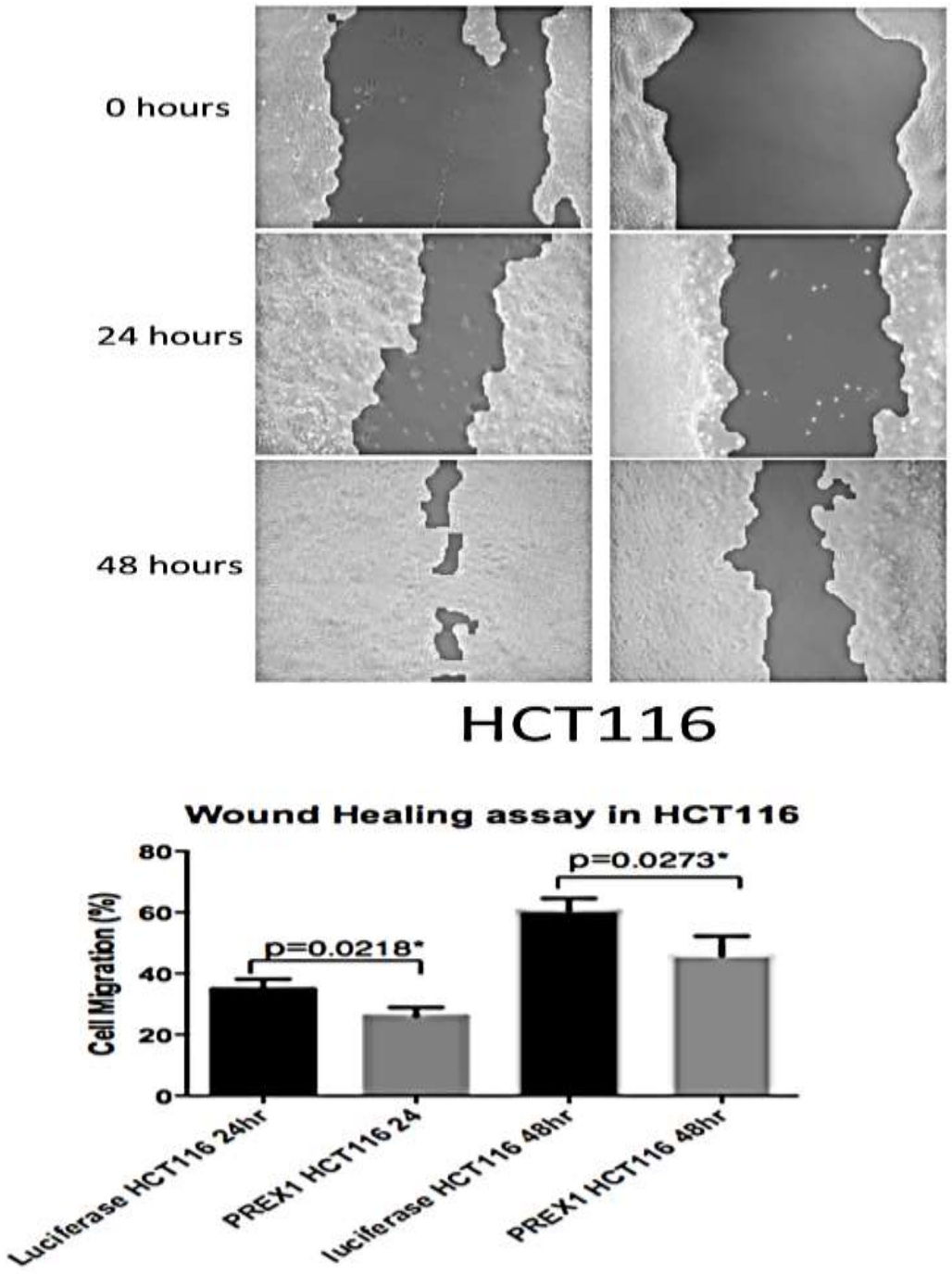


Figure 4-32. Wound healing assays.
After 72 h of PREX1 knockdown, wound healing assay was performed in HCT116 cells. PREX1 downregulation reduced the ability of cells to migrate through the scratch. The wound healing assays were performed in two independent experiments.

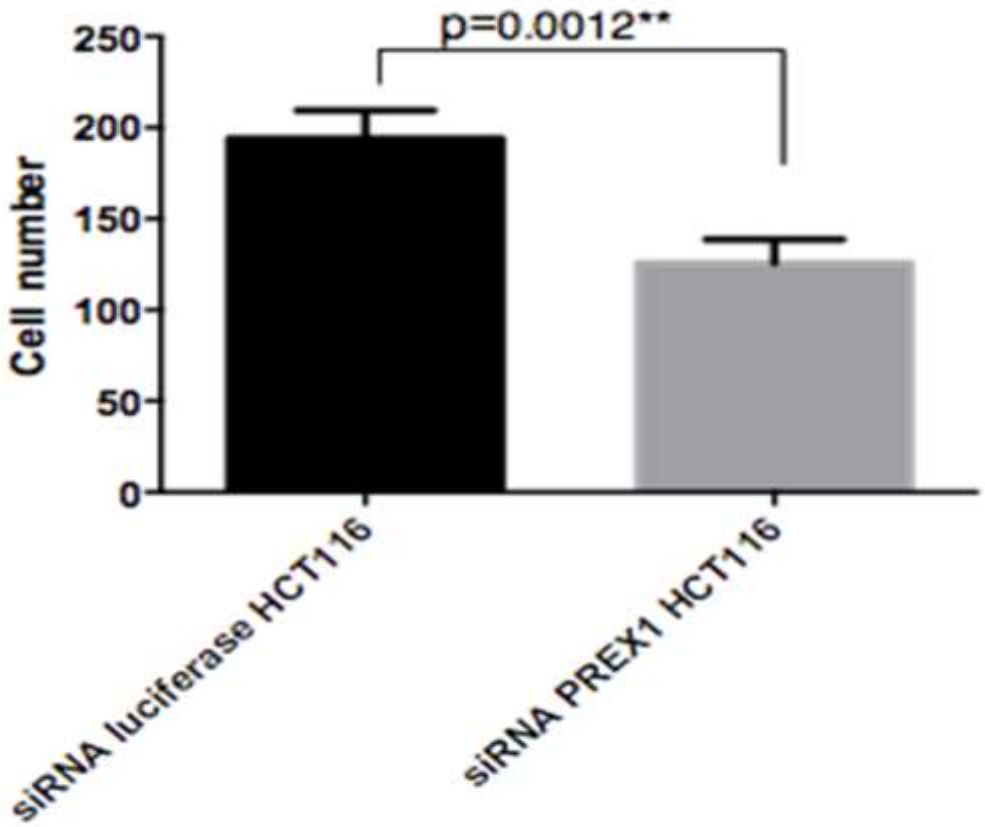


Figure 4-33. PREX1 increase cell invasion ability.
A significant decreased was observed in the number of HCT116 $^{siRNA\ PREX1}$cells that invaded the membrane when compared to that of HCT116 $^{siRNA\ Luciferase}$ cells. Values are expressed as means ± SD. The experiment was performed in duplicate.

4.1.3.3 Discussion

PREX1 activates RHO family GTPases by stimulating the transfer of GDP to GTP. This activation regulates cell motility and morphology (Herter et al., 2013, Waters et al., 2008, Yoshizawa et al., 2005). The oncogenic role of PREX1in cancer has been reported. However, PREX1 expression has not been studied in CRC cell lines or clinical tissues. Moreover, PREX1 role in CRC cell line growth and migration has not been investigated. Therefore, in this study, PREX1protein expression was studied in CRC clinical tissues. Furthermore, PREX1 was knocked down in CRC cell lines and cell growth and migration were monitored.

PREX1expression in human CRC primary tumour tissues was examined by IHC. Results showed that PREX1 expression was detected in the cytoplasm. Normal colonic epithelial cells did not express PREX1 in all cases. For the first time, we reported the up-regulation of PREX1 expression in 61% of CRC tumours. In other organ system PREX1 is not expressed in normal tissue but shows up-regulation in tumour tissue such as breast cancer, and melanoma (Montero et al., 2011, Sosa et al., 2010, Lindsay et al., 2011). These up-regulations are associated with tumour growth and lymph node metastases. PREX1 was overexpressed in CRC tissues, precisely in 47% of luminal tumour tissues, and the frequency increased in central and advancing tumours (61%). Thus, PREX1 overexpression in CRC might drive tumour as in other cancer.

PREX1 expression in CRC cell lines was also studied. Western blot analysis indicated that PREX1expression was weak in HT29 cells. Additionally, SW480 did not express PREX1, but SW620 (secondary tumour of SW480) weakly expressed PREX1, although both cell lines are 20q amplified. PREX1 was highly expressed in DLD1 and HCT116 cells. These two cell lines are not 20q amplified. Therefore, PREX1 overexpression in CRC is not associated with gene amplification as observed in breast cancer (Sosa et al., 2010). PREX1 overexpression might be a consequence of the loss of repression through histone deacetylases (HDACs) as observed in prostate cancer (Wong et al., 2011).

To study PREX1 effect on CRC, a PREX1 siRNA was transfected into CRC cell lines and growth and motility assays were performed. The proliferation rate of PREX1 knocked down CRC cells decreased when compared to that of the control cells. This effect was observed in the different tested CRC cell lines. Thus, PREX1

enhances CRC cell proliferation. PREX1 also enhances tumour growth in other organs system. PREX1 enhances tumour growth of pancreatic and breast cancers, and melanoma *in vivo* and *in vitro* (Qin et al., 2009, Kim et al., 2011, Campbell et al., 2013, Sosa et al., 2010).

PREX1 knockdown in CRC cell lines inhibited cell motility. In transwell migration, fewer cells migrated through the membrane compared following knockdown to the control cells for both SW620 and HCT116 cell lines (SW620 $^{siRNA\ PREX1}$,vs SW620 $^{siRNA\ Luciferase}$, $p< 0.0001$) indicating that PREX1 probably promotes cell migration in CRC. For further validation, wound healing assay confirmed that PREX1 promotes CRC cell lines migration. Furthermore, PREX1 knockdown reduced matrigel invasion of HCT116 cells. This phenomenon has also been reported in breast cancer cell lines (Sosa et al., 2010). In melanoma, PREX1 similarly promotes cell motility *in vivo* and *in vitro* (Lindsay et al., 2011).

In conclusion, this study is the first to investigate the expression of PREX1 in CRC. Moreover, this study explored the role of PREX1in cell proliferation and motility of CRC. Our study confirmed that PREX1 is up-regulated in invasive cancers and it promotes CRC proliferation and cell motility (both migration and invasion) *in vitro*. The PREX1 signalling pathway has not been studied in CRC cell lines and needs further investigation. Some studies investigated the potential of targeting the PREX1 pathway for cancer treatment. The expression data were not accompanied with clinical data in this study. Such data could be used to determine whether PREX1 can be considered as a novel molecular marker to indicate CRC progression and prognosis in patients.

4.1.4 Engulfment and cell motility (ELMO2)

4.1.4.1 Introduction

ELMO2 belongs to the family ELMO that has a role in cytoskeletal rearrangements requisite for cell motility and phagocytosis of apoptotic cells. The role of ELMO2 in cancer development and metastasis remains unclear (reviewed in more detail in section 1.6.4). Exploring the role of ELMO2 in CRC could reveal its role in cancer development and/or metastasis.

4.1.4.2 Result

4.1.4.2.1 Immunohistochemistry

ELMO2 protein expression has not been studied in CRC tissue. Nevertheless, ELMO2 expression has been studied in Breast cancer tissues and its up regulation is associated with associated with metastasised tumour (Li et al., 2013). We evaluated ELMO2 expression in 84 CRC cases arrayed in a TMA as previously described. As in PREX1, the data were divided into two different categories; no expression and expression of ELMO2 (). The ELMO2 expression was not detected in any of the non-tumour colonic epithelial tissues. Therefore, any expression detected was considered as ELMO2 tissue expression.

Expression of ELMO2 was detected in 24 cases luminal tumour cases (29%). The percentage of cases expressed ELMO2 slightly increased in central tumour in 37% of the cases and similar percentage was found in advancing tumour tissues .

Associations of ELMO2 expression in different tumour sites were investigated (Table 4-17, Table 4-18 and Table 4-19). As in PREX1expression, there were no significant associations found between ELMO2 expression patterns in different site of tumour. Furthermore, only 10% concordance found between cases expressed ELMO2 in both middle and edge tumour, and 15% of concordance found between luminal and middle tumour.

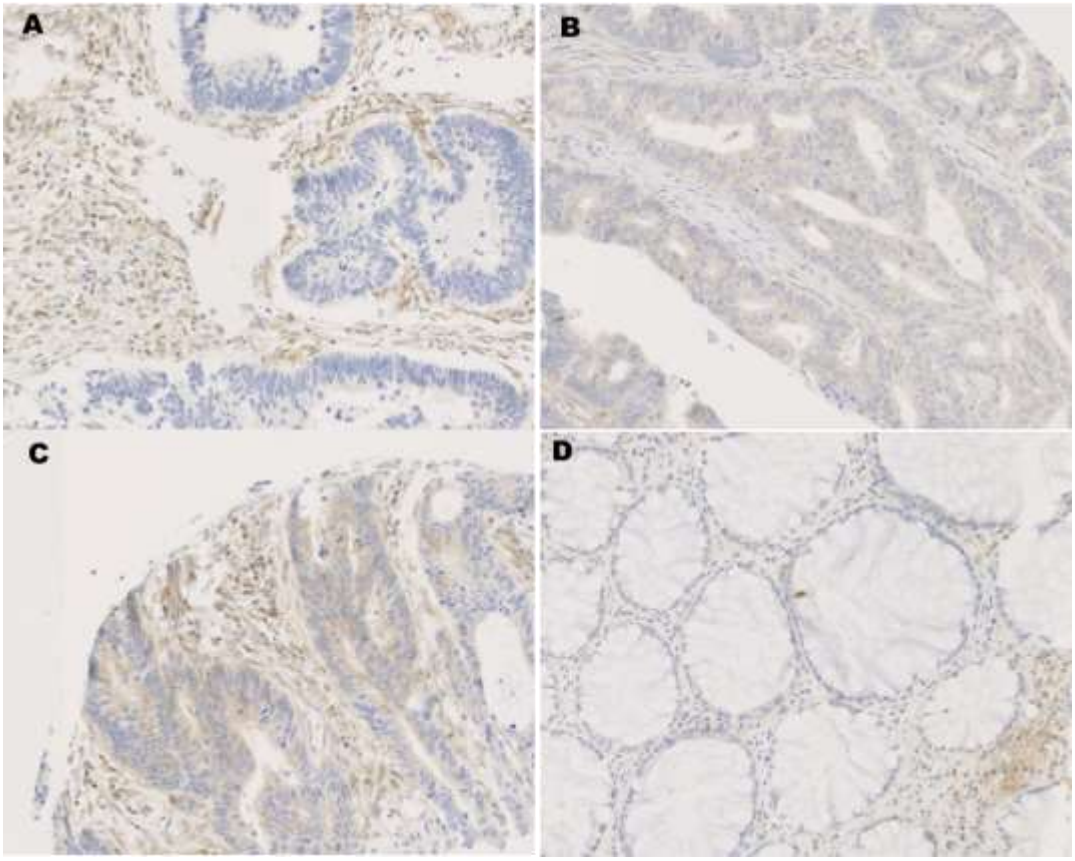


Figure 4-34 No expression of ELMO2 and Expression of ELMO2 staining.
Figure (A) is a no expression of ELMO2 in CRC tumour tissue. (B) Tumour tissue was weakly expressed ELMO2. (C) Tumour tissue was highly expressed ELMO2 (D) No ELMO2 expression detected in non-tumour tissues. ELMO2 showed cytoplasmic staining in all tumour tissues. all pictures were taken at X20.



Figure 4-35 Pie chart showed the frequencies of high and low expression of ELMO2
Immunohistochemistry of 84 CRC series was performed to study protein expression. This pie chart describe the frequency of protein expression in our series. The Blue parts indicate cells did not express ELMO2 protein and green part indicated the expression of ELMO2 detected, in different tumours sits. (A) ELMO2 Luminal Tumour Staining. (B) ELMO2 Middle Tumour Staining (C) ELMO2 Edge Tumour Staining

Table 4-15 ELMO2 staining overview

Immunohistochemistry of 84 CRC series was performed to study protein expression

	ELMO2 Luminal Tumour Staining	ELMO2 Middle Tumour Staining	ELMO2 Edge Tumour Staining	ELMO2 non-tumour tissue Staining
Minimum H scoring	0	0	0	0
Maximum H scoring	150	105	120	0

.

Table 4-16 Overall frequency of ELMO2 in CRC tissue in different matched tumour sites.

Immunohistochemistry of 84 CRC series was performed to study protein expression Overall frequency of Low expression and High expression of ELMO2 were listed. The Low in table indicated the frequency of no expression of ELMO2.

		Frequency	Percent (%)
ELMO2 Luminal Tumour Staining	No Expression	58	71
	Elmo2 expression	24	29
ELMO2 Middle Tumour Staining	No Expression	51	63
	Elmo2 expression	30	37
ELMO2 Edge Tumour Staining	No Expression	37	62
	Elmo2 expression	23	38
ELMO2 non-tumour tissue Staining	No Expression	59	100
	Elmo2 expression	0	0

Table 4-17 Crosstabulation of ELMO2 Middle Tumour Vs ELMO2 Edge Tumour

Immunohistochemistry of 84 CRC series was performed to study protein expression. In this table, the correlation of ELMO2 expression of advancing tumour compared to ELMO2 expression central tumour.

			ELMO2 Edge tumour		Total
			no ELMO2 expression	ELMO2 expression	
ELMO2 Middle tumour	no ELMO	Count	24 (41%)	12(21%)	36
	ELM expre	Count	12 (21%)	10 (17.2%)	22
Total		Count	36	22	58

Table 4-18 Crosstabulation of ELMO2 Middle Tumour Vs ELMO2 Luminal Tumour

Immunohistochemistry of 84 CRC series was performed to study protein expression. In this table, the correlation of ELMO2 expression of Luminal tumour compared to ELMO2 expression central tumour.

			ELMO2 Luminal tumour		Total
			no ELMO2 expression	ELMO2 expression	
ELMO2 Middle tumour	no ELMO 2	Count	39(49%)	12(15%)	51
	ELMO	Count	17(21%)	12(15%)	29
Total		Count	56	24	80

Table 4-19 Crosstabulation of ELMO2 Luminal Tumour Vs ELMO2 Edge Tumour

Immunohistochemistry of 84 CRC series was performed to study protein expression. In this table, the correlation of ELMO2 expression of Luminal tumour compared to ELOM2 expression advanced tumour.

			ELMO2 Luminal tumour		Total
			no ELMO2 expression	ELMO2 expression	
ELMO2 Edge tumour	no ELMO2	Count	26(44%)	15(25%)	41
	ELMO2	Count	11(19%)	7(7%)	18
Total		Count	37	22	59

4.1.4.2.2 ELMO2 Knockdown confirmation in mRNA and Protein expression levels

ELMO2 protein expression has not been studied before in CRC cell lines. In order to find cell lines suitable for Gene knockdown, ELMO2 protein expression was studied by western blotting (Figure 4-36). Intensity of the bands were measured and normalised to β-actin expression. The highest ELMO2 protein expression was observed in HT29 and DLD1. However, RKO and SW620 cells were moderately positive. ELMO2 knockdown was performed by transfection of siRNA Targeting ELMO2 into cell lines (cell line $^{siRNA\ ELMO2}$). ELMO2 was successfully knocked down in CRC cell lines. Validation of these knockdowns was achieved by Western blots. Knockdown of ELMO2 in CRC cell lines showed efficiencies between 55-95% Figure 4-36. Real time PCR was conducted and it showed that Elmo2 was downregulated by approximately 50% compared to the control Figure 4-36.

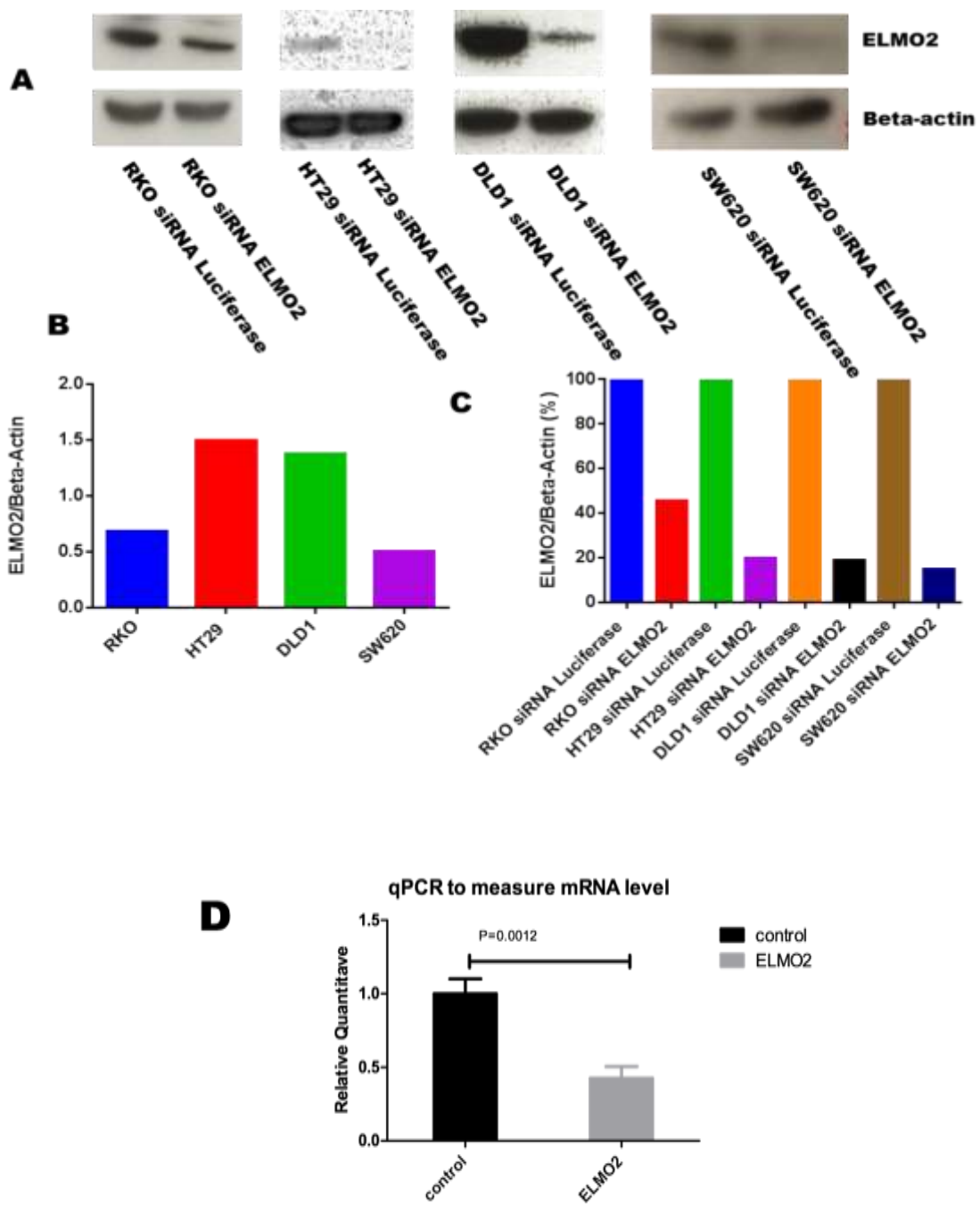


Figure 4-36 ELMO2 knockdown in four different colorectal cancer cell lines
Cell lysates (30µg) were analysed using 4–12% Bis-Tris Plus Gel. ELMO2 antibody was used to detect ELMO2 protein expression levels. The loading control was the housekeeping protein ß-actin (1:50,000). (B) Histogram represented western blot intensities analysed by ImageJ software. Band intensity detected by ELMO2 antibody was normalised by its relevant ß-actin band. (C) All CRC cell lines were transfected with a siRNA targeting ELMO2 (cell line $^{\text{siRNA ELMO2}}$) or a siRNA targeting luciferase (cell line $^{\text{siRNA Luciferase}}$). Knockdown was validated by western blot in all tested CRC cell lines. In RKO cell line, the efficiency of the knockdown was 55%. In SW620 cell line, the knockdown efficiency was 95%. Similarly for both HT29 and DLD1, the knockdown efficiencies were 80% and 81%, respectively. (D) SW620 cells were transfected with a siRNA targeting the ELMO2 gene. Knockdown was validated by RT-qPCR

4.1.4.2.3 ELMO2 enhances proliferation in CRC cell lines

There has not been any study investigated the role of ELMO2 in CRC. The role of ELMO2 in cell proliferation was investigated in several cell CRC cell lines. A time course assay was performed over 4 time points to assess the effects of ELMO2 knockdown on cell numbers using the Presto Blue assay.

The proliferation pattern of HT29 $^{siRNA\ ELMO2}$ cells significantly changed when compared to that of HT29 $^{siRNA\ Luciferase}$ cells (P value <0.0001***, Two way Anova test). For validation, cell cycle analysis showed that down regulation of ELMO2 resulted in more cells arrested in G1 and S phase compared to the control (p value = 0.00005*** and 0.0142*, respectively, unpaired T-test), Figure 4-37.

Further validation, proliferations assay was performed in SW620 and DLD1 cell lines. Similarly, down regulation of ELMO2 in SW620 inhibited proliferation when compared with control cells (p value= 0.0012*, Two way anova test) (Figure 4-38). Interestingly, DLD1 $^{siRNA\ ELMO2}$ did show similar result to HT29 and SW620 proliferation rates (P =0.0304, Two way anova test)

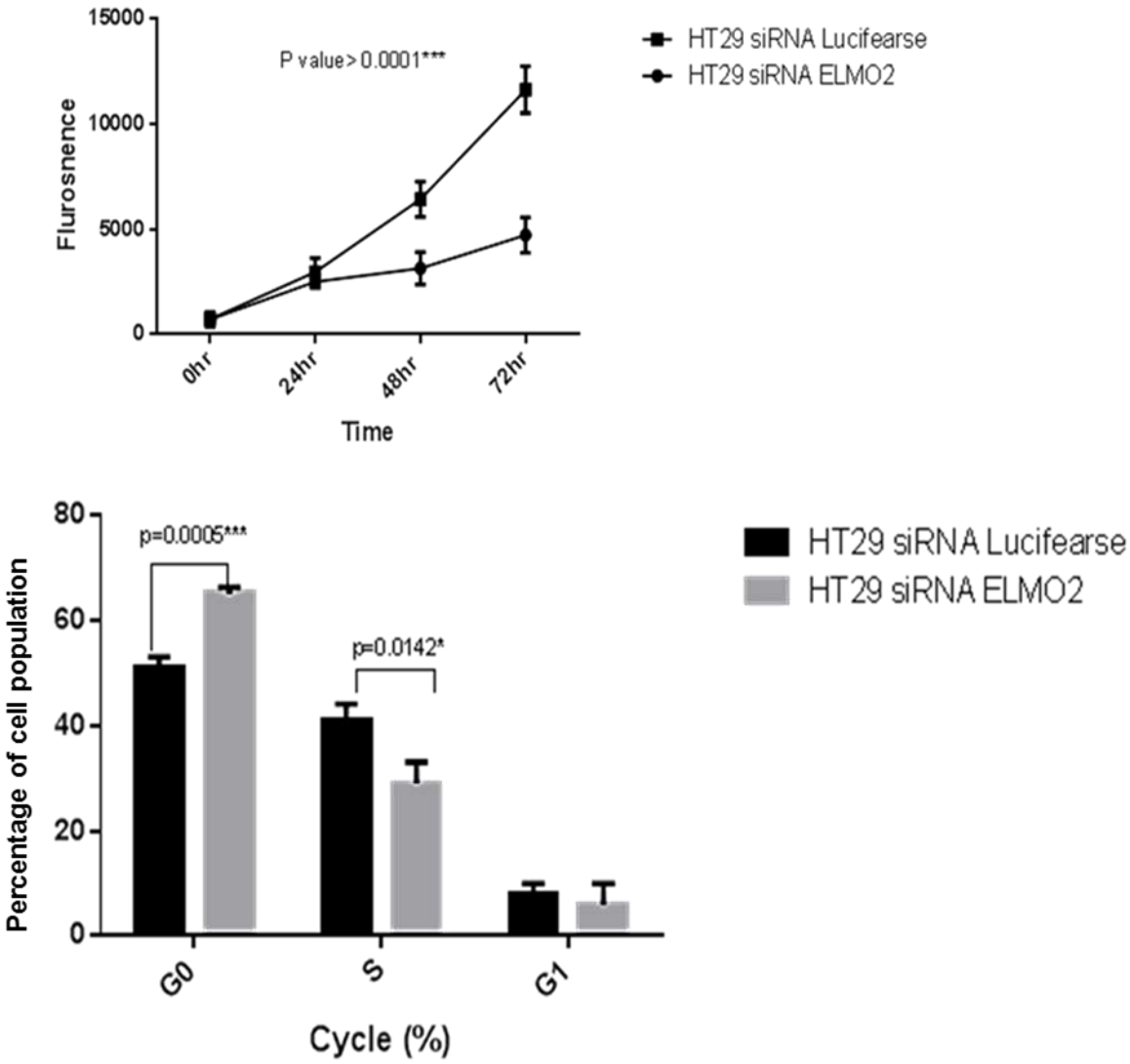


Figure 4-37 Effect of ELMO2 on cell proliferation and cell cycle in HT29.
Upper panel showed proliferation time course assay: Cells were harvested 48h after siRNA transfection. Then, cells ($2X10^4$) were seeded into 24 well-plates in triplicate. Presto Blue was added to each well, and then the fluorescence intensity (relative fluorescence units-RFUs) was measured using for excitation at 495nm and a filter for emission at 580nm. 4 time points after knockdown of ELMO2 HT29 cells viabilities were measured by fluorescence. The lower panel showed percentage of cells in each cell cycle phases in both ELMO2 Knockdown and control in HT29 were significantly different. Results analysis of cell cycle of HT29 was displayed as histogram which was designed by Prism software. All data were mean ± SD of three independent experiments

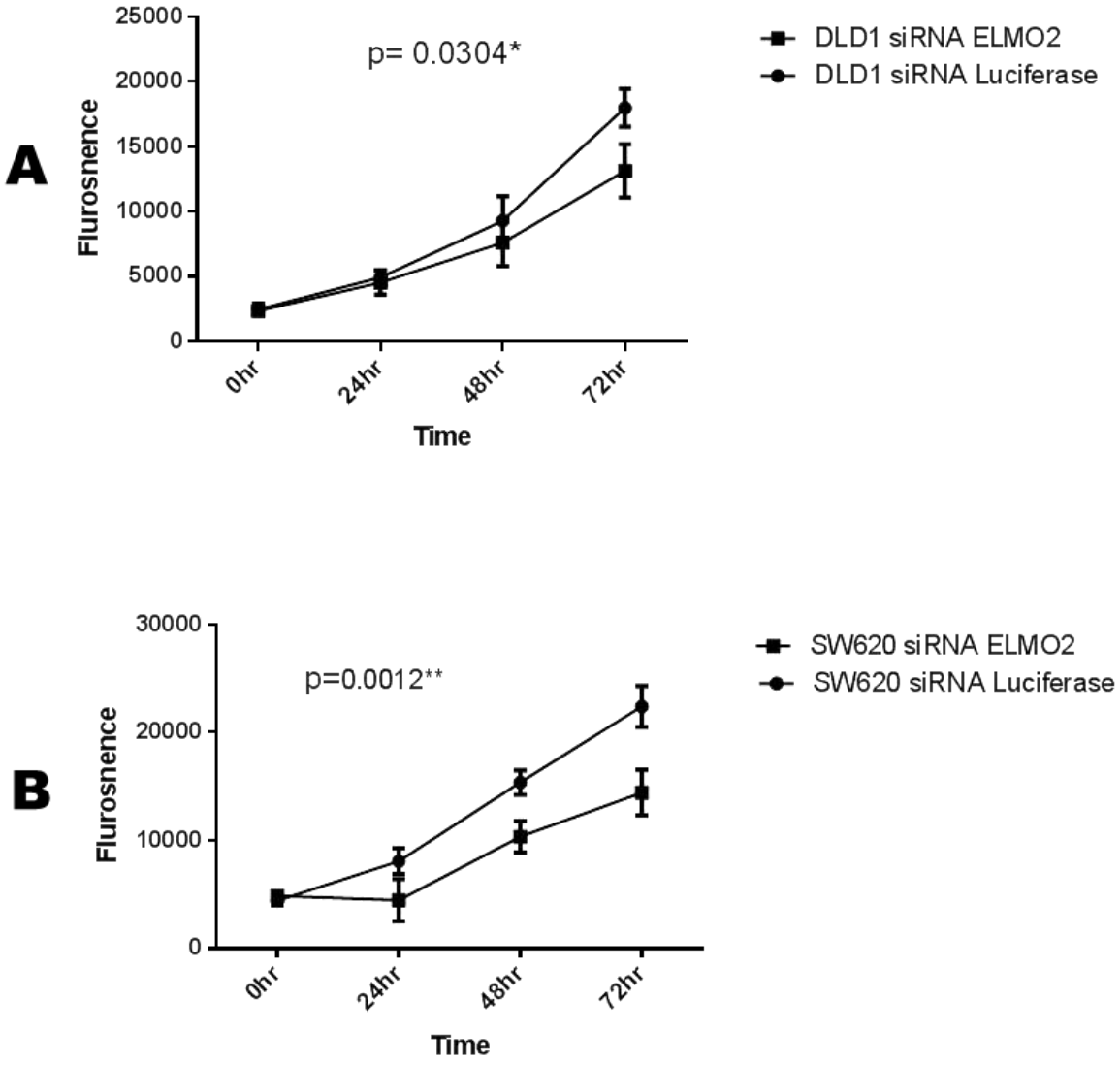


Figure 4-38 Effect of ELMO2 on cell proliferation in SW620 and DLD1.
Proliferation time course assay: Cells were harvested 48h after siRNA transfection. Then, cells ($2X10^4$) were seeded into 24 well-plates in triplicate. Presto Blue was added to each well, and then the fluorescence intensity (relative fluorescence units-RFUs) was measured using for excitation at 495nm and a filter for emission at 580nm. 4 time points after knockdown of ELMO2 SW620 and DLD1, cells viabilities were measured by fluorescence. Figures were designed by Prism software. All data were mean ± SD of three independent experiments.

4.1.4.2.4 ELMO2 enhances migration in CRC cell lines

Transwell migration assay was used to study the effect of ELMO2 on CRC cell lines motility. RKO cells were transfected with siRNA targeting ELMO2 and siRNA targeting Luciferase (control). RKO siRNA ELMO2 cells migrated more slowly than RKO siRNA Luciferase cells (p value= 0.0001***, Unpaired T-test) Figure 4-39. The same result was seen when HT29 was transfected with siRNA ELMO2, and cells significantly migrated slower than the control (p value= 0.0054**,unpaired T-test). In order to validate previous results, wound healing assay was performed to HT29 cell line. HT29 control migrated across the wound faster than control cells (p value= 0.002*, unpaired T-test) Figure 4-39.

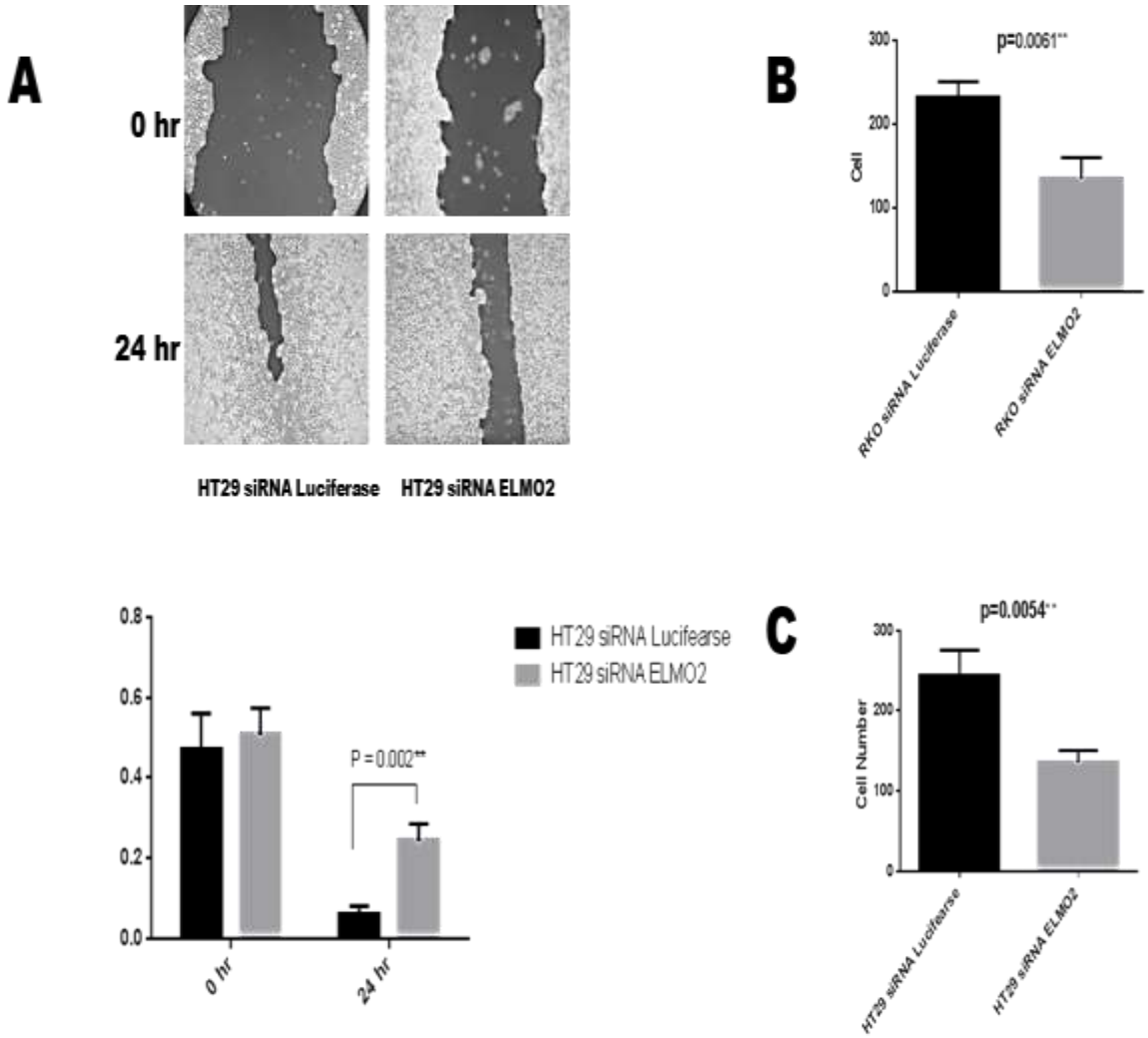


Figure 4-39 ELMO2 enhanced motility in wound healing Transwell migration assays.

Transwell migration assay was performed to study cell migration in CRC cell lines. Migration of RKO $^{siRNA\ ELMO2}$, and HT29 $^{siRNA\ ELMO2}$ cells were compared with relevant cell line siRNA Luciferase. For both cell lines tested, down regulation of ELMO2 in these cell lines caused slower migration compared to the control (RKO P value 0.0061**, and P value0.0054**). All results expressed as means ± SD. Transwell migration experiments were performed in triplicate. The wound healing assays were performed in two independent experiments.

4.1.4.3 Discussion

The ELMO Family has a role in cytoskeletal rearrangements. Down regulation of ELMO2 interrupts activation of RHO GTPase activation which reduces cell migration (Katoh and Negishi, 2003). Also, there is evidence that ELMO2 binds to ILK which leads to activation of RHO when activated by EGFR. ILK, ELMO2 and RHO form a complex that activates RAC1 (Ho and Dagnino, 2012). Other evidence shows that ELMO2 is involved in chromosome segregation regulation (Jackson et al., 2015, Rohena and Mooberry, 2014). Therefore, here for the first time we investigated ELMO2 role in CRC.

The expression of ELMO2 in primary CRC tissues was studied by IHC. ELMO2 expression was detected in tumour cell cytoplasm. The normal colonic epithelium did not express ELMO2 in all cases. However, ELMO2 expression was detected in CRC tissues (38%). Expression of ELMO2 was detected in 29% of luminal tumour CRC tissues. ELMO2 expression was found slightly increased by 37% in middle tumour and 38% in advancing tumour. These results might indicate up regulations of ELMO2 plays a role in CRCs tumorigenesis.

ELMO2 was knocked down using siRNA and cell proliferation and cell motility were tested. Knockdown of ELMO2 significantly reduced cell numbers in DLD1, SW620 and HT29. ELMO2 also inhibited breast cancer cell growth in vitro when it is knocked down (Abu-Thuraia et al., 2015). In light of these data, ELMO2 can be considered to promote cell growth in CRC and breast cancer cell lines. To investigate further the mechanism by which ELMO2 may influence cell numbers, cell cycle analysis was performed. Knockdown of ELMO2 showed considerable cell arrest at the G1 phase of the cell cycle compare to control cell. However, it has not been revealed which downstream pathways can be affected by ELMO2, which appear to promote proliferation.

It has been reported that ELMO2 promotes cell motility in breast cancer cell lines (Li et al., 2013, Abu-Thuraia et al., 2015). We used two methods to assess effect of ELMO2 on cell motility - transwell migration and wound healing assays. In transwell migration, the number of cell migrating across the membrane in both HT29 and RKO control cells were higher in number in control cells compared to

those with ELMO2 knockdown. There was validation of this with the wound healing assay showed that ELMO2 enhance migration of across the wound. Similarly, in breast cancer, knockdown of ELMO2 prevents metastasis of MDA-MB-231 cells to lungs in *vivo* (Li et al., 2013). Furthermore, ELMO2 promotes cell motility in *vitro* (Abu-Thuraia et al., 2015). It is has been reported that ILK promotes cells migration and invasion in CRC (Yan et al., 2014). ELMO2 activates RAC1 by EGF stimulation in other cell type. Since, ELMO2 forms a link between ILK and active RHO, and that activates RAC1, this may be the route through which ELMO2 promotes cell cycle progression and cell motility in CRC (Espina et al., 2008, Esufali et al., 2007).

In conclusion, this study explored for the first investigation of ELMO2 expression in CRC. ELMO2 did not express in normal colonic epithelial cells, and the expression was detected in CRCs. Our study also investigated the functional activity ELMO2 and showed is seems to stimulate cell growth and cell motility and suggests that ELMO2 has an oncogenic role in CRC. Studying the ELMO2 pathway would increase the understanding the protein which could lead to novel therapeutic ELMO2 targets. Furthermore, investigating ELMO2 expression in a larger sample size accompanied with clinical data could reveal the possibility of using ELMO2 as a molecular marker of prognosis in CRC.

4.1.5 Prostaglandin I2 (prostacyclin) synthase (PTGIS)

4.1.5.1 Introduction

PTGIS plays an important role in the prostaglandin endoperoxide synthase pathway (cyclooxygenase pathway). It is an enzyme that catalyses the conversion of prostaglandin H2 to PGI2. It may be implicated in CRC progression by preventing apoptosis (He et al., 1999). This gene was reviewed in details previously in section 1.6.5. The functional role of PTGIS functional role in CRC has not yet been studied, although it is located on 20q13, which is frequently amplified in CRC. Therefore, PTGIS functional role in CRC was investigated in this study.

4.1.5.2 Results

4.1.5.2.1 PTGIS did not affect cell proliferation and cell motility in CRC cell lines

PTGIS functional effect on CRC was studied in term of proliferation and cell motility. PTGIS expression in 4 CRC cell lines was measured by western blotting (Figure 4-40). Of these, SW480 and SW620 had 20q amplification and, HCT116 and RKO did not have this amplification. Expression level of PTGIS protein was similar in both cells with 20q amplification and cells without this amplification.

PTGIS knockdown was achieved by transfecting a siRNA targeting *PTGIS* gene (Figure 4-41). Proliferation was then assessed at 3 time points using the Methylene blue assay. PTGIS knockdown in HCT116, SW620 and SW480 cells did not affect the proliferation rate when compared to the control ($P = 0.976$, $P = 0.132$, and $P = 0.2034$, respectively, Two way anova) (Figure 4-42). A migration assay was performed to study the effect of PTGIS on cell motility. PTGIS knockdown did not affect cell migration of HCT116 cells (Figure 4-43).

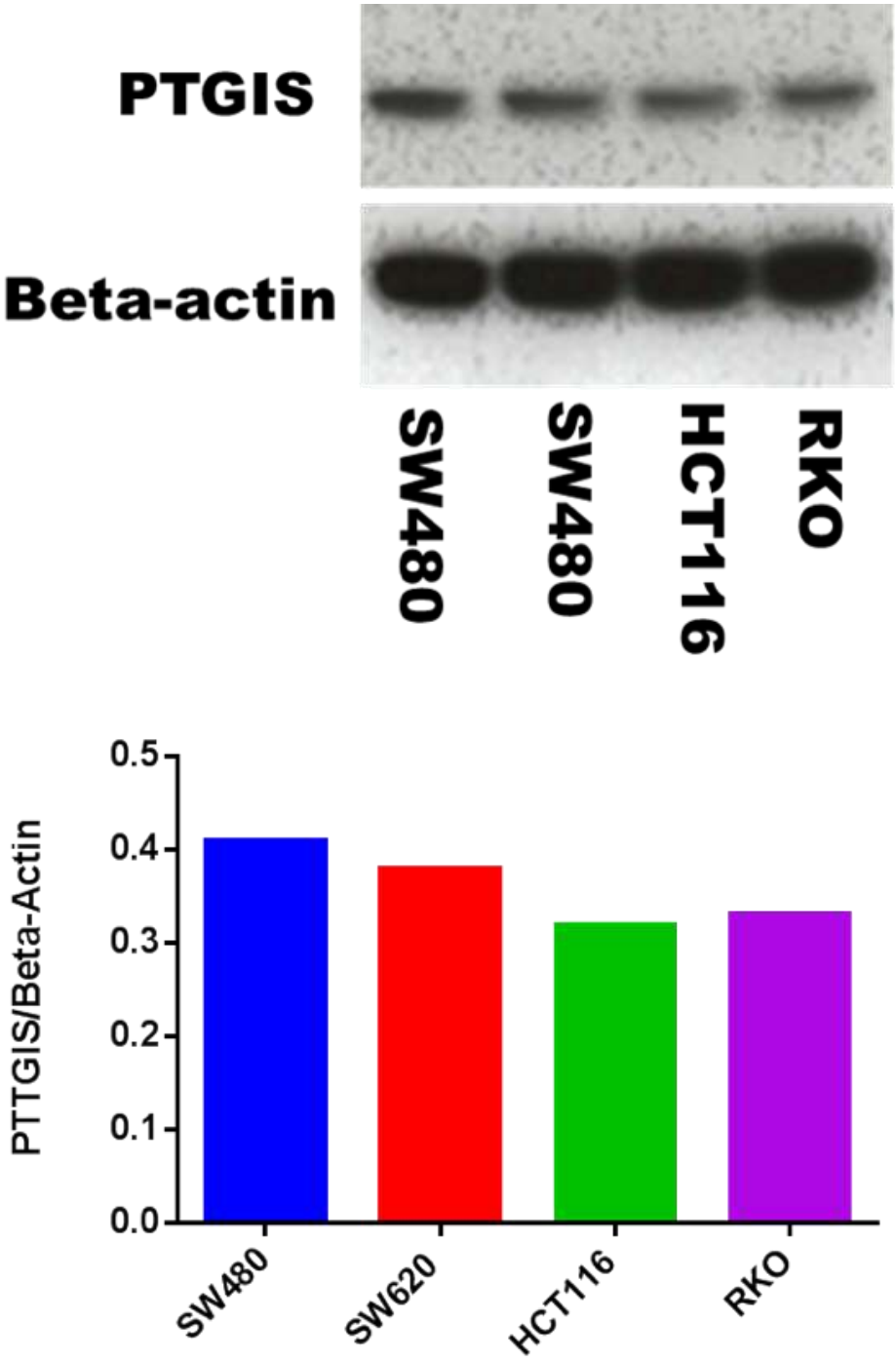


Figure 4-40 Western blot screening of PTGIS expression in 4CRC cell lines.

(Upper panel) Cell lysates (30µg) were analysed using 4–12% Bis-Tris Plus Gel. A PTGIS antibody was used to detect PTGIS protein expression levels. The loading control was the housekeeping protein ß-actin (1:50,000). (Lower panel) Histogram represented western blot intensities analysed by ImageJ software. Band intensity detected by PTGIS antibody was normalised by its relevant ß-actin band.

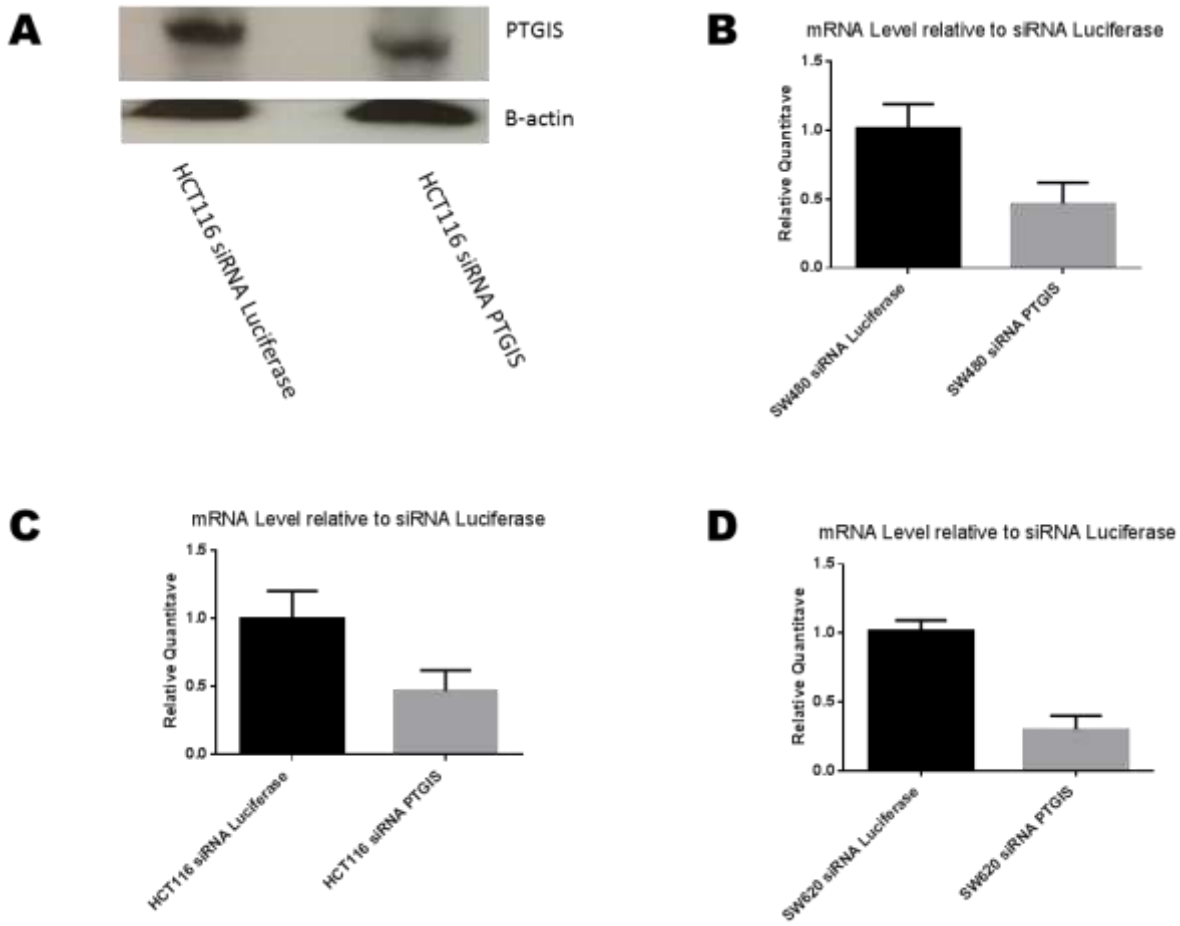


Figure 4-41. PTGIS knockdown in SW620, SW480, and HCT116 cells.
All cell lines were transfected with the PTGIS siRNA (cell line siRNA PTGIS) or a siRNA targeting Luciferase (cell line siRNA Luciferase). Two days after the knockdown, western blot analysis confirmed PTGIS downregulation in SW620 cells. β–actin was used as a loading control. (B), (C) and (D) Relative quantity of *PTGIS* mRNA in HCT116, SW620, and SW480 cells transfected with the PTGIS siRNA. PTGIS knockdown was confirmed by RT-qPCR.

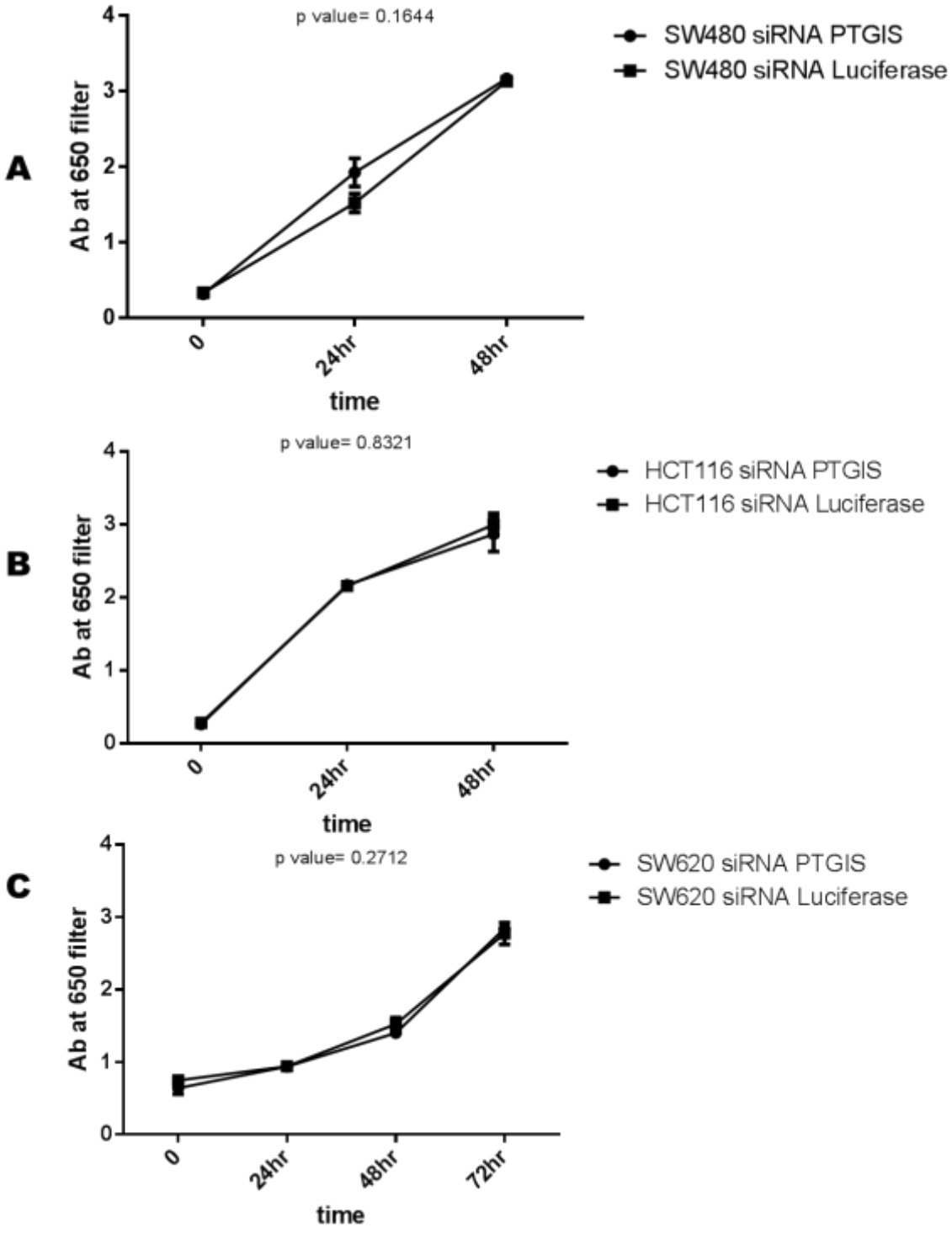


Figure 4-42. Effect of PTGIS on cell proliferation in SW620, SW480, and HCT116 cells.

(A) and (B) Proliferation time course assay: Proliferation was assessed at 3 time points after PTGIS knockdown in SW480 and HCT116 cells. Cells seeded into 24 well-plates in triplicate, and incubated at 37Cº and 5% CO2 for 4 hours. The cells were fixed by 100% methanol and stained with, Methylene blue. Then, ethanol/HCl (1:1) was added to release the dye from the DNA. The absorbance at 650nm wavelength nanometre (nm) was measured on a plate-reader. (C)Proliferation was assessed at 4 points in SW620 cells. All data are expressed as mean ± SD of three independent experiments

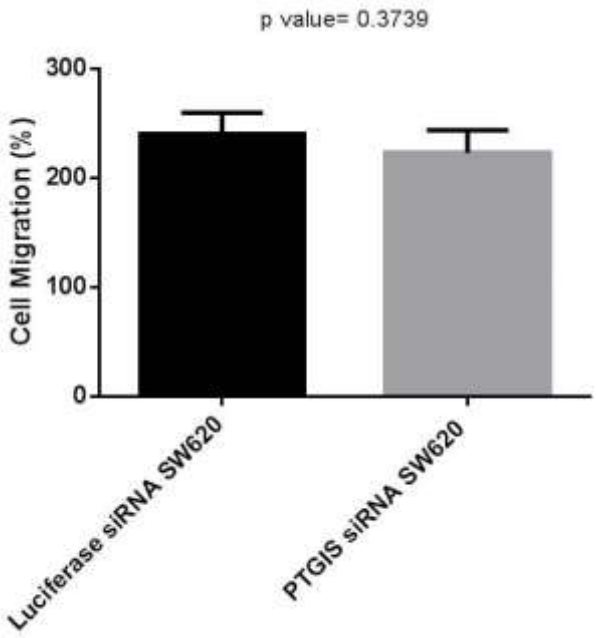


Figure 4-43. PTGIS did not affect cell motility in the transwell migration assay.

Transwell migration assay was performed to study cell migration in the SW620 cell line. Migration of SW620 $^{siRNA\ PTGIS}$ cells was compared to that of SW620 $^{siRNA\ Luciferase}$. PTGIS downregulation in the SW620 cell line had no significant effect on cell migration when compared to the control cells. Results are expressed as means ± SD. All experiments were performed in triplicate.

4.1.5.3 Discussion

PTGIS is considered as a potential oncogenic gene because PTGIS is an enzyme involved in the catalysis of PGH2 to PGI2 conversion. PGI2 is implicated in the activation of the nuclear receptor PPARδ. PPARδ is functionally active in CRC cell lines (Park et al., 2001a) and is a downstream effector of the APC/β-catenin pathway in CRC (He et al., 1999). Previous studies have showed that that PTGIS is highly expressed in CRC tissues (Lichao et al., 2012a). However, the PTGIS promoter is reportedly hypermethylated in half of the cases. The data, taken at face value, are mixed regarding the role of PTGIS as an oncogene or tumour suppressor.

The effect of PTGIS on the growth and motility of CRC cell lines has not been previously studied. Therefore, we used siRNA to knockdown PTGIS and test PTGIS function in CRC cell lines. Proliferation assay results showed no effect of PTGIS knockdown on cell proliferation in 3 tested cell lines. Both CRC cell lines, with 20q amplification and without amplification, showed no effect of PTGIS on cell proliferation. PTGIS effect on cell motility was assessed by using the transwell migration assay. No effect of PTGIS knockdown was observed on CRC cell motility. PTGIS expression has been reported in 80% of CRCs. PTGIS expression in CRC cell lines were studied by western blotting. PTGIS expressed in cell lines without 20q amplification and there was a higher expression in those with 20q amplification when compared with CRC cell lines without 20q amplification. Thus, we can speculate that PTGIS is merely overexpressed in CRC as a result of the 20q13 amplification.

However, PTGIS might play a role in the microenvironment in CRC. Vascular Endothelial Growth Factor (VEGF) is an important factor in angiogenesis regulation, and it induces PGI2. PGI2 is thought to contribute to vascular biology and angiogenesis (Galaup et al., 2006, Vane and Corin, 2003). Consequently, PTGIS coupled with the production of PGI2 might play a role in CRC metastasis through regulation of angiogenesis (Buchanan et al., 2004).

In conclusion, this study shows that PTGIS is expressed in CRC cell lines at the protein and mRNA levels. Our study shows that PTGIS did not promote cell proliferation and motility in CRC cell lines. These results suggest that PTGIS is overexpressed due to 20q13 amplification. However, this assumption does not

take into account its potential role in angiogenesis and in CRC development and metastasis.

5 Chapter Five: General Discussion

In this thesis, chromosome 20q amplification was investigated in colorectal cancer. The hypothesis was that 20q amplification drives tumour metastasis. This investigation started with validation of our aCGH data of a series of 20 CRC and their matched liver metastasis. Validation was carried out by qPCR and performed on six genes located at 20q to evaluate the DNA copy number. Then, 20q amplification in both colorectal cancers, primary and secondary, was compared.

The other hypothesis was that 20q contains genes which are tumour drivers. After validating the methodology of screening 20q amplification by qPCR, two genes were used to screen the 20q13 DNA copy number in another series of 103 cases. The association of 20q amplification with aneuploidy was studied. Furthermore, the associations of 20q amplification with mutations in *KRAS*, *PIK3CA* and *TP53* genes were studied.

After we studied 20q amplification in CRC, functional studies of genes located in 20q were performed. First of all, protein expressions of these genes were studied by immunohistochemistry. Eighty four primary CRC FFPE cases were reviewed. Luminal, central and advancing tumours, and non-tumour colon tissues were arrayed. Then, expressions of candidate genes in CRC cell lines were screened by Western blotting to find cell lines suitable for gene knockdown. For gene knockdown, siRNA was used and knockdown validated at protein and mRNA levels by Western blot and RT-PCR, respectively. After validation of gene knockdown, the effects in cell growth and motility were studied *in vitro*. CRC cell growth was studied by Presto blue assay. Then, validation of Presto blue assay was acquired by cell cycle analysis using flow cytometry. For cell motility, transwell migration and for further validation the wound healing assay was performed. Invasion assay was performed to assess cell motility in CRC cell lines.

5.1 DNA Copy Number Evaluation of 20q Genes in Colorectal Cancer and Liver Metastasis

CRCs initiate as adenoma polyp, developing to an advanced adenoma, and then to cancer. Genomic alterations drive the multistep process towards invasive CRC (Meijer et al., 1998a, Ried et al., 1996). One of those variations is DNA copy number variation. Studies have identified common chromosomal amplifications or deletions (Tsafrir et al., 2006, Sheffer et al., 2009a, Meijer et al., 1998a).

Amplification of 20q is identified in ~50% of CRCs and 70% of liver metastases (Diep et al., 2006a). Our array CGH data in a series of 20 CRC and their matched liver metastases have identified the frequent amplification of 20q13. These data were validated by qPCR based on 6 genes located at 20q13 cytoband. Correlations between relative quantitative results were high in DNA copy number with the genes tested. Our qPCR data showed high concordance with aCGH data in term of 20q amplification status. Therefore, qPCR can be used as tool to test genes amplification with appropriate exponential design (Chamizo et al., 2015).

The series of 15 CRC and their matched liver metastasis set showed amplification of 20q13 in primary tumours in 67% of cases and 60% of secondary tumours.

The frequencies of 20q amplification in primary and secondary tumours were generally similar. Therefore, 20q amplification did not drive liver metastasis. In another series of 103 CRC primary cases, amplification of 20q in primary CRC tumours was detected 46.5% of cases. CRCs has been reported to acquire 20q is amplified in ~50% of cases which agreed with our finding (Diep et al., 2006a, Loo et al., 2013). Thus, 20q amplification might be an important CRC driver.

The associations of 20q amplification with other genetic alterations were studied. CRC cases with 20q amplification coexisted with aneuploidy in high proportion of CRCs cases. In our study, only *TP53* was associated with CRC with 20q amplification. Both genetic alterations (20q amplification and TP53 mutations) are important in developing CRC, so CRC cells selective advantage to harbour these two genomic changes needs more investigation.

5.2 Evaluating Cancer Related Progress of Genes Located at 20q

The amplification of 20q is a common event in CRCs. Thus, the hypothesis was that 20q contains genes which are tumour drivers. Therefore, we investigated functional activities of several genes that map to 20q in CRC cell lines.

5.2.1 PTPN1 enhances cell motility in CRC cell lines.

PTPN1 plays a controversial role in cancer development as a tumour suppressor or oncogene (Lessard et al., 2010). However, PTPN1 in CRC is overexpressed and its overexpression associated with poor prognosis (Zhu et al., 2007, Chen et al., 2014). Our finding showed that the highest frequency of PTPN1 overexpression in CRCs was found in advancing tumour site. Consequently, PTPN1 overexpression might be due to its implication in cell motility regulation. Expression of PTPN1 in CRC cell lines was explored by western blotting. PTPN1 expressed in all CRC cell lines tested. High PTPN1 expression in CRC with 20q amplified might be a consequence of this amplification. Interestingly, high expression was also detected in CRC cell lines without 20q amplification. This indicates the importance of PTPN1 in driving CRC tumorigenesis.

Then, cancer related processes were tested in CRC cell lines. In our finding, PTPN1 did not change proliferation rate in CRC cell lines. However, in other studies, it promotes tumour growth in breast cancer and CRC through activation of SRC (Zhu et al., 2007, Arias-Romero et al., 2009). The differences between these studies and our study may be due to experimental methodology. We found PTPN1 increased cell migration in transwell migration and in wound healing assays. The consistency of PTPN1 effect on cell motility suggests that it is not tissue specific. These findings have been supported by previous investigations, in which PTPN1 promotes cell motility in CRC and breast cancer (Zhu et al., 2007, Arias-Romero et al., 2009). Regarding cell invasion, PTPN1 increased cell ability to invade the matrigel and this effect also has been reported previously (Zhu et al., 2007, Lessard et al., 2012). The cell motility study companied with IHC data indicates that over expression of PTPN1 in the edge of the tumour more likely to promote cell motility and invasiveness.

.

5.2.2 CD40 enhances cell number in CRC cell lines

CD40, TNF receptor superfamily member 5, expression is identified in hematopoietic and non-hematopoietic cells such as fibroblasts and endothelial cells (Banchereau et al., 1995, van Kooten and Banchereau, 1997). CD40 expression has been detected in several haematological and solid tumours. Its controversial role in cancer is also reported in different studies (Dallman et al., 2003, Vonderheide and Glennie, 2013, Bussolati et al., 2002, Tong et al., 2001, Sabel et al., 2000, Homig-Holzel et al., 2008). CD40 expression has not been detected in normal colon cells (Gelbmann et al., 2003, Cruickshank et al., 2004, Georgopoulos et al., 2007, Wu et al., 2008), whereas it is overexpressed in malignant colon tissues (Wu et al., 2008, Georgopoulos et al., 2007). The malignant colon cell has a selective advantage to express CD40, which indicates its oncogenic role, yet current finding showed contradicted conclusion. Therefore, role of CD40 in CRC was investigated by studying CD40 expression and, effect on cell growth and motility.

As CD40 maps to 20q, overexpression may be due to genomic amplification. However, in our results, CRC cell lines with and without this amplification showed CD40 overexpression. Therefore, 20q amplification is not the only mechanism that leads to CD40 overexpression in CRC cells. Furthermore, CD40 overexpression in CRC cell lines supports the possible role of CD40 as an oncogene. The Immunohistochemistry showed CD40 expression in CRC tissues. Cytoplasmic expression was not different from non-tumour colonic tissues. The same observation was detected in CD40L expression. These expressions might be not relevant with CD40/ CD40L functions, as both receptor and ligand function at the membrane. However, cytoplasmic expression might suggest a different role of CD40 in CRC. Moreover, only two cases co-expressed CD40 and CD40L were detected. Therefore, CD40 does not require CD40L co-expression.

CD40 promotes tumour proliferation at early stage of cancer development (Baxendale et al., 2005). As 20q amplification is an early event in CRC. Therefore, elevated CD40 expression in malignant CRC could play an important role in cell growth. *In vitro*, knockdown CD40 inhibited CRC cells proliferation. This finding was confirmed by cell cycle analysis which showed more apoptotic cells were found when CD40 knockdowned. Cell cycle analysis showed that CD40 promotes

cell proliferation in CRC by inhibiting apoptosis. However, it has been reported that CD40 promotes apoptosis in CRC cell lines (Wu et al., 2008, Georgopoulos et al., 2007). The differences in results might be because of the different methodology used in the study. In both studies, CD40 has been stimulated by CD40L and the effect was studied. However, our study knockdowned CD40 and the effects were observed. Finally, CD40 effect on CRC cell motility was studied. CD40 knockdown did not show any effect on cell migration in CRC. Further validation was carried out by wound healing assay. Likewise, CD40 knockdown did change cell migration in the assay. It is not reported whether CD40 affects cell motility or not. Therefore, our finding suggests that CD40 reduce cell apoptosis and did not regulate cell motility.

5.2.3 PREX1 enhances proliferation and motility in CRC cell lines

PREX1 activates RHO GTPases which regulate multiple cellular processes (Herter et al., 2013, Waters et al., 2008, Yoshizawa et al., 2005). Its reported role in cancer reported as an oncogene, in which promotes cell growth and motility in several tumours *in vitro* and *in vivo* (Qin et al., 2009, Kim et al., 2011, Campbell et al., 2013). PREX1is not expressed in normal pancreatic and breast cells, whereas it is overexpressed in pancreatic and breast malignant cells (Qin et al., 2009, Wong et al., 2011, Sosa et al., 2010). The expression of PREX1 has not been studied in CRC cell lines or clinical tissues. We found that PREX1 overexpressed in several CRC cell lines (both with and without 20q amplification). Therefore, PREX1 expression was not dependant on 20q amplification. Furthermore, PREX1 was overexpressed frequently in central and advancing CRC tumours. Moreover, normal colonic epithelial cells did not express PREX1. This might be an indication of its oncogenic role in it tumour growth and motility in CRC.

Knockdown of PREX1 inhibits tumour growth in breast cancer in *vitro* and *in vivo* (Sosa et al., 2010, Qin et al., 2009). Our finding agreed with pervious study, in which downregulated PREX1 inhibited CRC cell proliferation. Regarding cell motility, it promotes cell motility in several tumours. Two methods were used to assess PREX1 effects. All results suggest that PREX1 also promotes cell motility in CRC. It is not clear how PREX1 has effect on CRC. Thus, investigating PREX1 signalling pathway in CRC could reveal more of its role in CRC.

Future studies on PREX1 are important to understand its signalling pathways in CRC. Moreover, studying PREX1 inhibitors effect on CRC cell lines should reveal novel therapeutic approach in treating CRC.

5.2.4 ELMO2 enhanecs proliferation and motility in CRC cell lines

ELMO2 activates RHO GTPases which regulates cell motility (Katoh and Negishi, 2003). Furthermore, ELMO2 binds to ILK and RHO when it is stimulated by EGFR, and this complex activates RAC1 (Ho and Dagnino, 2012). Other evidence shows that ELMO2 is involved in chromosome segregation regulation. (Jackson et al., 2015, Rohena and Mooberry, 2014). Studies have investigated ELMO2 in breast cancer and shows that ELMO2 is expressed in breast cancer cell lines and tissues (Li et al., 2013).

Therefore, here for the first time we investigated ELMO2's role in CRC. ELMO2 was not expressed in non-tumour colon tissues. However, it is expressed in CRC tissues. CRC cell lines also expressed ELMO2 in non 20q amplified and in 20q amplified cells, which indicates that its overexpression is not dependent on 20q amplification. Furthermore, we found ELMO2 expression was higher in both central and advancing CRC tissues. These finding indicates that ELMO2 could play a role in CRC development and metastasis.

Knockdown of ELMO2 inhibited proliferation in CRC cell lines, which also caused more cell arrested at G1. Therefore, ELMO2 enhances proliferation by blocking transition from G1 to S phase. The minimal effect on proliferation of non-amplified 20q cell line (DLD1) might be because of 20q status.

ELMO2 promotes cell motility in breast cancer cell lines (Li et al., 2013, Abu-Thuraia et al., 2015). Similarly, ELMO2 knockdown reduced CRC cells' ability to migrate in a transwell migration. The ELMO2 knockdown in a wound healing assay also reduced cell motility. ELMO2 modulates the ILK binding ability to RHO; downregulation of ELMO2 possibly reduces the ability of ILK to activate RAC1, which regulates cell motility. ILK promotes cell migration in CRC (Yan et al., 2014). The activation of RAC1 also can promote cell motility and cell cycle progression in CRC (Espina et al., 2008, Esufali et al., 2007). Therefore, ELMO2 might activate RAC1 in CRC, which enhances cell proliferation and motility.

5.2.5 PTGIS role in colorectal cancer cell lines

PTIGS is an enzyme involved in the catalysis of PGH2 into PGI2. PGI2 is implicated in the activation of the nuclear receptor PPARδ. PPARδ is functionally active in CRC cell lines (Park et al., 2001a). PTGIS is highly expressed in CRC

tissues, and it is associated with liver metastasis cases (Lichao et al., 2012a). Furthermore, PTGIS is hypermethylated in 50 %of CRC cases. (Park et al., 2001a) PTGIS could be implicated in the APC/β-catenin pathway in CRC by activating PPARδ (He et al., 1999). However, the functionality of PTGIS in CRC cancer has not been studied.

The knockdown of PTGIS did not change the proliferation rate in CRC cell lines. The PTGIS effect on CRC cell motility was investigated. The knockdown did not affect the migration of the cells. Therefore, PTIGS overexpression in CRC might be due to 20q amplification. In other words, PTGIS is a passenger not cancer driver gene. However, its role in angiogenesis has not been investigated. Therefore, PTGIS might have a role in CRC metastasis through angiogenesis regulation.

5.3 Limitation of the thesis:

The limitation of DNA copy number evaluation of 20q genes in colorectal cancer and liver metastasis study were mainly the sample size. In series of CRC with their liver metastasis set, only 15 cases were studied, and any finding can be used as a pilot result for further research. Likewise, the sample size of the second series was not also on large scale, which might miss the small difference of less frequent tumour related-mutations; *KRAS* and *PI3KCA* mutations. Furthermore, the APC mutation is one of the most important events in early stage developing CRC. In our series, the status of APC mutation is unknown.

Investigating genes located in 20q13 role in CRC was carried out and several limitations identified. Regarding the protein expression studies on the candidate genes, the main limitation was the clinical sample size was relatively small. Clinical data of these CRC tissues were not available. This sample site was not linked with previous sample set. In functional studies, only knockdown was used to study the functional characteristics of candidate genes, and ectopic expression was not employed for validating the knockdown finding. Furthermore, all functional studies were performed *in vitro*, which does not reflect the cancer cells' surrounding environment as does in the *in vivo* study Regarding CD40 study, the CD40 stimulation effect on CRC was not examined.

5.4 Potential future studies:

Studying a larger size of CRC cases may identify small differences between those mutations and 20q amplified cases. The association of 20q amplification with drug response in CRC patients should be studied and as it may reveal 20q amplification as a marker for drug response. Then, developing a simple method to screen 20q status might be useful in the future in clinical applications. In addition, mRNA and protein profiling together with chromosomal aberrations data could identify potentially relevant genes to CRC progress. .

Future studies regarding candidates genes located on 20q13, the signalling pathway of PTPN1 in CRC should be studied by knocking down PTPN1 and studying its mRNA in a microarray expression platform. The PTPN1 inhibitor effect should be studied in CRC *in vitro* and *in vivo*, which could reveal a new

therapeutic strategy. For future study, CD40 effects on cell signalling in CRC need more investigation.

Future studies on PREX1 are important to understand its signalling pathways in CRC. Moreover, studying PREX1 inhibitors effect on CRC cell lines should reveal novel therapeutic approach in treating CRC. For future research, the ELMO2 pathway should be intensively studied in CRC. Investigating the link between ILK and ELMO2 and its role in the activation of RAC1 should be addressed in the future. Moreover, studying EGFR stimulation and its effect on ELMO2 and other downstream molecules would reveal the signalling pathway of ELMO2 in CRC. Finally, both ELMO2 and PREX1 activate RAC1 through RHO. The dual knockdown of both genes should also be performed and the effect on cell proliferation and migrations monitored. For future work, the PTGIS role in angiogenesis regulation should be investigated together with the coexistence of PTGIS and PGI2 expressions. Furthermore, the PTGIS effect on Wnt signalling should be explored.

5.5 Final Conclusion

To conclude, 20q amplification appeared to have a crucial role in colorectal cancer. The 20q13 is amplified frequently in primary tumours but it not positively associated with metastasis. Many genes located in 20q showed an oncogenic role in CRC development. Further investigation should shed light on the role of chromosome 20q amplification in CRC biology. Understanding their role in CRC development could reveal new avenue in understanding cancer biology and treatment.

6 Chapter Six: References

ABDEL-MISIH, S. R., SCHMIDT, C. R. & BLOOMSTON, P. M. 2009a. Update and review of the multidisciplinary management of stage IV colorectal cancer with liver metastases. *World J Surg Oncol,* 7**,** 72.

ABDEL-MISIH, S. R., SCHMIDT, C. R. & BLOOMSTON, P. M. 2009b. Update and review of the multidisciplinary management of stage IV colorectal cancer with liver metastases. *World J Surg Oncol,* 7**,** 72.

ABDEL-RAHMAN, W. M., MECKLIN, J. P. & PELTOMÄKI, P. 2006. The genetics of HNPCC: application to diagnosis and screening. *Crit Rev Oncol Hematol,* 58**,** 208-20.

ABU-THURAIA, A., GAUTHIER, R., CHIDIAC, R., FUKUI, Y., SCREATON, R. A., GRATTON, J. P. & COTE, J. F. 2015. Axl phosphorylates Elmo scaffold proteins to promote Rac activation and cell invasion. *Mol Cell Biol,* 35**,** 76-87.

AHUJA, N., MOHAN, A. L., LI, Q., STOLKER, J. M., HERMAN, J. G., HAMILTON, S. R., BAYLIN, S. B. & ISSA, J. P. 1997. Association between CpG island methylation and microsatellite instability in colorectal cancer. *Cancer Res,* 57**,** 3370-4.

AKASAKI, Y., LIU, G., MATUNDAN, H. H., NG, H., YUAN, X., ZENG, Z., BLACK, K. L. & YU, J. S. 2006. A peroxisome proliferator-activated receptor-gamma agonist, troglitazone, facilitates caspase-8 and -9 activities by increasing the enzymatic activity of protein-tyrosine phosphatase-1B on human glioma cells. *J Biol Chem,* 281**,** 6165-74.

AL-TASSAN, N., CHMIEL, N. H., MAYNARD, J., FLEMING, N., LIVINGSTON, A. L., WILLIAMS, G. T., HODGES, A. K., DAVIES, D. R., DAVID, S. S., SAMPSON, J. R. & CHEADLE, J. P. 2002. Inherited variants of MYH associated with somatic G:C-->T:A mutations in colorectal tumors. *Nat Genet,* 30**,** 227-32.

ALNABULSI, A., AGOUNI, A., MITRA, S., GARCIA-MURILLAS, I., CARPENTER, B., BIRD, S. & MURRAY, G. I. 2012. Cellular apoptosis susceptibility (chromosome segregation 1-like, CSE1L) gene is a key regulator of apoptosis, migration and invasion in colorectal cancer. *J Pathol*.

ANDERSEN, C. L., WIUF, C., KRUHØFFER, M., KORSGAARD, M., LAURBERG, S. & ØRNTOFT, T. F. 2007a. Frequent occurrence of uniparental disomy in colorectal cancer. *Carcinogenesis,* 28**,** 38-48.

ANDERSEN, C. L., WIUF, C., KRUHØFFER, M., KORSGAARD, M., LAURBERG, S. & ØRNTOFT, T. F. 2007b. Frequent occurrence of uniparental disomy in colorectal cancer. *Carcinogenesis,* 28**,** 38-48.

AOKI, K. & TAKETO, M. M. 2007. Adenomatous polyposis coli (APC): a multi-functional tumor suppressor gene. *J Cell Sci,* 120**,** 3327-35.

ARAGANE, H., SAKAKURA, C., NAKANISHI, M., YASUOKA, R., FUJITA, Y., TANIGUCHI, H., HAGIWARA, A., YAMAGUCHI, T., ABE, T., INAZAWA, J. & YAMAGISHI, H.

2001a. Chromosomal aberrations in colorectal cancers and liver metastases analyzed by comparative genomic hybridization. *Int J Cancer,* 94**,** 623-9.

ARAGANE, H., SAKAKURA, C., NAKANISHI, M., YASUOKA, R., FUJITA, Y., TANIGUCHI, H., HAGIWARA, A., YAMAGUCHI, T., ABE, T., INAZAWA, J. & YAMAGISHI, H. 2001b. Chromosomal aberrations in colorectal cancers and liver metastases analyzed by comparative genomic hybridization. *Int J Cancer,* 94**,** 623-9.

ARANGO, D., LAIHO, P., KOKKO, A., ALHOPURO, P., SAMMALKORPI, H., SALOVAARA, R., NICORICI, D., HAUTANIEMI, S., ALAZZOUZI, H., MECKLIN, J. P., JÄRVINEN, H., HEMMINKI, A., ASTOLA, J., SCHWARTZ, S. & AALTONEN, L. A. 2005. Gene-expression profiling predicts recurrence in Dukes' C colorectal cancer. *Gastroenterology,* 129**,** 874-84.

ARIAS-ROMERO, L. E., SAHA, S., VILLAMAR-CRUZ, O., YIP, S. C., ETHIER, S. P., ZHANG, Z. Y. & CHERNOFF, J. 2009. Activation of Src by protein tyrosine phosphatase 1B Is required for ErbB2 transformation of human breast epithelial cells. *Cancer Res,* 69**,** 4582-8.

ARMITAGE, N. C., BALLANTYNE, K. C., SHEFFIELD, J. P., CLARKE, P., EVANS, D. F. & HARDCASTLE, J. D. 1991. A prospective evaluation of the effect of tumor cell DNA content on recurrence in colorectal cancer. *Cancer,* 67**,** 2599-604.

ARMITAGE, R. J., FANSLOW, W. C., STROCKBINE, L., SATO, T. A., CLIFFORD, K. N., MACDUFF, B. M., ANDERSON, D. M., GIMPEL, S. D., DAVIS-SMITH, T., MALISZEWSKI, C. R. & ET AL. 1992. Molecular and biological characterization of a murine ligand for CD40. *Nature,* 357**,** 80-2.

ARVELO, F., SOJO, F. & COTTE, C. 2015. Biology of colorectal cancer. *Ecancermedicalscience,* 9**,** 520.

ASPENSTROM, P., RUUSALA, A. & PACHOLSKY, D. 2007. Taking Rho GTPases to the next level: the cellular functions of atypical Rho GTPases. *Exp Cell Res,* 313**,** 3673-9.

AUCLAIR, J., VAISSIÈRE, T., DESSEIGNE, F., LASSET, C., BONADONA, V., GIRAUD, S., SAURIN, J. C., JOLY, M. O., LEROUX, D., FAIVRE, L., AUDOYNAUD, C., MONTMAIN, G., RUANO, E., HERCEG, Z., PUISIEUX, A. & WANG, Q. 2011. Intensity-dependent constitutional MLH1 promoter methylation leads to early onset of colorectal cancer by affecting both alleles. *Genes Chromosomes Cancer,* 50**,** 178-85.

AUST, D. E., MUDERS, M., KÖHLER, A., SCHMIDT, M., DIEBOLD, J., MÜLLER, C., LÖHRS, U., WALDMAN, F. M. & BARETTON, G. B. 2004. Prognostic relevance of 20q13 gains in sporadic colorectal cancers: a FISH analysis. *Scand J Gastroenterol,* 39**,** 766-72.

BACHER, J. W., FLANAGAN, L. A., SMALLEY, R. L., NASSIF, N. A., BURGART, L. J., HALBERG, R. B., MEGID, W. M. & THIBODEAU, S. N. 2004. Development of a

fluorescent multiplex assay for detection of MSI-High tumors. *Dis Markers,* 20**,** 237-50.

BAKER, S. J., PREISINGER, A. C., JESSUP, J. M., PARASKEVA, C., MARKOWITZ, S., WILLSON, J. K., HAMILTON, S. & VOGELSTEIN, B. 1990. p53 gene mutations occur in combination with 17p allelic deletions as late events in colorectal tumorigenesis. *Cancer Res,* 50**,** 7717-22.

BALAGUER, F., CASTELLVI-BEL, S., CASTELLS, A., ANDREU, M., MUNOZ, J., GISBERT, J. P., LLOR, X., JOVER, R., DE CID, R., GONZALO, V., BESSA, X., XICOLA, R. M., PONS, E., ALENDA, C., PAYA, A., PIQUE, J. M. & GASTROINTESTINAL ONCOLOGY GROUP OF THE SPANISH GASTROENTEROLOGICAL, A. 2007. Identification of MYH mutation carriers in colorectal cancer: a multicenter, case-control, population-based study. *Clin Gastroenterol Hepatol,* 5**,** 379-87.

BANCHEREAU, J., DUBOIS, B., FAYETTE, J., BURDIN, N., BRIERE, F., MIOSSEC, P., RISSOAN, M. C., VAN KOOTEN, C. & CAUX, C. 1995. Functional CD40 antigen on B cells, dendritic cells and fibroblasts. *Adv Exp Med Biol,* 378**,** 79-83.

BARBER, M. A., DONALD, S., THELEN, S., ANDERSON, K. E., THELEN, M. & WELCH, H. C. 2007. Membrane translocation of P-Rex1 is mediated by G protein betagamma subunits and phosphoinositide 3-kinase. *J Biol Chem,* 282**,** 29967-76.

BAXENDALE, A. J., DAWSON, C. W., STEWART, S. E., MUDALIAR, V., REYNOLDS, G., GORDON, J., MURRAY, P. G., YOUNG, L. S. & ELIOPOULOS, A. G. 2005. Constitutive activation of the CD40 pathway promotes cell transformation and neoplastic growth. *Oncogene,* 24**,** 7913-23.

BEERENWINKEL, N., ANTAL, T., DINGLI, D., TRAULSEN, A., KINZLER, K. W., VELCULESCU, V. E., VOGELSTEIN, B. & NOWAK, M. A. 2007. Genetic progression and the waiting time to cancer. *PLoS Comput Biol,* 3**,** e225.

BELLAM, N. & PASCHE, B. 2010. Tgf-beta signaling alterations and colon cancer. *Cancer Treat Res,* 155**,** 85-103.

BELLIZZI, A. M. & FRANKEL, W. L. 2009. Colorectal cancer due to deficiency in DNA mismatch repair function: a review. *Adv Anat Pathol,* 16**,** 405-17.

BJORGE, J. D., PANG, A. & FUJITA, D. J. 2000. Identification of protein-tyrosine phosphatase 1B as the major tyrosine phosphatase activity capable of dephosphorylating and activating c-Src in several human breast cancer cell lines. *J Biol Chem,* 275**,** 41439-46.

BODMER, W. F., BAILEY, C. J., BODMER, J., BUSSEY, H. J., ELLIS, A., GORMAN, P., LUCIBELLO, F. C., MURDAY, V. A., RIDER, S. H., SCAMBLER, P. & ET AL. 1987. Localization of the gene for familial adenomatous polyposis on chromosome 5. *Nature,* 328**,** 614-6.

BOLAND, C. R., SHIN, S. K. & GOEL, A. 2009. Promoter methylation in the genesis of gastrointestinal cancer. *Yonsei Med J,* 50**,** 309-21.

BORRESEN, A. L., LOTHE, R. A., MELING, G. I., LYSTAD, S., MORRISON, P., LIPFORD, J., KANE, M. F., ROGNUM, T. O. & KOLODNER, R. D. 1995. Somatic mutations in the hMSH2 gene in microsatellite unstable colorectal carcinomas. *Hum Mol Genet,* 4**,** 2065-72.

BOSETTI, C., ROSATO, V., GALLUS, S., CUZICK, J. & LA VECCHIA, C. 2012. Aspirin and cancer risk: a quantitative review to 2011. *Ann Oncol,* 23**,** 1403-15.

BOUGHDADY, I. S., KINSELLA, A. R., HABOUBI, N. Y. & SCHOFIELD, P. F. 1992. K-ras gene mutations in adenomas and carcinomas of the colon. *Surg Oncol,* 1**,** 275-82.

BOYLE, T., KEEGEL, T., BULL, F., HEYWORTH, J. & FRITSCHI, L. 2012. Physical activity and risks of proximal and distal colon cancers: a systematic review and meta-analysis. *J Natl Cancer Inst,* 104**,** 1548-61.

BRENNER, H., BOUVIER, A. M., FOSCHI, R., HACKL, M., LARSEN, I. K., LEMMENS, V., MANGONE, L., FRANCISCI, S. & GROUP, E. W. 2012. Progress in colorectal cancer survival in Europe from the late 1980s to the early 21st century: the EUROCARE study. *Int J Cancer,* 131**,** 1649-58.

BRENNER, H., CHANG-CLAUDE, J., SEILER, C. M., RICKERT, A. & HOFFMEISTER, M. 2011. Protection from colorectal cancer after colonoscopy: a population-based, case-control study. *Ann Intern Med,* 154**,** 22-30.

BRENNER, H., KLOOR, M. & POX, C. P. 2014. Colorectal cancer. *Lancet,* 383**,** 1490-502.

BROWN-SHIMER, S., JOHNSON, K. A., HILL, D. E. & BRUSKIN, A. M. 1992. Effect of protein tyrosine phosphatase 1B expression on transformation by the human neu oncogene. *Cancer Res,* 52**,** 478-82.

BRUGNERA, E., HANEY, L., GRIMSLEY, C., LU, M., WALK, S. F., TOSELLO-TRAMPONT, A. C., MACARA, I. G., MADHANI, H., FINK, G. R. & RAVICHANDRAN, K. S. 2002. Unconventional Rac-GEF activity is mediated through the Dock180-ELMO complex. *Nat Cell Biol,* 4**,** 574-82.

BRUIN, S. C., KLIJN, C., LIEFERS, G. J., BRAAF, L. M., JOOSSE, S. A., VAN BEERS, E. H., VERWAAL, V. J., MORREAU, H., WESSELS, L. F., VAN VELTHUYSEN, M. L., TOLLENAAR, R. A. & VAN'T VEER, L. J. 2010a. Specific genomic aberrations in primary colorectal cancer are associated with liver metastases. *BMC Cancer,* 10**,** 662.

BRUIN, S. C., KLIJN, C., LIEFERS, G. J., BRAAF, L. M., JOOSSE, S. A., VAN BEERS, E. H., VERWAAL, V. J., MORREAU, H., WESSELS, L. F., VAN VELTHUYSEN, M. L., TOLLENAAR, R. A. & VAN'T VEER, L. J. 2010b. Specific genomic aberrations in

primary colorectal cancer are associated with liver metastases. *BMC Cancer,* 10**,** 662.

BUCHANAN, F. G., CHANG, W., SHENG, H., SHAO, J., MORROW, J. D. & DUBOIS, R. N. 2004. Up-regulation of the enzymes involved in prostacyclin synthesis via Ras induces vascular endothelial growth factor. *Gastroenterology,* 127**,** 1391-400.

BUSSOLATI, B., RUSSO, S., DEAMBROSIS, I., CANTALUPPI, V., VOLPE, A., FERRANDO, U. & CAMUSSI, G. 2002. Expression of CD154 on renal cell carcinomas and effect on cell proliferation, motility and platelet-activating factor synthesis. *Int J Cancer,* 100**,** 654-61.

CAFFREY, D. R., ZHAO, J., SONG, Z., SCHAFFER, M. E., HANEY, S. A., SUBRAMANIAN, R. R., SEYMOUR, A. B. & HUGHES, J. D. 2011. siRNA off-target effects can be reduced at concentrations that match their individual potency. *PLoS One,* 6**,** e21503.

CAMPBELL, A. D., LAWN, S., MCGARRY, L. C., WELCH, H. C., OZANNE, B. W. & NORMAN, J. C. 2013. P-Rex1 cooperates with PDGFRbeta to drive cellular migration in 3D microenvironments. *PLoS One,* 8**,** e53982.

CARRETERO-ORTEGA, J., WALSH, C. T., HERNANDEZ-GARCIA, R., REYES-CRUZ, G., BROWN, J. H. & VAZQUEZ-PRADO, J. 2010. Phosphatidylinositol 3,4,5-triphosphate-dependent Rac exchanger 1 (P-Rex-1), a guanine nucleotide exchange factor for Rac, mediates angiogenic responses to stromal cell-derived factor-1/chemokine stromal cell derived factor-1 (SDF-1/CXCL-12) linked to Rac activation, endothelial cell migration, and in vitro angiogenesis. *Mol Pharmacol,* 77**,** 435-42.

CARSON, J. D., VAN ALLER, G., LEHR, R., SINNAMON, R. H., KIRKPATRICK, R. B., AUGER, K. R., DHANAK, D., COPELAND, R. A., GONTAREK, R. R., TUMMINO, P. J. & LUO, L. 2008. Effects of oncogenic p110alpha subunit mutations on the lipid kinase activity of phosphoinositide 3-kinase. *Biochem J,* 409**,** 519-24.

CARVALHO, B., POSTMA, C., MONGERA, S., HOPMANS, E., DISKIN, S., VAN DE WIEL, M. A., VAN CRIEKINGE, W., THAS, O., MATTHÄI, A., CUESTA, M. A., TERHAAR SIVE DROSTE, J. S., CRAANEN, M., SCHRÖCK, E., YLSTRA, B. & MEIJER, G. A. 2009. Multiple putative oncogenes at the chromosome 20q amplicon contribute to colorectal adenoma to carcinoma progression. *Gut,* 58**,** 79-89.

CEBOLA, I., CUSTODIO, J., MUNOZ, M., DIEZ-VILLANUEVA, A., PARE, L., PRIETO, P., AUSSO, S., COLL-MULET, L., BOSCA, L., MORENO, V. & PEINADO, M. A. 2015. Epigenetics override pro-inflammatory PTGS transcriptomic signature towards selective hyperactivation of PGE2 in colorectal cancer. *Clin Epigenetics,* 7**,** 74.

CENTER, M. M., JEMAL, A., SMITH, R. A. & WARD, E. 2009. Worldwide variations in colorectal cancer. *CA Cancer J Clin,* 59**,** 366-78.

CHALHOUB, N. & BAKER, S. J. 2009. PTEN and the PI3-kinase pathway in cancer. *Annu Rev Pathol,* 4**,** 127-50.

CHAMIZO, C., ROJO, F. & MADOZ-GURPIDE, J. 2015. Determination of True ERBB2 Gene Amplification in Breast Cancer by Quantitative PCR Using a Reference and a Novel Control Gene. *Appl Immunohistochem Mol Morphol*.

CHAMORRO, M. N., SCHWARTZ, D. R., VONICA, A., BRIVANLOU, A. H., CHO, K. R. & VARMUS, H. E. 2005. FGF-20 and DKK1 are transcriptional targets of beta-catenin and FGF-20 is implicated in cancer and development. *EMBO J,* 24**,** 73-84.

CHAN, D. S., LAU, R., AUNE, D., VIEIRA, R., GREENWOOD, D. C., KAMPMAN, E. & NORAT, T. 2011. Red and processed meat and colorectal cancer incidence: meta-analysis of prospective studies. *PLoS One,* 6**,** e20456.

CHEN, Q., LI, Y., LI, Z., ZHAO, Q. & FAN, L. 2014. Overexpression of PTP1B in human colorectal cancer and its association with tumor progression and prognosis. *J Mol Histol,* 45**,** 153-9.

CHIARAVALLI, A. M., FURLAN, D., FACCO, C., TIBILETTI, M. G., DIONIGI, A., CASATI, B., ALBARELLO, L., RIVA, C. & CAPELLA, C. 2001. Immunohistochemical pattern of hMSH2/hMLH1 in familial and sporadic colorectal, gastric, endometrial and ovarian carcinomas with instability in microsatellite sequences. *Virchows Arch,* 438**,** 39-48.

CHOW, E. & MACRAE, F. 2005. A review of juvenile polyposis syndrome. *J Gastroenterol Hepatol,* 20**,** 1634-40.

CLEARY, S. P., COTTERCHIO, M., JENKINS, M. A., KIM, H., BRISTOW, R., GREEN, R., HAILE, R., HOPPER, J. L., LEMARCHAND, L., LINDOR, N., PARFREY, P., POTTER, J., YOUNGHUSBAND, B. & GALLINGER, S. 2009. Germline MutY human homologue mutations and colorectal cancer: a multisite case-control study. *Gastroenterology,* 136**,** 1251-60.

COTE, J. F. & VUORI, K. 2007. GEF what? Dock180 and related proteins help Rac to polarize cells in new ways. *Trends Cell Biol,* 17**,** 383-93.

CRAWFORD, H. C., FINGLETON, B. M., RUDOLPH-OWEN, L. A., GOSS, K. J., RUBINFELD, B., POLAKIS, P. & MATRISIAN, L. M. 1999. The metalloproteinase matrilysin is a target of beta-catenin transactivation in intestinal tumors. *Oncogene,* 18**,** 2883-91.

CRUICKSHANK, S. M., MCVAY, L. D., BAUMGART, D. C., FELSBURG, P. J. & CARDING, S. R. 2004. Colonic epithelial cell mediated suppression of CD4 T cell activation. *Gut,* 53**,** 678-84.

CUTLER, N. S., GRAVES-DEAL, R., LAFLEUR, B. J., GAO, Z., BOMAN, B. M., WHITEHEAD, R. H., TERRY, E., MORROW, J. D. & COFFEY, R. J. 2003. Stromal

production of prostacyclin confers an antiapoptotic effect to colonic epithelial cells. *Cancer Res,* 63**,** 1748-51.

DALLMAN, C., JOHNSON, P. W. & PACKHAM, G. 2003. Differential regulation of cell survival by CD40. *Apoptosis,* 8**,** 45-53.

DANIELSEN, S. A., LIND, G. E., BJØRNSLETT, M., MELING, G. I., ROGNUM, T. O., HEIM, S. & LOTHE, R. A. 2008. Novel mutations of the suppressor gene PTEN in colorectal carcinomas stratified by microsatellite instability- and TP53 mutation- status. *Hum Mutat,* 29**,** E252-62.

DE ANGELIS, P. M., CLAUSEN, O. P., SCHJØLBERG, A. & STOKKE, T. 1999a. Chromosomal gains and losses in primary colorectal carcinomas detected by CGH and their associations with tumour DNA ploidy, genotypes and phenotypes. *Br J Cancer,* 80**,** 526-35.

DE ANGELIS, P. M., CLAUSEN, O. P., SCHJØLBERG, A. & STOKKE, T. 1999b. Chromosomal gains and losses in primary colorectal carcinomas detected by CGH and their associations with tumour DNA ploidy, genotypes and phenotypes. *Br J Cancer,* 80**,** 526-35.

DELEKTORSKAIA, V. V., PEREVOSHCHIKOV, A. G., GOLOVKOV, D. A. & KUSHLINSKIĬ, N. E. 2005. [Immunohistochemical study of E-cadherin, beta-catenin and CD-44v6 expression in the cells of primary colon cancer and its metastases]. *Arkh Patol,* 67**,** 34-8.

DIEP, C. B., KLEIVI, K., RIBEIRO, F. R., TEIXEIRA, M. R., LINDGJAERDE, O. C. & LOTHE, R. A. 2006a. The order of genetic events associated with colorectal cancer progression inferred from meta-analysis of copy number changes. *Genes Chromosomes Cancer,* 45**,** 31-41.

DIEP, C. B., KLEIVI, K., RIBEIRO, F. R., TEIXEIRA, M. R., LINDGJAERDE, O. C. & LOTHE, R. A. 2006b. The order of genetic events associated with colorectal cancer progression inferred from meta-analysis of copy number changes. *Genes Chromosomes Cancer,* 45**,** 31-41.

DIEP, C. B., PARADA, L. A., TEIXEIRA, M. R., EKNAES, M., NESLAND, J. M., JOHANSSON, B. & LOTHE, R. A. 2003. Genetic profiling of colorectal cancer liver metastases by combined comparative genomic hybridization and G-banding analysis. *Genes Chromosomes Cancer,* 36**,** 189-97.

DIKOVSKAYA, D., SCHIFFMANN, D., NEWTON, I. P., OAKLEY, A., KROBOTH, K., SANSOM, O., JAMIESON, T. J., MENIEL, V., CLARKE, A. & NÄTHKE, I. S. 2007. Loss of APC induces polyploidy as a result of a combination of defects in mitosis and apoptosis. *J Cell Biol,* 176**,** 183-95.

DUBÉ, N., BOURDEAU, A., HEINONEN, K. M., CHENG, A., LOY, A. L. & TREMBLAY, M. L. 2005. Genetic ablation of protein tyrosine phosphatase 1B accelerates lymphomagenesis of p53-null mice through the regulation of B-cell development. *Cancer Res,* 65**,** 10088-95.

ELIOPOULOS, A. G. & YOUNG, L. S. 2004. The role of the CD40 pathway in the pathogenesis and treatment of cancer. *Curr Opin Pharmacol,* 4**,** 360-7.

ELMUNZER, B. J., HAYWARD, R. A., SCHOENFELD, P. S., SAINI, S. D., DESHPANDE, A. & WALJEE, A. K. 2012. Effect of flexible sigmoidoscopy-based screening on incidence and mortality of colorectal cancer: a systematic review and meta-analysis of randomized controlled trials. *PLoS Med,* 9**,** e1001352.

ESCHRICH, S., YANG, I., BLOOM, G., KWONG, K. Y., BOULWARE, D., CANTOR, A., COPPOLA, D., KRUHØFFER, M., AALTONEN, L., ORNTOFT, T. F., QUACKENBUSH, J. & YEATMAN, T. J. 2005. Molecular staging for survival prediction of colorectal cancer patients. *J Clin Oncol,* 23**,** 3526-35.

ESPINA, C., CESPEDES, M. V., GARCIA-CABEZAS, M. A., GOMEZ DEL PULGAR, M. T., BOLUDA, A., OROZ, L. G., BENITAH, S. A., CEJAS, P., NISTAL, M., MANGUES, R. & LACAL, J. C. 2008. A critical role for Rac1 in tumor progression of human colorectal adenocarcinoma cells. *Am J Pathol,* 172**,** 156-66.

ESTELLER, M. 2008. Epigenetics in cancer. *N Engl J Med,* 358**,** 1148-59.

ESUFALI, S., CHARAMES, G. S., PETHE, V. V., BUONGIORNO, P. & BAPAT, B. 2007. Activation of tumor-specific splice variant Rac1b by dishevelled promotes canonical Wnt signaling and decreased adhesion of colorectal cancer cells. *Cancer Res,* 67**,** 2469-79.

FADHIL, W., IBRAHEM, S., SETH, R., ABUALI, G., RAGUNATH, K., KAYE, P. & ILYAS, M. 2012. The utility of diagnostic biopsy specimens for predictive molecular testing in colorectal cancer. *Histopathology,* 61**,** 1117-24.

FADHIL, W., IBRAHEM, S., SETH, R. & ILYAS, M. 2010. Quick-multiplex-consensus (QMC)-PCR followed by high-resolution melting: a simple and robust method for mutation detection in formalin-fixed paraffin-embedded tissue. *J Clin Pathol,* 63**,** 134-40.

FADHIL, W., KINDLE, K., JACKSON, D., ZAITOUN, A., LANE, N., ROBINS, A. & ILYAS, M. 2014. DNA content analysis of colorectal cancer defines a distinct 'microsatellite and chromosome stable' group but does not predict response to radiotherapy. *Int J Exp Pathol,* 95**,** 16-23.

FAUX, M. C., ROSS, J. L., MEEKER, C., JOHNS, T., JI, H., SIMPSON, R. J., LAYTON, M. J. & BURGESS, A. W. 2004. Restoration of full-length adenomatous polyposis coli (APC) protein in a colon cancer cell line enhances cell adhesion. *J Cell Sci,* 117**,** 427-39.

FEARON, E. R. 2011a. Molecular genetics of colorectal cancer. *Annu Rev Pathol,* 6**,** 479-507.

FEARON, E. R. 2011b. Molecular genetics of colorectal cancer. *Annu Rev Pathol,* 6**,** 479-507.

FEARON, E. R. & VOGELSTEIN, B. 1990. A genetic model for colorectal tumorigenesis. *Cell,* 61**,** 759-67.

FEDIRKO, V., TRAMACERE, I., BAGNARDI, V., ROTA, M., SCOTTI, L., ISLAMI, F., NEGRI, E., STRAIF, K., ROMIEU, I., LA VECCHIA, C., BOFFETTA, P. & JENAB, M. 2011. Alcohol drinking and colorectal cancer risk: an overall and dose-response meta-analysis of published studies. *Ann Oncol,* 22**,** 1958-72.

FELTUS, F. A., LEE, E. K., COSTELLO, J. F., PLASS, C. & VERTINO, P. M. 2006. DNA motifs associated with aberrant CpG island methylation. *Genomics,* 87**,** 572-9.

FINKELSTEIN, S. D., SAYEGH, R., CHRISTENSEN, S. & SWALSKY, P. A. 1993. Genotypic classification of colorectal adenocarcinoma. Biologic behavior correlates with K-ras-2 mutation type. *Cancer,* 71**,** 3827-38.

FLYGER, H. L., LARSEN, J. K., NIELSEN, H. J. & CHRISTENSEN, I. J. 1999. DNA ploidy in colorectal cancer, heterogeneity within and between tumors and relation to survival. *Cytometry,* 38**,** 293-300.

FRANGIONI, J. V., BEAHM, P. H., SHIFRIN, V., JOST, C. A. & NEEL, B. G. 1992. The nontransmembrane tyrosine phosphatase PTP-1B localizes to the endoplasmic reticulum via its 35 amino acid C-terminal sequence. *Cell,* 68**,** 545-60.

FRIGOLA, J., MUNOZ, M., CLARK, S. J., MORENO, V., CAPELLA, G. & PEINADO, M. A. 2005. Hypermethylation of the prostacyclin synthase (PTGIS) promoter is a frequent event in colorectal cancer and associated with aneuploidy. *Oncogene,* 24**,** 7320-6.

GALAUP, A., CAZES, A., LE JAN, S., PHILIPPE, J., CONNAULT, E., LE COZ, E., MEKID, H., MIR, L. M., OPOLON, P., CORVOL, P., MONNOT, C. & GERMAIN, S. 2006. Angiopoietin-like 4 prevents metastasis through inhibition of vascular permeability and tumor cell motility and invasiveness. *Proc Natl Acad Sci U S A,* 103**,** 18721-6.

GALIATSATOS, P. & FOULKES, W. D. 2006. Familial adenomatous polyposis. *Am J Gastroenterol,* 101**,** 385-98.

GELBMANN, C. M., LEEB, S. N., VOGL, D., MAENDEL, M., HERFARTH, H., SCHOLMERICH, J., FALK, W. & ROGLER, G. 2003. Inducible CD40 expression mediates NFkappaB activation and cytokine secretion in human colonic fibroblasts. *Gut,* 52**,** 1448-56.

GEORGOPOULOS, N. T., MERRICK, A., SCOTT, N., SELBY, P. J., MELCHER, A. & TREJDOSIEWICZ, L. K. 2007. CD40-mediated death and cytokine secretion in colorectal cancer: a potential target for inflammatory tumour cell killing. *Int J Cancer,* 121**,** 1373-81.

GETZ, G., HÖFLING, H., MESIROV, J. P., GOLUB, T. R., MEYERSON, M., TIBSHIRANI, R. & LANDER, E. S. 2007. Comment on "The consensus coding sequences of human breast and colorectal cancers". *Science,* 317**,** 1500.

GILLET, J. P., VARMA, S. & GOTTESMAN, M. M. 2013. The clinical relevance of cancer cell lines. *J Natl Cancer Inst,* 105**,** 452-8.

GOEL, A., ARNOLD, C. N., NIEDZWIECKI, D., CHANG, D. K., RICCIARDIELLO, L., CARETHERS, J. M., DOWELL, J. M., WASSERMAN, L., COMPTON, C., MAYER, R. J., BERTAGNOLLI, M. M. & BOLAND, C. R. 2003. Characterization of sporadic colon cancer by patterns of genomic instability. *Cancer Res,* 63**,** 1608-14.

GOEL, A., NAGASAKA, T., ARNOLD, C. N., INOUE, T., HAMILTON, C., NIEDZWIECKI, D., COMPTON, C., MAYER, R. J., GOLDBERG, R., BERTAGNOLLI, M. M. & BOLAND, C. R. 2007. The CpG island methylator phenotype and chromosomal instability are inversely correlated in sporadic colorectal cancer. *Gastroenterology,* 132**,** 127-38.

GONZÁLEZ-AGUILERA, J. J., OLIART, S., AZCOITA, M. M. & FERNÁNDEZ-PERALTA, A. M. 2004. Simultaneous mutations in K-ras and TP53 are indicative of poor prognosis in sporadic colorectal cancer. *Am J Clin Oncol,* 27**,** 39-45.

GONZÁLEZ-RODRIGUEZ, A., ESCRIBANO, O., ALBA, J., RONDINONE, C. M., BENITO, M. & VALVERDE, A. M. 2007. Levels of protein tyrosine phosphatase 1B determine susceptibility to apoptosis in serum-deprived hepatocytes. *J Cell Physiol,* 212**,** 76-88.

GRADY, W. M. & CARETHERS, J. M. 2008a. Genomic and epigenetic instability in colorectal cancer pathogenesis. *Gastroenterology,* 135**,** 1079-99.

GRADY, W. M. & CARETHERS, J. M. 2008b. Genomic and epigenetic instability in colorectal cancer pathogenesis. *Gastroenterology,* 135**,** 1079-99.

GRIMSLEY, C. M., KINCHEN, J. M., TOSELLO-TRAMPONT, A. C., BRUGNERA, E., HANEY, L. B., LU, M., CHEN, Q., KLINGELE, D., HENGARTNER, M. O. & RAVICHANDRAN, K. S. 2004. Dock180 and ELMO1 proteins cooperate to promote evolutionarily conserved Rac-dependent cell migration. *J Biol Chem,* 279**,** 6087-97.

GRODEN, J., THLIVERIS, A., SAMOWITZ, W., CARLSON, M., GELBERT, L., ALBERTSEN, H., JOSLYN, G., STEVENS, J., SPIRIO, L., ROBERTSON, M. & ET AL. 1991. Identification and characterization of the familial adenomatous polyposis coli gene. *Cell,* 66**,** 589-600.

GROEN, E. J., ROOS, A., MUNTINGHE, F. L., ENTING, R. H., DE VRIES, J., KLEIBEUKER, J. H., WITJES, M. J., LINKS, T. P. & VAN BEEK, A. P. 2008. Extra-intestinal manifestations of familial adenomatous polyposis. *Ann Surg Oncol,* 15**,** 2439-50.

GUASTADISEGNI, C., COLAFRANCESCHI, M., OTTINI, L. & DOGLIOTTI, E. 2010. Microsatellite instability as a marker of prognosis and response to therapy: a meta-analysis of colorectal cancer survival data. *Eur J Cancer,* 46**,** 2788-98.

GUINNEY, J., DIENSTMANN, R., WANG, X., DE REYNIES, A., SCHLICKER, A., SONESON, C., MARISA, L., ROEPMAN, P., NYAMUNDANDA, G., ANGELINO, P., BOT, B. M., MORRIS, J. S., SIMON, I. M., GERSTER, S., FESSLER, E., DE SOUSA, E. M. F., MISSIAGLIA, E., RAMAY, H., BARRAS, D., HOMICSKO, K., MARU, D., MANYAM, G. C., BROOM, B., BOIGE, V., PEREZ-VILLAMIL, B., LADERAS, T., SALAZAR, R., GRAY, J. W., HANAHAN, D., TABERNERO, J., BERNARDS, R., FRIEND, S. H., LAURENT-PUIG, P., MEDEMA, J. P., SADANANDAM, A., WESSELS, L., DELORENZI, M., KOPETZ, S., VERMEULEN, L. & TEJPAR, S. 2015. The consensus molecular subtypes of colorectal cancer. *Nat Med,* 21**,** 1350-6.

GUMIENNY, T. L., BRUGNERA, E., TOSELLO-TRAMPONT, A. C., KINCHEN, J. M., HANEY, L. B., NISHIWAKI, K., WALK, S. F., NEMERGUT, M. E., MACARA, I. G., FRANCIS, R., SCHEDL, T., QIN, Y., VAN AELST, L., HENGARTNER, M. O. & RAVICHANDRAN, K. S. 2001. CED-12/ELMO, a novel member of the CrkII/Dock180/Rac pathway, is required for phagocytosis and cell migration. *Cell,* 107**,** 27-41.

HALFORD, S., SASIENI, P., ROWAN, A., WASAN, H., BODMER, W., TALBOT, I., HAWKINS, N., WARD, R. & TOMLINSON, I. 2002. Low-level microsatellite instability occurs in most colorectal cancers and is a nonrandomly distributed quantitative trait. *Cancer Res,* 62**,** 53-7.

HAMPEL, H., FRANKEL, W., PANESCU, J., LOCKMAN, J., SOTAMAA, K., FIX, D., COMERAS, I., LA JEUNESSE, J., NAKAGAWA, H., WESTMAN, J. A., PRIOR, T. W., CLENDENNING, M., PENZONE, P., LOMBARDI, J., DUNN, P., COHN, D. E., COPELAND, L., EATON, L., FOWLER, J., LEWANDOWSKI, G., VACCARELLO, L., BELL, J., REID, G. & DE LA CHAPELLE, A. 2006. Screening for Lynch syndrome (hereditary nonpolyposis colorectal cancer) among endometrial cancer patients. *Cancer Res,* 66**,** 7810-7.

HASEGAWA, H., KIYOKAWA, E., TANAKA, S., NAGASHIMA, K., GOTOH, N., SHIBUYA, M., KURATA, T. & MATSUDA, M. 1996. DOCK180, a major CRK-binding protein, alters cell morphology upon translocation to the cell membrane. *Mol Cell Biol,* 16**,** 1770-6.

HAYASHIDA, Y., HONDA, K., IDOGAWA, M., INO, Y., ONO, M., TSUCHIDA, A., AOKI, T., HIROHASHI, S. & YAMADA, T. 2005. E-cadherin regulates the association between beta-catenin and actinin-4. *Cancer Res,* 65**,** 8836-45.

HE, T. C., CHAN, T. A., VOGELSTEIN, B. & KINZLER, K. W. 1999. PPARdelta is an APC-regulated target of nonsteroidal anti-inflammatory drugs. *Cell,* 99**,** 335-45.

HE, T. C., SPARKS, A. B., RAGO, C., HERMEKING, H., ZAWEL, L., DA COSTA, L. T., MORIN, P. J., VOGELSTEIN, B. & KINZLER, K. W. 1998. Identification of c-MYC as a target of the APC pathway. *Science,* 281**,** 1509-12.

HEIMANN, T. M., MILLER, F., MARTINELLI, G., MESTER, J., KURTZ, R. J., SZPORN, A. & FASY, T. 1990. Significance of DNA content abnormalities in small rectal cancers. *Am J Surg,* 159**,** 199-202; discussion 202-3.

HEMMINKI, A., TOMLINSON, I., MARKIE, D., JARVINEN, H., SISTONEN, P., BJORKQVIST, A. M., KNUUTILA, S., SALOVAARA, R., BODMER, W., SHIBATA, D., DE LA CHAPELLE, A. & AALTONEN, L. A. 1997. Localization of a susceptibility locus for Peutz-Jeghers syndrome to 19p using comparative genomic hybridization and targeted linkage analysis. *Nat Genet,* 15**,** 87-90.

HENDRIX, N. D., WU, R., KUICK, R., SCHWARTZ, D. R., FEARON, E. R. & CHO, K. R. 2006. Fibroblast growth factor 9 has oncogenic activity and is a downstream target of Wnt signaling in ovarian endometrioid adenocarcinomas. *Cancer Res,* 66**,** 1354-62.

HERTER, J. M., ROSSAINT, J., BLOCK, H., WELCH, H. & ZARBOCK, A. 2013. Integrin activation by P-Rex1 is required for selectin-mediated slow leukocyte rolling and intravascular crawling. *Blood,* 121**,** 2301-10.

HIDAKA, S., YASUTAKE, T., TAKESHITA, H., KONDO, M., TSUJI, T., NANASHIMA, A., SAWAI, T., YAMAGUCHI, H., NAKAGOE, T., AYABE, H. & TAGAWA, Y. 2000a. Differences in 20q13.2 copy number between colorectal cancers with and without liver metastasis. *Clin Cancer Res,* 6**,** 2712-7.

HIDAKA, S., YASUTAKE, T., TAKESHITA, H., KONDO, M., TSUJI, T., NANASHIMA, A., SAWAI, T., YAMAGUCHI, H., NAKAGOE, T., AYABE, H. & TAGAWA, Y. 2000b. Differences in 20q13.2 copy number between colorectal cancers with and without liver metastasis. *Clin Cancer Res,* 6**,** 2712-7.

HILL, K., KRUGMANN, S., ANDREWS, S. R., COADWELL, W. J., FINAN, P., WELCH, H. C., HAWKINS, P. T. & STEPHENS, L. R. 2005. Regulation of P-Rex1 by phosphatidylinositol (3,4,5)-trisphosphate and Gbetagamma subunits. *J Biol Chem,* 280**,** 4166-73.

HO, E. & DAGNINO, L. 2012. Emerging role of ILK and ELMO2 in the integration of adhesion and migration pathways. *Cell Adh Migr,* 6**,** 168-72.

HOMIG-HOLZEL, C., HOJER, C., RASTELLI, J., CASOLA, S., STROBL, L. J., MULLER, W., QUINTANILLA-MARTINEZ, L., GEWIES, A., RULAND, J., RAJEWSKY, K. & ZIMBER-STROBL, U. 2008. Constitutive CD40 signaling in B cells selectively activates the noncanonical NF-kappaB pathway and promotes lymphomagenesis. *J Exp Med,* 205**,** 1317-29.

HOULSTON, R. S., CHEADLE, J., DOBBINS, S. E., TENESA, A., JONES, A. M., HOWARTH, K., SPAIN, S. L., BRODERICK, P., DOMINGO, E., FARRINGTON, S., PRENDERGAST, J. G., PITTMAN, A. M., THEODORATOU, E., SMITH, C. G.,

OLVER, B., WALTHER, A., BARNETSON, R. A., CHURCHMAN, M., JAEGER, E. E., PENEGAR, S., BARCLAY, E., MARTIN, L., GORMAN, M., MAGER, R., JOHNSTONE, E., MIDGLEY, R., NIITTYMAKI, I., TUUPANEN, S., COLLEY, J., IDZIASZCZYK, S., CONSORTIUM, C., THOMAS, H. J., LUCASSEN, A. M., EVANS, D. G., MAHER, E. R., CONSORTIUM, C., GROUP, C. C., GROUP, C. C., MAUGHAN, T., DIMAS, A., DERMITZAKIS, E., CAZIER, J. B., AALTONEN, L. A., PHAROAH, P., KERR, D. J., CARVAJAL-CARMONA, L. G., CAMPBELL, H., DUNLOP, M. G. & TOMLINSON, I. P. 2010. Meta-analysis of three genome-wide association studies identifies susceptibility loci for colorectal cancer at 1q41, 3q26.2, 12q13.13 and 20q13.33. *Nat Genet,* 42**,** 973-7.

IACOPETTA, B., GRIEU, F. & AMANUEL, B. 2010. Microsatellite instability in colorectal cancer. *Asia Pac J Clin Oncol,* 6**,** 260-9.

IACOPETTA, B., RUSSO, A., BAZAN, V., DARDANONI, G., GEBBIA, N., SOUSSI, T., KERR, D., ELSALEH, H., SOONG, R., KANDIOLER, D., JANSCHEK, E., KAPPEL, S., LUNG, M., LEUNG, C. S., KO, J. M., YUEN, S., HO, J., LEUNG, S. Y., CRAPEZ, E., DUFFOUR, J., YCHOU, M., LEAHY, D. T., O'DONOGHUE, D. P., AGNESE, V., CASCIO, S., DI FEDE, G., CHIECO-BIANCHI, L., BERTORELLE, R., BELLUCO, C., GIARETTI, W., CASTAGNOLA, P., RICEVUTO, E., FICORELLA, C., BOSARI, S., ARIZZI, C. D., MIYAKI, M., ONDA, M., KAMPMAN, E., DIERGAARDE, B., ROYDS, J., LOTHE, R. A., DIEP, C. B., MELING, G. I., OSTROWSKI, J., TRZECIAK, L., GUZINSKA-USTYMOWICZ, K., ZALEWSKI, B., CAPELLÁ, G. M., MORENO, V., PEINADO, M. A., LÖNNROTH, C., LUNDHOLM, K., SUN, X. F., JANSSON, A., BOUZOURENE, H., HSIEH, L. L., TANG, R., SMITH, D. R., ALLEN-MERSH, T. G., KHAN, Z. A., SHORTHOUSE, A. J., SILVERMAN, M. L., KATO, S., ISHIOKA, C. & GROUP, T.-C. C. 2006. Functional categories of TP53 mutation in colorectal cancer: results of an International Collaborative Study. *Ann Oncol,* 17**,** 842-7.

ILYAS, M., STRAUB, J., TOMLINSON, I. P. & BODMER, W. F. 1999. Genetic pathways in colorectal and other cancers. *Eur J Cancer,* 35**,** 1986-2002.

ISHIKAWA, K., MIYAMOTO, M., YOSHIOKA, T., KATO, T., KAJI, M., OHBUCHI, T., HIRANO, S., ITOH, T., DOSAKA-AKITA, H. & KONDO, S. 2008. Up-regulation of CD40 with juxtacrine activity in human nonsmall lung cancer cells correlates with poor prognosis. *Cancer,* 113**,** 530-41.

ISHIKAWA, T., ICHIKAWA, Y., MITSUHASHI, M., MOMIYAMA, N., CHISHIMA, T., TANAKA, K., YAMAOKA, H., MIYAZAKIC, K., NAGASHIMA, Y., AKITAYA, T. & SHIMADA, H. 1996. Matrilysin is associated with progression of colorectal tumor. *Cancer Lett,* 107**,** 5-10.

ITALIANO, A., SAINT-PAUL, M. C., CAROLI-BOSC, F. X., FRANÇOIS, E., BOURGEON, A., BENCHIMOL, D., GUGENHEIM, J. & MICHIELS, J. F. 2005. Epidermal growth factor receptor (EGFR) status in primary colorectal tumors correlates with EGFR expression in related metastatic sites: biological and clinical implications. *Ann Oncol,* 16**,** 1503-7.

JACKSON, B. C., IVANOVA, I. A. & DAGNINO, L. 2015. An ELMO2-RhoG-ILK network modulates microtubule dynamics. *Mol Biol Cell,* 26**,** 2712-25.

JAFFE, A. B. & HALL, A. 2005. Rho GTPases: biochemistry and biology. *Annu Rev Cell Dev Biol,* 21**,** 247-69.

JASMINE, F., RAHAMAN, R., DODSWORTH, C., ROY, S., PAUL, R., RAZA, M., PAUL-BRUTUS, R., KAMAL, M., AHSAN, H. & KIBRIYA, M. G. 2012a. A genome-wide study of cytogenetic changes in colorectal cancer using SNP microarrays: opportunities for future personalized treatment. *PLoS One,* 7**,** e31968.

JASMINE, F., RAHAMAN, R., DODSWORTH, C., ROY, S., PAUL, R., RAZA, M., PAUL-BRUTUS, R., KAMAL, M., AHSAN, H. & KIBRIYA, M. G. 2012b. A genome-wide study of cytogenetic changes in colorectal cancer using SNP microarrays: opportunities for future personalized treatment. *PLoS One,* 7**,** e31968.

JASS, J. R. 2007. Classification of colorectal cancer based on correlation of clinical, morphological and molecular features. *Histopathology,* 50**,** 113-30.

JESS, T., RUNGOE, C. & PEYRIN-BIROULET, L. 2012. Risk of colorectal cancer in patients with ulcerative colitis: a meta-analysis of population-based cohort studies. *Clin Gastroenterol Hepatol,* 10**,** 639-45.

JOHNSON, P. W., WATT, S. M., BETTS, D. R., DAVIES, D., JORDAN, S., NORTON, A. J. & LISTER, T. A. 1993. Isolated follicular lymphoma cells are resistant to apoptosis and can be grown in vitro in the CD40/stromal cell system. *Blood,* 82**,** 1848-57.

JONES, S., CHEN, W. D., PARMIGIANI, G., DIEHL, F., BEERENWINKEL, N., ANTAL, T., TRAULSEN, A., NOWAK, M. A., SIEGEL, C., VELCULESCU, V. E., KINZLER, K. W., VOGELSTEIN, B., WILLIS, J. & MARKOWITZ, S. D. 2008. Comparative lesion sequencing provides insights into tumor evolution. *Proc Natl Acad Sci U S A,* 105**,** 4283-8.

JULIEN, S. G., DUBÉ, N., HARDY, S. & TREMBLAY, M. L. 2011. Inside the human cancer tyrosine phosphatome. *Nat Rev Cancer,* 11**,** 35-49.

KANG, Y. & MASSAGUÉ, J. 2004. Epithelial-mesenchymal transitions: twist in development and metastasis. *Cell,* 118**,** 277-9.

KARPUSAS, M., HSU, Y. M., WANG, J. H., THOMPSON, J., LEDERMAN, S., CHESS, L. & THOMAS, D. 1995. 2 A crystal structure of an extracellular fragment of human CD40 ligand. *Structure,* 3**,** 1031-9.

KATAYAMA, H., SASAI, K., KAWAI, H., YUAN, Z. M., BONDARUK, J., SUZUKI, F., FUJII, S., ARLINGHAUS, R. B., CZERNIAK, B. A. & SEN, S. 2004. Phosphorylation by aurora kinase A induces Mdm2-mediated destabilization and inhibition of p53. *Nat Genet,* 36**,** 55-62.

KATOH, H. & NEGISHI, M. 2003. RhoG activates Rac1 by direct interaction with the Dock180-binding protein Elmo. *Nature,* 424**,** 461-4.

KAU, T. R., WAY, J. C. & SILVER, P. A. 2004. Nuclear transport and cancer: from mechanism to intervention. *Nat Rev Cancer,* 4**,** 106-17.

KAWADA, K., HASEGAWA, S., MURAKAMI, T., ITATANI, Y., HOSOGI, H., SONOSHITA, M., KITAMURA, T., FUJISHITA, T., IWAMOTO, M., MATSUMOTO, T., MATSUSUE, R., HIDA, K., AKIYAMA, G., OKOSHI, K., YAMADA, M., KAWAMURA, J., TAKETO, M. M. & SAKAI, Y. 2011. Molecular mechanisms of liver metastasis. *Int J Clin Oncol,* 16**,** 464-72.

KIM, E. K., YUN, S. J., HA, J. M., KIM, Y. W., JIN, I. H., YUN, J., SHIN, H. K., SONG, S. H., KIM, J. H., LEE, J. S., KIM, C. D. & BAE, S. S. 2011. Selective activation of Akt1 by mammalian target of rapamycin complex 2 regulates cancer cell migration, invasion, and metastasis. *Oncogene,* 30**,** 2954-63.

KIM, J. C., CHOI, J. S., ROH, S. A., CHO, D. H., KIM, T. W. & KIM, Y. S. 2010. Promoter methylation of specific genes is associated with the phenotype and progression of colorectal adenocarcinomas. *Ann Surg Oncol,* 17**,** 1767-76.

KIM, Y. H., MIN, B. H., CHOI, H. K., KIM, S. J., KIM, K. M., KIM, J. Y., CHANG, D. K., SON, H. J., RHEE, P. L., KIM, J. J., RHEE, J. C. & CHUN, H. K. 2009. Sporadic colorectal carcinomas with low-level microsatellite instability in Korea: do they form a distinct subgroup with distinguished clinicopathological features? *J Surg Oncol,* 99**,** 351-5.

KINZLER, K. W. & VOGELSTEIN, B. 1996. Lessons from hereditary colorectal cancer. *Cell,* 87**,** 159-70.

KITADA, S., ZAPATA, J. M., ANDREEFF, M. & REED, J. C. 1999. Bryostatin and CD40-ligand enhance apoptosis resistance and induce expression of cell survival genes in B-cell chronic lymphocytic leukaemia. *Br J Haematol,* 106**,** 995-1004.

KLEIN, C. A. & STOECKLEIN, N. H. 2009. Lessons from an aggressive cancer: evolutionary dynamics in esophageal carcinoma. *Cancer Res,* 69**,** 5285-8.

KOLCH, W. 2000. Meaningful relationships: the regulation of the Ras/Raf/MEK/ERK pathway by protein interactions. *Biochem J,* 351 Pt 2**,** 289-305.

KORN, W. M., YASUTAKE, T., KUO, W. L., WARREN, R. S., COLLINS, C., TOMITA, M., GRAY, J. & WALDMAN, F. M. 1999a. Chromosome arm 20q gains and other genomic alterations in colorectal cancer metastatic to liver, as analyzed by comparative genomic hybridization and fluorescence in situ hybridization. *Genes Chromosomes Cancer,* 25**,** 82-90.

KORN, W. M., YASUTAKE, T., KUO, W. L., WARREN, R. S., COLLINS, C., TOMITA, M., GRAY, J. & WALDMAN, F. M. 1999b. Chromosome arm 20q gains and other genomic alterations in colorectal cancer metastatic to liver, as analyzed by comparative genomic hybridization and fluorescence in situ hybridization. *Genes Chromosomes Cancer,* 25**,** 82-90.

KOSTIC, A. D., GEVERS, D., PEDAMALLU, C. S., MICHAUD, M., DUKE, F., EARL, A. M., OJESINA, A. I., JUNG, J., BASS, A. J., TABERNERO, J., BASELGA, J., LIU, C., SHIVDASANI, R. A., OGINO, S., BIRREN, B. W., HUTTENHOWER, C., GARRETT, W. S. & MEYERSON, M. 2012. Genomic analysis identifies association of Fusobacterium with colorectal carcinoma. *Genome Res,* 22**,** 292-8.

KOUNTOURAKIS, P., PAVLAKIS, K., PSYRRI, A., RONTOGIANNI, D., XIROS, N., PATSOURIS, E., PECTASIDES, D. & ECONOMOPOULOS, T. 2006. Clinicopathologic significance of EGFR and Her-2/neu in colorectal adenocarcinomas. *Cancer J,* 12**,** 229-36.

KRAJEWSKA, M., MOSS, S. F., KRAJEWSKI, S., SONG, K., HOLT, P. R. & REED, J. C. 1996. Elevated expression of Bcl-X and reduced Bak in primary colorectal adenocarcinomas. *Cancer Res,* 56**,** 2422-7.

KROBOTH, K., NEWTON, I. P., KITA, K., DIKOVSKAYA, D., ZUMBRUNN, J., WATERMAN-STORER, C. M. & NÄTHKE, I. S. 2007. Lack of adenomatous polyposis coli protein correlates with a decrease in cell migration and overall changes in microtubule stability. *Mol Biol Cell,* 18**,** 910-8.

KWON, C. H., PARK, H. J., CHOI, J. H., LEE, J. R., KIM, H. K., JO, H. J., KIM, H. S., OH, N., SONG, G. A. & PARK DO, Y. 2015. Snail and serpinA1 promote tumor progression and predict prognosis in colorectal cancer. *Oncotarget,* 6**,** 20312-26.

LAURENT-PUIG, P., CAYRE, A., MANCEAU, G., BUC, E., BACHET, J. B., LECOMTE, T., ROUGIER, P., LIEVRE, A., LANDI, B., BOIGE, V., DUCREUX, M., YCHOU, M., BIBEAU, F., BOUCHÉ, O., REID, J., STONE, S. & PENAULT-LLORCA, F. 2009. Analysis of PTEN, BRAF, and EGFR status in determining benefit from cetuximab therapy in wild-type KRAS metastatic colon cancer. *J Clin Oncol,* 27**,** 5924-30.

LEARY, R. J., LIN, J. C., CUMMINS, J., BOCA, S., WOOD, L. D., PARSONS, D. W., JONES, S., SJÖBLOM, T., PARK, B. H., PARSONS, R., WILLIS, J., DAWSON, D., WILLSON, J. K., NIKOLSKAYA, T., NIKOLSKY, Y., KOPELOVICH, L., PAPADOPOULOS, N., PENNACCHIO, L. A., WANG, T. L., MARKOWITZ, S. D., PARMIGIANI, G., KINZLER, K. W., VOGELSTEIN, B. & VELCULESCU, V. E. 2008. Integrated analysis of homozygous deletions, focal amplifications, and sequence alterations in breast and colorectal cancers. *Proc Natl Acad Sci U S A,* 105**,** 16224-9.

LEEMAN, M. F., CURRAN, S. & MURRAY, G. I. 2003. New insights into the roles of matrix metalloproteinases in colorectal cancer development and progression. *J Pathol,* 201**,** 528-34.

LENGAUER, C., KINZLER, K. W. & VOGELSTEIN, B. 1997. Genetic instability in colorectal cancers. *Nature,* 386**,** 623-7.

LESLIE, A., PRATT, N. R., GILLESPIE, K., SALES, M., KERNOHAN, N. M., SMITH, G., WOLF, C. R., CAREY, F. A. & STEELE, R. J. 2003. Mutations of APC, K-ras, and p53 are associated with specific chromosomal aberrations in colorectal adenocarcinomas. *Cancer Res,* 63**,** 4656-61.

LESSARD, L., LABBÉ, D. P., DEBLOIS, G., BÉGIN, L. R., HARDY, S., MES-MASSON, A. M., SAAD, F., TROTMAN, L. C., GIGUÈRE, V. & TREMBLAY, M. L. 2012. PTP1B is an androgen receptor-regulated phosphatase that promotes the progression of prostate cancer. *Cancer Res,* 72**,** 1529-37.

LESSARD, L., STUIBLE, M. & TREMBLAY, M. L. 2010. The two faces of PTP1B in cancer. *Biochim Biophys Acta,* 1804**,** 613-9.

LI, H., YANG, L., FU, H., YAN, J., WANG, Y., GUO, H., HAO, X., XU, X., JIN, T. & ZHANG, N. 2013. Association between Galphai2 and ELMO1/Dock180 connects chemokine signalling with Rac activation and metastasis. *Nat Commun,* 4**,** 1706.

LI, W., ZHU, T. & GUAN, K. L. 2004. Transformation potential of Ras isoforms correlates with activation of phosphatidylinositol 3-kinase but not ERK. *J Biol Chem,* 279**,** 37398-406.

LIANG, P. S., CHEN, T. Y. & GIOVANNUCCI, E. 2009. Cigarette smoking and colorectal cancer incidence and mortality: systematic review and meta-analysis. *Int J Cancer,* 124**,** 2406-15.

LICHAO, S., LIANG, P., CHUNGUANG, G., FANG, L., ZHIHUA, Y. & YULIANG, R. 2012a. Overexpression of PTGIS could predict liver metastasis and is correlated with poor prognosis in colon cancer patients. *Pathol Oncol Res,* 18**,** 563-9.

LICHAO, S., LIANG, P., CHUNGUANG, G., FANG, L., ZHIHUA, Y. & YULIANG, R. 2012b. Overexpression of PTGIS could predict liver metastasis and is correlated with poor prognosis in colon cancer patients. *Pathol Oncol Res,* 18**,** 563-9.

LIÈVRE, A., BACHET, J. B., BOIGE, V., CAYRE, A., LE CORRE, D., BUC, E., YCHOU, M., BOUCHÉ, O., LANDI, B., LOUVET, C., ANDRÉ, T., BIBEAU, F., DIEBOLD, M. D., ROUGIER, P., DUCREUX, M., TOMASIC, G., EMILE, J. F., PENAULT-LLORCA, F. & LAURENT-PUIG, P. 2008. KRAS mutations as an independent prognostic factor in patients with advanced colorectal cancer treated with cetuximab. *J Clin Oncol,* 26**,** 374-9.

LIFE-TECHNOLOGIES. 2011. *Real-Time PCR: Understanding Ct Application Note* [Online]. USA: Life Technologies. Available: http://www.thermofisher.com/uk/en/home/life-science/pcr/real-time-pcr/qpcr-education/pcr-understanding-ct-application-note.html 2015].

LIM, H., GUPTA, R. A., MA, W. G., PARIA, B. C., MOLLER, D. E., MORROW, J. D., DUBOIS, R. N., TRZASKOS, J. M. & DEY, S. K. 1999. Cyclo-oxygenase-2-derived prostacyclin mediates embryo implantation in the mouse via PPARdelta. *Genes Dev,* 13**,** 1561-74.

LINDSAY, C. R., LAWN, S., CAMPBELL, A. D., FALLER, W. J., RAMBOW, F., MORT, R. L., TIMPSON, P., LI, A., CAMMARERI, P., RIDGWAY, R. A., MORTON, J. P., DOYLE, B., HEGARTY, S., RAFFERTY, M., MURPHY, I. G., MCDERMOTT, E. W., SHEAHAN, K., PEDONE, K., FINN, A. J., GROBEN, P. A., THOMAS, N. E., HAO, H., CARSON, C., NORMAN, J. C., MACHESKY, L. M., GALLAGHER, W. M., JACKSON, I. J., VAN KEMPEN, L., BEERMANN, F., DER, C., LARUE, L., WELCH, H. C., OZANNE, B. W. & SANSOM, O. J. 2011. P-Rex1 is required for efficient melanoblast migration and melanoma metastasis. *Nat Commun,* 2**,** 555.

LITVINOV, S. V., BALZAR, M., WINTER, M. J., BAKKER, H. A., BRIAIRE-DE BRUIJN, I. H., PRINS, F., FLEUREN, G. J. & WARNAAR, S. O. 1997. Epithelial cell adhesion molecule (Ep-CAM) modulates cell-cell interactions mediated by classic cadherins. *J Cell Biol,* 139**,** 1337-48.

LIU, F., HILL, D. E. & CHERNOFF, J. 1996. Direct binding of the proline-rich region of protein tyrosine phosphatase 1B to the Src homology 3 domain of p130(Cas). *J Biol Chem,* 271**,** 31290-5.

LOO, L. W., TIIRIKAINEN, M., CHENG, I., LUM-JONES, A., SEIFRIED, A., CHURCH, J. M., GRYFE, R., WEISENBERGER, D. J., LINDOR, N. M., GALLINGER, S., HAILE, R. W., DUGGAN, D. J., THIBODEAU, S. N., CASEY, G. & LE MARCHAND, L. 2013. Integrated analysis of genome-wide copy number alterations and gene expression in microsatellite stable, CpG island methylator phenotype-negative colon cancer. *Genes Chromosomes Cancer,* 52**,** 450-66.

LU, X., MALUMBRES, R., SHIELDS, B., JIANG, X., SAROSIEK, K. A., NATKUNAM, Y., TIGANIS, T. & LOSSOS, I. S. 2008. PTP1B is a negative regulator of interleukin 4-induced STAT6 signaling. *Blood,* 112**,** 4098-108.

LUBBE, S. J., DI BERNARDO, M. C., CHANDLER, I. P. & HOULSTON, R. S. 2009. Clinical implications of the colorectal cancer risk associated with MUTYH mutation. *J Clin Oncol,* 27**,** 3975-80.

LUCATO, C. M., HALLS, M. L., OOMS, L. M., LIU, H. J., MITCHELL, C. A., WHISSTOCK, J. C. & ELLISDON, A. M. 2015. The Phosphatidylinositol (3,4,5)-Trisphosphate-dependent Rac Exchanger 1.Ras-related C3 Botulinum Toxin Substrate 1 (P-Rex1.Rac1) Complex Reveals the Basis of Rac1 Activation in Breast Cancer Cells. *J Biol Chem,* 290**,** 20827-40.

LUSTIG, B., JERCHOW, B., SACHS, M., WEILER, S., PIETSCH, T., KARSTEN, U., VAN DE WETERING, M., CLEVERS, H., SCHLAG, P. M., BIRCHMEIER, W. & BEHRENS, J. 2002. Negative feedback loop of Wnt signaling through upregulation of conductin/axin2 in colorectal and liver tumors. *Mol Cell Biol,* 22**,** 1184-93.

LYNCH, H. T. & DE LA CHAPELLE, A. 2003. Hereditary colorectal cancer. *N Engl J Med,* 348**,** 919-32.

LYNCH, H. T., SMYRK, T. C., LANSPA, S. J., LYNCH, P. M., WATSON, P., STRAYHORN, P. C., BRONSON, E. K., LYNCH, J. F., PRILUCK, I. A. & APPELMAN, H. D. 1990.

Phenotypic variation in colorectal adenoma/cancer expression in two families. Hereditary flat adenoma syndrome. *Cancer,* 66**,** 909-15.

MA, Y., YANG, Y., WANG, F., ZHANG, P., SHI, C., ZOU, Y. & QIN, H. 2013. Obesity and risk of colorectal cancer: a systematic review of prospective studies. *PLoS One,* 8**,** e53916.

MAEDA, K., NISHIGUCHI, Y., KANG, S. M., YASHIRO, M., ONODA, N., SAWADA, T., ISHIKAWA, T. & HIRAKAWA, K. 2001. Expression of thrombospondin-1 inversely correlated with tumor vascularity and hematogenous metastasis in colon cancer. *Oncol Rep,* 8**,** 763-6.

MALLORY, S. B. 1995. Cowden syndrome (multiple hamartoma syndrome). *Dermatol Clin,* 13**,** 27-31.

MALUMBRES, M. & BARBACID, M. 2003. RAS oncogenes: the first 30 years. *Nat Rev Cancer,* 3**,** 459-65.

MC DONNELL, S., CHAUDHRY, V., MANSILLA-SOTO, J., ZENG, Z. S., SHU, W. P. & GUILLEM, J. G. 1999. Metastatic and non-metastatic colorectal cancer (CRC) cells induce host metalloproteinase production in vivo. *Clin Exp Metastasis,* 17**,** 341-9.

MEIJER, G. A., HERMSEN, M. A., BAAK, J. P., VAN DIEST, P. J., MEUWISSEN, S. G., BELIËN, J. A., HOOVERS, J. M., JOENJE, H., SNIJDERS, P. J. & WALBOOMERS, J. M. 1998a. Progression from colorectal adenoma to carcinoma is associated with non-random chromosomal gains as detected by comparative genomic hybridisation. *J Clin Pathol,* 51**,** 901-9.

MEIJER, G. A., HERMSEN, M. A., BAAK, J. P., VAN DIEST, P. J., MEUWISSEN, S. G., BELIËN, J. A., HOOVERS, J. M., JOENJE, H., SNIJDERS, P. J. & WALBOOMERS, J. M. 1998b. Progression from colorectal adenoma to carcinoma is associated with non-random chromosomal gains as detected by comparative genomic hybridisation. *J Clin Pathol,* 51**,** 901-9.

MESSICK, C. A., SANCHEZ, J., DEJULIUS, K. L., CHURCH, J. M. & KALADY, M. F. 2009. Genetic and molecular diversity of colon cancer hepatic metastases. *Surgery,* 146**,** 227-31.

MIYAKI, M., IIJIMA, T., HOSONO, K., ISHII, R., YASUNO, M., MORI, T., TOI, M., HISHIMA, T., SHITARA, N., TAMURA, K., UTSUNOMIYA, J., KOBAYASHI, N., KUROKI, T. & IWAMA, T. 2000. Somatic mutations of LKB1 and beta-catenin genes in gastrointestinal polyps from patients with Peutz-Jeghers syndrome. *Cancer Res,* 60**,** 6311-3.

MONTERO, J. C., SEOANE, S., OCANA, A. & PANDIELLA, A. 2011. P-Rex1 participates in Neuregulin-ErbB signal transduction and its expression correlates with patient outcome in breast cancer. *Oncogene,* 30**,** 1059-71.

MOSIMANN, C., HAUSMANN, G. & BASLER, K. 2009. Beta-catenin hits chromatin: regulation of Wnt target gene activation. *Nat Rev Mol Cell Biol,* 10**,** 276-86.

MUNEMITSU, S., ALBERT, I., SOUZA, B., RUBINFELD, B. & POLAKIS, P. 1995. Regulation of intracellular beta-catenin levels by the adenomatous polyposis coli (APC) tumor-suppressor protein. *Proc Natl Acad Sci U S A,* 92**,** 3046-50.

MUNOZ-BELLVIS, L., FONTANILLO, C., GONZALEZ-GONZALEZ, M., GARCIA, E., IGLESIAS, M., ESTEBAN, C., GUTIERREZ, M. L., ABAD, M. M., BENGOECHEA, O., DE LAS RIVAS, J., ORFAO, A. & SAYAGUES, J. M. 2012. Unique genetic profile of sporadic colorectal cancer liver metastasis versus primary tumors as defined by high-density single-nucleotide polymorphism arrays. *Mod Pathol,* 25**,** 590-601.

NAGASAKA, T., GOEL, A., NOTOHARA, K., TAKAHATA, T., SASAMOTO, H., UCHIDA, T., NISHIDA, N., TANAKA, N., BOLAND, C. R. & MATSUBARA, N. 2008. Methylation pattern of the O6-methylguanine-DNA methyltransferase gene in colon during progressive colorectal tumorigenesis. *Int J Cancer,* 122**,** 2429-36.

NAKAO, K., MEHTA, K. R., FRIDLYAND, J., MOORE, D. H., JAIN, A. N., LAFUENTE, A., WIENCKE, J. W., TERDIMAN, J. P. & WALDMAN, F. M. 2004. High-resolution analysis of DNA copy number alterations in colorectal cancer by array-based comparative genomic hybridization. *Carcinogenesis,* 25**,** 1345-57.

NANASHIMA, A., YAMAGUCHI, H., YASUTAKE, T., SAWAI, T., KUSANO, H., TAGAWA, Y., NAKAGOE, T. & AYABE, H. 1997a. Gain of chromosome 20 is a frequent aberration in liver metastasis of colorectal cancers. *Dig Dis Sci,* 42**,** 1388-93.

NANASHIMA, A., YAMAGUCHI, H., YASUTAKE, T., SAWAI, T., KUSANO, H., TAGAWA, Y., NAKAGOE, T. & AYABE, H. 1997b. Gain of chromosome 20 is a frequent aberration in liver metastasis of colorectal cancers. *Dig Dis Sci,* 42**,** 1388-93.

NANNEY, L. B., DAVIDSON, M. K., GATES, R. E., KANO, M. & KING, L. E. 1997. Altered distribution and expression of protein tyrosine phosphatases in normal human skin as compared to squamous cell carcinomas. *J Cutan Pathol,* 24**,** 521-32.

NIELSEN, M., FRANKEN, P. F., REINARDS, T. H., WEISS, M. M., WAGNER, A., VAN DER KLIFT, H., KLOOSTERMAN, S., HOUWING-DUISTERMAAT, J. J., AALFS, C. M., AUSEMS, M. G., BROCKER-VRIENDS, A. H., GOMEZ GARCIA, E. B., HOOGERBRUGGE, N., MENKO, F. H., SIJMONS, R. H., VERHOEF, S., KUIPERS, E. J., MORREAU, H., BREUNING, M. H., TOPS, C. M., WIJNEN, J. T., VASEN, H. F., FODDE, R. & HES, F. J. 2005. Multiplicity in polyp count and extracolonic manifestations in 40 Dutch patients with MYH associated polyposis coli (MAP). *J Med Genet,* 42**,** e54.

NIELSEN, M., HES, F. J., NAGENGAST, F. M., WEISS, M. M., MATHUS-VLIEGEN, E. M., MORREAU, H., BREUNING, M. H., WIJNEN, J. T., TOPS, C. M. & VASEN, H. F.

2007. Germline mutations in APC and MUTYH are responsible for the majority of families with attenuated familial adenomatous polyposis. *Clin Genet,* 71**,** 427-33.

PALLES, C., CAZIER, J. B., HOWARTH, K. M., DOMINGO, E., JONES, A. M., BRODERICK, P., KEMP, Z., SPAIN, S. L., GUARINO, E., SALGUERO, I., SHERBORNE, A., CHUBB, D., CARVAJAL-CARMONA, L. G., MA, Y., KAUR, K., DOBBINS, S., BARCLAY, E., GORMAN, M., MARTIN, L., KOVAC, M. B., HUMPHRAY, S., CONSORTIUM, C., CONSORTIUM, W. G. S., LUCASSEN, A., HOLMES, C. C., BENTLEY, D., DONNELLY, P., TAYLOR, J., PETRIDIS, C., ROYLANCE, R., SAWYER, E. J., KERR, D. J., CLARK, S., GRIMES, J., KEARSEY, S. E., THOMAS, H. J., MCVEAN, G., HOULSTON, R. S. & TOMLINSON, I. 2013. Germline mutations affecting the proofreading domains of POLE and POLD1 predispose to colorectal adenomas and carcinomas. *Nat Genet,* 45**,** 136-44.

PARADA, L. A., MARAÑON, A., HALLÉN, M., TRANBERG, K. G., STENRAM, U., BARDI, G. & JOHANSSON, B. 1999. Cytogenetic analyses of secondary liver tumors reveal significant differences in genomic imbalances between primary and metastatic colon carcinomas. *Clin Exp Metastasis,* 17**,** 471-9.

PARK, B. H., VOGELSTEIN, B. & KINZLER, K. W. 2001a. Genetic disruption of PPARdelta decreases the tumorigenicity of human colon cancer cells. *Proc Natl Acad Sci U S A,* 98**,** 2598-603.

PARK, B. H., VOGELSTEIN, B. & KINZLER, K. W. 2001b. Genetic disruption of PPARdelta decreases the tumorigenicity of human colon cancer cells. *Proc Natl Acad Sci U S A,* 98**,** 2598-603.

PERUCHO, M. 1999. Correspondence re: C.R. Boland et al., A National Cancer Institute workshop on microsatellite instability for cancer detection and familial predisposition: development of international criteria for the determination of microsatellite instability in colorectal cancer. Cancer Res., 58: 5248-5257, 1998. *Cancer Res,* 59**,** 249-56.

PETERS, U., BIEN, S. & ZUBAIR, N. 2015. Genetic architecture of colorectal cancer. *Gut*.

PETRIE, R. J., DOYLE, A. D. & YAMADA, K. M. 2009. Random versus directionally persistent cell migration. *Nat Rev Mol Cell Biol,* 10**,** 538-49.

PHAM, L. V., TAMAYO, A. T., YOSHIMURA, L. C., LO, P., TERRY, N., REID, P. S. & FORD, R. J. 2002. A CD40 Signalosome anchored in lipid rafts leads to constitutive activation of NF-kappaB and autonomous cell growth in B cell lymphomas. *Immunity,* 16**,** 37-50.

PHELPS, R. A., CHIDESTER, S., DEHGHANIZADEH, S., PHELPS, J., SANDOVAL, I. T., RAI, K., BROADBENT, T., SARKAR, S., BURT, R. W. & JONES, D. A. 2009. A two-step model for colon adenoma initiation and progression caused by APC loss. *Cell,* 137**,** 623-34.

PHILLIPS, W. A., ST CLAIR, F., MUNDAY, A. D., THOMAS, R. J. & MITCHELL, C. A. 1998. Increased levels of phosphatidylinositol 3-kinase activity in colorectal tumors. *Cancer,* 83**,** 41-7.

PINO, M. S. & CHUNG, D. C. 2010. The chromosomal instability pathway in colon cancer. *Gastroenterology,* 138**,** 2059-72.

POLAKIS, P. 2007. The many ways of Wnt in cancer. *Curr Opin Genet Dev,* 17**,** 45-51.

POSTMA, C., HERMSEN, M. A., COFFA, J., BAAK, J. P., MUELLER, J. D., MUELLER, E., BETHKE, B., SCHOUTEN, J. P., STOLTE, M. & MEIJER, G. A. 2005a. Chromosomal instability in flat adenomas and carcinomas of the colon. *J Pathol,* 205**,** 514-21.

POSTMA, C., HERMSEN, M. A., COFFA, J., BAAK, J. P., MUELLER, J. D., MUELLER, E., BETHKE, B., SCHOUTEN, J. P., STOLTE, M. & MEIJER, G. A. 2005b. Chromosomal instability in flat adenomas and carcinomas of the colon. *J Pathol,* 205**,** 514-21.

PRITCHARD, C. C. & GRADY, W. M. 2011. Colorectal cancer molecular biology moves into clinical practice. *Gut,* 60**,** 116-29.

QIN, J., XIE, Y., WANG, B., HOSHINO, M., WOLFF, D. W., ZHAO, J., SCOFIELD, M. A., DOWD, F. J., LIN, M. F. & TU, Y. 2009. Upregulation of PIP3-dependent Rac exchanger 1 (P-Rex1) promotes prostate cancer metastasis. *Oncogene,* 28**,** 1853-63.

RAFTOPOULOS, I., DAVARIS, P., KARATZAS, G., KARAYANNACOS, P. & KOURAKLIS, G. 1998. Level of alpha-catenin expression in colorectal cancer correlates with invasiveness, metastatic potential, and survival. *J Surg Oncol,* 68**,** 92-9.

RASHID, A., SHEN, L., MORRIS, J. S., ISSA, J. P. & HAMILTON, S. R. 2001. CpG island methylation in colorectal adenomas. *Am J Pathol,* 159**,** 1129-35.

REHA-KRANTZ, L. J. 2010. DNA polymerase proofreading: Multiple roles maintain genome stability. *Biochim Biophys Acta,* 1804**,** 1049-63.

RIED, T., KNUTZEN, R., STEINBECK, R., BLEGEN, H., SCHROCK, E., HESELMEYER, K., DU MANOIR, S. & AUER, G. 1996. Comparative genomic hybridization reveals a specific pattern of chromosomal gains and losses during the genesis of colorectal tumors. *Genes Chromosomes Cancer,* 15**,** 234-45.

RODRIGUEZ-VICIANA, P., WARNE, P. H., DHAND, R., VANHAESEBROECK, B., GOUT, I., FRY, M. J., WATERFIELD, M. D. & DOWNWARD, J. 1994. Phosphatidylinositol-3-OH kinase as a direct target of Ras. *Nature,* 370**,** 527-32.

RODRIGUEZ-VICIANA, P., WARNE, P. H., VANHAESEBROECK, B., WATERFIELD, M. D. & DOWNWARD, J. 1996. Activation of phosphoinositide 3-kinase by interaction with Ras and by point mutation. *EMBO J,* 15**,** 2442-51.

ROHENA, C. C. & MOOBERRY, S. L. 2014. Recent progress with microtubule stabilizers: new compounds, binding modes and cellular activities. *Nat Prod Rep,* 31**,** 335-55.

ROONEY, P. H., BOONSONG, A., MCKAY, J. A., MARSH, S., STEVENSON, D. A., MURRAY, G. I., CURRAN, S., HAITES, N. E., CASSIDY, J. & MCLEOD, H. L. 2001a. Colorectal cancer genomics: evidence for multiple genotypes which influence survival. *Br J Cancer,* 85**,** 1492-8.

ROONEY, P. H., BOONSONG, A., MCKAY, J. A., MARSH, S., STEVENSON, D. A., MURRAY, G. I., CURRAN, S., HAITES, N. E., CASSIDY, J. & MCLEOD, H. L. 2001b. Colorectal cancer genomics: evidence for multiple genotypes which influence survival. *Br J Cancer,* 85**,** 1492-8.

ROTHWELL, P. M., FOWKES, F. G., BELCH, J. F., OGAWA, H., WARLOW, C. P. & MEADE, T. W. 2011. Effect of daily aspirin on long-term risk of death due to cancer: analysis of individual patient data from randomised trials. *Lancet,* 377**,** 31-41.

ROWAN, A., HALFORD, S., GAASENBEEK, M., KEMP, Z., SIEBER, O., VOLIKOS, E., DOUGLAS, E., FIEGLER, H., CARTER, N., TALBOT, I., SILVER, A. & TOMLINSON, I. 2005. Refining molecular analysis in the pathways of colorectal carcinogenesis. *Clin Gastroenterol Hepatol,* 3**,** 1115-23.

RUSSO, A., BAZAN, V., IACOPETTA, B., KERR, D., SOUSSI, T., GEBBIA, N. & GROUP, T.-C. C. S. 2005. The TP53 colorectal cancer international collaborative study on the prognostic and predictive significance of p53 mutation: influence of tumor site, type of mutation, and adjuvant treatment. *J Clin Oncol,* 23**,** 7518-28.

RUSTGI, A. K. 2007. The genetics of hereditary colon cancer. *Genes Dev,* 21**,** 2525-38.

SABEL, M. S., YAMADA, M., KAWAGUCHI, Y., CHEN, F. A., TAKITA, H. & BANKERT, R. B. 2000. CD40 expression on human lung cancer correlates with metastatic spread. *Cancer Immunol Immunother,* 49**,** 101-8.

SAMOWITZ, W. S., ALBERTSEN, H., HERRICK, J., LEVIN, T. R., SWEENEY, C., MURTAUGH, M. A., WOLFF, R. K. & SLATTERY, M. L. 2005. Evaluation of a large, population-based sample supports a CpG island methylator phenotype in colon cancer. *Gastroenterology,* 129**,** 837-45.

SANCHEZ, J. A., KRUMROY, L., PLUMMER, S., AUNG, P., MERKULOVA, A., SKACEL, M., DEJULIUS, K. L., MANILICH, E., CHURCH, J. M., CASEY, G. & KALADY, M. F. 2009. Genetic and epigenetic classifications define clinical phenotypes and determine patient outcomes in colorectal cancer. *Br J Surg,* 96**,** 1196-204.

SANGWAN, V., PALIOURAS, G. N., CHENG, A., DUBÉ, N., TREMBLAY, M. L. & PARK, M. 2006. Protein-tyrosine phosphatase 1B deficiency protects against Fas-induced hepatic failure. *J Biol Chem,* 281**,** 221-8.

SANKARANARAYANAN, R., SWAMINATHAN, R., BRENNER, H., CHEN, K., CHIA, K. S., CHEN, J. G., LAW, S. C., AHN, Y. O., XIANG, Y. B., YEOLE, B. B., SHIN, H. R., SHANTA, V., WOO, Z. H., MARTIN, N., SUMITSAWAN, Y., SRIPLUNG, H., BARBOZA, A. O., ESER, S., NENE, B. M., SUWANRUNGRUANG, K., JAYALEKSHMI, P., DIKSHIT, R., WABINGA, H., ESTEBAN, D. B., LAUDICO, A., BHURGRI, Y., BAH, E. & AL-HAMDAN, N. 2010. Cancer survival in Africa, Asia, and Central America: a population-based study. *Lancet Oncol,* 11**,** 165-73.

SASTRY, S. K. & ELFERINK, L. A. 2011. Checks and balances: interplay of RTKs and PTPs in cancer progression. *Biochem Pharmacol,* 82**,** 435-40.

SAYAGUÉS, J. M., FONTANILLO, C., ABAD, M. E. M., GONZÁLEZ-GONZÁLEZ, M., SARASQUETE, M. E., CHILLON, M. E. C., GARCIA, E., BENGOECHEA, O., FONSECA, E., GONZALEZ-DIAZ, M., DE LAS RIVAS, J., MUÑOZ-BELLVIS, L. & ORFAO, A. 2010a. Mapping of genetic abnormalities of primary tumours from metastatic CRC by high-resolution SNP arrays. *PLoS One,* 5**,** e13752.

SAYAGUÉS, J. M., FONTANILLO, C., ABAD, M. E. M., GONZÁLEZ-GONZÁLEZ, M., SARASQUETE, M. E., CHILLON, M. E. C., GARCIA, E., BENGOECHEA, O., FONSECA, E., GONZALEZ-DIAZ, M., DE LAS RIVAS, J., MUÑOZ-BELLVIS, L. & ORFAO, A. 2010b. Mapping of genetic abnormalities of primary tumours from metastatic CRC by high-resolution SNP arrays. *PLoS One,* 5**,** e13752.

SCHMIDT, A. & HALL, A. 2002. Guanine nucleotide exchange factors for Rho GTPases: turning on the switch. *Genes Dev,* 16**,** 1587-609.

SCHUMACHER, F. R., SCHMIT, S. L., JIAO, S., EDLUND, C. K., WANG, H., ZHANG, B., HSU, L., HUANG, S. C., FISCHER, C. P., HARJU, J. F., IDOS, G. E., LEJBKOWICZ, F., MANION, F. J., MCDONNELL, K., MCNEIL, C. E., MELAS, M., RENNERT, H. S., SHI, W., THOMAS, D. C., VAN DEN BERG, D. J., HUTTER, C. M., ARAGAKI, A. K., BUTTERBACH, K., CAAN, B. J., CARLSON, C. S., CHANOCK, S. J., CURTIS, K. R., FUCHS, C. S., GALA, M., GIOVANNUCC, E. L., GOGARTEN, S. M., HAYES, R. B., HENDERSON, B., HUNTER, D. J., JACKSON, R. D., KOLONEL, L. N., KOOPERBERG, C., KURY, S., LACROIX, A., LAURIE, C. C., LAURIE, C. A., LEMIRE, M., LEVINE, D., MA, J., MAKAR, K. W., QU, C., TAVERNA, D., ULRICH, C. M., WU, K., KONO, S., WEST, D. W., BERNDT, S. I., BEZIEAU, S., BRENNER, H., CAMPBELL, P. T., CHAN, A. T., CHANG-CLAUDE, J., COETZEE, G. A., CONTI, D. V., DUGGAN, D., FIGUEIREDO, J. C., FORTINI, B. K., GALLINGER, S. J., GAUDERMAN, W. J., GILES, G., GREEN, R., HAILE, R., HARRISON, T. A., HOFFMEISTER, M., HOPPER, J. L., HUDSON, T. J., JACOBS, E., IWASAKI, M., JEE, S. H., JENKINS, M., JIA, W. H., JOSHI, A., LI, L., LINDOR, N. M., MATSUO, K., MORENO, V., MUKHERJEE, B., NEWCOMB, P. A., POTTER, J. D., RASKIN, L., RENNERT, G., ROSSE, S., SEVERI, G., SCHOEN, R. E., SEMINARA, D., SHU, X. O., SLATTERY, M. L., TSUGANE, S., WHITE, E., XIANG, Y. B., ZANKE, B. W., ZHENG, W., LE MARCHAND, L., CASEY, G., GRUBER, S. B., et al. 2015. Genome-wide association study of colorectal cancer identifies six new susceptibility loci. *Nat Commun,* 6**,** 7138.

SCOTT, L. M., LAWRENCE, H. R., SEBTI, S. M., LAWRENCE, N. J. & WU, J. 2010. Targeting protein tyrosine phosphatases for anticancer drug discovery. *Curr Pharm Des,* 16**,** 1843-62.

SEGDITSAS, S. & TOMLINSON, I. 2006. Colorectal cancer and genetic alterations in the Wnt pathway. *Oncogene,* 25**,** 7531-7.

SESHAGIRI, S. 2013. The burden of faulty proofreading in colon cancer. *Nat Genet,* 45**,** 121-2.

SETH, R., CROOK, S., IBRAHEM, S., FADHIL, W., JACKSON, D. & ILYAS, M. 2009. Concomitant mutations and splice variants in KRAS and BRAF demonstrate complex perturbation of the Ras/Raf signalling pathway in advanced colorectal cancer. *Gut,* 58**,** 1234-41.

SHEFFER, M., BACOLOD, M. D., ZUK, O., GIARDINA, S. F., PINCAS, H., BARANY, F., PATY, P. B., GERALD, W. L., NOTTERMAN, D. A. & DOMANY, E. 2009a. Association of survival and disease progression with chromosomal instability: a genomic exploration of colorectal cancer. *Proc Natl Acad Sci U S A,* 106**,** 7131-6.

SHEFFER, M., BACOLOD, M. D., ZUK, O., GIARDINA, S. F., PINCAS, H., BARANY, F., PATY, P. B., GERALD, W. L., NOTTERMAN, D. A. & DOMANY, E. 2009b. Association of survival and disease progression with chromosomal instability: a genomic exploration of colorectal cancer. *Proc Natl Acad Sci U S A,* 106**,** 7131-6.

SHOJI, Y., MIYAMOTO, M., ISHIKAWA, K., YOSHIOKA, T., MISHRA, R., ICHINOKAWA, K., MATSUMURA, Y., ITOH, T., SHINOHARA, T., HIRANO, S. & KONDO, S. 2011. The CD40-CD154 interaction would correlate with proliferation and immune escape in pancreatic ductal adenocarcinoma. *J Surg Oncol,* 103**,** 230-8.

SIEGEL, R., DESANTIS, C., VIRGO, K., STEIN, K., MARIOTTO, A., SMITH, T., COOPER, D., GANSLER, T., LERRO, C., FEDEWA, S., LIN, C., LEACH, C., CANNADY, R. S., CHO, H., SCOPPA, S., HACHEY, M., KIRCH, R., JEMAL, A. & WARD, E. 2012. Cancer treatment and survivorship statistics, 2012. *CA Cancer J Clin,* 62**,** 220-41.

SILLARS-HARDEBOL, A. H., CARVALHO, B., BELIËN, J. A., DE WIT, M., DELIS-VAN DIEMEN, P. M., TIJSSEN, M., VAN DE WIEL, M. A., PONTÉN, F., FIJNEMAN, R. J. & MEIJER, G. A. 2012a. BCL2L1 has a functional role in colorectal cancer and its protein expression is associated with chromosome 20q gain. *J Pathol,* 226**,** 442-50.

SILLARS-HARDEBOL, A. H., CARVALHO, B., BELIËN, J. A., DE WIT, M., DELIS-VAN DIEMEN, P. M., TIJSSEN, M., VAN DE WIEL, M. A., PONTÉN, F., MEIJER, G. A. & FIJNEMAN, R. J. 2012b. CSE1L, DIDO1 and RBM39 in colorectal adenoma to carcinoma progression. *Cell Oncol (Dordr)*.

SILLARS-HARDEBOL, A. H., CARVALHO, B., TIJSSEN, M., BELIËN, J. A., DE WIT, M., DELIS-VAN DIEMEN, P. M., PONTÉN, F., VAN DE WIEL, M. A., FIJNEMAN, R. J. & MEIJER, G. A. 2011a. TPX2 and AURKA promote 20q amplicon-driven colorectal adenoma to carcinoma progression. *Gut*.

SILLARS-HARDEBOL, A. H., CARVALHO, B., TIJSSEN, M., BELIËN, J. A., DE WIT, M., DELIS-VAN DIEMEN, P. M., PONTÉN, F., VAN DE WIEL, M. A., FIJNEMAN, R. J. & MEIJER, G. A. 2011b. TPX2 and AURKA promote 20q amplicon-driven colorectal adenoma to carcinoma progression. *Gut*.

SILVER, A., SENGUPTA, N., PROPPER, D., WILSON, P., HAGEMANN, T., PATEL, A., PARKER, A., GHOSH, A., FEAKINS, R., DORUDI, S. & SURAWEERA, N. 2012. A distinct DNA methylation profile associated with microsatellite and chromosomal stable sporadic colorectal cancers. *Int J Cancer,* 130**,** 1082-92.

SJÖBLOM, T., JONES, S., WOOD, L. D., PARSONS, D. W., LIN, J., BARBER, T. D., MANDELKER, D., LEARY, R. J., PTAK, J., SILLIMAN, N., SZABO, S., BUCKHAULTS, P., FARRELL, C., MEEH, P., MARKOWITZ, S. D., WILLIS, J., DAWSON, D., WILLSON, J. K., GAZDAR, A. F., HARTIGAN, J., WU, L., LIU, C., PARMIGIANI, G., PARK, B. H., BACHMAN, K. E., PAPADOPOULOS, N., VOGELSTEIN, B., KINZLER, K. W. & VELCULESCU, V. E. 2006. The consensus coding sequences of human breast and colorectal cancers. *Science,* 314**,** 268-74.

SMITH, G., CAREY, F. A., BEATTIE, J., WILKIE, M. J., LIGHTFOOT, T. J., COXHEAD, J., GARNER, R. C., STEELE, R. J. & WOLF, C. R. 2002. Mutations in APC, Kirsten-ras, and p53--alternative genetic pathways to colorectal cancer. *Proc Natl Acad Sci U S A,* 99**,** 9433-8.

SNOW, A. K., TUOHY, T. M., SARGENT, N. R., SMITH, L. J., BURT, R. W. & NEKLASON, D. W. 2014. APC promoter 1B deletion in seven American families with familial adenomatous polyposis. *Clin Genet*.

SONNENBERG, A. & GENTA, R. M. 2013. Helicobacter pylori is a risk factor for colonic neoplasms. *Am J Gastroenterol,* 108**,** 208-15.

SOSA, M. S., LOPEZ-HABER, C., YANG, C., WANG, H., LEMMON, M. A., BUSILLO, J. M., LUO, J., BENOVIC, J. L., KLEIN-SZANTO, A., YAGI, H., GUTKIND, J. S., PARSONS, R. E. & KAZANIETZ, M. G. 2010. Identification of the Rac-GEF P-Rex1 as an essential mediator of ErbB signaling in breast cancer. *Mol Cell,* 40**,** 877-92.

STOCK, C., PULTE, D., HAUG, U. & BRENNER, H. 2012. Subsite-specific colorectal cancer risk in the colorectal endoscopy era. *Gastrointest Endosc,* 75**,** 621-30.

STOFFEL, E., MUKHERJEE, B., RAYMOND, V. M., TAYOB, N., KASTRINOS, F., SPARR, J., WANG, F., BANDIPALLIAM, P., SYNGAL, S. & GRUBER, S. B. 2009. Calculation of risk of colorectal and endometrial cancer among patients with Lynch syndrome. *Gastroenterology,* 137**,** 1621-7.

STRESEMANN, C. & LYKO, F. 2008. Modes of action of the DNA methyltransferase inhibitors azacytidine and decitabine. *Int J Cancer,* 123**,** 8-13.

STUIBLE, M., ABELLA, J. V., FELDHAMMER, M., NOSSOV, M., SANGWAN, V., BLAGOEV, B., PARK, M. & TREMBLAY, M. L. 2010. PTP1B targets the endosomal sorting machinery: dephosphorylation of regulatory sites on the endosomal sorting complex required for transport component STAM2. *J Biol Chem,* 285**,** 23899-907.

STUIBLE, M., DOODY, K. M. & TREMBLAY, M. L. 2008. PTP1B and TC-PTP: regulators of transformation and tumorigenesis. *Cancer Metastasis Rev,* 27**,** 215-30.

STUIBLE, M. & TREMBLAY, M. L. 2010. In control at the ER: PTP1B and the down-regulation of RTKs by dephosphorylation and endocytosis. *Trends Cell Biol,* 20**,** 672-9.

TABACH, Y., KOGAN-SAKIN, I., BUGANIM, Y., SOLOMON, H., GOLDFINGER, N., HOVLAND, R., KE, X. S., OYAN, A. M., KALLAND, K. H., ROTTER, V. & DOMANY, E. 2011. Amplification of the 20q chromosomal arm occurs early in tumorigenic transformation and may initiate cancer. *PLoS One,* 6**,** e14632.

TAKAHASHI, Y., KITADAI, Y., BUCANA, C. D., CLEARY, K. R. & ELLIS, L. M. 1995. Expression of vascular endothelial growth factor and its receptor, KDR, correlates with vascularity, metastasis, and proliferation of human colon cancer. *Cancer Res,* 55**,** 3964-8.

TAKAYAMA, T., OHI, M., HAYASHI, T., MIYANISHI, K., NOBUOKA, A., NAKAJIMA, T., SATOH, T., TAKIMOTO, R., KATO, J., SAKAMAKI, S. & NIITSU, Y. 2001. Analysis of K-ras, APC, and beta-catenin in aberrant crypt foci in sporadic adenoma, cancer, and familial adenomatous polyposis. *Gastroenterology,* 121**,** 599-611.

TANG, R., HO, Y. S., YOU, Y. T., HSU, K. C., CHEN, J. S., CHANGCHIEN, C. R. & WANG, J. Y. 1995. Prognostic evaluation of DNA flow cytometric and histopathologic parameters of colorectal cancer. *Cancer,* 76**,** 1724-30.

TAYLOR, D. P., BURT, R. W., WILLIAMS, M. S., HAUG, P. J. & CANNON-ALBRIGHT, L. A. 2010. Population-based family history-specific risks for colorectal cancer: a constellation approach. *Gastroenterology,* 138**,** 877-85.

THEODORATOU, E., CAMPBELL, H., TENESA, A., HOULSTON, R., WEBB, E., LUBBE, S., BRODERICK, P., GALLINGER, S., CROITORU, E. M., JENKINS, M. A., WIN, A. K., CLEARY, S. P., KOESSLER, T., PHAROAH, P. D., KURY, S., BEZIEAU, S., BUECHER, B., ELLIS, N. A., PETERLONGO, P., OFFIT, K., AALTONEN, L. A., ENHOLM, S., LINDBLOM, A., ZHOU, X. L., TOMLINSON, I. P., MORENO, V., BLANCO, I., CAPELLA, G., BARNETSON, R., PORTEOUS, M. E., DUNLOP, M. G. & FARRINGTON, S. M. 2010. A large-scale meta-analysis to refine colorectal cancer risk estimates associated with MUTYH variants. *Br J Cancer,* 103**,** 1875-84.

THIBODEAU, S. N., BREN, G. & SCHAID, D. 1993. Microsatellite instability in cancer of the proximal colon. *Science,* 260**,** 816-9.

TONG, A. W., PAPAYOTI, M. H., NETTO, G., ARMSTRONG, D. T., ORDONEZ, G., LAWSON, J. M. & STONE, M. J. 2001. Growth-inhibitory effects of CD40 ligand (CD154) and its endogenous expression in human breast cancer. *Clin Cancer Res,* 7**,** 691-703.

TSAFRIR, D., BACOLOD, M., SELVANAYAGAM, Z., TSAFRIR, I., SHIA, J., ZENG, Z., LIU, H., KRIER, C., STENGEL, R. F., BARANY, F., GERALD, W. L., PATY, P. B., DOMANY, E. & NOTTERMAN, D. A. 2006. Relationship of gene expression and chromosomal abnormalities in colorectal cancer. *Cancer Res,* 66**,** 2129-37.

TSUKAMOTO, N., KOBAYASHI, N., AZUMA, S., YAMAMOTO, T. & INOUE, J. 1999. Two differently regulated nuclear factor kappaB activation pathways triggered by the cytoplasmic tail of CD40. *Proc Natl Acad Sci U S A,* 96**,** 1234-9.

UMETANI, N., SASAKI, S., MASAKI, T., WATANABE, T., MATSUDA, K. & MUTO, T. 2000. Involvement of APC and K-ras mutation in non-polypoid colorectal tumorigenesis. *Br J Cancer,* 82**,** 9-15.

VAN BEERS, E. H., JOOSSE, S. A., LIGTENBERG, M. J., FLES, R., HOGERVORST, F. B., VERHOEF, S. & NEDERLOF, P. M. 2006. A multiplex PCR predictor for aCGH success of FFPE samples. *Br J Cancer,* 94**,** 333-7.

VAN KOOTEN, C. & BANCHEREAU, J. 1997. Functions of CD40 on B cells, dendritic cells and other cells. *Curr Opin Immunol,* 9**,** 330-7.

VAN KOOTEN, C. & BANCHEREAU, J. 2000. CD40-CD40 ligand. *J Leukoc Biol,* 67**,** 2-17.

VANE, J. & CORIN, R. E. 2003. Prostacyclin: a vascular mediator. *Eur J Vasc Endovasc Surg,* 26**,** 571-8.

VASEN, H. F. 2000. Clinical diagnosis and management of hereditary colorectal cancer syndromes. *J Clin Oncol,* 18**,** 81S-92S.

VASEN, H. F., TOMLINSON, I. & CASTELLS, A. 2015. Clinical management of hereditary colorectal cancer syndromes. *Nat Rev Gastroenterol Hepatol,* 12**,** 88-97.

VILAR, E. & GRUBER, S. B. 2010. Microsatellite instability in colorectal cancer-the stable evidence. *Nat Rev Clin Oncol,* 7**,** 153-62.

VIVANCO, I. & SAWYERS, C. L. 2002a. The phosphatidylinositol 3-Kinase AKT pathway in human cancer. *Nat Rev Cancer,* 2**,** 489-501.

VIVANCO, I. & SAWYERS, C. L. 2002b. The phosphatidylinositol 3-Kinase AKT pathway in human cancer. *Nat Rev Cancer,* 2**,** 489-501.

VOGELSTEIN, B., FEARON, E. R., HAMILTON, S. R., KERN, S. E., PREISINGER, A. C., LEPPERT, M., NAKAMURA, Y., WHITE, R., SMITS, A. M. & BOS, J. L. 1988. Genetic alterations during colorectal-tumor development. *N Engl J Med,* 319**,** 525-32.

VONDERHEIDE, R. H. & GLENNIE, M. J. 2013. Agonistic CD40 antibodies and cancer therapy. *Clin Cancer Res,* 19**,** 1035-43.

VOUSDEN, K. H. & PRIVES, C. 2009. Blinded by the Light: The Growing Complexity of p53. *Cell,* 137**,** 413-31.

WALTHER, A., HOULSTON, R. & TOMLINSON, I. 2008. Association between chromosomal instability and prognosis in colorectal cancer: a meta-analysis. *Gut,* 57**,** 941-50.

WALTHER, A., JOHNSTONE, E., SWANTON, C., MIDGLEY, R., TOMLINSON, I. & KERR, D. 2009. Genetic prognostic and predictive markers in colorectal cancer. *Nat Rev Cancer,* 9**,** 489-99.

WANG, Y., JATKOE, T., ZHANG, Y., MUTCH, M. G., TALANTOV, D., JIANG, J., MCLEOD, H. L. & ATKINS, D. 2004. Gene expression profiles and molecular markers to predict recurrence of Dukes' B colon cancer. *J Clin Oncol,* 22**,** 1564-71.

WARABI, M., NEMOTO, T., OHASHI, K., KITAGAWA, M. & HIROKAWA, K. 2000. Expression of protein tyrosine phosphatases and its significance in esophageal cancer. *Exp Mol Pathol,* 68**,** 187-95.

WATERS, J. E., ASTLE, M. V., OOMS, L. M., BALAMATSIAS, D., GURUNG, R. & MITCHELL, C. A. 2008. P-Rex1 - a multidomain protein that regulates neurite differentiation. *J Cell Sci,* 121**,** 2892-903.

WEISENBERGER, D. J., SIEGMUND, K. D., CAMPAN, M., YOUNG, J., LONG, T. I., FAASSE, M. A., KANG, G. H., WIDSCHWENDTER, M., WEENER, D., BUCHANAN, D., KOH, H., SIMMS, L., BARKER, M., LEGGETT, B., LEVINE, J., KIM, M., FRENCH, A. J., THIBODEAU, S. N., JASS, J., HAILE, R. & LAIRD, P. W. 2006. CpG island methylator phenotype underlies sporadic microsatellite instability and is tightly associated with BRAF mutation in colorectal cancer. *Nat Genet,* 38**,** 787-93.

WEITZ, J., KOCH, M., DEBUS, J., HÖHLER, T., GALLE, P. R. & BÜCHLER, M. W. 2005. Colorectal cancer. *Lancet,* 365**,** 153-65.

WELCH, H. C., COADWELL, W. J., ELLSON, C. D., FERGUSON, G. J., ANDREWS, S. R., ERDJUMENT-BROMAGE, H., TEMPST, P., HAWKINS, P. T. & STEPHENS, L. R. 2002. P-Rex1, a PtdIns(3,4,5)P3- and Gbetagamma-regulated guanine-nucleotide exchange factor for Rac. *Cell,* 108**,** 809-21.

WIELENGA, V. J., SMITS, R., KORINEK, V., SMIT, L., KIELMAN, M., FODDE, R., CLEVERS, H. & PALS, S. T. 1999. Expression of CD44 in Apc and Tcf mutant mice implies regulation by the WNT pathway. *Am J Pathol,* 154**,** 515-23.

WINTER, M. J., NAGELKERKEN, B., MERTENS, A. E., REES-BAKKER, H. A., BRIAIRE-DE BRUIJN, I. H. & LITVINOV, S. V. 2003. Expression of Ep-CAM shifts the state of cadherin-mediated adhesions from strong to weak. *Exp Cell Res,* 285**,** 50-8.

WONG, C. Y., WURIYANGHAN, H., XIE, Y., LIN, M. F., ABEL, P. W. & TU, Y. 2011. Epigenetic regulation of phosphatidylinositol 3,4,5-triphosphate-dependent Rac exchanger 1 gene expression in prostate cancer cells. *J Biol Chem,* 286**,** 25813-22.

WOOD, L. D., PARSONS, D. W., JONES, S., LIN, J., SJÖBLOM, T., LEARY, R. J., SHEN, D., BOCA, S. M., BARBER, T., PTAK, J., SILLIMAN, N., SZABO, S., DEZSO, Z., USTYANKSKY, V., NIKOLSKAYA, T., NIKOLSKY, Y., KARCHIN, R., WILSON, P. A., KAMINKER, J. S., ZHANG, Z., CROSHAW, R., WILLIS, J., DAWSON, D., SHIPITSIN, M., WILLSON, J. K., SUKUMAR, S., POLYAK, K., PARK, B. H., PETHIYAGODA, C. L., PANT, P. V., BALLINGER, D. G., SPARKS, A. B., HARTIGAN, J., SMITH, D. R., SUH, E., PAPADOPOULOS, N., BUCKHAULTS, P., MARKOWITZ, S. D., PARMIGIANI, G., KINZLER, K. W., VELCULESCU, V. E. & VOGELSTEIN, B. 2007. The genomic landscapes of human breast and colorectal cancers. *Science,* 318**,** 1108-13.

WOODFORD-THOMAS, T. A., RHODES, J. D. & DIXON, J. E. 1992. Expression of a protein tyrosine phosphatase in normal and v-src-transformed mouse 3T3 fibroblasts. *J Cell Biol,* 117**,** 401-14.

WRIGHT, C. M., DENT, O. F., NEWLAND, R. C., BARKER, M., CHAPUIS, P. H., BOKEY, E. L., YOUNG, J. P., LEGGETT, B. A., JASS, J. R. & MACDONALD, G. A. 2005. Low level microsatellite instability may be associated with reduced cancer specific survival in sporadic stage C colorectal carcinoma. *Gut,* 54**,** 103-8.

WU, Y., WANG, L., HE, X., XU, H., ZHOU, L., ZHAO, F. & ZHANG, Y. 2008. Expression of CD40 and growth-inhibitory activity of CD40 ligand in colon cancer ex vivo. *Cell Immunol,* 253**,** 102-9.

XIE, X., WANG, C. Y., CAO, Y. X., WANG, W., ZHUANG, R., CHEN, L. H., DANG, N. N., FANG, L. & JIN, B. Q. 2005. Expression pattern of epithelial cell adhesion molecule on normal and malignant colon tissues. *World J Gastroenterol,* 11**,** 344-7.

YAN, Z., YIN, H., WANG, R., WU, D., SUN, W., LIU, B. & SU, Q. 2014. Overexpression of integrin-linked kinase (ILK) promotes migration and invasion of colorectal cancer cells by inducing epithelial-mesenchymal transition via NF-kappaB signaling. *Acta Histochem,* 116**,** 527-33.

YANG, H., OU, C. C., FELDMAN, R. I., NICOSIA, S. V., KRUK, P. A. & CHENG, J. Q. 2004. Aurora-A kinase regulates telomerase activity through c-Myc in human ovarian and breast epithelial cells. *Cancer Res,* 64**,** 463-7.

YIP, S. C., SAHA, S. & CHERNOFF, J. 2010. PTP1B: a double agent in metabolism and oncogenesis. *Trends Biochem Sci,* 35**,** 442-9.

YOSHIZAWA, M., KAWAUCHI, T., SONE, M., NISHIMURA, Y. V., TERAO, M., CHIHAMA, K., NABESHIMA, Y. & HOSHINO, M. 2005. Involvement of a Rac activator,P-Rex1, in neurotrophin-derived signaling and neuronal migration. *J Neurosci,* 25**,** 4406-19.

ZHAO, L. & VOGT, P. K. 2008. Class I PI3K in oncogenic cellular transformation. *Oncogene,* 27**,** 5486-96.

ZHU, S., BJORGE, J. D. & FUJITA, D. J. 2007. PTP1B contributes to the oncogenic properties of colon cancer cells through Src activation. *Cancer Res,* 67**,** 10129-37.

7 Chapter Seven: Appendix

7.1 Appendix 2: DNA extraction

Six to ten 10 micron thick sections were cut from each tissue blocks. For the purposes of microdissection, the tissues were cut onto slides and left over night to dry at 37°c. Then, the slides were stained with nuclear Fast Red (NFR). The normal tissues and stroma were removed by needle microdissection under a dissecting microscope (EMT 8523, MEIJI-LABAX, Tokyo, Japan).

The slides then underwent rehydration by ethanol (100% 30 sec, 90% 30 sec and 70% 30 sec) and incubated overnight at 37 Cû with 1X sodium thiocyanate solution (80518, Fluka, BioChemika, Switzerland). The slides then washed twice with phosphate buffered saline (PBS) for 10 min each and then air dried. Finally the tumour tissue was scraped into 1.5 ml eppendorf tube.

For the non-microdissected cases, the sections were directly placed into 1.5 ml eppendorf tube. The DNA extraction was done in sets of samples using the QIAamp DNA FFPE tissue kit (Qiagen) according to the manufacture's instruction.

7.2 Appendix2: BCA protein Assay kit instruction

Preparation of Standards and Working Reagent (required for both assay procedures)

A. Preparation of Diluted Albumin (BSA) Standards

Use Table 1 as a guide to prepare a set of protein standards. Dilute the contents of one Albumin Standard (BSA) ampule into several clean vials, preferably using the same diluent as the sample(s). Each 1 ml ampule of 2.0 mg/ml Albumin Standard is sufficient to prepare a set of diluted standards for either working range suggested in Table 1. There will be sufficient volume for three replications of each diluted standard.

Table 1. Preparation of Diluted Albumin (BSA) Standards

Dilution Scheme for Standard Test Tube Protocol and Microplate Procedure (Working Range = 20–2,000 µg/ml)			
Vial	**Volume of Diluent**	**Volume and Source of BSA**	**Final BSA Concentration**
A	0	300 µl of Stock	2,000 µg/ml
B	125 µl	375 µl of Stock	1,500 µg/ml
C	325 µl	325 µl of Stock	1,000 µg/ml
D	175 µl	175 µl of vial B dilution	750 µg/ml
E	325 µl	325 µl of vial C dilution	500 µg/ml
F	325 µl	325 µl of vial E dilution	250 µg/ml
G	325 µl	325 µl of vial F dilution	125 µg/ml
H	400 µl	100 µl of vial G dilution	25 µg/ml
I	400 µl	0	0 µg/ml = Blank
Dilution Scheme for Enhanced Test Tube Protocol (Working Range = 5–250 µg/ml)			
Vial	**Volume of Diluent**	**Volume and Source of BSA**	**Final BSA Concentration**
A	700 µl	100 µl of Stock	250 µg/ml
B	400 µl	400 µl of vial A dilution	125 µg/ml
C	450 µl	300 µl of vial B dilution	50 µg/ml
D	400 µl	400 µl of vial C dilution	25 µg/ml
E	400 µl	100 µl of vial D dilution	5 µg/ml
F	400 µl	0	0 µg/ml = Blank

B. Preparation of the BCA Working Reagent (WR)

1. Use the following formula to determine the total volume of WR required:

   (# standards + # unknowns) × (# replicates) × (volume of WR per sample) = total volume WR required

   Example: for the standard test-tube procedure with 3 unknowns and 2 replicates of each sample:

   (9 standards + 3 unknowns) × (2 replicates) × (2 ml) = 48 ml WR required

   Note: 2.0 ml of the WR is required for each sample in the test-tube procedure, while only 200 µl of WR reagent is required for each sample in the microplate procedure.

2. Prepare WR by mixing 50 parts of BCA Reagent A with 1 part of BCA Reagent B (50:1, Reagent A:B). For the above example, combine 50 ml of Reagent A with 1 ml of Reagent B.

   Note: When Reagent B is first added to Reagent A, turbidity is observed that quickly disappears upon mixing to yield a clear, green WR. Prepare sufficient volume of WR based on the number of samples to be assayed. The WR is stable for several days when stored in a closed container at room temperature (RT).

Microplate Procedure (Sample to WR ratio = 1:8)

1. Pipette 25 µl of each standard or unknown sample replicate into a microplate well (working range = 20-2,000 µg/ml).

   Note: If sample size is limited, 10 µl of each unknown sample and standard can be used (sample to WR ratio = 1:20). However, the working range of the assay in this case will be limited to 125-2,000 µg/ml.

2. Add 200 µl of the WR to each well and mix plate thoroughly on a plate shaker for 30 seconds.
3. Cover plate and incubate at 37°C for 30 minutes.
4. Cool plate to RT.
5. Measure the absorbance at or near 562 nm on a plate reader.

   Notes:
   - Wavelengths from 540-590 nm have been used successfully with this method.
   - Because plate readers use a shorter light path length than cuvette spectrophotometers, the Microplate Procedure requires a greater sample to WR ratio to obtain the same sensitivity as the standard Test Tube Procedure. If higher 562 nm measurements are desired, increase the incubation time to 2 hours.